DOCTOR OF PHILOSOPHY

Patterns and processes of saltmarsh area change at three spatial scales

Ladd, Cai J.T.

Award date:
2018

Awarding institution:
Bangor University

Patterns and processes of saltmarsh area change at three spatial scales

Thesis submitted in candidature for
the Degree of Doctor of Philosophy at Bangor University, Wales

by
Cai J. T. Ladd

School of Ocean Sciences,
Bangor University,
Menai Bridge,
Anglesey, Wales
LL59 5AB

June 2018

Coleg Cymraeg Cenedlaethol

PRIFYSGOL BANGOR UNIVERSITY

Summary

Ecosystems around the globe are being degraded by anthropogenic activity. Coastal ecosystems are considered especially vulnerable given that human populations are concentrated at the coast. Extensive areas of saltmarsh habitat have already been lost to land reclamation, and the continued existence of natural marsh systems is in question. Understanding how saltmarsh plants interact within a changing coastal environment is seen as a vital step in protecting remaining habitat and delivering successful restoration. This thesis examines patterns of saltmarsh change across Great Britain (GB), and the biological and environmental drivers responsible for change, in order to better understand marsh persistence.

Studies have tended to assess marsh persistence based on their capacity to grow vertically with sea level rise. Long-term horizontal marsh dynamics are often overlooked. *Chapter 2* examines 100 years of saltmarsh area change across GB and found that sea level rise and sediment supply determined whether saltmarshes expanded or eroded. All marshes were keeping pace with sea level rise, highlighting the importance of considering horizontal dynamics in long-term marsh change.

Identifying the limits on horizontal saltmarsh growth onto tidal flats has been valuable in assessing potential impacts of coastal change on open-coast marsh systems, however little work has been done on identifying limits of marsh extent within estuaries. *Chapter 3* examines saltmarsh extent change between 1948 and 2013 in three sheltered estuaries along western GB, and shows that changes in the position of tidal channels limited marsh extent. Channels periodically migrated across the estuary causing marsh erosion. On the opposite bank, marshes tended to expand, indicating the capacity of marshes to cycle between phases of expansion and erosion retaining a dynamic persistence within estuaries.

Horizontal erosion of saltmarsh creeks causes vegetated marsh debris to accumulate at the creek base. Indications are that these deposits limit further erosion and promote recovery through trapping sediment if they persist. However, biotic and abiotic controls on debris longevity are unclear. *Chapter 4* examines monthly creek change over a year and shows that failed bank debris with high root content slow debris erosion rates, thereby promoting sediment trapping and recovery. Thus, plant growth plays an important role on saltmarsh stability.

By investigating marsh change over different spatio-temporal scales, a picture emerges of how biological and environmental drivers collectively influence change in saltmarsh extent. This offers important insight into how management interventions could target the drivers of marsh change at each scale in order to build marsh resilience, and is discussed in chapter 5.

Contents

List of appendices

List of figures

List of tables

Acknowledgements

I am indebted to my main supervisor, Dr Martin Skov, for his support and encouragement during the PhD. Working with you has been a please during the past four years, and I hope our collaborations will continue on well into the future. I am also grateful to my supervisory team, Dr Jaco Baas and Dr Dei Huws, whom were always available for support and guidance throughout the PhD. My thanks to Prof. James Scourse for valuable feedback on my work and progress. Thank you to Prof. Stuart Jenkins, Dr Jan Hiddink, Dr Andrew Davies and Prof. Tjeerd Bouma, for the thrilling discussions, constructive feedback and support. Special thanks to Prof. Tom Spencer, Prof. David Thomas, and Dr Ian McCarthy for a successful Viva, and for the detailed feedback on the first submission of this work. Your comments have helped improve the work substantially.

To the saltmarsh gang, Dr Hilary Ford, Dr Rachel Kingham, Dr Jordi Pagès, Mollie Duggan-Edwards and Angus Garbutt, working with you all these past years has been wonderful. Thank you so much for all the help – I would not have succeeded in completing this thesis without you. I would also like to thank everyone involved in the CBESS and ResilCoast projects for their support, advice and company. The best of luck you all in your future careers.

My sincere gratitude to the volunteers that have helped me with fieldwork and data processing, especially Julie Wright, Maria Hayden-Hughes and Rachel Wright. Thank you Ben Powell, Peter Hughes and Aled Owen help with deploying the ADV in the field, and thank you to all the technical and research staff at the School of Ocean Sciences for access to lab space and equipment. Special thanks to Dr Jonathan Malarkey, who has helped me on countless occasions to understand the mechanics of water and sediment flow. I am also indebted to Alex Vierod, who helped me set up MicMac on the HPC system and gave me a crash-course in using Linux.

Finally, thank you to Emma, Mum, Dad, Grandma, and all my dear friends for all the support and encouragement you've given me these past four years.

The Coleg Cymraeg Cenedlaethol and HPC Wales are gratefully acknowledged for financial support of this PhD.

I dedicate this work to the memory of Eilir Hedd Morgan, mentor and friend. Cysga'n dawel Eilir.

1 General introduction

Ecosystems around the globe face mounting pressures from anthropogenic activities that may cause catastrophic and permanent losses to ecosystem structure and functioning (Scheffer et al., 2012). Already, there are examples of ecosystems that have irreversibly changed through species extinction (Barnosky et al., 2011) and habitat loss (Vitousek, 1994). Ecosystem degradation is having a detrimental effect on human health and wellbeing (Myers et al., 2013), and efforts to restore degraded systems is met with limited success: only a third of ecosystem projects manage to fully restore ecological functioning to levels equivalent to those found in natural systems (Jones and Schmitz, 2009). As a consequence, there is a strong motivation for ecologists and resource managers to understand the causes and processes that lead to ecosystem collapse, and importantly, how to prevent them (Biggs et al., 2009). Identifying the biological mechanisms and physical processes that determine ecosystem resilience is an important step towards informing conservation policy and ecological theory about how best to protect the future of ecosystems in an anthropogenically dominated world (Walker, 1995; Thrush et al., 2009; Altieri et al., 2013).

This thesis adds to the discussion of ecosystem resilience by exploring how biological and physical processes interact across spatio-temporal scales to shape a potentially vulnerable ecosystem: the salt marsh. Section 1.1 documents the character, value and historical exploitation of saltmarsh ecosystems. Section 1.2 presents an overview of how saltmarsh change can be interpreted using the stable state and resilience frameworks. Section 1.3 reviews current understanding of the mechanistic causes for lateral saltmarsh erosion and expansion. Section 1.4 considers how processes of marsh change are influenced by larger-scale coastal dynamics. Section 1.5 summarises how patterns and drivers of lateral marsh change could be reconciled at different spatio-temporal scale domains. Section 1.6 sets out the aims and objectives of the thesis.

1.1 The saltmarsh ecosystem

Saltmarshes are formed by halophytic vegetation that colonise sheltered intertidal zones in temperate regions of the globe (Allen, 2000). The vegetation is organised in distinct zones from the sea to the land (Allen, 2000), from the creek bank to the marsh interior- (Kim et al., 2012; Kim et al., 2013) and with small-scale variation in marsh elevation (Belluco et al., 2006). Plant

zonation is largely due to the variable tolerance of species to sea-water inundation, salinity and hydrological disturbance (Allen, 2000). Feedbacks between environmental forcing and biological processes are responsible for the establishment and persistence of salt marshes, meaning marshes are considered classic examples of a biogeomorphic system (Murray et al., 2008). Marshes make up just under 5.5 million hectares of the global coastline (Mcowen et al., 2017) (Figure 1.1) and support diverse faunal communities including both marine and terrestrial invertebrates (Ford et al., 2013), fish (Shenker and Dean, 1979) and birds (Sharps et al., 2015).

The saltmarsh ecosystem is recognised globally for its importance in delivering a diverse range of natural goods and services to human societies (Costanza et al., 1997). Saltmarshes are an important store for 'blue carbon', accumulating an estimated 162 Mg of Carbon per hectare within the upper 1 m of soil (Duarte et al., 2013); this level exceeds the 123 Mg C ha^{-1} average of carbon stored by rainforests (Lal, 2005). Dense growth of stiff plants are effective at dissipating wave energy (Bouma et al., 2005; Möller et al., 2014) and so marshes protect coastlines from flooding during storm surges (Shepard et al., 2011; Spencer et al., 2015), with great potential savings on constructing artificial coastal flood defences. Thus, US marshes saved \$8,236 ha^{-1} yr^{-1} by reducing hurricane damages to coastlines (Costanza et al., 2008); in the 1990s in the UK, the wave dampening by an 80 m wide marsh would reduce construction cost of artificial coastal defences by \$8,000 per linear metre (King and Lester, 1995). Marshes are also important for agricultural production. In the UK, the value of saltmarsh lamb can be

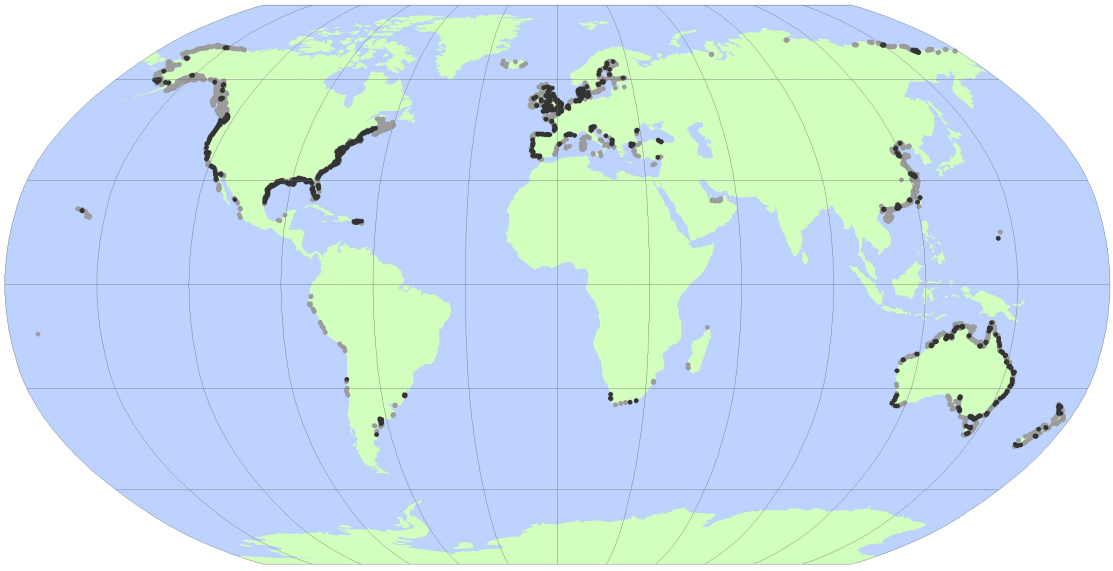

Figure 1.1 Distribution coastal (light grey) and estuarine (dark grey) salt marshes around the globe. Adapted from Mcowen et al. (2017).

~100% greater than terrestrially–reared meat (MEA, 2005). Salt marshes are effective at trapping heavy-metal and organic pollution (Bai et al., 2011) and they provide nursey grounds that sustain recreational fishing in South-east USA at an estimated value of US$6471/acre and $981/acre capitalized value (Bell, 1997).

Vast tracts of salt marsh have been embanked and drained for conversion to agricultural and urban land since human habitation of the coast began (Valiela et al., 2009; Hatvany et al., 2015; Jongepier et al., 2015). Salt marshes have also been extensively modified for commercial exploitation including salt pond creation for salt extraction, hay harvesting and turf stripping (Gedan et al., 2009). Similar changes have befallen other coastal systems, and direct human impact has collectively resulted in the loss of 67% of coastal wetlands across the globe (Lotze et al., 2006). There has been a recent paradigm shift in the attitudes towards saltmarsh management. Motivation for 'marsh conversion' has been replaced by 'marsh conservation' across much of the northern hemisphere (Hatvany et al., 2015). However, indirect effects of human activity are compounding already-vulnerable systems. Climate change is increasing the severity of storm flood damage to coastal ecosystems (Leonardi and Fagherazzi, 2015) and warmer mean annual air temperature is facilitating shifts in habitat from salt marshes to mangroves in sub-tropical to temperate regions of the world (Osland et al., 2016; Gabler et al., 2017). Sea-level rise is of particular concern when marshes are unable to retreat inland due to embanked coastline; a phenomenon known as coastal squeeze (Nicholls et al., 2007). There is considerable debate at present as to the capacity of global marshes to trap sediment and grow with sea level rise: estimates range from predicting high marsh resilience to sea level rise, to anticipating large-scale global losses in marsh cover (Crosby et al., 2016; Kirwan et al., 2016; Spencer et al., 2016). There is paucity in research on the global patterns of marsh change and, in particular, the mechanisms that drive spatio-temporal variation marsh cover. Lateral extent of marshes appears to be highly vulnerable to even moderate changes in mean sea level (Mariotti and Fagherazzi, 2013; Mariotti and Carr, 2014). Elevated rates of sea level rise have also been implicated as the cause for the widening and expansion of saltmarsh creek channel networks; sea level rise can increase the tidal prism, that lead to the internal dissection of marshes in sediment supply-limited systems (Hughes, 2012; Ganju et al., 2015). Coastal eutrophication through nutrient loading (Deegan et al., 2012), trophic cascades (Silliman et al., 2005; Altieri et al., 2013), and reductions in sediment flux to the coastline through land use change (Syvitski et al., 2005) and dredging (Cox et al., 2003) are also implicated in the degradation of plant health. Degraded vegetation can disrupt plant capacity to bind soils,

thereby accelerating erosion risks (Francalanci et al., 2013). The threat of continued direct human effects (e.g., land conversion) or indirect human effects (affecting natural coastal processes that impinge on marsh functioning) on marshes has stimulated the formation of ambitious legislative initiatives for the protection and restoration of marsh systems around the globe (Mcowen et al., 2017). In support of such action, calls have been made to better understand the mechanisms and drivers of saltmarsh dynamics (Bouma et al., 2014) and there is a growing attempt to understand how natural and human processes impact on the vulnerability of marsh systems and how these affect marsh resilience (Altieri et al., 2013; Angelini et al., 2016).

1.2 Salt marshes as an alternative stable state

Salt marshes exist at the interface between lower-elevation tidal flats and higher-elevation upland vegetation, separated by abrupt ecotones. Salt marshes, tidal flats and upland vegetation are all said to represent 'alternative stable states' of the coastal landscape. Any given state can be considered 'stable' when feedbacks between biological and environmental processes act to reinforce and maintain that particular state in the face of disturbance and environmental change (Petraitis, 2013). Ecosystems are said to be 'resilient' when they are able to maintain their ecological functioning (stable state) despite disturbance and environmental change (Holling, 1973). Resilience operates through ecosystems being able to resist change, being able to recover and/or being able to adapt to change (Francis and Bekera, 2014). A loss of resilience can result in a reconfiguration of the landscape. Resilience can be overcome by stochastic distance events, such as the partial or full transformation of vegetated saltmarsh into bare tidal flat caused by channel migration (Pringle, 1995). Resilience can also be overcome gradually, as a tipping point is reached, such as overcoming marsh ability to maintain optimum positions in the tidal frame with elevated sea level rise (Kirwan et al., 2010). A loss of resilience in one ecosystem can cause a shift to an alternative stable state (Scheffer et al., 2012). Shifts between alternative stable states can either signify serious environmental deterioration (Scheffer et al., 2001), or represent part of cyclical behaviour whereby landscapes periodically shifts between two or more states (Angeler et al., 2015). Shifts between saltmarshes and tidal flats have received particular attention, because erosion of salt marshes would negatively affect the ecosystem services they provide (Koch et al., 2009). In many cases, however, shifts between tidal flats and marshes are part of long-term cyclical patterns of change: periods of marsh dominance exchange with periods of tidal flat dominance over decades or centuries (Allen,

2000). Without longer-term and/or larger scale empirical observations, it may be difficult to evaluate whether patterns or periods of saltmarsh erosion are indicative of unidirectional environmental deterioration or simply part of a natural cyclical pattern of change. Thus, a precise understanding of the mechanisms that determine lateral marsh dynamics is key to interpreting coastal landscape change.

1.3 Saltmarsh lateral dynamics

1.3.1 Establishment of marshes onto the tidal flat

Establishment of marshes onto tidal flats requires stable sediments that are suitably elevated above the water column. Sediments are subject to high mobility due to tide/wave action, however the presence of extracellular polymeric substances (EPS) secreted by microorganisms and the presence of surficial biofilms act to reduce sediment erodibility (Malarkey et al., 2015). Stabilized sediments on the intertidal allow macroalgal turfs to develop onto the tidal flat, further stabilising and trapping sediments. Sediment biostabilisation can raise bed elevations (Allen, 2000) allowing pioneer marsh vegetation to develop and initiating the transition from tidal flat (loss of resilience) to salt marsh configuration (gain of resilience) (Wang and Temmerman, 2013).

The precise mechanism by which the regime shift from tidal flat to saltmarsh occur depends on whether pioneer marsh plants establish from horizontally-growing roots of already-established marsh platforms (Silinski et al., 2016), from rhizome fragments, or from seedling germination (Huiskes et al., 1995; Minchinton, 2006; Wolters et al., 2008). In order for pioneer marsh seedlings, such as *Salicornia europaea agg.* (henceforth *Salicornia*) and *Spartina anglica* (henceforth *Spartina*), to establish onto tidal flats, a series of prolonged and stochastic disturbance-free periods, known as 'Windows of Opportunity', are required: *i.* seeding establishment and rapid development a rootlet before the next tide to avoid floating away; *ii.* development of sufficiently long roots over ~3 days to avoid dislodgement from current- and wave exposure during inundation, and; *iii.* periods of low storm activity over months, allowing shoots to develop sufficient root growth to tolerate storm-induced elevation changes on the tidal flat (Wiehe, 1935; Balke et al., 2014; Hu et al., 2015a) (Figure 1.2). Over a period of hours to months, favourable conditions of plant growth need minimal environmental disturbance. If the disturbance is too great, plants will fail to establish, and the landscape remains in the tidal-flat state.

The likelihood of successful marsh establishment onto tidal flats is dependent on a range of biotic and abiotic controls. Biotic factors include: presence of macroalga, which prevent seeds being washed away and shelter seeds from extreme temperature fluctuations (Davy et al., 2001) or ensnare seedlings and tear from the ground as wrack floats away with the tide (Jensen and Jefferies, 1984); invertebrate bioturbation that dislodges seeds (Gerdol and Hughes, 1993; van Wesenbeeck et al., 2007); grazing on seeds and seedlings (Kiehl et al., 1996); and seed recruitment potential (Erfanzadeh et al., 2010). Physical factors include: salinity levels, water stress, anaerobic soils (which especially affects *Spartina* growth) and grain size (Hacker and Bertness, 1999; Marani et al., 2006). Other stressors are described in greater detail for *Salicornia* by Davy et al. (2001), and for *Spartina* by Goodman et al. (1969). For a given coastal location, the underlying biotic and environmental conditions are crucial in determining the likelihood of coastal areas shifting between marsh and tidal flat states (van Belzen et al., 2017).

Where conditions are favourable for pioneer plants to establish on the intertidal, *Salicornia* growth tends to be gregarious in colonisation (Davy et al., 2001), whilst *Spartina* plants can expand clonally to form circular tussocks that, under optimal conditions, can reach 3 m in diameter after 5 years (Hubbard, 1965) (Figure 1.3 a). The presence of vegetation on the tidal flat effectively trap sediments from the incoming tide (Li and Yang, 2009) and initiate the rapid conversion of 'tidal flat' to 'marsh' state (D'Alpaos, 2011).

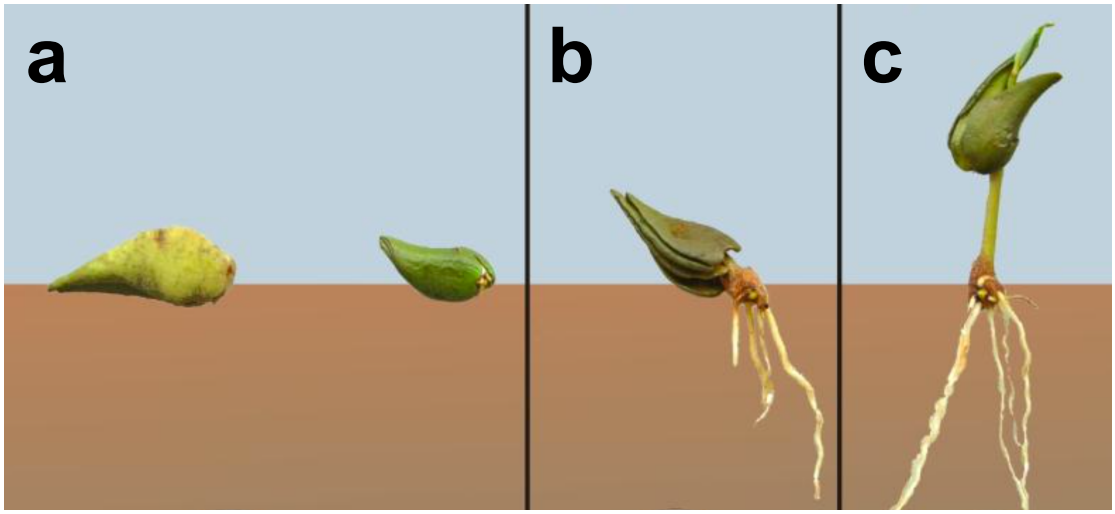

Figure 1.2 The establishment of a pioneer marsh seedling on a tidal flat. **a** During ebb tide, a seed deposited onto the tidal flat must rapidly develop a rootlet of sufficient length to avoid being floated away with the incoming tide. **b** The seed root must develop a sufficient length to resist wave and current action during spring tides. **c** The propagule root must grow sufficiently large to avoid dislodgement from storms and floods that destabilise the surrounding tidal flat. Adapted from Balke (2013).

Successful establishment of *Salicornia* onto the tidal flat can facilitate the colonisation of other, larger, plants that eventually outcompete *Salicornia* through shading (Ellison, 1987). Increased plant biomass increases the efficacy of sediment trapping, which in turn increases nutrient loading on the marsh and stimulates the growth of tall dense tussocks (Bouma et al., 2005). Sediment trapping and the incorporation of organic material into the soil raises tussocks higher in the water column, reducing inundation stress and further promoting plant growth. A positive feedback is thus initiated, whereby sediment capture promotes the ability of plants to trap more sediment. The positive feedback acts to reinforce marsh resilience (van Hulzen et al., 2007).

In *Spartina* marshes, the positive feedback is short-term. Large tussocks present an obstacle to current flow during tidal inundation, which causes scouring at the front and edges of tussocks to form a gully. Gully formation restricts further lateral expansion and makes the high-elevation edge vulnerable to wave and current action (van Wesenbeeck et al., 2008), often resulting in tussocks eroding away (Balke et al., 2012) (Figure 1.3 b). At the tidal-landscape scale, however, the formation of multiple tussock patches decreases overall incoming tidal energy through friction (Friess et al., 2012) thereby reducing gully scouring around tussocks. Tussocks closest to the land merge and form closed swards, whilst tussocks closest to the sea cycle through phases of formation and collapse (Figure 1.4 a) marking a distinct ecotone between salt marsh and tidal flat regimes (Figure 1.4 b). The localised action of plant growth on sediment trapping has a strong internal, bottom-up dynamic, responsible for moderating the local environment and allowing lateral marsh expansion across the tidal flat.

Actions of pioneer plant growth and favourable environmental conditions can trigger the threshold shift from tidal flat to salt marsh states (Wiehe, 1935; Balke et al., 2014). The now-

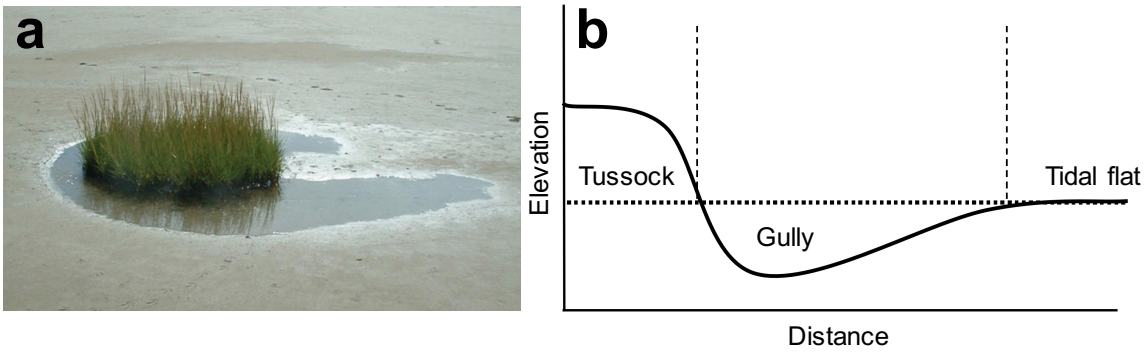

Figure 1.3 a Image of a *Spartina* tussock surrounded by a gully. **b** Cross-section representation of the high-elevation *Spartina* tussock and low-elevation gully relative to the surrounding tidal flat. Adapted from van Wesenbeeck et al. (2008).

established marsh surface rapidly accretes to mean sea level, and will continue to gain elevation, albeit at lower rates due to reduced inundation time of sediment-laden waters (French, 2006). The marsh surface can also grow vertically through autochthonous incorporation of plant material through below-ground growth (French, 2006), but at greatly reduced rates compared to external sediment import. As the elevation increases, marsh plant communities transition through pioneer, low, mid, high and transitional zones (Allen, 2000). In organogenic marshes where deposition is mostly autochthonous, plants may have the capacity to moderate rates of organic matter accumulation in the soil. Plants are therefore able to modify elevations relative to the tidal frame to suit their optimal growth ranges (Marani et al., 2013).

The combination of processes responsible for initiating marsh colonisation afford considerable resilience to salt marshes: algal turfs can prevent pioneer marsh seeds being washed away and shelter them from extreme temperature fluctuations (Davy et al., 2001); alga and plant growth physically trap sediments during tidal inundation, reducing inundation stress and promoting plant growth (van Hulzen et al., 2007). In more established marsh deposits, plants increase resilience through reducing soil anoxia and associated phytotoxicity by ventilating soils through root water uptake (Dacey and Howes, 1984), diffusing oxygen into the soil from plant tissues (Pezeshki, 2001), establishing permanently aerated soil layers (Marani et al., 2006), and

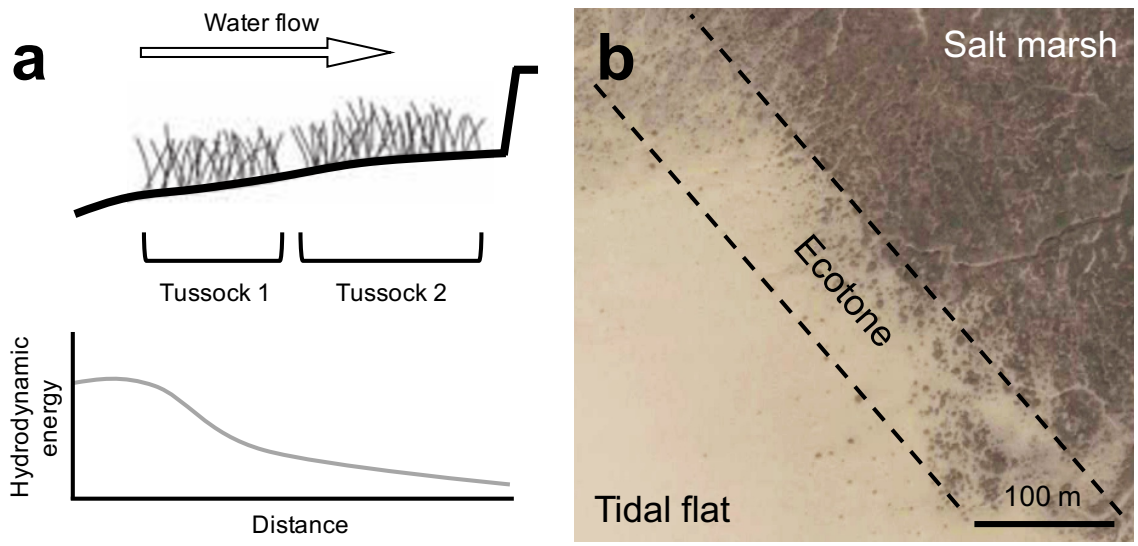

Figure 1.4 a Representation of *Spartina* tussocks developing on the tidal flat and reduction in hydrodynamic energy due to friction between the incoming tide and plant structure. **b** Across the coast, tussocks merge to form a closed sward at the top of the shore, whereas the interface between marsh and tidal flat persists as a patchwork ecotone of vegetated and bare ground where tussocks continually form and degrade. Adapted from Friess et al. (2012).

by growing alongside mussels that aerate the soil and improve plant growth (Angelini et al., 2016). Plant growth also enhances resilience by resisting soil erodibility through root binding and through the incorporation of cohesive organic matter into the soil (Ford et al., 2016). Collectively, the multitude of environment-modifying roles played by biota can provide an internal, 'bottom-up' dynamic to enhance salt marsh resilience.

1.3.2 Saltmarsh edge cyclical erosion and re-expansion

At the salt marsh-tidal flat interface, sediment trapping and organic incorporation into the soil creates small differences in elevation between the marsh edge and the tidal flat over time: above-ground plant growth of marshes traps sediments and dissipates wave/current energy (Bouma et al., 2005), whilst below-ground roots bind soils and resist erosion (Ford et al., 2016). The marsh can gradually grow vertically (van de Koppel et al., 2005). Meanwhile, the unstable tidal flat fluctuates in height relative to the tidal frame, driven by seasonal variation in wave/current energy (Bouma et al., 2016). Differences between the vertically-growing salt marsh and the seasonally fluctuating tidal flat directly in front of the marsh edge can give rise to a pronounced marsh cliff. The cliff becomes increasingly unstable as the elevation differences between the salt marsh and tidal flat grow (Mariotti and Fagherazzi, 2010) until a precarious stage is reached, where even benign wind waves and tidal current action can trigger a dramatic lateral marsh edge retreat (Callaghan et al., 2010). A catastrophic shift in ecosystem state from 'vegetated' salt marsh (state 2) to 'bare' tidal flat (state 1) can follow (Figure 1.5 a). The rate of marsh cliff erosion is typically an order of magnitude faster than the vertical accretion rates that led to the marsh cliff becoming unstable (van de Koppel et al., 2005; van der Wal et al., 2008). Plant-sediment interactions that operate at a local scale can undermine marsh resilience and trigger erosion (Rietkerk et al., 2004).

The release of sediment from lateral marsh erosion provides a local source for accretion immediately in front of the marsh edge. Once the elevation is sufficiently high to match the flooding tolerance of plants, and when hydrological disturbance levels are within plant tolerance levels, seedlings can germinate once more and the cycle of marsh expansion is reinitiated in front of the eroded cliff (van der Wal et al., 2008; Balke et al., 2014) (Figure 1.5 b). Cyclical phases of marsh erosion and expansion have long been documented as a natural phenomenon of saltmarsh lateral dynamics (Yapp et al., 1917; Jakobsen, 1954; van Straaten, 1954; Greensmith and Tucker, 1965; Allen, 2000; van de Koppel et al., 2005; Pedersen and

Bartholdy, 2007; van der Wal et al., 2008; Haslett and Allen, 2014). As well as representing an internal, bottom-up dynamic heavily influenced by plant growth (van de Koppel et al., 2005), saltmarsh cycles can also occur in response to the long-term fluctuations in sea level (Chauhan, 2009), or from alterations to tidal ebb-flood asymmetry due to embankment (Kestner, 1975).

Cycles of erosion and expansion, in some cases, have been described in the context of loss and gain of resilience: root-grazing crabs kill marsh plants and destabilise soils, which releases unconsolidated sediments that are both unsuitable for crab burrowing and promote plant recolonization (Altieri et al., 2013); waterlogging can kill plants and form low-elevation and expanding salt pans. The expanding pan eventually connects with a nearby creek, which ameliorates the conditions for plants through allowing tidal inundation to flush out toxins and aerate the soil, thereby facilitating rapid marsh recovery (Wilson et al., 2014; Mariotti, 2016).

1.3.3 Saltmarsh creek dynamics

As the marsh evolves on the intertidal, so does the marsh creek network. Creeks play an important functional role for supplying the inner marsh with sediment. Creeks are either 'inherited' from small deformations on the tidal flat around which plants establish (Friedrichs and Perry, 2001) (Figure 1.6 a), or develop from elaboration of the scour channels initially formed around tussocks (Temmerman et al., 2007) (Figure 1.6 b). Creeks can also be artificial (Pye and French, 1993a), having been excavated for a variety of reasons including to increase drainage and reduce mosquito breeding ground (Gedan et al., 2009), or enhance sedimentation around plants so they rapidly grow vertically and can be reclaimed (Ranwell, 1967). With every flood tide that overtops the marsh, suspended sediments are trapped by plants, so the

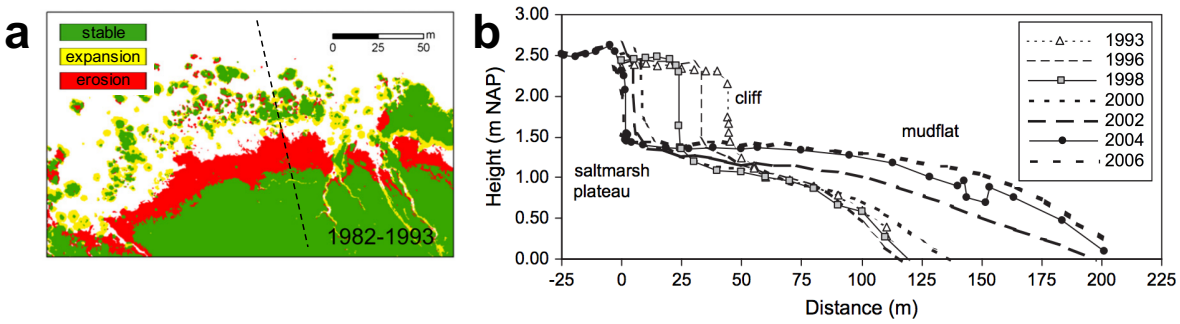

Figure 1.5 a Map showing regions of a coastline where marsh has expanded (yellow), eroded (red) and remained stable (green) between 1982 and 1993, and a transect (dashed line) showing **b** how a cross-section of the marsh has changed between 1993 and 2006 in Zuidgors marsh, Westerschelde estuary south-west Netherlands. Retreat of the marsh plateau by cliff erosion can release sediment that allows pioneer species to reestablish on the tidal flat. Adapted from van der Wal et al. (2008).

concentration of suspended sediment decreases with distance from a creek. Preferential deposition near the creek bank produces 'levees' (Temmerman et al., 2005). Over time, the levees move downslope due to gravity (Mariotti et al., 2016) and collapse into the creek as slump blocks (Gabet, 1998). Slump blocks armour creek banks and account for slow lateral migration rates typical of vegetated channel banks (Coco et al., 2013; Motta et al., 2014). A weakening of vegetation stabilisation can cause creeks to erode and widen in a process called internal dissection (Deegan et al., 2012). Increased tidal pumping along the creeks as a result of sea level rise can also cause creeks to widen (van der Wal and Pye, 2004). Channel widening can cause marsh loss (Ganju et al., 2017).

1.4 Coastal morphology on constraining marsh size

Patterns of natural saltmarsh expansion and decline operate within pre-defined physical boundaries at the terrestrial and seaward end of the marsh. At the terrestrial end, the boundary is usually at an intertidal level equating to the reach of the highest astronomical tides (HAT). Above HAT, marsh vegetation is competitively excluded by faster-growing, less salt-tolerant terrestrial plants (Traut, 2005). At the seaward limit the marsh boundary is usually set by plant physiological tolerance to tidal inundation frequency (Balke et al., 2016) and hydrological disturbance (Callaghan et al., 2010).

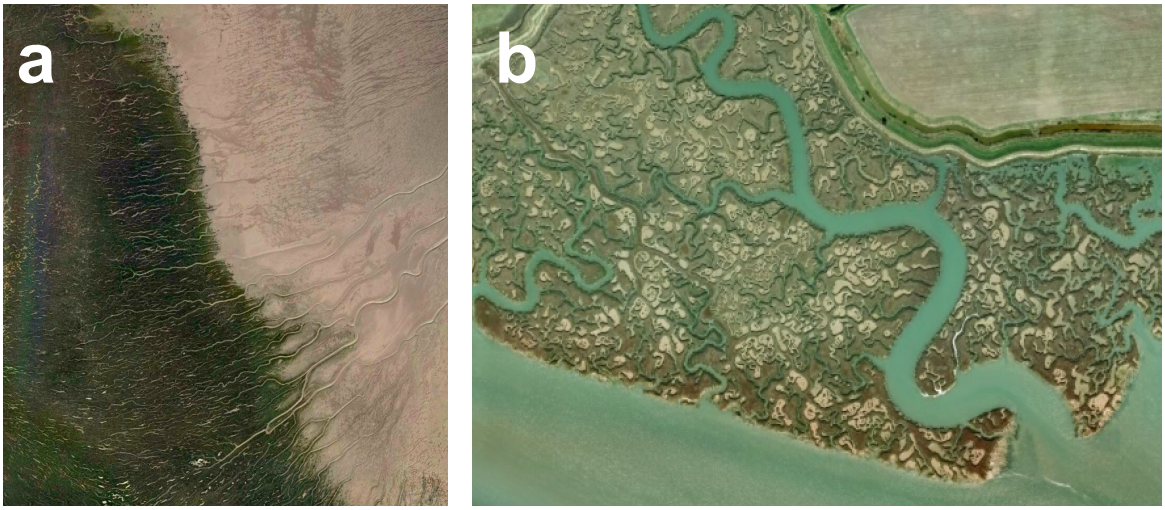

Figure 1.6 Saltmarsh creek networks emerge either through **a** the elaboration of gullies between plant patches to create straight channels perpendicular to the flow of tidal currents (Plaat van Valkenisse marsh, Scheldt estuary, southwest Netherlands), or **b** colonisation of plants onto an inherited dendritic tidal channel network already established on the tidal flat (Abbotts Hall marsh, Blackwater estuary, southern England).

The upper- and lower-limits of the marsh boundary are themselves subject to change over time. Chauhan (2009) describe how successive phases of cyclical marsh expansion and decline occurred as sea level fell across north-west UK during the Holocene; historical lower limits of marshes can be seen as abandoned cliffs in the marsh interior that leave a terraced topography on the marsh platform. Spatial or temporal variation in sea level changes the effective area over which marsh dynamics can occur. Sea level rise increases the accommodation space (the area available for sediment to be deposited) of estuaries and, provided there is a sufficient sediment source, enhances flood-driven transport and sediment infill. The rate of sediment infill declines as the estuary approaches a new dynamic equilibrium (Pethick, 1994; Dronkers, 2005). Estuarine infill raises tidal flat elevations upon which marshes can evolve (Beets and van der Spek, 2000) (Figure 1.7).

Shorter-term fluxes in sediment supply at the coast also occur in the absence of a varying sea level. In estuaries, strong asymmetric tides drive sediment fluxes over decadal timescales, with alternate cycles of flood-dominance (that import sediment) and ebb-dominance (that export sediment). As estuaries infill, tidal flats grow vertically and tidal channels become deeper. Deep channels can cause estuaries to switch from flood-dominance to ebb-dominance and lead to the erosion of tidal flats and sediment export from the estuary (Dronkers, 1986; Townend et al., 2007; Pye and Blott, 2014). As estuaries empty of sediment, the tide regime can flip again and become flood-dominant in a cyclical manner (Brown and Davies, 2010). Along the open coast, longshore drift controls the emergence and loss of back-barrier systems (Aagaard et al., 2004).

Modification of the foreshore size and profile in front of marshes influence the wave climate and inundation frequency at the marsh edge. As marshes erode, the released sediment can supply vertical growth (Ganju et al., 2017), or losses of salt marsh in one area can fuel marsh growth elsewhere in the sedimentary system (Pringle, 1995). Hydrological conditions at the marsh edge exert a strong control on whether conditions favour plant settlement or marsh cliff erosion (Marani et al., 2010; Bouma et al., 2014; Hu et al., 2015b) (Figure 1.7). Sediment transport is therefore critical in exerting a long-term control on the maximum extent that a marsh can attain (Marker, 1967; Moore et al., 2009; de Groot et al., 2011a). Sediment flux exerts an external, top-down forcing on lateral marsh dynamics.

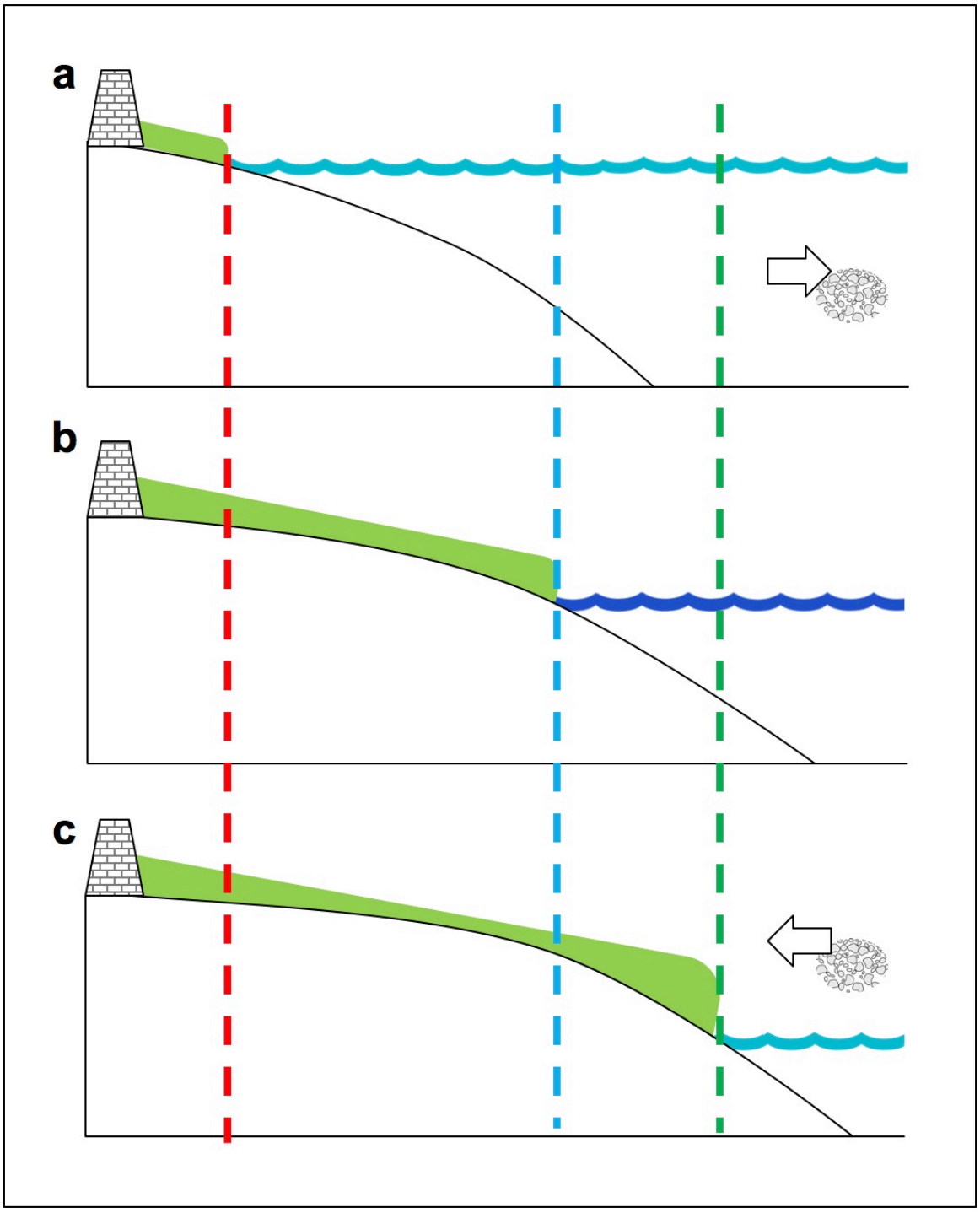

Figure 1.7 Representation of the effect of varying sea level rise and sediment transport on the size of the foreshore over which marshes can occupy, between a sea wall and mean sea level. **a** Either a rise in sea level rise or sediment export changes the hydrological energy reaching the coast and shortens the width over which marshes can expand, relative to **b**. **c** Sediment import and a fall in sea level can reduce hydrological stress and increase the area over which marshes can expand in relation to **b**.

1.5 Saltmarsh resilience and scale

The above review shows how marsh resilience depends on a complex interplay between plants, hydrology, and sedimentation. Internal, bottom-up dynamics of biotia on sediment control that influence marsh formation and stability are moderated by external, top-down forcing by environmental conditions. Saltmarshes therefore appear to sit as a biogeomorphic landscape between environmental and biological dominance. Plant-water-sediment interactions operate at an array of different physical and temporal scales; thus, the interpretation of observed patterns of lateral marsh change will be influence by the scale of study (selected examples in Table 1.1).

Considerable debate remains as to whether shifts in vegetation composition in a given location is best viewed as merely stages in the evolution of the landscape, or whether it represents a fundamental shift in environmental conditions (Phillips, 1995). Cowell and Thom (1994) identify four spatio-temporal dimensions that provide a framework for practically clustering observational patterns and causes of change in coastal morphodynamics (Figure 1.8; labelled boxes). When considering lateral marsh dynamics within this framework, patterns and drivers of change observed in any given dimension will often only inform future changes at that dimension (Table 1.1). For example, observations of the recovery phase of vegetation in front of an eroding marsh cliff (van der Wal et al., 2008) at the *event* scale may not be helpful for informing that marshes along a coastline are eroding due to changing wave exposure profile (Leonardi et al., 2016) at an *engineering* scale.

Table 1.1 Examples of the conclusions that can be reached about marsh resilience from three studies examining the patterns and drivers of lateral marsh change at different spatial-temporal scales.

Author	Space and time scale	Process	Conclusion
Angelini et al. (2016)	50 m over 10-20 years	Plant patches growing on mussel mounds can survive droughts. During wetter conditions, plants grow laterally through clonal expansion and facilitate marsh recovery.	Marshes are resilient
van der Wal et al. (2008)	1 km over 30 years	Marsh edge sedimentation produces a marsh cliff that is vulnerable to erosion. Once erosion is initiated, marsh debris protects from further erosion, elevates the fronting tidal flat, and reinitiates marsh growth in a cyclical fashion.	Marshes alternate between losing and gaining resilience.
Leonardi et al. (2016)	70 km over 83 years	Marsh edges are exposed to persistent erosion due to wave exposure maintained by a rising sea level.	Marshes are not resilient

Numerous studies extrapolate trends of lateral marsh change beyond the context set by the dimension their observations inform on (usually at instantaneous or event scales across engineering scales, e.g. van Wesenbeeck et al., 2008; Feagin et al., 2009; Wang and Temmerman, 2013; Kirwan et al., 2016), and patterns and drivers of lateral marsh change at the higher dimensions of *engineering* scale are poorly studied (e.g. Weston, 2014; Hu et al., 2015b; Jongepier et al., 2015). This thesis builds on the logic of the Cowell and Thom (1994) framework (Figure 1.8) to generate an understanding of the patterns and drivers of lateral marsh change at creeks (*instantaneous*), estuaries (*event*) and regions (*engineering*) scales. It is hypothesised that: lateral erosion of creeks by tidal current action is resisted by sediment

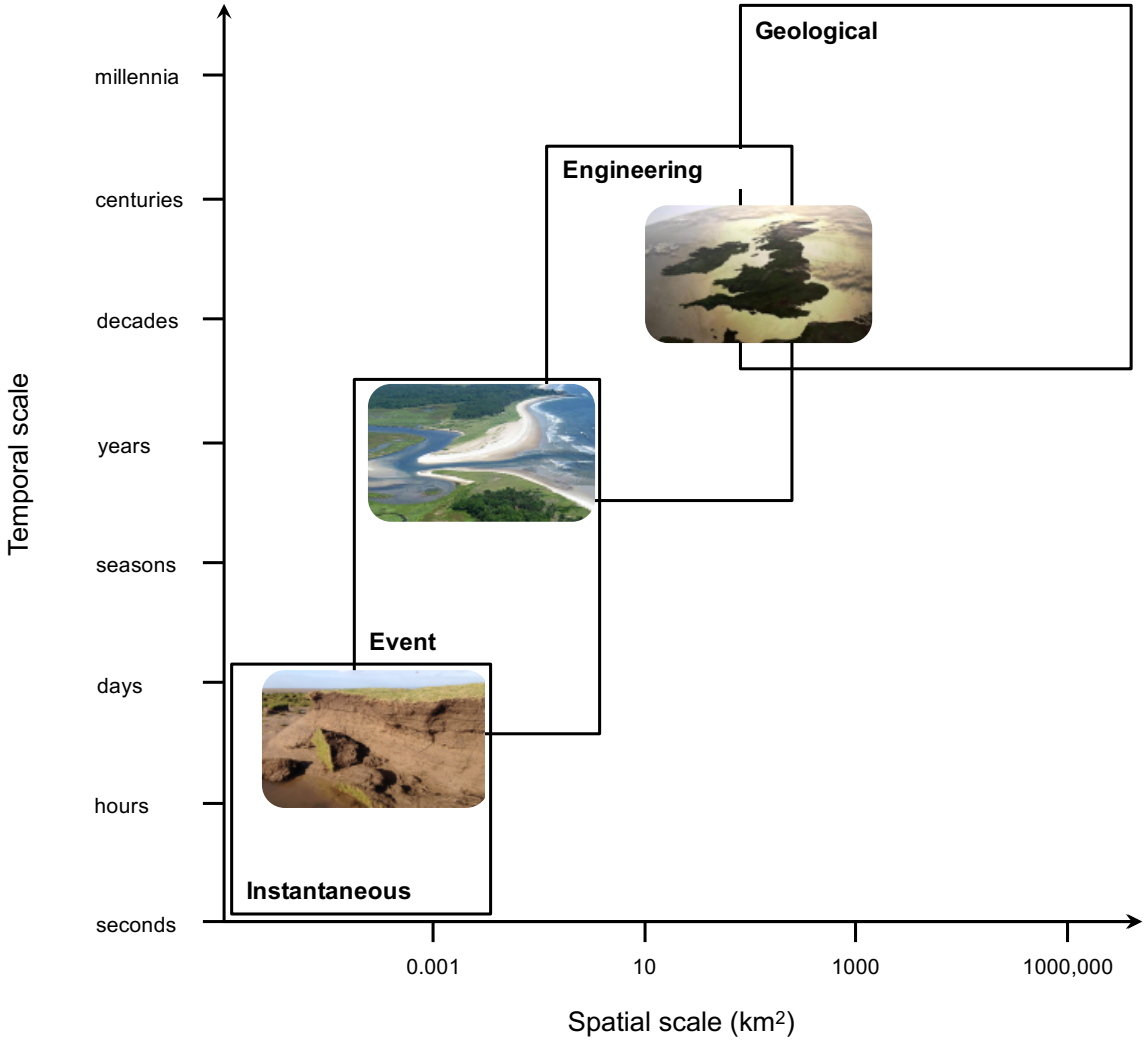

Figure 1.8 Conceptual plot of spatial and temporal scales involved in coastal evolution. *Instantaneous* scales capture morphological changes after wave/tide impacts over a single tidal cycle. *Event* scales represent morphological change across time spans ranging from that of a single event, such as a storm, through to seasonal variations in environmental conditions. *Engineering* scales involve multiple *events* that collectively shape coastal morphology. *Geological* scales represent millennial fluctuations in boundary conditions primarily driven by the effects of Milankovich cycles. Consideration of how lateral saltmarsh dynamics could be structured within this framework is demonstrated with pictures of a creek, estuary and region (Great Britain) within their respective scale domain, and explanation in the text. Adapted from Cowell and Thom (1994).

binding and trapping by plants (Figure 1.8; *instantaneous*); lateral marsh erosion by tidal channel migration is compensated for by expansion elsewhere in estuaries in a cyclical pattern (Figure 1.8; *event*); and, between-estuary variation in lateral marsh erosion and accretion is explained by sediment availability, which is in turn determined by variation in estuarine morphology (affecting tidal amplitude and asymmetric sediment flux) and climate (storm and flooding frequency) (Figure 1.8; *engineering/geological*). From this perspective, it is plausible that vegetation-associated processes are important regulators of marsh change at the *instantaneous* scale, whilst at *geological* scales, plant-derived processes have limited control and marsh change is more likely explained by large-scale physical processes, such as climate variability and variation in sediment sources at the coast. This thesis asks at what point can an observation of marsh change made in one dimension inform about changes operating at other dimensions? Do biotic processes associated with vegetation influence larger-scale lateral marsh dynamics?

1.6 Study aims and objectives

The aim of this study is to investigate the patterns and drivers of lateral change in estuarine saltmarshes of Great Britain, with a focus on three dimensional scales: saltmarsh creeks, estuaries and geographical region of the UK (Figure 1.8).

At each scale dimension, the study objectives are as follows:

i. The 'regional' scale (dimension *engineering/geological* in Figure 1.8) will be addressed in Chapter 2. Changes in saltmarsh areal extent will be captured from historical maps and aerial photographs at ~30-year intervals from 1848 to 2016, covering 25 estuaries in 6 geographical regions of Great Britain. The causes of areal extent change, specifically from the 1970s onwards, will be determined from climate data and process-measurements of estuarine properties;
ii. The 'estuary' scale (dimension *event* Figure 1.8) will be addressed in Chapter 3. Maps and aerial photographs will be used to capture change in the areal extent of individual marshes from 1848 to 2016, and positions of tidal channel change between 1946 and 2016 across 3 estuaries within Cardigan Bay, North-West Wales. The study examines the influence of tidal channel position, estuarine morphology and climate on the areal extent of marshes;

iii. The ‘creek’ scale (dimension *instantaneous* Figure 1.8) will be addressed in Chapter 4. Three-dimensional reconstructions captured monthly between October 2014 and October 2015 will be used to compare creek basin/bank erosion-accretion rates with slump block dissolution rates, for 30 five-metre transects in a salt marsh within Glaslyn-Dwyryd estuary of Cardigan Bay, North-West Wales. In turn, slump blocks erosion rates will be correlated with biotic (species richness, biomass, root content) and environmental (grain size, organic matter content) properties to determine whether biotic or environmental factors influence creek bank erosion.

The dissertation hypothesises that: $H_{1.1}$ the influence of biological factors on lateral marsh change weakens with increase in physical and temporal scales; and, conversely, $H_{1.2}$, the influence of physical processes on marsh lateral change strengthens with increase in spatio-temporal scales.

2 Identifying long-term drivers of saltmarsh lateral expansion and erosion

Cai J. T. Ladd[1], Mollie F. Duggan-Edwards[1], Tjeerd J. Bouma[2], Jordi F. Pagès[1], Martin W. Skov[1]

In review: Nature Communications

Summary

Global losses of salt marshes threaten valuable ecosystem services including natural coastal protection. Recent evidence shows marsh vertical growth can keep pace with relative sea level rise (RSLR). Yet, many sites undergo periodic and rapid changes in lateral extent, the causes of which lack common explanation. Here we show that long-term (150-year), large-scale patterns of lateral marsh change can be explained by interactions of RSLR (driving marsh loss) and sediment supply (countering loss). Marshes in Great Britain shifted from expanding to eroding in regions where sediment supply fell below threshold levels that enabled marsh growth to keep pace with RSLR. Human activity and extreme storm events could not explain the patterns of marsh change. The study provides long-term and large-scale confirmation that sediment supply is a critical regulator of marsh lateral erosion. Current global declines in sediment flux to the coast are likely to diminish the resilience of salt marshes and other sedimentary ecosystems to RSLR. Monitoring and managing suspended sediment supply is not common-place, but may be critical to mitigating coastal impacts from climate change.

[1]School of Ocean Sciences, Bangor University, Menai Bridge, LL57 4UN, UK, [2]Royal Netherlands Institute for Sea Research (NIOZ), Department of Estuarine and Delta Systems, and Utrecht University, P.O. Box 140, 4400 AC Yerseke, Netherlands.

Author contributions

C.J.T.L., J.F.P. and M.W.S. designed the observational study and statistical analyses. C.J.T.L. and M.F.D-E. collected and processed the saltmarsh extent data and C.J.T.L. collated and processed the monitoring data. C.J.T.L. wrote the initial manuscript. All authors contributed to and approved the final manuscript.

Notes

Changes have been made to the format of figure and table text, referencing style and appendices of the manuscript submitted to Nature Communications in order to match the style of this thesis.

2.1 Introduction

The threat of sea level rise has dominated theoretical and empirical saltmarsh research for more than thirty years, from concerns that over 90% of global marshes could drown by 2100 (Crosby et al., 2016). Recent results show the vertical growth of marshes is adept at keeping pace with sea level rise (Kirwan et al., 2010; Kirwan and Megonigal, 2013; Kirwan et al., 2016); an irony, given that fear of marsh loss by drowning has had an overriding influence on conservation policy since the 1970s (Hatvany et al., 2015). Despite the vertical resilience to sea level rise, there are many documented cases from Europe, North America and Asia where marshes have undergone extensive lateral changes in cover, expanding or eroding hundreds of meters in just a few years (Yang et al., 2001; Lotze et al., 2006; Gunnell et al., 2013). This study heeds the call to investigate the drivers causing lateral marsh change, shifting the current emphasis away from a predominant focus on vertical growth dynamics alone (Mariotti and Fagherazzi, 2010; Hu et al., 2015a; Bouma et al., 2016). The causes for lateral marsh change need to be understood if natural coastal protection by marshes is to be effectively managed (Temmerman et al., 2013; Bouma et al., 2014).

Salt marshes are comprised of halophytic plants the cover of which expands seaward onto bare tidal flats during disturbance-free periods (Balke et al., 2014). Seaward expansion is limited by plant tolerance to tidal inundation and the exposure to large waves and currents (Callaghan et al., 2010; Bouma et al., 2014; Hu et al., 2015a). Salt marshes are highly dynamic and changes in the physical environment drive cycles of marsh expansion and decline that can last over seasons (van Proosdij et al., 2006), decades (Haslett and Allen, 2014) or centuries (Chauhan, 2009). Cyclical changes in saltmarsh extent were first reported 100 years ago (Yapp et al., 1917) and several hypotheses have been posed to explain their causes (Cox et al., 2003; van de Koppel et al., 2005; Mariotti and Fagherazzi, 2010). Recent empirical evidence has shown that seasonal sediment flux on the tidal flat fronting the marsh edge can trigger longer-term periods of expansion or erosion (Bouma et al., 2016). During rough winter weather, wave erosion lowers the surface of the tidal flat, forming a marsh cliff vulnerable to wave attack (Callaghan et al., 2010; Mariotti and Fagherazzi, 2010; Bouma et al., 2016). In calmer spring/summer weather, sediment deposition onto the tidal flat increases the chance of seedling establishment and clonal expansion onto the foreshore (Bouma et al., 2016; Silinski et al., 2016; Cao et al., 2017). However, the further the marsh extends seaward the greater is the risk of marsh hydrological erosion and the poorer is the chance of successful plant colonisation (Bouma et

al., 2016). Thus, periods of marsh lateral expansion may eventually be countered by marsh erosion.

Climate change drives sea level rise and increases the severity of storm (Haigh et al., 2016), precipitation and flooding events (Christensen and Christensen, 2003), which collectively act to raise the water depths and wave/current erosion over tidal flats, thereby increasing the likelihood of initiating lateral marsh erosion (Mariotti and Fagherazzi, 2010; Mariotti and Carr, 2014; Hu et al., 2015c). Previous studies have indicated that sediment supply from marine or riverine sources can diminish this erosion risk when the replenishment of sediment is sufficiently large to cause tidal flats to elevate through accretion (Hoitink et al., 2003; Traini et al., 2015; Ganju et al., 2017). For example, marshes in the macrotidal Bay of Fundy, Canada, are resilient to erosion because new sources of sediment from ice rafting are transported to the saltmarsh edge by large-amplitude tides (van Proosdij et al., 2006). In contrast, marshes in the microtidal Venice Lagoon, Italy, are erosion prone due to low river sediment fluxes, as well as limited tide-driven sediment mobilisation and transport (Fagherazzi et al., 2013). Marsh change is also associated with human activity. Globally, land reclamation has reduced the extent of marshes (Gedan et al., 2009), while the introduction of invasive marsh building plants, *Spartina* species, has expanded marshes (Gedan et al., 2009). Large fluctuations in marsh cover have also been linked to changes in hydrology and sediment transport driven by coastal development and land-use change (Yang et al., 2001; Kirwan et al., 2011).

While numerical models have pioneered the mechanistic understanding of lateral marsh dynamics (Mariotti and Fagherazzi, 2010; Mariotti and Carr, 2014; Hu et al., 2015a), empirical evidence has lagged behind and been limited to isolated sites (Cox et al., 2003; Gunnell et al., 2013), or have been concerned with single explanatory drivers of change (Weston, 2014; Gabler et al., 2017). To address this gap, the following study asks which key climate drivers primarily explain large-scale, long-term lateral marsh change? The coastline of Great Britain was selected as a suitable large-scale study area, due to the availability of freely-accessible, long-term records of coastal change and climate data. The first objective of the study was to collate measures of marsh extent from maps and aerial photographs dating back 150 years for 25 estuaries across Great Britain. The second objective was to collate measures of vertical marsh accretion rates for the study sites from existing literature, and compare against rates of local sea level rise. The third objective was to collate empirical data on key environmental

drivers associated with marsh lateral change and compare to rate changes in lateral marsh expansion or erosion in each study estuary.

2.2 Methods

2.2.1 Study sites

Change in saltmarsh extent were examined across 25 estuaries and embayments located in 6 regions across Great Britain: the Solway, Morecambe and Cardigan regions located along the west coast, in the Irish Sea; and the Wash, Essex-Kent and Solent regions along the east/south-east, in the North Sea and English Channel (Figure 2.1). In total, these estuaries occupied 19,000 ha of salt marsh (~ 40% of the total marsh area in GB) (Phelan et al., 2011). Estuaries were shallow, generally well-mixed with semidiurnal meso- to macro-tidal ranges. Tidal asymmetry: flood-dominance were common along the west coast, Wash region and many of the Essex-Kent regions, whereas in the Solent region, all the estuaries were ebb dominant (Manning and Whitehouse, 2012). Typical estuary morphology ranged from bar-built to embayment/coastal plains (Pye and Blott, 2014). Relative sea level rise increased along an axis from the north-west to the south-east due to isostatic adjustment of the British Isles following deglaciation at the end of the Last Glacial Maximum (Bradley et al., 2009). Along a similar axis, tidal amplitude and estuary depth generally decreased, and sediment type changed from sand- to silt/clay-dominance (Goudie, 2013). All regions had historically undergone embankment works, with extensive stepwise reclamation in the Wash and the Essex-Kent regions (Davidson et al., 1991). Fluvial suspended sediment flux to the coastline was low for all regions (Worrall et al., 2013).

2.2.2 Lateral and vertical saltmarsh change

Saltmarsh area for the entirety of each estuary was quantified at approximately every 30 years between 1846 and 2016 using a combination of Ordnance Survey (OS) maps, aerial photographs and additional estimates taken from Cooper et al. (2001) and Baily and Pearson (2007) for the Essex-Kent and Solent regions respectively. OS maps were accessed via the EDINA Digimap Resource Centre. Dates when maps were surveyed were taken from Oliver (2013) as the timestamp. For the Cardigan regions, aerial photographs were taken from the Royal Commission on Ancient Historical Monuments Wales. Photographs were scanned and georeferenced onto OS 1:25,000 rasters in the British National Grid projection. Pixel size corresponded to ca. 0.25 × 0.25 m in the field. Marsh extent from OS maps and aerial

photographs were delineated manually at a scale of 1:7,500 by placing vertices along the marsh edge approximately every 5 m.

In all cases, embankments represented the landward extent of the salt marsh and were easily defined. To account for boundary precision of the seaward marsh edge, visual comparisons

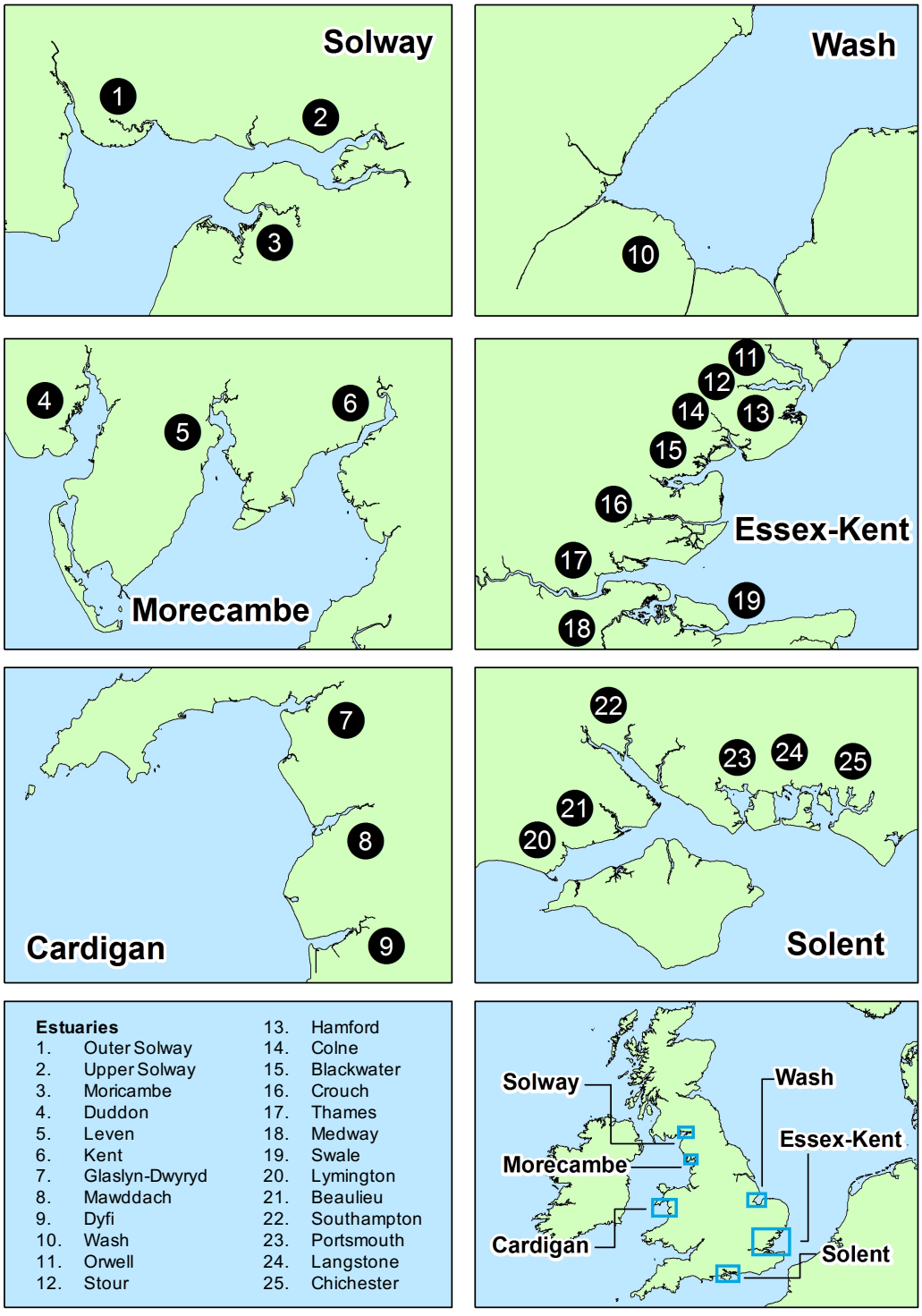

Figure 2.1 Estuaries examined within each region**.** A total of 25 estuaries separted into 6 regions across Great Britain.

between the georeferenced images and a reference shapefile (see Phelan et al., 2011) was done to ensure accuracy of the georeferencing procedure. The chronometric accuracy of successive OS map revisions also had to be considered (Baily and Inkpen, 2013). Maps where successive revisions showed no change in marsh extent were disregarded, on the assumption that the revisions were only partial and did not resurvey the marsh (Appendix I). A search for site-specific literature was done to verify whether observations of significant change in marsh extent could be considered 'real', or were likely caused by differences in map surveyors' interpretation of where the marsh edge lay (Appendix III). In the case of the Wash, large areas of marshland were reclaimed during the study period. To account for this, the area of reclaimed land was calculated, then subtracted from the marsh extent in the previous map revision and included this value as an additional measurement of marsh area between map revisions. Methods used to calculate an error term for each measure of marsh area is described in Appendix I. A linear rate of saltmarsh change per year was calculated for each estuary and used as the response variable in statistical modelling. Due to the non-linear change of marshes in the Wash region, an average rate of marsh change was calculated from rate changes following each reclamation phase. Rates of marsh change, and the dates over which this rate was taken, are shown in Table 2.1. Observed rates of lateral marsh change were compared against published empirical measurements of vertical accretion on the saltmarsh surface on the same sites. All accretion rates were measured near the marsh low intertidal edge using a range of techniques including Caesium radio-isotope dating, Sediment Elevation Tables and Marker Horizons (see references in Table 2.3). Differential in vertical accretion versus rate of sea level rise was calculated to determine whether accretion was positive (vertical accretion > relative sea level rise) or negative (vertical accretion < relative sea level rise). Dates over which accretion rates were taken are shown in Table 2.1.

2.2.3 Predictor variables

For each estuary, data was collated on key hydrological, sedimentological and climatological variables known to structure saltmarsh extent within estuaries. Records of key predictor variables were insufficiently regular or absent for the entire 1846-2016 period. Consequently, considerations of lateral marsh change were constrained to the period between 1970 and 2016. Temporally- and spatially-averaged estimates of estuarine suspended sediment concentration (SSC_E; described in more detail below) were taken from Manning and Whitehouse (2012). Estimated bedload sediment flux volume (in or out of the estuary) were taken from Bray et al.

(1991), HR Wallingford et al. (2002), Brown and Davies (2010) and Halcrow (2010). Due to differences in the precision of modelled bedload sediment flux estimates between studies, all values were rounded to their nearest 10^{th} value, representing a magnitude flux either into (positive) or out (negative) of the estuary at the estuary mouth. Estimates of relative sea level rise (RSLR) were taken from the UK Climate Projections (UKCP09) User Interface (Lowe et al., 2009) for baseline changes between 1990 and 2016 under a 'low' CO_2 emissions scenario, with 50% percentile for each estuary at a resolution of approximately 0.9°. UKCP09 data was chosen over conventional tide gauge data because of limitations in the ability to calculate RSLR from short timeseries, as is the case for a number of sites across Great Britain (Woodworth and Player, 2003). Frequency of storm events were calculated using daily averaged wind speed data from the UK Met Office Integrated Data Archive System (Met Office, 2013). Stations were selected based on their proximity to each estuary. The temporal range for each station varied considerably, although at most limited to between 1957 and 2016. As a consequence, some stations nearby had low number of samples and were rejected for further analysis. The final representation of stations was limited to one per region, and storm events recorded by that station were assumed to be representative of all estuaries for the respective region. Prior to analysis, wind speed data was screened for quality and completeness (see Watson et al. (2015) for method). Frequency of storm events were then estimated from annual datasets as a count above an absolute threshold of 23 ms^{-1} ('strong gale' on the Beaufort scale), and rate of change in number of events per year was used in the statistical analysis. Rate change in river flood frequency events were calculated using number of Peaks-Over-Threshold per water year data provided by the National River Flow Archive (Robson and Reed, 1999).

Predictor variables, and the timescale over which they were measured, are noted in Table 2.1. Measurements of RSLR, taken from UKCP (Lowe et al., 2009), did not extend back in time beyond 1990. However, rate change in mean sea level has remained relatively constant since 1901 across the UK, with the exception of some interannual variability (Woodworth et al., 2009). UKCP estimates of RSLR were therefore considered appropriate for comparing against marsh extent change from the 1970s onwards. Process measurements of bedload sediment flux and suspended sediment concentrations were based on parameters of estuary shape, size and hydrological regime taken between 2000-2010. Changes in bedload sediment fluxes are considered stable under current rates of sea level rise (Halcrow, 2010). Sediment sources or sinks are also expected to persist between 500 and 2000 years across the UK (HR Wallingford,

Table 2.1 Site characteristics for all 25 estuaries divided into 6 regions. Parentheses indicate the timescales over which rates were measured, or in which empirical data was used to derive values. These dates are representative of either the entire Great Britain, a whole region, or a specific estuary.

	Lateral expansion (ha/yr)	Vertical accretion (mm/yr) ± S.D.	Relative sea level rise (mm/yr)	Suspended sediment conc. (mg/l)
			(1990-2015)	(2000)
Solway	(1970-2016)	(1961)		
Outer Solway	0.14	21.43 ± 10.56	1.60	404.22
Upper Solway	2.22	11.79 ± 18.12	1.60	404.22
Moricambe	0.27	25.40 ± 0.00	1.60	404.22
Morecambe	(1967-2010)			
Duddon	2.84	NA	2.00	291.49
Leven	3.35	NA	2.00	313.42
Kent	2.62	NA	2.00	313.42
Cardigan	(1969-2013)			
Glaslyn-Dwyryd	1.56	NA	2.40	89.37
Mawddach	1.48	NA	2.40	NA
Dyfi	3.89	10.29 ± 4.06 (1988-1989)	2.40	111.03
Wash	(1972-2016)			
Wash	1.27	48.00 ± 26.87 (1956-1962)	2.80	295.97
Essex-Kent	(1973-1998)			
Orwell	-1.85	NA	2.80	64.46
Stour	-6.39	NA	2.80	64.46
Hamford	-9.98	NA	2.80	59.51
Colne	-3.81	NA	2.80	78.69
Blackwater	-7.99	4.84 ± 5.00 (1963-1998)	2.80	122.68
Crouch	-6.50	6.70 ± 0.00 (1897-1994)	2.80	106.40
Thames	-3.93	3.93 ± 1.38 (1963-1998)	2.80	NA
Medway	-13.22	4.05 ± 2.05 (1989)	2.80	86.05
Swale	-4.11	NA	2.80	NA
Solent	(1971-2001)			
Lymington	-4.86	5.2 ± 0.00 (1893-1995)	2.80	42.54
Beaulieu	-2.44	3.3 ± 0.00 (1893-1995)	2.80	54.12
Southampton	-4.31	4.8 ± 0.14 (1870-1995)	2.80	102.87
Portsmouth	-2.72	NA	2.80	83.39
Langstone	-1.45	1.5 ± 0.00 (1907-1995)	2.80	79.57
Chichester	-5.77	NA	2.80	78.56

Table 2.1 continued.

	Bedload sediment flux (m^3/yr)	Wind storm frequency (n/yr)	River flood frequency (n/yr)	Unvegetated/ vegetated marsh ratio
				(*2006-2009*)
Solway	(*2010*)	(*1961-2008*)		
Outer Solway	10,000,000	0.02	1.34 (*1979-2014*)	0.020
Upper Solway	100,000	0.02	-1.36 (*1963-2014*)	0.032
Moricambe	0	0.02	0.00	0.057
Morecambe	(*2010*)	(*1957-2015*)		
Duddon	10,000	0.01	0.79 (*1968-2014*)	0.138
Leven	1,000,000	-0.15	0.44 (*1939-2014*)	0.182
Kent	10,000,000	-0.15	0.28 (*1968-2014*)	0.092
Cardigan	(2010)	(*1957-2015*)		
Glaslyn-Dwyryd	NA	0.09	0.34 (*1961-2014*)	0.138
Mawddach	NA	0.09	NA	0.203
Dyfi	-1,000,000	0.09	0.02 (*1962-2013*)	0.106
Wash	(*2002*)	(*1969-2015*)		
Wash	10,000,000	-0.01	0.04 (*1939-1996*)	0.085
Essex-Kent	(*2002*)	(*1957-2015*)		
Orwell	10,000	0.04	0.11 (*1964-1996*)	0.387
Stour	10,000	0.04	-0.13 (*1928-1992*)	0.403
Hamford	1,000	0.04	0.00	0.985
Colne	10,000	0.04	0.07 (*1959-2014*)	0.315
Blackwater	10,000	0.04	0.10 (*1932-1968*)	0.616
Crouch	1,000,000	-0.50	0.21 (*1976-2014*)	0.397
Thames	-1,000,000	-0.50	0.27 (*1883-2014*)	0.492
Medway	100,000	-0.13	-0.02 (*1956-2014*)	0.420
Swale	10,000	-0.13	0.00	0.353
Solent	(*1998*)	(*1957-2015*)		
Lymington	0	0.06	0.57 (*1960-2014*)	0.539
Beaulieu	0	0.06	NA	0.644
Southampton	10,000	0.06	0.05 (*1972-2014*)	0.492
Portsmouth	1,000	0.06	0.26 (*1951-2014*)	2.138
Langstone	1,000	0.06	0.11 (*1979-2014*)	1.131
Chichester	1,000	0.06	0.04 (*1967-2014*)	1.070

2017). SSC_E measurements are sensitive to change in tidal range (see section 2.2.4). Pelling and Green (2014) demonstrate how increases in sea level by 1,000 mm resulted in little response from the tides. For present rates of sea level rise and current tidal ranges, both bedload sediment fluxes and SSC_E process measurements are considered representative for the duration of the study period between 1970 and 2016. Timescales over which vertical marsh accretion rates were calculated extended beyond the scope of the study in some cases as far back as 1870 where isotope dating was used (notably in the Solent and Essex-Kent regions). Given that rates of sea level rise have remained constant over the time period, vertical accretion rates were considered comparable to lateral rates of marsh change. The analysis also considered the influences of introductions of the marsh-building plant *Spartina spp.* Dates of *Spartina spp.* colonisation were taken from Goodman et al. (1959), Hubbard and Stebbings (1967) and Harwood and Scott (1999). The analysis also considered the influences of significant construction events. Information on coastal engineering works were taken from Marshall (1962), Kestner (1962) and Burd (1992) for the Solway, Wash and Essex-Kent regions respectively.

2.2.4 Quantifying suspended sediment concentration

Estuarine maximum static time- and depth-averaged fine cohesive suspended sediment concentration (SSC_E) was obtained from the EstProc-Defra database (see Manning and Whitehouse, 2012), which used an analytically-derived solution from Manning and Whitehouse (2012), quantified by:

$$SSC_E = \frac{\frac{1}{2}\gamma\rho f {U_A}^2}{D_A \alpha} \quad (1)$$

$$\alpha = \frac{0.7\ {W_S}^2}{K_Z} \quad (2)$$

$$K_Z = f U_A D_A \quad (3)$$

where:

γ is a sediment erosion rate coefficient;

ρ is a water density coefficient;

f is a bed friction coefficient;

α is the half-life of coarse cohesive sediments in suspension;

U_A is the analytically-derived average tidal current amplitude over a tidal cycle;

D_A is the analytically-derived average estuary depth over a tidal cycle;

W_S^2 is the time- and depth-averaged particle settling velocity; and

K_Z is the eddy diffusivity

Combining equations (1), (2) and (3) gives:

$$SSC_E = \frac{\frac{1}{2}\gamma\rho f^2 {U_A}^3 D_A}{0.7\,{W_S}^2} \qquad (4)$$

Equations (1) and (4) represent a simple description of sediment dynamics based on the assumption of a balance between sediment erosion and deposition, represented as:

$$SSC_E D_A \alpha = \frac{\gamma\rho f {U_A}^2}{2} \qquad (5)$$

Estuary depth, D_A, and tidal current amplitude, U_A, are simplified representations of estuarine morphology from direct observations of each study estuary (Manning and Whitehouse, 2012). The sediment erosion rate coefficient, γ, and the time- and depth-averaged particle settling velocity, W_S^2, are empirical observations defined from a large-scale study of coastal suspended sediments from the Holderness coastline (Prandle et al., 2001), given as ~0.0001 and 0.001 ms^{-1} respectively. The bed friction coefficient, f, was also empirically-derived by observation of erosion rate from UK estuaries, taken as ~0.002 (Prandle, 2003). Root mean square value of the tidal current amplitude was taken in order to represent mean amplitude. Tidal current amplitude was raised to the power 2 to exceed shear stress of the sediment, initiating seabed erosion (Lavelle et al., 1984; Prandle, 2003). Validation studies show SSC_E predictions fit empirical values of SSC in British estuaries (Prandle et al., 2005). The assumptions used to estimate SSC_E are that estuaries are shallow (< 40 m), strongly tidal, funnel-shaped and with plenty of sediment to be mobilised from the bed or from external sources. All estuaries used in

the study had average mean depths between 1.9 and 12.1 m, are meso- to macro-tidal with ranges between 1.56 and 6.36 m, and satisfy the estuarine 'funnel-shape' criteria requisite for calculating SSC_E (Prandle, 2004). In Great Britain, estuarine sediment input from fluvial sources was only regionally important in the south-east (Odd and Murphy, 1992), and flux to the coast across Britain did not significantly change since 1974 (Worrall et al., 2013). The marine environment was the dominant source of fine sediments to British estuaries: in the west, strong tidal currents caused upwelling and transport of fine sediments to the coastline (Halcrow, 2010); in the east, tidal currents transported eroded cliff deposits to the Wash (HR Wallingford et al., 2002) and Greater Thames area and therefore Essex-Kent coastline (HR Wallingford et al., 2002). Localised cliff erosion and dissipation of dredged materials also supplied estuaries along the Essex-Kent coastline (HR Wallingford et al., 2002) and the English Channel (Bray et al., 2017) with fine sediment. Consequently, estuaries in the study region satisfy the level of sediment supply required for calculating SSC_E (Prandle, 2004). Saltmarsh erosion can elevate SSC in some localities, in which case time-averaged SSC calculations over-estimate external sediment supply available to marshes (Ganju et al., 2015). For such cases, recent work has shown that the unvegetated/vegetated ratio (UVVR) within a given marsh complex is a better proxy for external sediment supply (Ganju et al., 2017). UVVR was calculated for each study estuary and the statistical analysis described below was repeated; once using UVVR and once using SSC_E. The two analyses reached the same conclusions (Appendix II); UVVR and SSC_E were strongly correlated (Adj. $R^2 = 0.69$), indicating SSC_E was not inflated in estuaries characterised by net marsh erosion. SSC_E therefore appeared to be a reliable estimator of external sediment supply for the study marshes.

2.2.5 Statistical treatment

All statistical analyses were implemented in R. Predictor variables were cube-transformed to meet assumptions of normality and equal variance. Predictor variables RSLR and SSC_E were found to be highly collinear (VIF>10), therefore a Partial Least Squares Regression (PLSR) model (Carrascal et al., 2009) using the software package 'pls' (Mevik et al., 2016) was used to identify which combination of predictor variables provided the highest relative importance in explaining variance in Y. To validate findings from the PLSR model, two separate Linear Regression models were built, excluding each covariate in turn, to identify which suite of variables best explained rate of marsh change. Prior to running the models, all model assumptions were tested. To identify groupings across the study sites, pairwise Euclidean

distances were calculated between all 25 estuaries and identified six clearly defined regions (Figure 2.1). 'Region' was used as a random variable to test for spatial autocorrelation, however no significant effect was found. A Stepwise Linear Regression model was therefore used to select the minimal adequate model. A One-Way ANOVA with post-hoc analysis was used to identify significant differences between regions in rates of marsh change and predictor variables using the software package 'multcomp' (Hothorn et al., 2016). For further details on the full statistical analysis, refer to Appendix IV.

2.3 Results

2.3.1 Patterns of regional marsh change

Between 1856 and 2016, five of the six regions increased in marsh cover by 29% to 158% between 1846 and 2016 (Figure 2.2 a-e, h) and marshes overall expanded by 11%. South-east

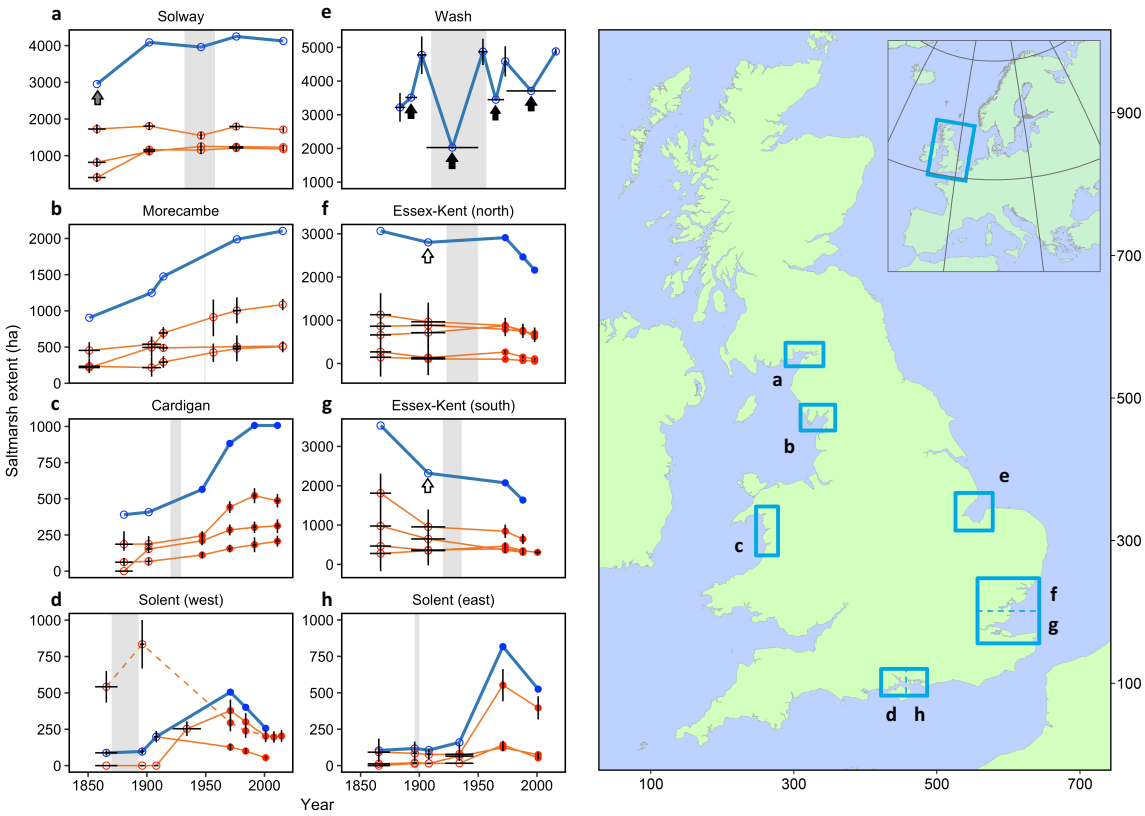

Figure 2.2 Change in estuarine-scale marsh extent across Great Britain. Regional- (blue line) and estuarine-scale (orange line) change in areal extent of salt marshes between 1856 and 2016 from photographs (filled circles) or maps (hollow circles). Arrows indicate occurrences of embankment (solid arrow), canalisation (grey arrow) or natural de-embankment (hollow arrow). Grey shading indicates *Spartina spp.* colonisation in each region. Vertical error bars indicate 95% confidence intervals in marsh area extent. Horizontal lines indicate the dates over which surveys of marsh extent were carried out. Essex-Kent and Solent regions have been subdivided for ease of presentation. Regional-scale marsh change (blue line) only includes marsh extent measures for all estuary in a given region and year. Marsh change in Southampton estuary (panel d: dashed line) was excluded from the regional-scale marsh change line due to paucity of contiguous cover in saltmarsh extent across multiple years.

Britain was the only region to consistently lose marsh cover (Figure 2.2 f-g). The largest lateral expansion occurred in the south, where Solent marshes had grown 307% by the 1970s before declining to their current levels, 29% greater than in 1868 (Figure 2.2 d, h). The north-eastern Wash region lost large areas of salt marsh on four occasions due to land reclamation (Figure 2.2 e; arrows); however, new marshes always expanded laterally on the seaward side of embankments, leading to a 52% overall increase in marsh area. In estuaries where marsh areal extent had been increasing, trends of marsh expansion generally preceded the arrival of *Spartina* (Figure 2.2 a-c, e; grey shading), with the exception of the Solent region, where marsh expansion was recorded after *Spartina* invasion (Figure 2.2 d, h; grey shading). Estuaries where significant canalisation work (Figure 2.2 a) and land reclamation (Figure 2.2 e) occurred were followed by net marsh expansion. Eroding marshes of the Essex-Kent region saw a prolonged period of little marsh change between 1900 and 1970, during which the presence of *Spartina* was first recorded, and several de-embankment events occurred (Figure 2.2 f-g). From 1970 onwards, the trend of marsh decline continued. All marshes were found to be accreting above the rate of local sea level rise (Table 2.3; parameter VA-RSLR).

2.3.2 Drivers of regional marsh change

For the period between 1970 and 2016, relative sea level rise and estimated suspended sediment concentration in combination best explained (26% of variation) the rate of marsh lateral changes in estuaries across Great Britain (Table 2.2). Marsh expansion had a positive linear relationship with SSC_E, and a negative linear relationship with RSLR (Table 2.2). The impact of these key predictors on saltmarsh change can be understood on a map of Great Britain (Figure 2.2): moving from the north-west to the south-east, RSLR increases whilst SSC_E decreases (Figure 2.3 a-b). Across this gradient, marshes expanded in the north-west, and eroded in the south-east, (Figure 2.3 c). Marsh behaviour shifted from eroding to expanding

Table 2.2 Model results for key drivers of estuarine-scale marsh change. Partial Least Squares Regression (PLSR) results showing Regression coefficients (RC), Variable Importance in the Projection (VIP) and loading weights (first component) for each predictor variable that best explained rate of saltmarsh change between 1970 and 2016. Bold numerical values show VIP > 1 combined with loading weights > 0.3 to indicate relative importance and main loading in the PLSR model.

Predictor variables	RC	VIP	Loading weights (comp 1)
Percentage variance explained in rate of marsh change = 25.80%			
Suspended sediment concentration	1.46	**1.476**	**0.660**
Relative sea level rise rate	-1.45	**1.459**	**-0.653**
Bedload sediment flux	0.76	0.762	0.341
Wind storm frequency rate	0.28	0.282	0.126
River flood frequency rate	0.18	0.184	-

when SSC_E increased and RSLR concurrently decreased (Figure 2.3 d). Bedload sediment flux and change in the frequency of wind storm and river flood events accounted for little variation in marsh lateral change and did not contribute to the explanatory model (Table 2.2).

2.4 Discussion

2.4.1 Marsh change trends between 1846 and 2016

Over the past 150 years, the study found a stronger tendency for seaward lateral marsh expansion than of marsh erosion in estuaries across Great Britain. Lateral marsh expansion has been attributed to the invasion of *Spartina spp.* or following land reclamation along other coastlines. *Spartina* can colonise lower on the intertidal than other marsh plants, leading to net marsh expansion where they successfully invade (An et al., 2007). Land reclamation can temporarily reduce flood-duration of tides, driving sediment deposition in front of the embankment if a plentiful nearshore sediment source exists (Kestner, 1975). The higher-

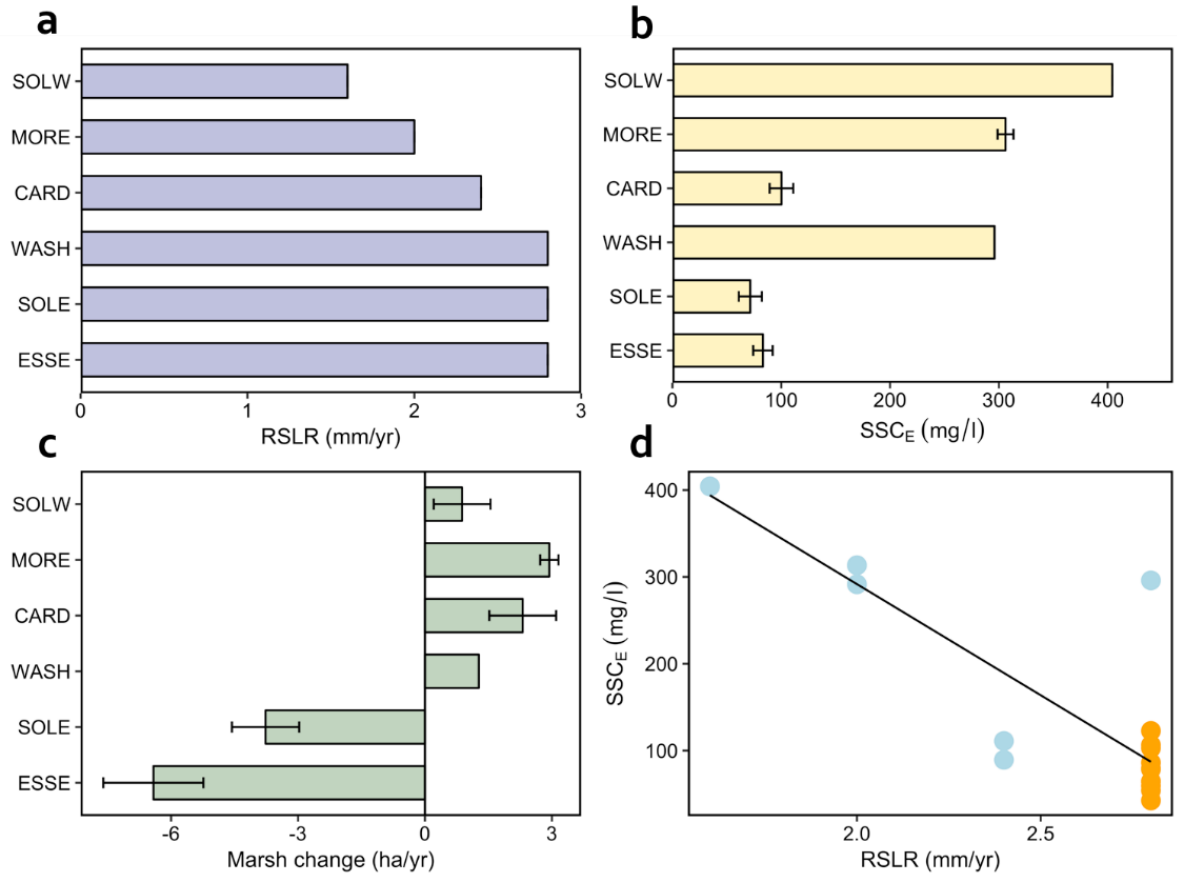

Figure 2.3 Relationships in key drivers of estuarine- and regional-scale marsh change. Mean ± S.E values per region for **a** rate of relative sea level rise (RSLR) between 1990 and 2015; **b** estimated estuarine suspended sediment concentration (SSC_E) in 2000; and **c** rate of marsh change between 1969 and 2016. Regions were, from north-west to south-east GB: Solway (SOLW), Morecambe (MORE), Cardigan (CARD), the Wash, Solent (SOLE) and Essex-Kent (ESSE). **d** Relationship between RSLR and SSC_E for all estuaries, coloured by whether marshes expanded (blue) or eroded (orange).

elevation tidal flat can then become colonised by marsh plants, and expand seaward until a new dynamic equilibrium is reached (Jongepier et al., 2015).

In the Solway and Wash regions, marshes expanded after significant phases of construction at the coast had occurred. Sediment supply in these estuaries therefore appear to be plentiful, allowing marshes to expand. Marshes in Solway, Morecambe and Cardigan regions along the west-coast of GB appeared to be expanding prior to the invasion of *Spartina*. Although *Spartina* likely quickened the rate of marsh expansion in some estuaries like the Cardigan region (Chater and Jones, 1957), colonisation alone does not appear to explain long-term marsh change in the region. Marshes in the Solent region expanded after *Spartina* was introduced into the estuary. *Spartina* colonisation had been particularly successful in the estuaries in the Solent region (Hubbard, 1965; Gray et al., 1991) and now make up the dominant plant species in the region (Baily and Pearson, 2007). In the nearby Poole Harbour (west of the study area), *Spartina* colonisation increased marsh area extent by 800 ha in 30 years (Raybould, 2005). *Spartina* appears to grow best in organic-rich sediments which contain more nutrients and preserve more moisture than sandy sediments (Li et al., 2014). Sediments in the Solent region are much finer and so organically enriched compared to the other study estuaries (Goudie, 2013). Better growing conditions for *Spartina* may explain why it was so successful at colonising the Solent, thus driving marsh expansion. There was a shift from net expansion to erosion at some point between 1910 and 1970 for west Solent, and 1930 and 1970 for east. Due to a lack of map revisions during this period, it is unclear whether marshes occupied a larger area than indicated from Figure 2.2 d and h alone. The causes of *Spartina* dieback since the 1970s remain unclear (Baily and Pearson, 2007). Studies have, however, reported marsh loss through lateral marsh erosion, indicating losses may be related to dynamics at the salt marsh-tidal flat interface (Johnson, 2000).

Table 2.3 Rates of lateral marsh change between 1969 and 2016, and the rate of marsh vertical accretion (VA) minus the rate of relative sea level rise (RSLR) over the period 1870 to 1998, for each region. Values are means ± S.E.

Region	Lateral expansion (ha/yr)	VA-RSLR differential (mm/yr)
Solway	0.88 ± 1.17	17.30 ± 14.53 (Marshall, 1962)
Morecambe	2.94 ± 0.37	-
Cardigan	2.31 ± 1.37	10.05 ± 4.06 (Shi, 1993)
Wash	1.27 ± 0.00	47.72 ± 26.87 (Kestner, 1975)
Essex-Kent	-6.42 ± 3.55	4.36 ± 3.56 (van der Wal and Pye, 2004)
Solent	-3.59 ± 1.65	4.25 ± 0.84 (Cundy and Croudace, 1996)

Marshes along the Essex-Kent region consistently eroded, with the exception of a period of little marsh change between 1900 and 1970. Between 1900 and 1970, *Spartina* was first recorded, and several de-embankment events occurred. *Spartina* colonisation has contributed to marsh expansion in some areas of the Essex-Kent region (van der Wal and Pye, 2004). Periods of de-embankment due to breaching of old sea walls has also resulted in marsh expansion whereby plants colonise formerly reclaimed land (Burd, 1992). From 1970 onwards, the trend of marsh decline continued. A lack of marsh extent measures during the 1900 and 1970 may overlook over any trend of rapid expansion or decline, however it is likely that invasion of *Spartina* and phases of de-embankment provided a temporary respite from an otherwise prolonged trend of marsh decline across the Essex-Kent region. These findings suggest *Spartina* introduction was not a main cause for marsh change over longer timescales in most estuaries. Long-term patterns of marsh lateral change across Great Britain do not appear to be driven by direct human impact alone, but were influenced by large-scale physical drivers.

2.4.2 Causes of lateral marsh change between 1970 and 2016

For the period between 1970 and 2016, concentrations of suspended sediment within the estuaries and the rate of relative sea level rise best explained whether marshes expanded or eroded at an estuarine scale. Shifts from lateral marsh erosion to expansion have been reported in numerical models when suspended sediment concentrations of more than ~300 mg/l coincide with relatively low sea level rise rates (less than 5 mm/yr; as observed across the study region) (Mariotti and Fagherazzi, 2010). Results from this study are in agreement with these numerical models and provide the first empirical support that large-scale and long-term shifts in the lateral extent of marshes are driven by the rate of sea level rise and availability of suspended sediment.

The model did leave 74% of variation in marsh change unexplained. This was likely due to local-scale processes including: anthropogenic impacts, such as local hydrological changes due to reclamation, dredging activity and coastal eutrophication (van der Wal and Pye, 2004; Baily and Pearson, 2007); temporal variation in hydrodynamics, such as migrating tidal channels (Pringle, 1995); variation of tidal asymmetry (Townend et al., 2007) and evolution of tidal flat profiles (Bouma et al., 2014) that collectively influence wave height/current velocity at the marsh edge; and within-estuary variation in substrate sand-content that is known to influence soil erosion rates (Mariotti and Carr, 2014; Ford et al., 2016). These small-scale processes will inevitably accrue much variation in marsh behaviour over the large physical and temporal

scales involved. The fact that RSLR and SSC_E can nevertheless explain a quarter of the variation in the long-term and large-scale changes of marshes to us suggests they are of key importance.

Change in the frequency of wind storm events accounted for little variation in marsh lateral change. The importance of wind-waves in regulating erosion-expansion of marshes is well recognised (Callaghan et al., 2010), however the direct impact of storms on marsh change is less clear. Storms can deposit sediment onto marshes if near-shore sediment sources exist, thus promoting accretion (de Groot et al., 2011b). Storms can also cause erosion at marsh edge (van der Wal and Pye, 2004) or induce marsh die-off through smothering of deposited sediments (Pringle, 1995). Differences in the response of marshes to storms may explain why change in storm frequency over time was not identified as a significant factor driving marsh areal extent change in this study. The use of frequency of wind storm change as a predictor of lateral marsh erosion may also oversimplify the relationship between wind-wave power and marsh erosion. Over the study period, a positive phase of North Atlantic Oscillation atmospheric phenomenon (Deser et al., 2017) has been associated with increased occurrence and frequency of strong south westerly winds over extended winter periods (Corbel et al., 2007). Changes in wind direction can change wave fetch along estuaries, and hence wave height at the marsh edge (Rohweder et al., 2008). Interaction between the timing of storm event and the stage of tide are also important determinants of wave energy at the coast. Storms occurring at high tide have a greater impact on marsh change (Pringle, 1995). Tide heights also vary with the 18.6-year lunar nodal cycle, which may change the exposure profile of marshes to storms over time (Baart et al., 2011). It is conceivable that, in areas where marshes are subject to high rates of sea level rise and low suspended sediment supply, the additional impact of storm-induced marsh change may be greater than this study suggests. Further research should address specifically how storminess affect lateral marsh change in macrotidal estuaries, as has been done along open-coast microtidal marshes of the U.S. (Leonardi et al., 2016).

2.4.3 Relationship between vertical and lateral marsh change

All marshes accreted above the rate of local sea level rise, yet some were eroding laterally, implying vertical accretion on its own was not a reliable predictor of marsh long-term stability. It is clearly risky to base evaluations of marsh resilience to environmental change solely on their vertical growth response to relative sea level rise, as has been the tendency (Kirwan et al.,

2016). While the vertical growth of marshes in southern Britain is keeping pace with sea level (van der Wal and Pye, 2004), they are clearly also in the process of long-term lateral erosion. Such contradictory patterns in vertical and lateral marsh change have been previously reported in numerical models (Mariotti and Carr, 2014) and demonstrated empirically (Ganju et al., 2017); they highlight that lateral change in marsh extent may be a better predictor of saltmarsh resilience than comparing marsh vertical growth to sea level rise alone (Balke et al., 2014; Bouma et al., 2016).

2.4.4 Conclusion

Global declines in sediment flux to the coast alongside increasing rates of sea level rise could lead to large-scale marsh loss, such as those along the east coast of the U.S.A. (Weston, 2014). Schemes involving managed realignment of the coastline with engineering solutions to control sediment flux and tidal inundation can be used to build large-scale and long-term marsh resilience in historically eroding systems including San Francisco Bay, U.S.A. (Stralberg et al., 2011), and the Scheldt estuary, Netherlands (Vandenbruwaene et al., 2011). Despite such large investments into the restoration of saltmarsh flood protection (Temmerman et al., 2013) the monitoring of key processes, such as short-term sediment dynamics at the marsh edge, is sparse (Bouma et al., 2016). This hampers the ability to predict whether marsh restoration schemes are likely to succeed or fail (Wolters et al., 2005). There is a need for establishing global monitoring of sediment fluxes near marshes and other coastal systems, similar to the Sediment Elevation Table array (Cahoon et al., 2006) used to record saltmarsh and mangrove vertical accretion rates across the globe.

The evidence presented here contributes to an emerging emphasis on investigating the causes for spatial shifts in coastal systems, including mudflats (Murray et al., 2014), seagrass beds (Suykerbuyk et al., 2016) and mangroves (Gabler et al., 2017). Access to long-term data is facilitating a shift away from a focus on sea level rise alone to consider also the influences of other anthropogenic and macroclimatic drivers of coastline change (Osland et al., 2016). Having shed light on the key drivers of long-term saltmarsh lateral change, researchers should now capitalise on advances in satellite remote sensing (Dorji et al., 2016; Mcowen et al., 2017) and novel and cheap instruments to quantify the short-term sediment dynamics at the coast (Hu et al., 2015b) to evaluate coastal resilience against human- and environment-induced change at a global scale.

3 Long-term estuarine geomorphological responses to periodic shifts of tidal channels

Summary

Temporal shifts in estuarine tidal channels can cause rapid erosion of saltmarshes. Yet, its larger-scale and longer-term influence on the distribution and areal cover of marshes is not well understood. This study used historical maps and aerial photographs between 1891 and 2013 to correlate with tidal channel position the cover and distribution of saltmarshes of three sheltered estuaries in Wales (UK). Aerial images were GIS-georeferenced to delineate marshes and channels across the entirety of each estuary. A series of transects were placed normal to the estuary centreline and distances from the seaward marsh edge and nearest tidal channel to a baseline behind the marsh were calculated for each photograph year. Change maps, age maps, locational probability plots, and long-term river flow and wind speed-direction data were used to investigate marsh-channel relationships. Total marsh cover expanded by 1.2-3.0 ha yr^{-1} over the study period in all estuaries. Upper estuary marshes covered a greater proportion of estuarine width and were more temporally stable than low estuary marshes. Despite a net increase in marsh extent, phases of marsh erosion and expansion occurred simultaneously within each estuary; marshes on one side of the estuary expanded whilst marshes on the opposite bank eroded. A mixed effects model confirmed that periodic shifts in channel positions set up long-lasting restrictions in the distribution of marshes, and explain much of the spatial variation in marsh area cover, as well the distance that single marshes extend out onto tidal flats. The distance of marsh protrusion onto the tidal flat tracked the position of tidal channels: marshes contracted when channels shifted towards them, and expanded when channels moved away. Thus, when some marsh complexes in the estuary eroded, other marshes expanded, giving rise to an estuarine-scale compensatory mechanism that acted to retain a constant marsh cover at the estuarine scale. The frequency and extent of channel shifts observed were typical for the region. There were no changes over the period in background triggers of shifts, such as average or extreme flood-wind events and channel migration is likely to be an intrinsic control of estuarine saltmarsh dynamics and cover. Channel erosion may preserve pioneer marsh species, and hence the capacity for rapid recovery, whilst reductions of channel meandering in the upper estuary may allow marshes to develop erosion-resistant soils. This implies two distinct marsh resilience mechanisms exist in macrotidal estuaries.

3.1 Introduction

Salt marshes occasionally undergo abrupt and rapid lateral erosion and expansion, which often lack clear explanations. For instance, alternate phases of expansion and erosion ranging between -8 and 6 m yr^{-1} in the Westerschelde Estuary, SW Netherlands, have and been attributed to changing wind wave and tidal current forcing (Cox et al., 2003). Lateral erosion of the seaward margin of salt marshes is initiated by differential sedimentation rates between the tidal flat and marsh edge that exaggerate elevation differences and expose the marsh edge to erosion (Bouma et al., 2016). Hydrological forcing is responsible for sediment transport at the coast and, thus, an indirect determinant of whether marshes erode or expand (Hu et al. 2015b). Seasonal or protracted changes in wave exposure are known to affect lateral marsh erosion and expansion on open coast salt marshes (Callaghan et al., 2010; Francalanci et al., 2013; Mariotti and Fagherazzi, 2013; Hu et al., 2015c). However, waves cannot explain lateral marsh shifts in many estuaries where fetch is small and wave action is minimal. Within estuaries, lateral marsh change has alternatively been linked to the periodic movement of tidal channels and their associated erosive forcing (Pringle, 1995; Ward et al., 1998; Cox et al., 2003; Traini et al., 2015). While channel shifts undoubtedly account for some marsh erosion, the extent to which they explain longer-term and estuarine-scale marsh distribution remains unclear.

Tidal channels are conduits for sediment and water flow, and responsible for the geomorphic evolution of estuaries and their associated ecosystems (Fagherazzi and Overeem, 2007; Hughes, 2012; Coco et al., 2013). Characterised by a sinuous planform (Fagherazzi et al., 2004) that is proportional to channel width (Marani et al., 2004; van der Wegen et al., 2008), tidal channels are well-developed in well-mixed sandy estuaries with tidal ranges greater than 2 m (Lanzoni and Seminara, 2002; Hume et al., 2007). The relative influence of tidal currents on sediment transport decreases up the estuary as variation in river flow become more important (Dronkers, 1986). Tidal channels migrate across tidal flats through slow ‘elaboration’ in response to displaced bidirectional flood and ebb currents flows to form cuspate meanders (Li et al., 2008). Point-bars also form from residual flow (Seminara, 2006) and are periodically perforated by tidal barbs in the direction of dominant flow (Barwis, 1977). Channels continually evolve through feedbacks in feature evolution and channel flow displacement (Hughes, 2012). Rapid ‘avulsion’ of channels can also occur during stochastic high-flow events (e.g. flooding) that is capable of eroding sediment from channel margins (Braudrick et al.,

2009). Over centuries, estuaries cycle through phases of sediment import and export as a result of changes in the dominance of asymmetric tidal currents (Dronkers, 1986). During sediment import phases, tidal channels become shallower and form multiple 'flood' channels across the tidal flat, with a main ebb channel in the centre of the estuary (Hughes, 2012). Small differences in the slope between the bottom of flood channel and the channel banks increase the likelihood of channel shifts (Hughes, 2012). Migrating tidal channels are important regulators of overall estuarine morphology and are likely to explain some degree of variation in marsh extent.

Periodic shifts in estuarine channels have been shown to trigger switching between expansion and erosion in single marsh locations (Yapp et al., 1917; Gao and Collins, 1997; Cox et al., 2003; van de Koppel et al., 2005b; Ollerhead et al., 2005; van der Wal et al., 2008; Chauhan, 2009; Haslett and Allen, 2014). Yet, the effects of channel migrations are likely extend well beyond single sites. Pringle (1995) reported the near total loss of Silverdale marsh, Morecambe Bay (~150 ha) in 20 years following the migration of a tidal channel, whilst on the opposite side of the bay, tidal flats rapidly became vegetated to form an extensive marsh (Gray, 1972). Thus it seems that, while channel shifts can lead to dramatic erosion of sites towards which the channel shifted, it may well be coupled to compensatory expansion at sites that the channels moved way from. Such 'estuarine-scale compensation' may be an inherent mechanism for sustaining net marsh extent at larger scales, but the principle has not been rigorously investigated. Channel migration in other fluvial systems including rivers is an important regulator of ecosystem structure (Yang et al., 1999; Francis, 2009). Bays and estuaries make up large portions of global marsh cover and provide suitable macrocosms to explore marsh compensation at landscape-scales.

This study examines the extent to which shifts in estuarine channels explain the patters of erosion and expansion of salt marshes, focusing on twelve salt marshes in three estuaries along the Welsh coastline, Great Britain. Using historical maps and aerial photographs, this study identifies marsh change at *i.* estuarine, *ii.* individual-marsh and *iii.* within-marsh scales to investigate how tidal channels structure marshes at the estuarine-scale. The study tests the prediction that erosion at one marsh is compensated for by expansion at another marsh, and result in no net change of marsh cover at the estuarine scale. The study also investigates if changes in marsh cover are secondarily explained by changes in normal and extreme river flows and change in wind speed and/or direction.

3.2 Methods

3.2.1 Study Site

Saltmarsh erosion-accretion patterns were studied in thirteen saltmarshes across three estuaries, Glaslyn-Dwyryd, Mawddach and Dyfi (Figure 3.1), located in Cardigan Bay on the West coast of Wales, United Kingdom. All three estuaries were formed from drowned river and glacial valleys that were flooded during the later stages of the Holocene transgression (Howe and Thomas, 1963; Larcombe and Jago, 1996). Sediment infill of estuaries along Cardigan Bay began after deglaciation, largely driven by flood-dominant tidal transport of fine sands (Larcombe and Jago, 1994). Marco-sequence soil cores from the Dyfi shows salt marshes first emerged around 6,000 yBP, thereafter, pollen records indicate a gradual conversion from 'low' to 'high' marsh and, eventually, to *Phragimes*-dominated brackish marsh at 5,150±90 yBP (Wilks, 1979). As the intertidal elevation rose further, marsh areas were colonised by alder-carr forest and underwent succession to true terrestrial conditions (Wilks, 1979). The rise in intertidal elevation continued until 4,700 yBP signalling a return to peri-marine conditions and the submersion of forests (Wilks, 1979). Shi and Lamb (1991) suggest that, at 3,050 yBP, marshes began to encroach onto the submerged forest peats, covering their extent fully by 1,510 yBP. This sequence of is believed to be in response to post-glacial sea level transgression, and likely representative of other situations across the UK including Glaslyn-Dwyryd and Mawddach estuaries (Wilks, 1979; Shi and Lamb, 1991; Larcombe and Jago, 1994).

Estuary size and tidal prism have been reduced by railway embankment and embankments on the river flood plains in the late 1800s, with a major reclamation scheme in the Glaslyn-Dwyryd estuary, resulting in the closing of the Glaslyn estuary entirely (Rhind and Jones, 1995; Robins and Davies, 2011). At present, estuaries have average depths of 4-10 m (Manning and Whitehouse, 2012) and are sheltered from north-westerly wind-generated waves by spit development at the estuary mouths comprised of sand in the Glaslyn-Dwyryd estuary, and shingle in the Mawddach and Dyfi estuaries (Brown, 2007). The spits are oriented in a south-north axis, indicative of the general south-to-north movement of bedload sediments within Cardigan Bay and prevalent wind direction (Brown, 2007). The Cardigan Bay estuaries had narrow entrances (0.4-1.5 km wide) relative to their long saline intrusion lengths of 10-15 km. The three estuaries were macrotidal, with spring and neap tidal ranges of 1.8 m and 4.28 m for Glaslyn-Dwyryd, and 1.76 m and 4 m for Mawddach, and 1.76 m and 4.04 m for Dyfi estuaries (Manning and Whitehouse, 2012). Coupled with their narrow morphologies, strong tidal flows

along the length of the estuaries produce velocities around 1 ms^{-1} during flood tides (Larcombe and Jago, 1996) that, for the Dyfi, produce greater tidal flows of 1,400 and 280 m^3 s^{-1} during spring and neap tides respectively compared to the mean freshwater flows of 20 m^3 s^{-1} (Shi and Lamb, 1991).

Tides are asymmetrical and dominate sediment transport (Larcombe and Jago, 1996; Brown and Davies, 2010). Imported offshore terrigenous deposits (Jago, 1980; Elliott and Gardiner, 1981; Shi and Lamb, 1991; Larcombe and Jago, 1994) are largely non-cohesive, medium grained sediments, with median diameters between 240 and 350 µm (Pethick, 1996). Sediment import from flood-dominant tides has been substantial, reducing the estuary accommodation

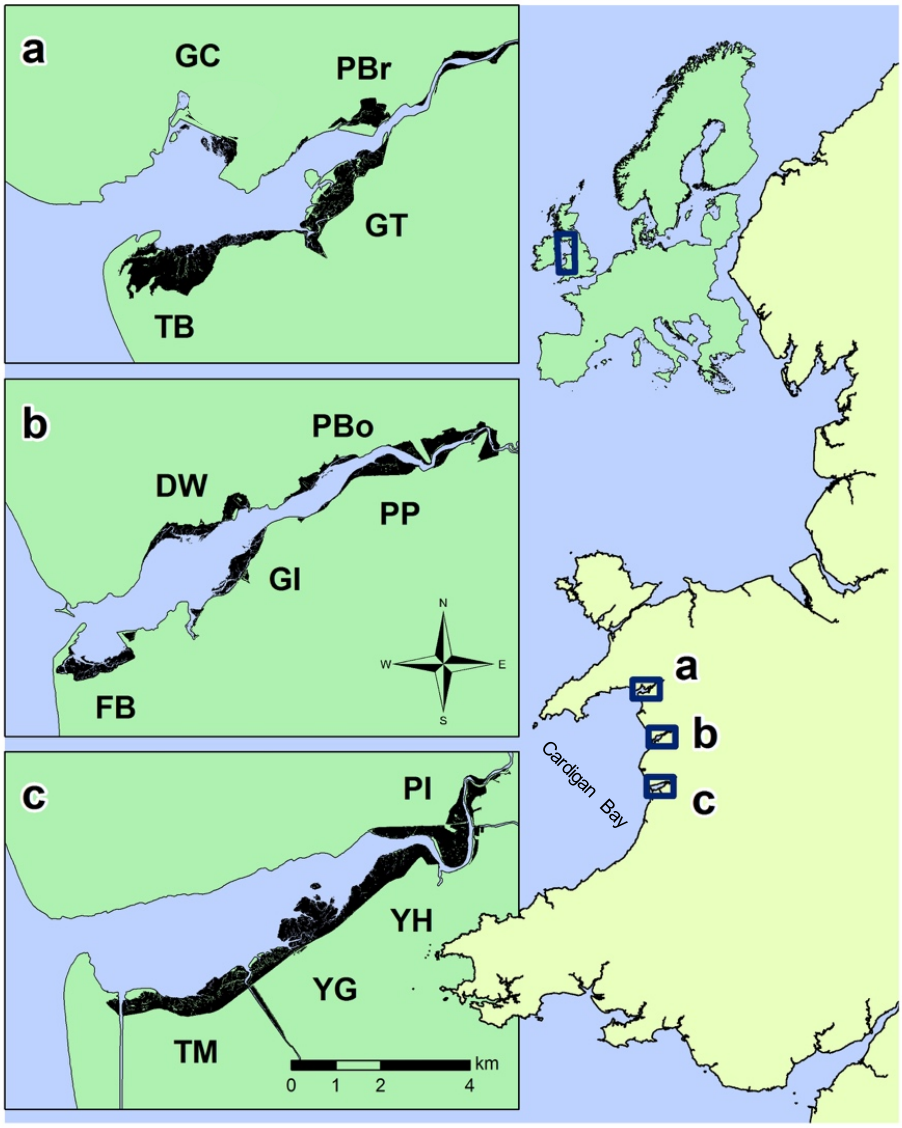

Figure 3.1 Locations of the three estuary complexes in Cardigan Bay, West Wales: **a** Glaslyn-Dwyryd, **b** Mawddach and **c** Dyfi. Labels refer to the names of saltmarsh complexes (GC: Glaslyn Cob; TB: Traeth Bach; GT: Glastraeth; PBr: Pont Briwet; FB: Fairbourne; DW: Dwynant; GI: Garth Isaf; PP: Penmaenpool; PBo: Pont Borthwnog; TM: Traeth Maelgwyn; YG: Ynys Greigiog; YH: Ynys Hir and PI: Penmaen Isa).

space (Shi, 1993) despite sea level rise rates of 2.5 mm yr^{-1} since 1990 (Pye and Blott, 2014). Net sediment import has formed shallow morphologies with well-developed intertidal flats, salt marshes and tidal channels (Brown, 2007). Presently, the three estuaries are considered dynamically stable (Haynes and Dobson, 1969), although work by Brown and Davies (2010) demonstrate net sediment export at the mouth of the Dyfi estuary due to stronger ebb flow in a main ebb-dominated channel, than channels through the flood-dominated tidal flats and salt marshes. Since the 1950s the main ebb tidal channel has tended to stay in the northern portion of each estuary (Fisher, 1991; Shi et al., 1995) therefore the largest marshes tend to occur on the southern banks, whilst the shallow flood channels seaward of the marsh edge are highly dynamic.

Salt marshes in the Cardigan Bay are typical estuarine marshes (Pye and Blott, 2014) and show a full complement of marsh zones from pioneer- through to upper-marsh zones. A change from pioneer to upper-marsh tends to occur upon moving up-estuary, as the average surface elevation tends to increase (Table 3.1).

Table 3.1 Site characteristics of marshes in Glaslyn-Dwyryd, Mawddach and Dyfi estuaries.

Estuary	Marsh	Estuary position	Dominant marsh zone	Average surface elevation (m OD)	Percentage silt-clay content (%)
Glaslyn-Dwyryd	Glaslyn Cob (GC)	Lower	mid-upper	1.70 ± 0.52	8.6
	Traeth Bach (TB)	Lower	pioneer; mid-upper	2.01 ± 0.44	-
	Glastraeth (GT)	Mid	mid-upper	2.36 ± 0.29	22.6
	Pont Briwet (PBr)	Upper	mid-upper	2.55 ± 0.75	29.2
Mawddach	Fairbourne (FB)	Lower	pioneer; low-mid; mid-upper	2.00 ± 0.70	3.6
	Dwynant (DW)	Mid	pioneer	1.76 ± 0.64	1.2
	Garth Isaf (GI)	Mid	pioneer	1.47 ± 0.53	-
	Penmaenpool (PP)	Upper	mid-upper	2.44 ± 0.61	-
	Pont Borthwnog (PBo)	Upper	mid-upper	2.19 ± 0.69	27
Dyfi	Traeth Maelgwyn (TM)	Lower	pioneer; mid-upper	1.85 ± 0.63	8.5
	Ynys Greigiog (YG)	Mid	pioneer; low-mid	1.88 ± 0.66	-
	Ynys Hir (YH)	Upper	*mid-upper	2.27 ± 0.58	-
	Penmaen Isa (PI)	Upper	*mid-upper	2.78 ± 0.86	52.2

Saltmarsh plant community compositions (National Vegetation Classification) taken from CCW (2003) and expressed as marsh zones according to definitions by JNCC (2004).
Average surface elevations for each marsh taken from the Environment Agency, UK (available at: https://data.gov.uk/publisher/environment-agency).
Percentage silt-clay content in the low-marsh taken from Duggan-Edwards (unpublished).

Plant assemblages are dominated by *Spartina anglica*, *Salicornia europaea agg.*, and *Puccinellia maritima* in the low marsh, with Mawddach estuary having the highest diversity of low- and pioneer-marsh. Mid-marsh and high-marsh zones are dominated by *Festuca rubra* and *Juncus maritimus* (Prosser and Wallace, 2004). Sheep grazing is classified as intensive (>5 sheep ha^{-1} yr^{-1}; Woodend, 2010) across all estuaries with the exception of the Mawddach estuary, which is classified as light (<2 sheep ha^{-1} yr^{-1}; Woodend, 2010). Moderate cattle stocking densities of 0.3-0.7 cattle ha^{-1} yr^{-1} are sustained on the Morfa Harlech marsh, outer Glaslyn-Dwyryd estuary. Grazing by a population of ~2,500 geese along the upper-estuary marshes of the Dyfi is considered of moderate intensity (Prosser and Wallace, 2004; Kingham, 2013). Marsh sediment types of Glaslyn-Dwyryd and Mawddach have broadly been classified as having "an absence of mud and fine silt" (Goudie, 2013). Marshes tend to increase in clay-silt content upon moving up-estuary (Table 3.1). Sediment deposits in the mid-marsh zone of the outer Dyfi estuary show successive seasonal accretion phases, as denoted by alternate laminae of sand and fibrous organic and silty sediment layers. Sediment layers are formed by sand deposition during winter, and vegetation growth during summer (Shi et al., 1993). Pyatt and Collin (1999) showed how silt-clay content tended to reduce upon moving from the high-, mid-, to low-marsh zones. Short-term sediment sequences reported elsewhere in the Dyfi, or for the Glaslyn-Dwyryd and Mawddach estuaries, are unavailable.

3.2.2 Processing historical maps and aerial photographs

A collection of Ordnance Survey (OS) maps and aerial photographs taken between 1891 and 2013 were used to measure change in saltmarsh extent over time. Only material that covered the entirety of each estuary was used. Change in tidal channel position was also extracted from aerial photographs, however, due to inconsistencies in updating tidal channel positions and smaller tidal channel often not being recorded (Carr, 1962), OS maps were not used to delineate the position change of tidal channels (Table 3.2).

OS maps were accessed via the EDINA Digimap Resource Centre (EDINA; available at: http://digimap.edina.ac.uk/webhelp/resources/index.html). Maps are scanned by EDINA at a resolution of 300 dpi, and the digitised map sheets were georeferenced using OS book of indexes for each grid to a British National Grid coordinate system on a GIS. No Root Mean Square Error term was reported during the EDINA digitising process, so RMSE was calculated by the author (see Appendix I). Survey date for each map was taken from Oliver (2013). First

edition and revision sheets in the County Series 1:10,560 were used to vectorise saltmarsh extent in each estuary manually using the online EDINA Historical Digimap Ancient Roam interface.

Aerial photographs were scanned at a resolution of ca. 400 dpi and georeferenced in a Geographic Information System (GIS) to British National Grid using a Thin Plate Spline algorithm with Lancsoz resampling suited to coarse-resolution historical image rectification (Bookstein, 1997). A combination of Ordnance Survey (OS) 1:25,000 raster maps (EDINA) and Environment Agency (EA) 1:7,500 orthorectified images from 2006-2009 (Phelan et al., 2011) were used to match the unrectified photographs to well-distrusted control points including cross-roads, building corners and salt marsh creeks. Rectifications were visually inspected for distortions and poor overlap and adjusted where necessary. Resulting georeferenced images had pixel sizes corresponding to ca. 0.25 × 0.25 m in the field.

3.2.3 Delineating saltmarsh extent and tidal channels

Marshes and channels for the entirety of each estuary were delineated manually at a standard scale of 1:7,500. To aid in distinguishing between features, aerial image contrast was set to

Table 3.2 Metadata on Ordnance Survey maps and aerial photographs used to calculate saltmarsh extent and tidal channel positions.

Site	Date	Decade group	Scale	Source	Image type
Glaslyn-Dwyryd	1891 (1st edition)	1890s	1:10560	EDINA	Map
	1901 (1st revision)	1900s	1:10560	EDINA	Map
	2nd May 1946	1950s	1:7,500	RCAHMW	B&W
	21st May 1971	1970s	1:7,500	RCAHMW	B&W
	1st May 1990	1990s	1:20,000	CRAPW	B&W
	31st December 1993	1990s	1:7,500	Bush and Davies (2013)	Colour
	29th September 2011	2010s	1:7,500	Phelan et al. (2011)	Colour
Mawddach	1890 (1st edition)	1890s	1:10560	EDINA	Map
	1901 (1st revision)	1900s	1:10560	EDINA	Map
	1948	1950s	1:7,500	CRAPW	B&W
	28th June 1969	1970s	1:10,000	Bush and Davies (2013)	B&W
	1st May 1990	1990s	1:20,000	CRAPW	B&W
	2013	2010s	1:10,000	Bush and Davies (2013)	Colour
Dyfi	1891 (1st edition)	1890s	1:10560	EDINA	Map
	1902 (1st revision)	1900s	1:10560	EDINA	Map
	1st May 1946	1950s	1:7,500	RCAHMW	B&W
	5th December 1958	1960s	1:7,500	RCAHMW	B&W
	29th June 1961	1960s	1:7,500	RCAHMW	B&W
	22nd June 1971	1970s	1:7,500	RCAHMW	B&W
	12th October 1972	1970s	1:7,500	RCAHMW	B&W
	19th July 1982	1980s	1:10,000	CRAPW	Colour
	1st May 1990	1990s	1:20,000	CRAPW	B&W
	2000	2000s	1:10,000	Bush and Davies (2013)	Colour
	6th January 2009	2010s	1:10,000	Google Earth	Colour

50% to exaggerate ‘dark’ vegetated surfaces / wet channels from ‘light’ bare tidal flats. Vertices were placed every 10 meters along the margins of saltmarshes and tidal channels. Marsh patches less than 5 m in diameter, creeks narrower than 10 m, and unvegetated features in the interior of saltmarshes such as salt pans were overlooked. In most cases, salt marshes were bounded by embankments that allowed for simple identification of the landward marsh boundary. For the Traeth Bach saltmarsh in the Glaslyn-Dwyryd estuary (Figure 3.1 a; TB), however, the marsh transitions to sand dune plant communities (Prosser and Wallace, 2004) making a specific boundary difficult to define. In this instance, a horizontal boundary was placed at the bottom of the marsh. The channel edge was identified as the transition between light (dry) and dark (wet) pixels in each images. Condition of the tide when images were captured was not known therefore a standard channel edge between years is difficult to justify. However potential error of several meters was usually offset by variation by tens of meters in channel position over time, so this method was considered acceptable. The final digitized layer was inspected against OS maps, an EA vectorised marsh layer (available at: https://data.gov.uk/dataset/saltmarsh-extents1), and marsh extent delineated from earlier / later image sets, as a quality control measure for identifying possible spurious delineations (i.e. suspect areas that may have been initially misclassified as marsh/channel due to large differences between years). These areas were then re-examined to ensure the delineation was fair.

After salt marsh and tidal channels were delineated, the area of each marsh was calculated. Distances from the salt marsh edge to the back of the marsh were calculated along transects normal to the estuary centreline placed every 200 m down the estuary. Distances from the nearest tidal channel and back of the marsh were also calculated along the same transects. Distances were standardised by estuary width and position of the estuary bank in order to generalise marsh change (Appendix V). Several maps for each estuary were created to interpret temporal marsh change. In a GIS, a ‘fishnet’ layer with 10 m ×10 m cell size was draped over each estuary and the presence/absence if marsh occurred within a cell noted for each year. The 10 m ×10 m scale was chosen to match the resolution used when delineating the marsh and tidal channel edge. Marsh was defined as ‘present’ in cells when any part of a marsh shapefile intersected that cell. Cells were then classified into four different types of long-term behaviour, they were labelled as: (1) ‘stable tidal flat’, where salt marsh was never observed; (2) ‘stable marsh’, where marshes consistently occurred; (3) ‘expanding, where a cell switched from marsh being absent to then being present, and; (4) ‘eroding’, where a cell switched from marsh

being present to then being absent. GIS maps were drawn to show the spatial distribution of these four marsh behaviours within estuaries between two time periods. GIS maps were also drawn to show how the spatial distribution of marsh behaviours changed across multiple years within each estuary. In order to represent areas of the fishnet where cells had fluctuated between marsh being present, absent and present again (or the reciprocal of being absent, present, then absent), cells were labelled as 'dynamic'. GIS maps were also drawn to show the age of marshes. This was done by calculating the time elapsed between the most recent cell labelling marsh as 'present' and the first cell that labelled marsh as being 'absent' along the time sequence. For example, a cell where marsh was registered as 'present' in 2013, 'present' in 1990, and 'absent' in 1971, the age of the marsh was given as 'between 23 and 42 years'. 'Locational probability analysis' was used to represent temporal change in tidal channel movement across each estuary. Locational probability is a cell-by-cell probability that a channel occurs in that cell based on presence/absence of the channel occurring in that cell. For example, if part of the channel occurs in a cell in every image, that pixel receives a locational probability score of 100%. Values are weighted by the total length of the record (Graf, 2000; Burningham, 2008).

3.2.4 River flow and wind data

Daily river flow data for a river gauge (float with counterweight) at "Dyfi at Dyfi Bridge" (ID: 64001; coordinates: 52°36'3"N, 3°51'17"W) was taken from the National River Flow Archive (available at: https://nrfa.ceh.ac.uk/nrfa-data). Data is quality-controlled before being made available for download, so no post-processing of the data was done (Robson and Reed, 1999). Daily wind speed and direction at "Aberporth" weather station (ID: 1198; coordinates: 1198, 52°8'21"N, 4°34'12"W) were taken from the Met Office Integrated Data Archive System (MIDAS) distributed by the British Atmospheric Data Centre (BADC) (available at: http://badc.nerc.ac.uk/data/ukmo-midas/WPS.html). Station was selected based the closest station to the estuary with a long temporal dataset range. Prior to analysis, wind speed data was screened for quality and completeness. MIDAS assign a 'flag' to measurements that have an unreliable observation, and were excluded from further analysis. Any duplicated values were also removed. Any given year was only used in later calculations when the dataset held ≥75% number of days per year, and that each month had ≥50% days per month (Watson et al., 2015).

3.2.5 Statistical Analysis

All statistical analyses were implemented in R. A mixed effects model was used to determine the effect of explanatory variables 'normalised position in estuary (%)', 'normalised estuary width (%)', 'normalised distance of channel to land (%)' and 'year factor' on the response variable 'normalised saltmarsh width (%)'. Only transects where marshes occurred at least once during the survey period were used in the analysis. All variables were verified for normality and checked for outliers. No transformations of the variables were required, and no outliers were removed. Multicollinearity between predictor variables was tested for using Variance Inflation Factor (VIF) tables, whereby variables that successive had a VIF score of >3 were excluded and resampled (Zuur et al., 2010). Estuary position and width were highly correlated (r=0.75), therefore normalised estuary width (%) was dropped from further analysis. Maximal mixed-effects models (including interaction terms) with Restricted Maximum Likelihood (REML) estimation and AIC scores were used to determine whether inclusion of 'estuary' and 'year' as random factors significantly improved the model fit (Zuur et al., 2009), and found inclusion of a random intercept (estuary) was sufficient. Minimal adequate model was selected using F tests and AIC scores by comparing between simpler models, and the final model was checked for homoscedasticity using the 'cftest' function of the 'multcomp' package (Hothorn et al., 2016). A time series analysis was used to determine whether daily river flow (between 1976 and 2013), wind speed, and wind direction had changed significantly over time (Crawley, 2013). Change over time was first detrended from seasonal variability using the 'stl' function; a locally weighted regression procedure (Cleveland et al., 1990). Mixed effects models were then used to determine whether applying both 'seasonal' and 'long-term trend' fits (model 1) better explained change in predictor value over time (i.e. river or wind change) than when a 'seasonal' fit alone was considered (model 2). If model 1 was significantly different (Chi^2) and had a lower AIC value than model 2, this would indicate a long-term trend existed in the data. Mixed effects models were used in order to reduce the effects of temporal pseudo-replication. Model fixed effects were the 'seasonal' and 'long-term trend' fits. The Restricted Maximum Likelihood (REML) approach was used on each mixed effects model for a fair comparison between the models (Zuur et al., 2009). 'Year' was designated as a random effect to allow for different intercepts for different years in each model. A linear regression model was used to determine whether annual maximum flood events changed over time. Model output was first checked for heteroscedacity in the model residuals and for the presence of outliers to ensure assumption of Heterogeneity of Variance were met.

3.3 Results

3.3.1 Spatially-Explicit Marsh Change

Over 67 years, 35-43% of marshes across the entirety of each estuary expanded (Figure 3.2; green), while 1-8% eroded (Figure 3.2; red). Stable marshes (Figure 3.2; black) represented 33-41% of observation cells. Stable areas were particularly frequent in the upper estuary, while expansion (Figure 3.2; green) was concentrated in the lower estuary. Many marshes were 'dynamic' at their down-shore limit (Figure 3.2; blue), especially in the Dyfi estuary, where 31% of marsh areas fluctuated between expansion and erosion. A series of maps showing where marshes in each estuary expanded/eroded between each survey year are shown in Appendix VI. A map showing the age of marshes in each estuary is shown in Appendix VII.

Between 1887 and 2013, the total marsh area per estuary expanded at rates between 1.2 and 3.0 ha yr^{-1} (Figures 3.3 a-c). Marsh expansion in the Glaslyn-Dwyryd and Mawddach estuaries was gradual (Figures 3.3 a and b), whilst marsh expansion the Dyfi was non-linear over the study period; there was an accelerated phase of marsh growth after the 1950s, followed by a phase of erosion in the Dyfi estuary after 2001 (Figure 3.3 c). At the 'individual-marsh' scale, marshes at the bottom of each estuary consistently expanded by between 420 and 2,400% (Figure 3.3 d-f; light dashed line). Marshes in the mid and upper parts of Glaslyn-Dwyryd and Mawddach estuaries fluctuated between expansion and erosion at their margins (Figure 3.3 d and 3.3 e; dotted and dark dashed lines), although they expanded overall by 30 to 190%. Alternate phases of erosion at one marsh and expansion at another over the same period was evident for upper-estuary marshes of GT and PBr in the Glaslyn-Dwyryd estuary (Figure 3.3 d), and for the mid-estuary marshes of GI and DW in the Mawddach estuary (Figure 3.3 e).

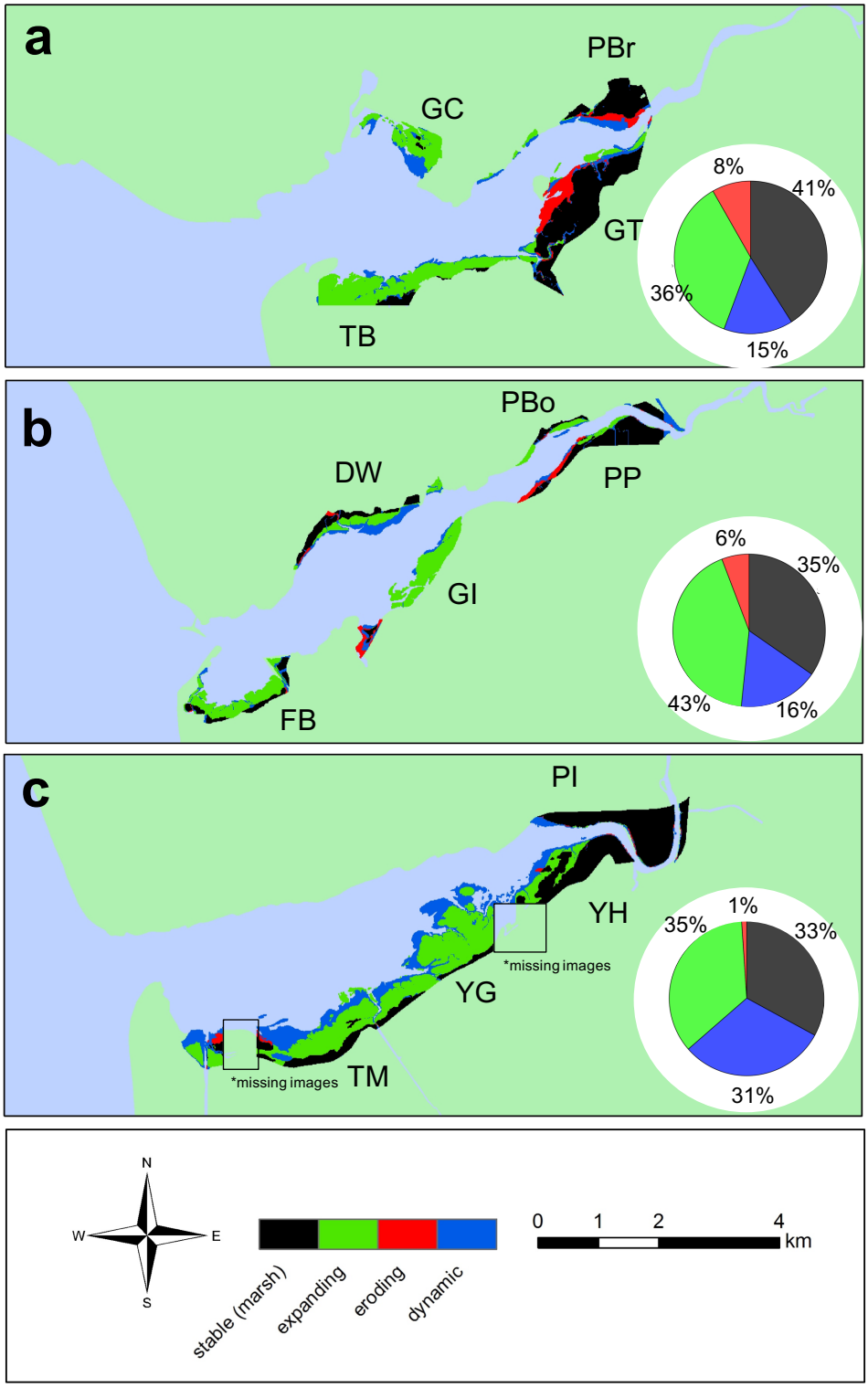

Figure 3.2 Maps summarising saltmarsh change for **a** Glaslyn-Dwyryd, **b** Mawddach and **c** Dyfi estuaries between 1946 and 2013. Black areas represent stable marsh that has remained unchanged throughout the study period. Red and green areas show marsh erosion and expansion respectively. Rectangles on the map labelled 'missing images' show areas of the estuary where aerial photographs were unavailable for measuring marsh areal cover (Dyfi estuary, for years 1971-1972). Descriptions of marsh change over time have therefore been omitted in these areas. Blue areas indicate fluctuations in marsh extent. Percentage total of each category are summarized as pie-charts. Labels refer to the names of saltmarsh complexes (GC: Glaslyn Cob; TB: Traeth Bach; GT: Glastraeth; PBr: Pont Briwet; FB: Fairbourne; DW: Dwynant; GI: Garth Isaf; PP: Penmaenpool; PBo: Pont Borthwnog; TM: Traeth Maelgwyn; YG: Ynys Greigiog; YH: Ynys Hir and PI: Penmaen Isa).

Marsh GT, Glaslyn-Dwyryd estuary and marsh PP, Mawddach estuary exhibited simultaneous marsh edge retreat and expansion across their length over the study period (exemplified in Figure 3.4). A similar pattern was seen along marsh TB, Glaslyn-Dwyryd estuary and marsh GI, Mawddach estuary (Appendix VI). All four marshes were amongst the longest marshes in the study estuaries, occupying 2 to 3 km stretches of the southern bank in each case. Patterns marsh erosion and accretion phases are all easily discernible in the 'total change' map, which summarises marsh change per estuary over the entire study period (Figure 3.2 a and b), as well as the 'sequential change' maps (Appendix VI) and the 'age map', which show when the present marsh extent was initiated (Appendix VII).

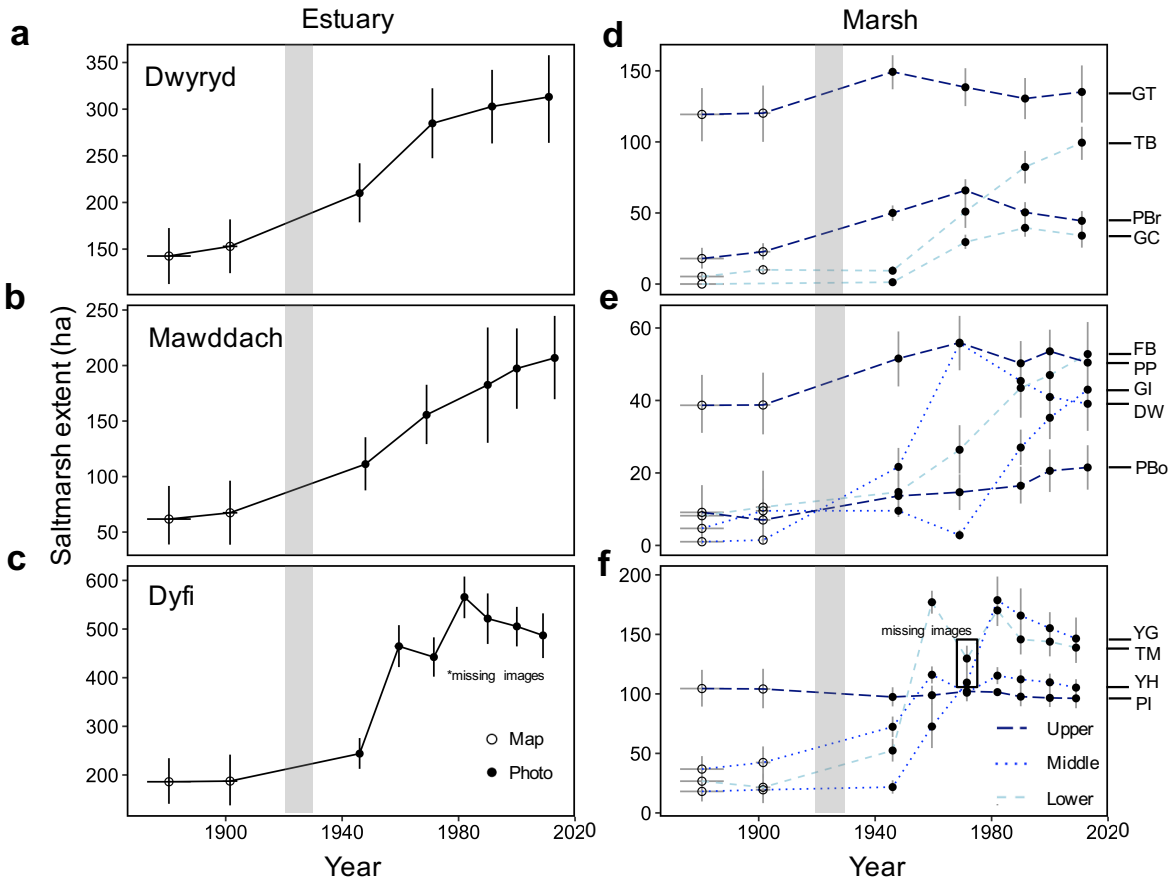

Figure 3.3 Change in saltmarsh extent between 1887 and 2013 for the Glaslyn-Dwyryd, Mawddach and Dyfi estuaries at **a-c** an estuarine-scale and **d-f** individual-marsh scale. Extent measurements were taken from maps (hollow circles) and aerial photographs (filled circles). Lines in **d-f** indicate whether marshes were located in the lower (dashed), middle (dotted) and upper (solid line) estuary. Labels refer to the names of saltmarsh complexes (GC: Glaslyn Cob; TB: Traeth Bach; GT: Glastraeth; PBr: Pont Briwet; FB: Fairbourne; DW: Dwynant; GI: Garth Isaf; PP: Penmaenpool; PBo: Pont Borthwnog; TM: Traeth Maelgwyn; YG: Ynys Greigiog; YH: Ynys Hir and PI: Penmaen Isa). Vertical error bars represent 95% confidence interval in marsh extent. Horizontal error bars represent date ranges over which surveying for maps was done, or when areal images were captured. Grey shading indicates *Spartina spp.* colonisation in each estuary. Years with missing images (asterisk) are underestimates of the true saltmarsh extent.

Patterns of simultaneous erosion-accretion phases between marshes in the Dyfi estuary were not observed (Figure 3.3 f). Marshes in the Dyfi estuary expanded until 1980, after which they began to erode (Appendix VI); the exception was the upper-estuary Penmaen Isa marsh, which remained stable throughout the study period (Figure 3.3 f; marsh 'PI').

3.3.2 Marsh-Channel Relationships

There was an effect of tidal channel position on saltmarsh extent across all estuaries, that weakened upon moving from the upper to the lower estuary (Figure 3.5, Figure 3.6, and Table 3.3). Saltmarshes occupied 75-95% of the estuary width at the heads of estuaries, but less than 20% at the mouth of estuaries. Variation in marsh width over time was constant across the

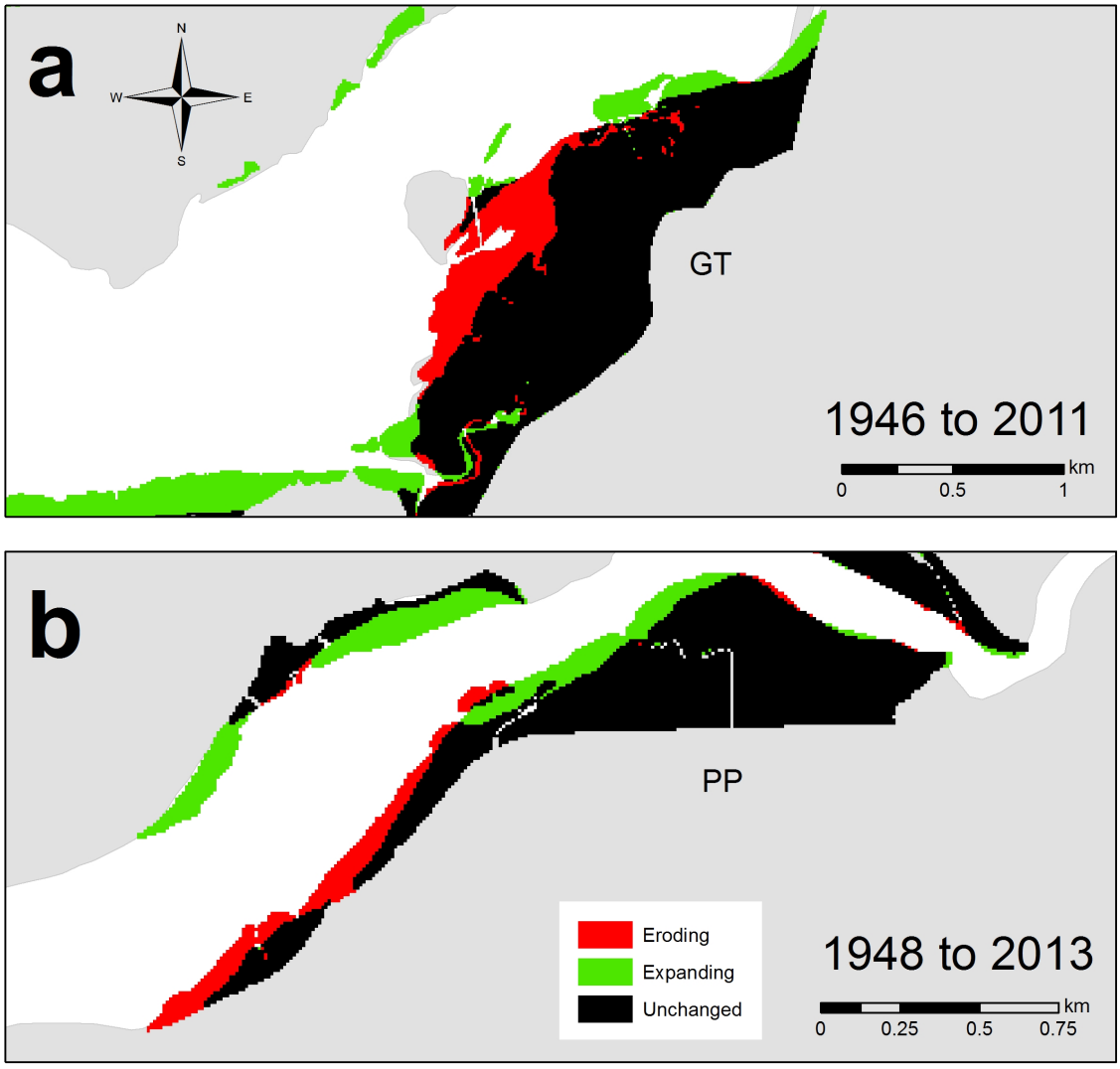

Figure 3.4 Change in saltmarsh shoreline for **a** Glaslyn-Dwyryd estuary between 1946 and 2011, and **b** Mawddach estuary between 1948 and 2013. Black areas represent stable marsh that has remained unchanged throughout the study period. Red and green areas show areas where marshes have eroded or expanded respectively Labels refer to the names of saltmarsh complexes (GT: Glastraeth, and; PP: Penmaenpool).

length of each estuary, with the exception of increases in the centres of Mawddach and Dyfi estuaries (Figure 3.5; error bars of green areas) where the largest expansion of marshes occurred during the study (Figure 3.2). The percentage of estuarine width between channel and land (Figure 3.5; blue line) varied considerably along the length of the estuary, ranging between 0% (flowing against the estuary bank) and 90 % near the top of the Dyfi estuary. The distances of channel shifts as a percentage of the estuary width was high (Figure 3.5; error bars of blue line), occurring across 75% of the estuary in some cases. Marshes tended to be much closer to a tidal channel in the upper estuary than in the lower estuary, where error bars overlapped suggesting an interaction between the movement of the marsh edge and tidal channel (Figure 3.5; error bars of green areas). Both the location where marshes occurred in the estuary and the position of tidal channels regulated marsh size (Table 3.3). Nearer the upper estuary, channels that migrated further out into the estuary were characterised by larger marshes. When moving from the upper- to lower-estuary, marshes became proportionally smaller in size compared to the estuary width and the association between position of tidal channels and marsh width weakened (Figure 3.6). The location of tidal channels between 1946 and 2013 for each estuary is shown in Appendix VIII.

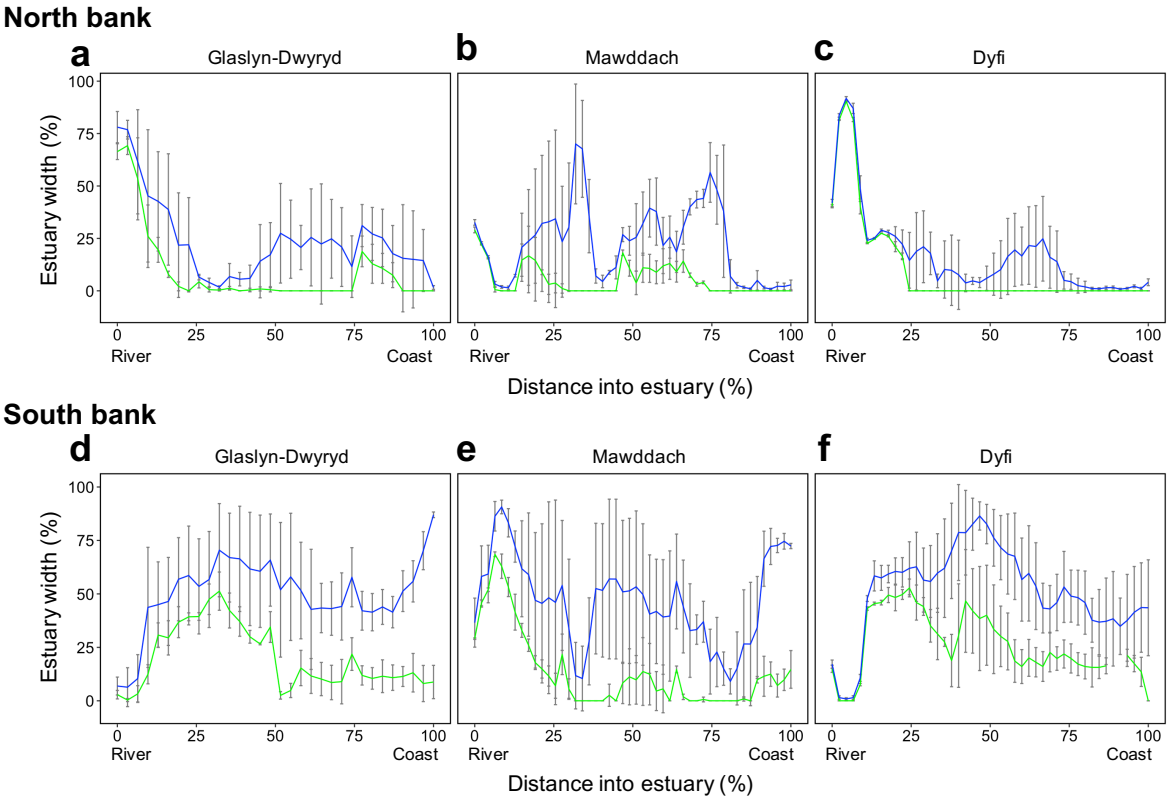

Figure 3.5 The mean normalised estuarine width occupied by salt marsh (green line) and the mean normalised distance of the nearest tidal channel into the estuary (blue line) at intervals of 200 m from the upper to the lower estuary expressed as a percentage for **a-c** the northern and **d-f** southern banks of Glaslyn-Dwyryd, Mawddach and Dyfi estuaries respectively between 1946 and 2013. Error bars represent S.D.

3.3.3 Predicting Marsh Size and Channel Position in Estuaries

Upon moving from one estuary bank to the other, the likelihood of encountering a marsh decreased (Figure 3.7 a; filled circles) as the likelihood of encountering a tidal channel increased (Figure 3.7 a; hollow circles). Marshes were less likely to occur on northern bank (from 50% to 5%) than southern banks (from 80 to 25%) upon moving a quarter of the way into the estuary because tidal channels were displaced northward. The northward displacement of tidal channels was more pronounced in the lower estuary (Figure 3.7 b; hollow circles) than the upper estuary (Figure 3.7 c; hollow circles). Salt marshes were more stable in the upper estuary than lower estuary: there was a high likelihood (75%) of encountering marshes extending 25% of the estuary width on the southern bank of the upper estuary (Figure 3.7 b; filled circles). At 25% of the estuary width in the lower estuary, however, likelihood of encountering saltmarsh dropped to 0% (Figure 3.7 c; filled circles).

3.3.4 Drivers of Channel Migration

Gaps in river flow data prior to 1963, and between 1971 and 1975, meant that any influence of flood events that may have occurred during this period on channel meandering or marsh extent could not be deduced. Between 1962 and 2013, however, the daily average river flow at the top of the Dyfi estuary showed high inter-seasonal variability (low flow during summer, high flow during winter) (Figure 3.8 a; grey line), with little change in the annual mean flow (Figure 3.8 a; blue line). For the longest timeseries between 1975 and 2013, no long-term trend was detected ($Chi^2 = 0.95$, $p = 0.330$; Appendix IX). Frequency of annual maximum flood events did not change significantly over time ($F_{1,41}=3.701$, $p=0.061$) when two large flood events in 1964 and 1965 were excluded as outliers. Both points had double flow rates compared to other years (Figure 3.8 a; black points). Daily average wind speeds also showed high inter-seasonal

Table 3.3 Predictor variables of normalised saltmarsh width (normalised by the width of the estuary), selected from a minimal adequate model (mixed effects model with 'estuary' as a random intercept).

Model variable	Estimate	SE	*z*-Value	*P* value
Best model fit: all estuaries (AIC = 5529.9)				
Chan*Est	-0.010	0.001	-8.180	2.22×10^{-16}***
Chan	0.671	0.056	12.005	$< 2.00 \times 10^{-16}$***
Est	0.142	0.069	2.058	0.040*
Chan*Est*Year	0.000	0.000	1.179	0.238
Chan*Year	0.006	0.007	0.918	0.359
Est*Year	-0.003	0.008	-0.327	0.744
Year	-0.061	0.390	-0.155	0.877

Chan = % normalised distance of channel from the land (0% represents channel is right up against the landward boundary); Est = % normalized estuary length (river to coast); Year = survey year.
* indicates interaction
*$P < 0.05$, **$P < 0.01$, ***$P < 0.001$, n.s. = not significant.

variability (Figure 3.8 b; grey lines), but no long-term trend in the annual average speed between 1957 and 2017 (Figure 3.8 b; blue line) ($Chi^2 = 1.96$, $p = 0.161$; Appendix IX). Time series analysis of wind data between 1957 and 2017 indicated a trend other than seasonal variation existed ($Chi^2 = 5.82$, $p = 0.016$; Appendix IX). Between 1957 and 1980, wind direction moved south-westerly by three-quarters of a degree a year ($F_{1,22} = 7.197$, $p = 0.014$), although the trend was weak ($R^2 = 0.21$). After 1980, no significant trend was found. Wind directions in 17- to 22-year periods are shown in Figure 3.8 b.

3.4 Discussion

From a long-term analysis of salt marsh lateral change in three sheltered estuaries in Wales, this study shows that tidal channels play a major role in regulating the position and cover of marshes. The maximum down-shore extent, and thus the 'per-marsh' and 'across-estuary' marsh cover, was restricted by the presence of the tidal channel, although the influence of the channel on the marsh weakened towards the bottom of the estuary (nearest the sea).

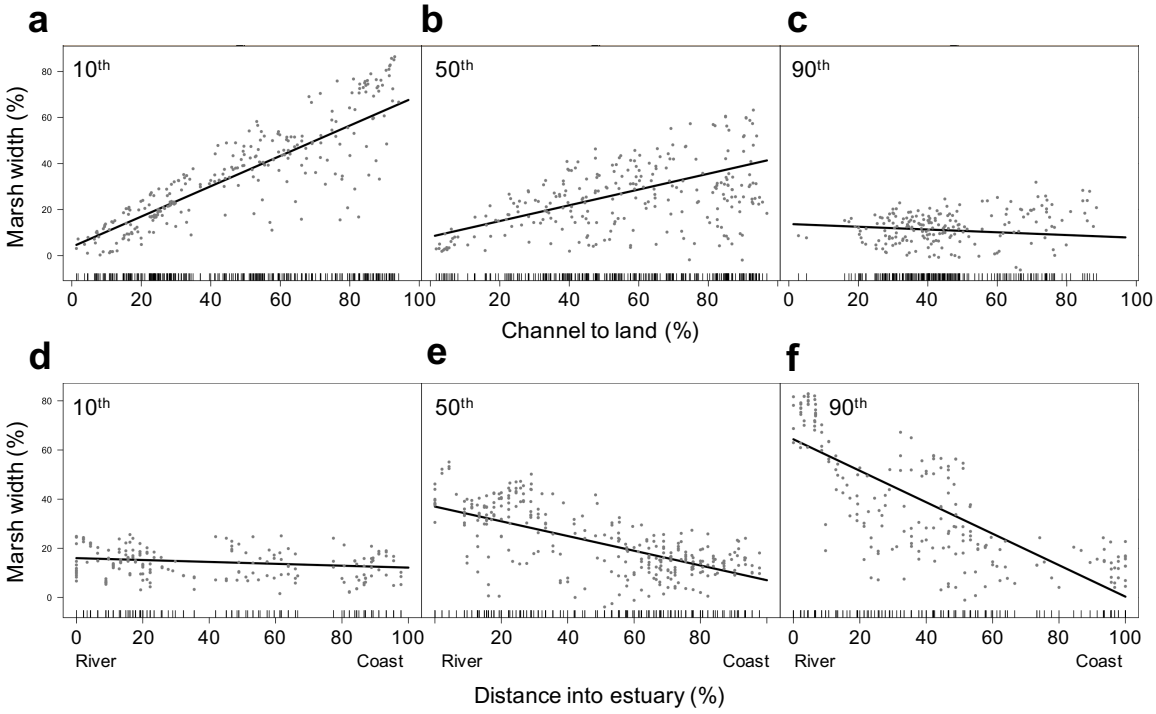

Figure 3.6 Relationships between the normalised marsh width across the estuary, and a significant interactive term between **a-c** normalised distance of channel from the land and **d-f** normalized distance into estuary (river to coast), identified from a mixed effects model with 'estuary' as a random intercept. Each predictor in the interaction is plotted separately by the 10th, 50th and 90th quantiles (top-left corner) of the interacting predictor, to visualise the changing strength of the relationship. Data points represent distribution of standardized partial residuals. Solid lines represent model-fit though the data. Tick marks along the bottom of each plot denote deciles of the distribution of each predictor value.

Migration of the channels drove cycles of marsh expansion and erosion across estuary banks in two of the estuaries (Glaslyn-Dwyryd and Mawddach), and particularly explained marsh extent in the mid- and upper-reaches of each estuary. Tidal channels along the Dyfi estuary were consistently located towards the northern bank, which likely prevented a cyclical erosion-accretion behaviour from occurring.

The method used to map marsh change (Figures 3.2 and 3.4, and Appendices VI, VII and VIII) recorded each 10×10 m cell as containing saltmarsh if any fraction of the cell space was intersected by digitized marsh extent. In some cases, the allocation of marsh presence in a cell may overstate the degree of marsh expansion/stability, or misclassify a marsh as 'stable' if the marsh extent if in reality marsh in that cell had been eroding. Nevertheless, these maps are of sufficient resolution to reveal estuarine-scale trends of change in marsh areal extent from the 1940s onwards. This study did not consider changes in the saltmarsh creek network over time, which could indicate marsh erosion if channels widen and proliferate across the marsh.

Channel widening in marshes, a process, called internal dissection, is observed along coastlines of southern England (van der Wal and Pye, 2004). Internal dissection can be induced by pollution that impacts on plant health (Deegan et al., 2012), can be generated by embankment construction that increase hydrological forcing at the seawall and thus marsh erosion (Carpenter and Pye, 1996), or may occur through increased tidal currents with sea level rise

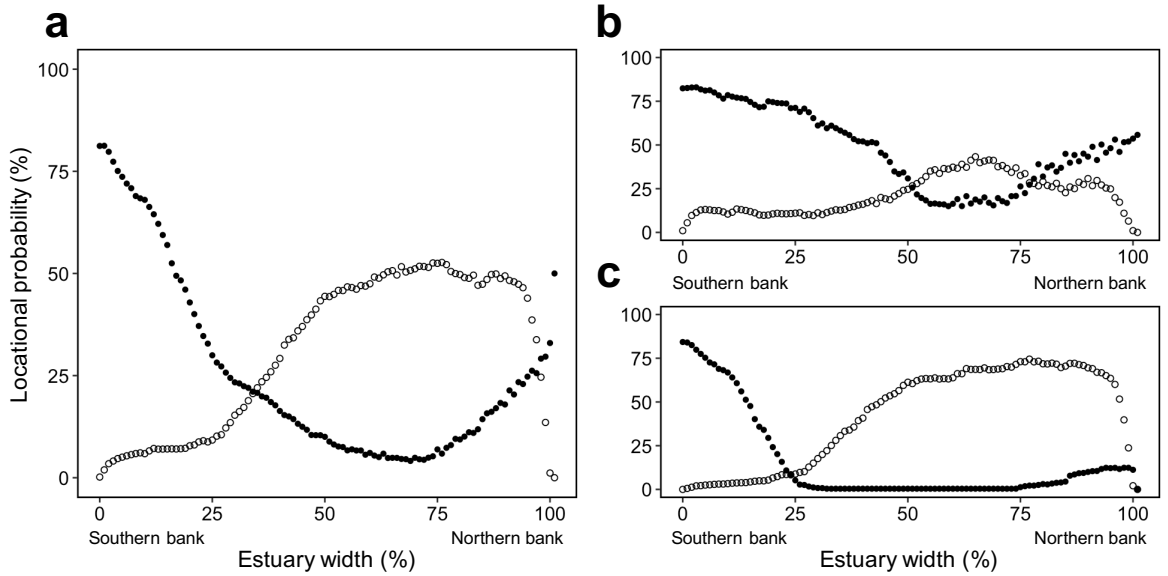

Figure 3.7 Likelihood of encountering salt marsh (filled circle) and tidal channel (hollow circle) upon moving from the southern (0%) to the northern bank (100%) for Glaslyn-Dwyryd, Mawddach and Dyfi estuaries across all years between 1946 and 2013, expressed as percentage for **a** all parts of the estuary, **b** the upper estuary only, and **c** the lower estuary only.

that scour creeks, particularly where sediment influx is insufficient to maintain creek planform (Rinaldo et al., 1999). Marshes in the present study appeared to be receiving sufficient sediment sources with sea level rise (*Chapter 2*) thus internal dissection did not appear to be a significant factor of marsh loss in the estuaries studied here.

3.4.1 Channel limit on marsh size

The relationship between channel and marsh was weakest in the lower estuary, and was likely due to differences in the stages of marsh development along the lengths of estuaries. At the top of each estuary, marshes consistently occupied a large proportion of the estuary width, meaning

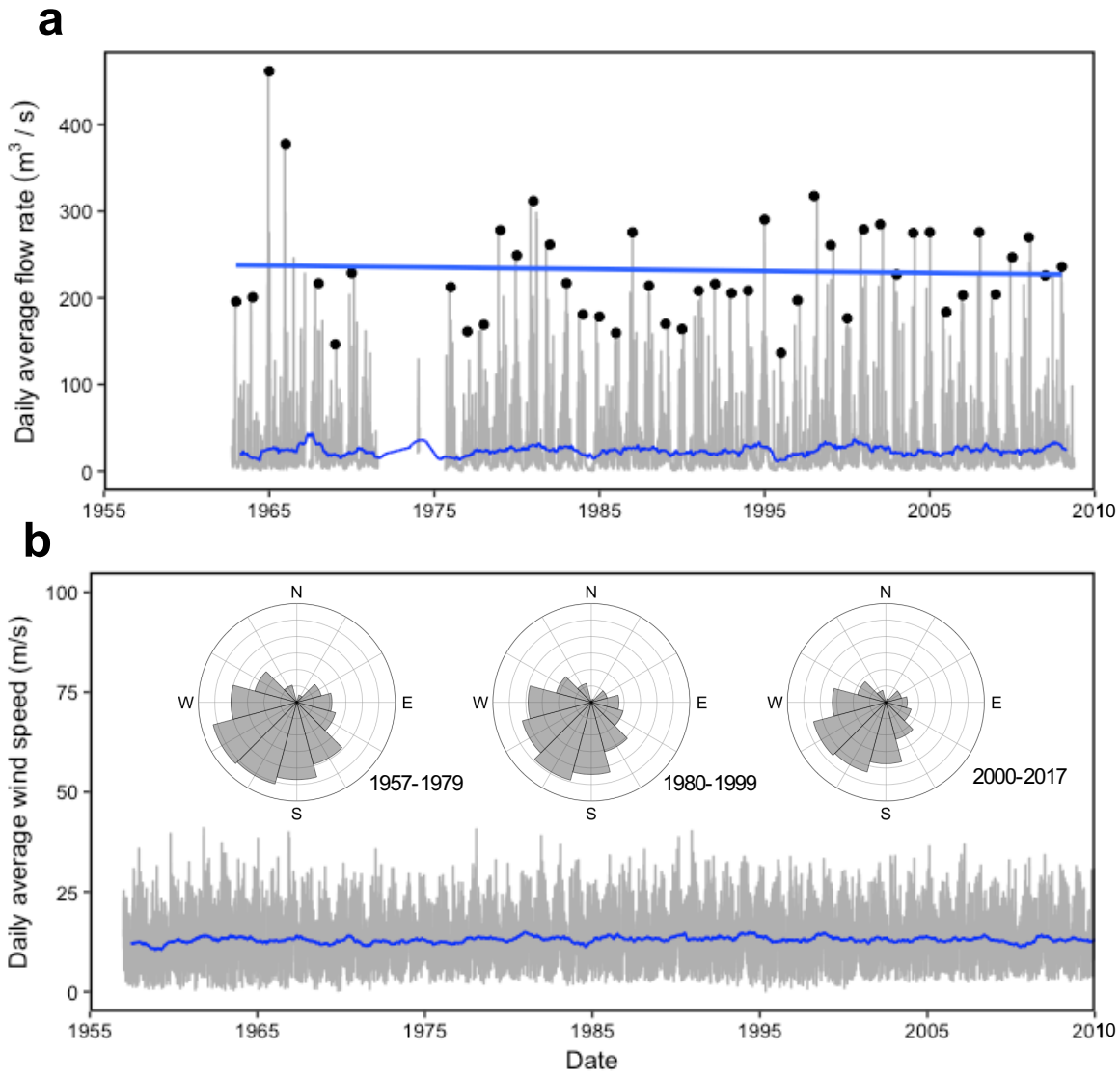

Figure 3.8 a Daily average river flow rate (grey line), maximum annual flood event per water year (black circle) and annual moving average (blue line) for the Dyfi river at the estuary mouth (river gauge, ID 64001, 52°36'3"N, 3°51'17"W). Best fit line indicates no trend in the maximum annual flood events. **b** Daily average wind speed (grey line), annual moving average (blue line) and wind direction for the periods 1957-1979, 1980-1999 and 2000-2017 respectively (wind station, station ID 1198, 52°8'21"N, 4°34'12"W).

marshes extended sufficiently far into the estuary and were therefore exposed to fluctuating tidal channels throughout the study period. In contrast, marshes nearer the bottom of the estuary needed to develop sufficiently before coming into contact with fluctuating tidal channels: marshes in the 1950-1960s were narrower in the lower estuary and were unaffected by channel movement. Causes for marsh expansion are discussed in section 3.4.3.

The only marsh that was not exposed to migrating channels was Fairbourne marsh (lower-estuary in Mawddach) which continued to expand over the study period. This was likely due to the railway development east of Fairbourne marsh built in 1895, which promoted sedimentation and restricted channel migrating close to the shore (Robins and Davies, 2011) thereby allowing the marsh to expand. Across all estuaries, tidal channel positions were displaced toward the northern bank by the Coriolis effect (Brown, 2007). Therefore, marshes were larger on the southern bank in Glaslyn-Dwyryd and Mawddach estuaries, and absent from the northern bank along the mid- and lower-estuary of the Dyfi. The emergent relationship between salt marsh width and tidal channel position suggests a common control on the maximum attainable size of marshes within estuaries. Previous work has shown that seaward marsh limits are determined by tidal range (Balke et al., 2016), wave exposure (Callaghan et al., 2010; Bouma et al., 2016), salinity (Odum, 1988), bioturbation (van Wesenbeeck et al., 2007) or soil anoxia (He et al., 2015). This study demonstrates the often overlooked importance of tidal channels as long-term regulators of marsh width.

3.4.2 Channel migration and marsh expansion-erosion patterns

Channel migration imposed a limit on maximum marsh extent, however fluctuations of the channel position also initiated local phases of marsh expansion or erosion that, in the Glaslyn-Dwyryd and Mawddach estuaries, were out of phase: erosion at the edge of one marsh was 'compensated' for by marsh expansion elsewhere in the estuary. These 'compensatory' phases of expansion and erosion occurred: *i.* between marshes on opposite estuary banks, *ii.* between marshes in bottom-, mid- and upper-estuary, and *iii.* within single marshes. In the Dyfi estuary, no such 'compensatory' mechanism could be observed. This was likely due to the persistence of a tidal channel along the northern bank of the estuary (lower and mid portions), which could prevent saltmarshes from forming.

The estuarine marshes in this study were generally very dynamic at their seaward limit, and switched several times between expansion and erosion over the 67-year study. Previous studies that have described cyclical patterns of expansion and erosion have tended to consider only single marsh sites (van de Koppel et al., 2005b; van der Wal et al., 2008; Wang and Temmerman, 2013) or describe marsh cyclicity along open coast/embayment marshes (Kestner, 1962; Greensmith and Tucker, 1965; Harmsworth and Long, 1986; Moller et al., 1999; Chauhan, 2009; Haslett and Allen, 2014). There was no obvious cause for migration of tidal channels, thus the dynamics reported here occur in the absence of extreme events. This study shows a cyclical marsh expansion-erosion pattern also emerges at the estuarine scale due to meandering tidal channels. Compensatory marsh expansion following erosion may be a common property of estuarine marshes which are more likely to reside adjacently to active migrating tidal channels (Gray, 1972; Pringle, 1995), than are salt marshes on open coasts.

3.4.3 Estuarine-scale marsh expansion

The greatest changes in marsh extent occurred in the lower estuary, where marshes expanded throughout the study period before being limited by tidal channels, resulting in a net increase at the estuarine-scale. The phase of expansion may be explained by the arrival of *Spartina anglica*, an invasive marsh builder that can colonise lower on the intertidal (Hubbard, 1965), and tidal sediment transport fluxes. The spread of *Spartina* has been monitored in the Dyfi estuary over a number of years. *Spartina* was introduced to the estuary in 1920 (Chater and Jones, 1957) and initially spread slowly until 1939, after which successive surveys in 1945, 1962 and 1970s report rapid expansion across the estuary (Chater and Jones, 1957; Buck, 1993; Prosser and Wallace, 2004) (Figure 3.3; grey bars). Although there was no detailed record of *Spartina* spread in the Glaslyn-Dwyryd and Mawddach estuaries, *Spartina* is now extensive throughout both estuaries (Prosser and Wallace, 2004), and characteristic *Spartina* patches are visible in the aerial photographs (e.g. rapid emergence of Garth Isa marsh in the Mawddach). According to Figure 3.3 a and b, however, marshes expanded prior to the arrival of *Spartina* in the Glaslyn-Dwyryd and Mawddach estuaries. In order for the native flora to colonise the intertidal, increases in the tidal flat elevation would have had to occur to allow seedlings to establish (Temmerman et al., 2005). Local sediment sources to the tidal flats fronting the saltmarsh are mainly derived from redistribution within the estuary, or from offshore sources transported into the estuary via tidal asymmetry (Haynes and Dobson, 1969; Friedrichs and Perry, 2001; Brown and Davies, 2010). Coastal engineering works may also have modified the

tidal prism, promoting sediment import (Robins and Davies, 2011). Similar causes for marsh expansion have been reported across western UK (Jago, 1980; Blott et al., 2006; Moore et al., 2009; Halcrow, 2010). In the Glaslyn-Dwyryd and Mawddach estuaries where marsh 'compensation' was observed, there appear two discrete spatial scales of marsh change: cyclical erosion-expansion between marshes that occur over several years, versus the net expansion of marshes that occurred over decades due to changes in species composition and sediment supply.

3.4.4 Estuarine-scale marsh configuration

Marshes towards the mouths of estuaries occupied a lesser proportion of the total estuarine width than did marshes towards the heads of estuaries. Such a planform has previously been described in idealised tidally-dominated estuarine systems, whose morphologies are shaped by first-order control of high tidal current energy near the estuary mouth (Dyer, 1973), then by second-order meandering of tidal channels (*Chapter 3*). Energy reduces higher up the estuary as tidal currents interact with river flow, causing a minimum in average hydrological forcing at the 'meandering' zone (Dyer, 1973). The 'meandering' zone represented the upper position of all estuaries in this study. At the upper estuary, tidal channel position variability over time was markedly lower (10-20% distance into estuary in Figure 3.5 d-f and Appendix VIII) than elsewhere in the estuary. An apparent consequence of less extreme tidal channel migration along the upper estuaries was that marshes remained mostly stable throughout the study period (>63 year-old deposits; Appendix VII). Only periodic erosion-accretion phases at the marsh edge were observed. Marshes in the upper estuary also tended to have higher clay-silt fraction (Table 3.1) and were generally situated higher in the tidal frame than marshes in the lower estuary (Table 3.1). In the absence of high hydrological forcing, marshes are able to grow vertically through both allochthonous and autochthonous sediment accumulation. Sediment accumulation enriches the organic matter content of soils (French, 2006) and creates more amenable conditions for less saline-tolerant marsh plants species through lower tidal inundation frequencies (Yapp et al., 1917). Such mid-upper marsh plant communities predominated the upper estuary in all cases (Table 3.1). Organically-enriched soils can be more resistant to erosion than unconsolidated sandy sediments (Mitchener and Torfs, 1996; Ford et al., 2016), and soils tend to become compacted as they slowly accrete, reducing their erodibility (Chen et al., 2012). High-marsh plant species, particularly *Juncus maritimus*, have also been shown to contribute more autochthonous accretion into soils than any other marsh community

type (Sousa et al., 2017). High-marsh plant communities may therefore engineer more resistant soils. Enhanced resistance to scholastic disturbance events, such as river flooding, would likely enhance marsh resilience. High soil resistance may protect marshes into the future, especially given that flood events are expected to worsen as a consequence of climate change (Robins et al., 2016).

In the mid- and low-estuary, marshes may not have sufficient time to accumulate erosion-resistant soils before tidal channel meandering causes marsh erosion. Many of these marshes, however, are composed of pioneer- to low-mid zones (Table 3.1). Pioneer marsh species can capitalise on periods of low disturbance to expand their range (Wiehe, 1935; Balke et al., 2014) and the maintenance of larger areas of pioneer marsh likely increase the capacity for recovery following disturbance due to greater propagule density within the area (Erfanzadeh et al., 2010). Marshes within the mid- and lower-estuary may therefore be erosion-prone, but have a high capacity for recovery, and therefore to persist in more dynamic regions of the estuary. This study observed net marsh expansion in the outer estuary, likely caused by sediment influx and *Spartina* invasion. Consequently, this study cannot comment on whether the marshes are held in a transient state by periodic rapid phases of erosion through tidal channel migration (although this has been observed in other marshes situated in the lower estuary lower estuaries (Pringle, 1995)). However, there may hypothetically exist two distinct marsh configurations across the length of an estuary, in response to a gradient of hydrological forcing: high-estuary 'resistor' marshes, which engineer soils to resist erosion and persist over long periods, and lower- and mid-estuaries 'recoverer' marshes, which are erosion-prone, but have a high capacity for recovery and therefore maintain a dynamic persistence in the lower estuary. Alternative expressions of the same ecosystem type to optimise resilience across hydrological forcing gradients have recently been described in barrier sand dunes (Stallins and Corenblit, 2017). Further work should adjudicate whether a similar scenario operate within estuarine marshes.

3.5 Conclusions

This study examined the patterns of saltmarsh and tidal channel movement with historical maps and aerial images for the entirety of three estuaries for the Cardigan Bay area between 1946 and 2013. Investigation of the general characteristics of the sizes of marshes in relation to tidal channel position revealed that:

1. Marshes are limited in extent by the position of the nearest tidal channel, imposing a maximum attainable size of marshes in tidally-dominated estuaries.
2. Once a maximum size is reached, minor changes in marsh extent can occur through cyclical phases of marsh expansion and decline in a 'compensatory' mechanism between marshes on opposite estuary banks, along the estuary length and within individual marshes, that in the mid and upper estuaries where cycles occurred showed little net marsh change.
3. Marshes in the lower estuary have expanded due to *Spartina* invasion and sediment import through tidal asymmetry, whereas marshes in the upper-estuary have remained stable except for cyclical dynamics at the marsh edge.
4. The ability of pioneer marsh plants to colonise the intertidal after channels migrate, and the ability of high-marsh plants to resist erosion may indicate different mechanisms by which marshes remain resilient in macrotidal estuaries.

4 Short-term bank erosion promotes long-term marsh resilience

Summary

Saltmarsh creek banks are regarded as stable features because failed bank material, known as slump blocks, persist and armour creek banks. Sea level rise (increasing creek flow velocity) and eutrophication (degrading plant structure) threaten to cause creek widening, a mechanism of marsh loss. It is therefore important to determine the limits of whether slump blocks are able to provide a resilience mechanism against creek erosion. High-resolution Digital Elevation Models were used to measure monthly change of 30 creeks and 3 slump blocks in each creek between 2014 and 2015. Creek basin and bank erosion was measured at a range of scales (directly behind a slump block, within 25, 50 and 100 cm of a block and across the entire creek basin) and related to slump block properties and creek hydrology. Step-wise regression was used to determine the influences of biotic (plant properties) and abiotic (water flow and soil properties) variables on slump block soil erosion rate. Creek bank expansion-erosion rates immediately behind a slump block and volume change around the block was positively related to the rates of slump block erosion ($R^2 = 0.18$ and $R^2 = 0.50$ respectively). When vegetated and bare blocks were considered separately, vegetated block erosion had a slightly stronger association with creek bank erosion than bare blocks ($R^2 = 0.42$ and $R^2 = 0.15$ respectively), whereas erosion of bare blocks had a stronger association with volume change at the creek basin than vegetated blocks ($R^2 = 0.39$ and $R^2 = 0.48$ respectively). There were no significant relationships between creek basin or bank erosion with peak current speed, and all associations weakened over larger scales. Erosion rate of vegetated blocks decreased with greater root matter content (R^2=0.59) and for bare blocks, erosion rate increased with peak current speed ($R^2 = 0.51$) and with lower clay-silt fraction ($R^2 = 0.38$). This study indicates that slow erosion of slump blocks can lead to creek edge recovery by reducing erosion at the creek basin and creek bank. Management aimed at enhancing below-ground root growth in soils could increase the overall resistance of salt marshes to erosion.

4.1 Introduction

Identifying the physical and environmental processes responsible for lateral marsh loss and recovery is crucial for saltmarsh stability in the face of growing human pressure on the coastline (Kirwan et al., 2016). Saltmarsh creek banks are a potential site for lateral marsh loss. Creek widening can reduce marsh size, in a process called internal dissection (van der Wal and Pye, 2004). Consequently, there is considerable interest in understanding mechanisms and drivers of marsh creek bank dynamics. Creek banks typically appear to be in an eroding state, characterised by rotational slipping of failed vegetated bank debris near the top and mud ridges near the base indicative of surface flow transporting eroded material to the creek bottom (Allen, 1985). Despite this, marsh creeks have been shown to migrate negligibly over time (Allen, 1985). Along the creek banks of an organogenic microtidal saltmarsh in north-west San Francisco Bay, US, Gabet (1998) observed that failed bank debris protected creek edges from erosion: so-called 'slump blocks' displaced current flows and caused the accumulation of sediment from the water column to form a low elevation table near the base of the creek suitable for new marsh growth. Blocks gradually eroded, triggering another phase of bank erosion and slump block deposition at the base of the creek. Gabet (1998) argued slump block formation was responsible for slow lateral migration rates of creeks across the marsh. Slump blocks have also been shown to obstruct water flow in creeks so decreased current flow behind the blockage leads to sedimentation and eventual conversion of creek to marsh (Goudie, 2013). Slump blocks have been shown to be a ubiquitous feature of laterally eroding marsh banks (Allen, 1989), and may therefore constitute a resilience mechanism influencing creek bank erosion and recovery.

Slump blocks form because current flow influences different parts of the creek bank. Saltmarsh soils in the upper ~30 cm are highly resistant to erosion because plant roots bind sediments (Ford et al., 2016). With increasing depth, soils become compacted and thus increasingly resistant to erosion. Soils immediately beneath the root layer are therefore the most vulnerable to erosion (Chen et al., 2012). At the exposed creek bank edge, mechanical particle erosion by tidal current action preferentially erode the weaker soils beneath the root layer (Chen et al., 2011). Tension cracks form as a portion of the root-dense creek bank begins to break away from the marsh platform by gravity (Mariotti et al., 2016). Water trapped in the cracks increase porewater pressure and enlarge the cracks (Francalanci et al., 2013). Successive wetting and drying with the tides expand and shrink soils repeatedly, exacerbating crack formation (Allen,

1989). Crustacean burrowing may also destabilise creek banks (Allen, 2000). Eventually, portions of creek bank break away as slump blocks. Slump blocks are deposited in several ways: rotational slipping on curved bank edges; sideways shearing of soil clumps from tension cracks that topple into the creek, and; collapsing of a cantilever from an undercut bank. Cantilever failure can occur either by: shearing of the overhang at the tension crack (shear failure); bending at the tension crack and collapsing by rotation (beam failure), and; collapse of the bottom half a cantilever (tensile fracture) (Thorne and Tovey, 1981). Rotational slipping is more common along muddy banks, whereas cantilever failure trends to occur in sandy environments (Allen, 1989). The final creek morphology often appears as spherical 'shells' at the eroding bank, possibly tiered along larger creeks (Allen, 1985).

Once formed, slump blocks may have several outcomes on creek bank erosion: The slump block may persist and trap sediment, leading to recovery of the creek bank in a cyclical manner (e.g. Allen, 1985; Goudie, 2013). Alternatively, the slump block is removed over time (Allen, 1989) in a process called end-point control (Thorne and Tovey, 1981), that initiates a new phase of creek bank erosion. Slow erosion rates allow creek banks on opposite sides to recover, so that there is no net loss of marsh as creeks migrate across the marsh (e.g. Gabet, 1998). Fast erosion rates could lead to creek widening, a process known as internal dissection, causing losses in marsh extent (van der Wal et al., 2008; Ganju et al., 2017). Internal dissection has been associated with increased erodibility due to higher flow by sea level rise and reductions of sediment supply (D'Alpaos, 2011) and loss of soil stability by vegetation degradation from eutrophication (Lottig and Fox, 2007; Alber et al., 2008; Deegan et al., 2012). The longevity of slump blocks is therefore crucial in determining the long-term fate of creek bank erosion and is likely determined by competing physical and biological processes (Figure 4.1)

The aim of this study was to determine the conditions when slump blocks, a product of marsh bank erosion, operate as a mechanism of resilience to promote marsh recovery. The study asks do slump blocks represent a resilience mechanism in creeks? And what factors determine the capacity of blocks to protect the marsh edge?

4.2 Methods

4.2.1 Site Description

The study took place at a single salt marsh within the Glaslyn-Dwyryd estuary, west Wales, UK. Glaslyn-Dwyryd is part of Cardigan Bay opening out to the Eastern Irish Sea. The estuary constitutes two conjoining estuaries with a single sand spit restricting the main entrance. The tidally-active area of the estuary is 16 km^2, now much reduced since the construction of a cob that closed the Glaslyn estuary at Glaslyn Cob in 1811. The remaining estuary is shallow, with a mean depth of 4.3 m, has a long saline intrusion length of 10.4 km (Manning and Whitehouse, 2012), and is macrotidal with spring tidal ranges in excess of 5 meters. Consequently, the estuary is strongly asymmetrical with tidally-dominated sediment transport. River flow from the Glaslyn and Dwyryd rivers that drain into the estuary have similar annual flow rates of around 6 m^3 s^{-1} (Manning and Whitehouse, 2012); National River Flow Archive, available at: https://nrfa.ceh.ac.uk/), and rates of relative sea level rise were low, at 2.4 mm yr^{-1}. Marshes throughout the estuary had been expanding since the middle of the 19th century at a rate of 1.6 ha yr^{-1} (*Chapter 2*). The study area was a ~0.1 km^2 area located in the eastern end of Traeth Bach saltmarsh, located on the southern bank in the middle of Glaslyn-Dwyryd estuary (Figure 4.2).

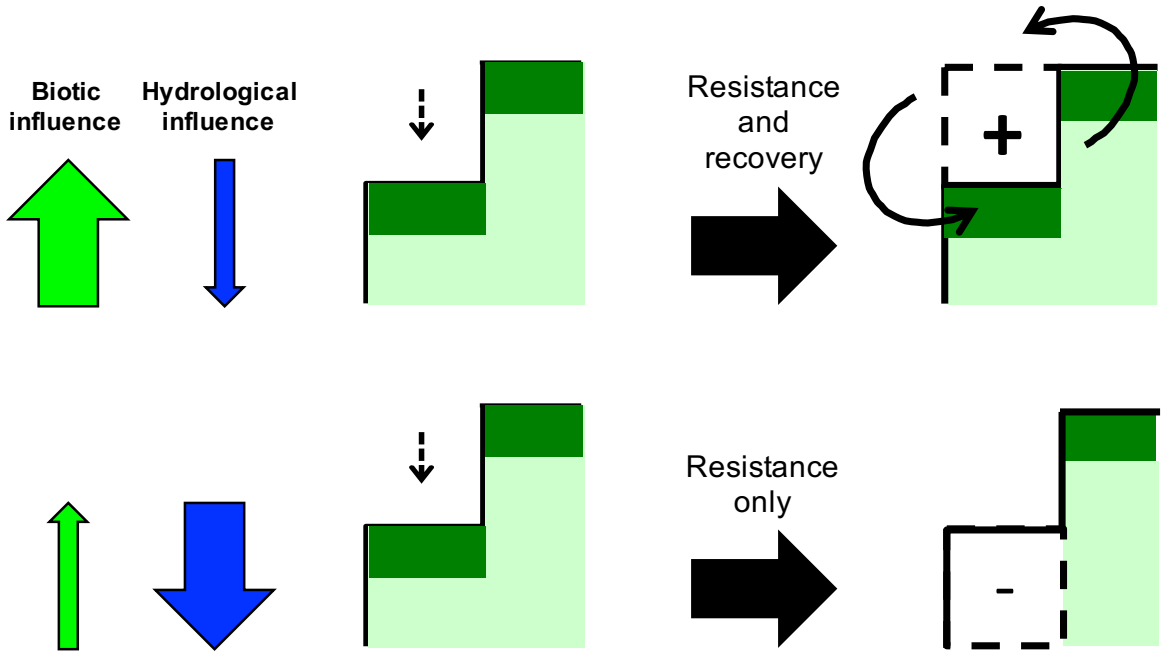

Figure 4.1 Heuristic to describe the potential role of slump blocks in influencing bank erosion. a When slump block resistance to erosion is greater than the hydrological force, the block can trap sediment from the water column and promote plant growth, leading to recovery of the bank edge in a cyclical process. b When hydrological forcing is greater than the resistance of a slump block to erosion, the slump block eventually erodes away and a new phase of bank erosion occurs.

Marsh deposits were between 50 and 70 years old (*Chapter 2*), and had a prominent eroding marsh cliff (~1.5 above the tidal flat) at the eastern end, with pioneer marsh species at the western end at the time of the study. Plant species consist of low- and mid-marsh species dominated by *Festuca rubra* dominated the higher elevated marshes, whilst *Spartina anglica* dominated the waterlogged areas behind creek levees. The site has intensive (>5 sheep yr ha^{-1}) sheep grazing (Prosser and Wallace, 2004).

4.2.2 Field survey

The creek network for study was extracted from a 1 m resolution LiDAR composite surface Digital Elevation Model (DEM) using the Hydrology toolset in ArcGIS. DEM was taken in 15/03/2009 provided through the Environment Agency (EA; available at https://data.gov.uk/dataset/lidar-composite-dsm-1m1). The creek network was divided into 5 m sections and classified as either 1st, 2nd or 3rd order channels. From this pool of 5 m creek sections, thirty were randomly selected. All transects were at least 20 m apart. Within each transect, 5 slump blocks were identified and 3 blocks randomly chosen for further analysis.

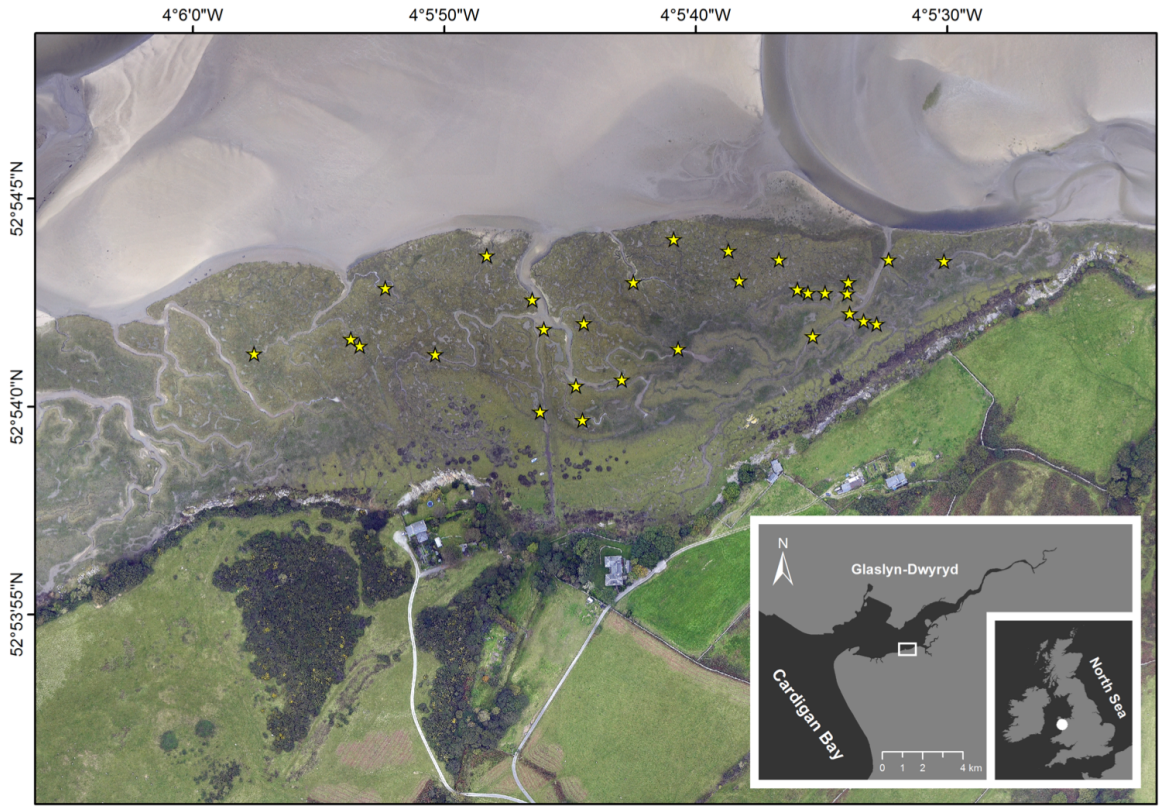

Figure 4.2 The study area in the Glaslyn-Dwyryd estuary, Cardigan Bay, UK.

4.2.3 Soil and vegetation characteristics

At each station, two stainless steel rings 3.1 cm in height, 7.5 cm in diameter were used to collect soil cores from the centre of a slump block just outside each creek transect. The first core was used to measure bulk density, moisture content, organic matter content and grain size, whilst the other core was used to measure dry root weight. Moisture content and bulk density were derived after drying at 105°C for 72 hours. A ~20 g subsample soil was used for estimating organic content, by loss on ignition (375°C, 24 h) (Ball, 1964). Grainsize analysis was done on a 5 g of dried soil, after 30% H_20_2 treatment; grain was classified into 100 size fractions between 0.2 and 2.0 µm using a Mastersizer 2000 and grouped into clay (0.2-2 µm), silt (2-50 µm), fine sand (50–200 µm) and coarse sand (200–2000 µm) fractions (Blott and Pye, 2012). The second soil core was carefully washed on a 2 mm sieve to extract total root dry mass (60°C, 24 h). Vegetation characteristics were measured within a 0.05 m^2 quadrat placed on each slump block. Plant species cover was assessed by eye, where cover exceeded >100% in the presence of a canopy. Diversity was calculated by species count. In each quadrat, an average of 5 plant heights was taken to the nearest 0.5 cm.

4.3.3. Peak flow velocity

Three Acoustic Doppler Velocimeters (ADVs, Nortek Vector) were used to capture the peak flood and ebb flow of the tidal current in each creek transect during spring tide. ADVs were moved between creek transects to capture peak flow between 20/07/16 and 16/09/16. The ADVs were placed in the centre of each creek ~25 cm from the creek bed with the North (X) axis faced toward oncoming flow. Bursts of 64 Hz every 2 minutes 30 seconds captured peak flow on the flood and ebb tides in each creek. A pressure sensor was used to isolate flow during each tide, and maximum peak and trough velocities were extracted in R (Figure 4.3).

4.2.4 Generating high-resolution creek surface models

Stereophotogrammetry was used to create high-resolution 3D reconstructions of each creek over multiple time periods, in order to quantify geomorphic change over time. 'Structure from Motion', a photogrammetry technique, was used to calculate the relative 3D positions of points extracted from commonly shared features visible in overlapping 2D image pairs (Egels and Kasser, 2003). The 3D 'point clouds' were converted to absolute scale using control points visible in the final model, for which XYZ coordinates were known. The rectified point clouds

were then converted to Digital Elevation Models allowing volume, elevation and area change of creeks and slump blocks, and rugosity (slump block presence) to be calculated.

4.2.5 Generating high-resolution creek surface models

Stereophotogrammetry was used to create high-resolution 3D reconstructions of each creek over multiple time periods, in order to quantify geomorphic change over time. 'Structure from Motion', a photogrammetry technique, was used to calculate the relative 3D positions of points extracted from commonly shared features visible in overlapping 2D image pairs (Egels and Kasser, 2003). The 3D 'point clouds' were converted to absolute scale using control points visible in the final model, for which XYZ coordinates were known. The rectified point clouds were then converted to Digital Elevation Models allowing volume, elevation and area change of creeks and slump blocks, and rugosity (slump block presence) to be calculated.

4.2.6 Image acquisition

Optimal image acquisition was based on methods used by Bretar et al. (2013). A commercially-available 12.1 megapixel Canon Powershot D20 digital camera was used for creek image acquisition. Before capturing photographs, the focal length was set to infinite, ISO was set to

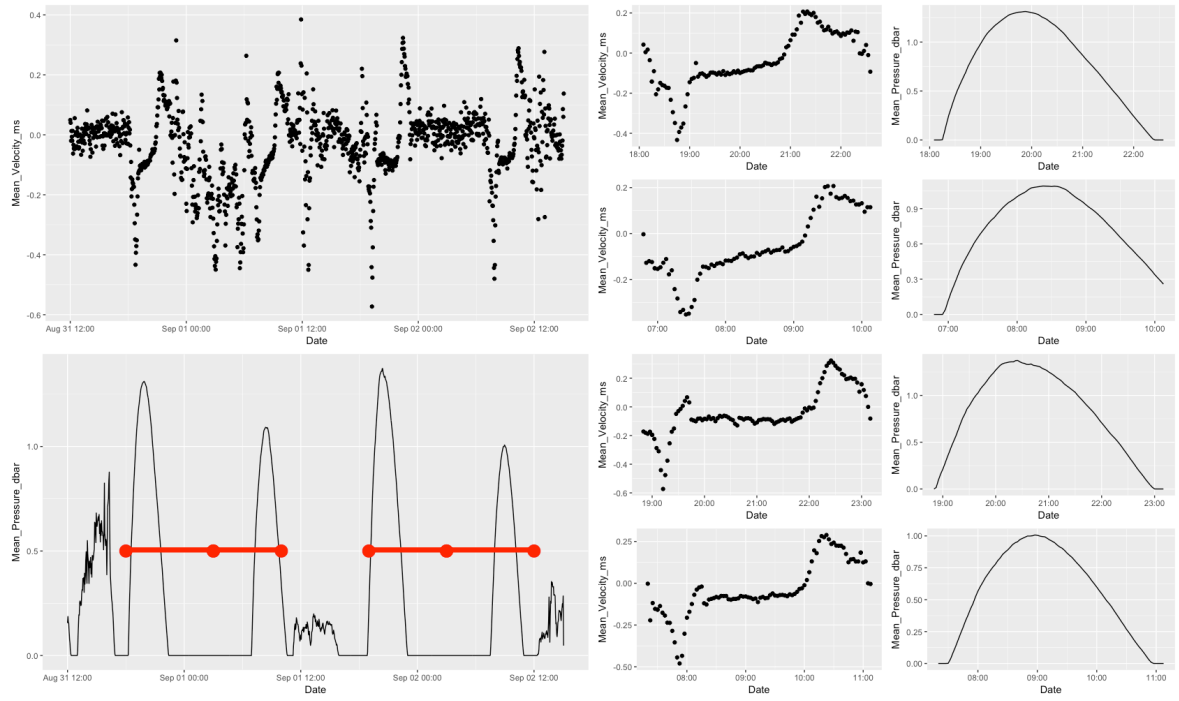

Figure 4.3 Example of velocity and pressure change over four tidal cycles in a saltmarsh creek measured from the current-facing probe of an Acoustic Doppler Velocimeter. When velocity and pressure change is subset to each tidal cycle, peak flood and ebb velocities can be extracted.

zero and white-balance was disabled. Installation of an open-source firmware update called CHDK allowed the use of an intervalometer to capture an image every 2 seconds once initiated.

Prior to commencing the year-long study, four 1.3 m fencing pins with a bracket on top were inserted into the outer edges of each creek (one at each end of the transect on both sides of the creek) to be used as Ground Control Points. At the start of each survey, four 25 cm^3 wooden cubes, pained red-blue-white to contrast the green-brown of the saltmarsh, were placed securely into the bracket to serve as well-distributed control points against which any change in creek geomorphology could be referenced. Care was taken to ensure the same cube was placed in the same bracket with the same orientation in each successive survey. Half-way into the survey period, X, Y coordinates (British National Grid, BNG) and elevation (meters, relative to Ordnance Datum Newlyn) of the centre of each cube were taken using a Leica Viva CS10 rtkGPS system. Points were only taken if an XYZ accuracy of 0.001 m was achieved. On occasion, this level of accuracy was unattainable because of a weak connection to the GNSS RTK Network, resulting in points having an accuracy ~0.003 instead. This was considered sufficient for the study of long-term geomorphic change.

In the field, photographs were only captured on overcast days to avoid light oversaturation when too sunny and image blurring when raining. Images were captured by mounting the camera on a telescopic pole, held oblique above a creek and angled downward ~2 m from the ground to capture vertical aerial images that were similarly oriented and perpendicular to the ground surface. Once the image capture sequence was initiated, the pole-and-camera was moved to capture a parallel strip to capture ~10 images that overlapped by ~90% for each creek. After acquisition, each image set was inspected to confirm the entire creek transect was captured and images had sufficient overlap.

4.2.7 Image processing

Georeferenced dense point clouds, Digital Terrain Models (DEMs) and orthorectified images of each creek were created using the open-source Apero-MicMac software (http://micmac.ensg.eu/index.php/Apero), a set of multi-view stereo software packages to generate 3D models from 2D images (Bretar et al., 2013). All processing was done using the High Performance Computing Wales / Supercomputing Wales network (https://portal.hpcwales.co.uk/). Creation of model outputs involves the completion of a

number of steps: *i*. a search among all image pairs for common tie-points to extract their position using a scale-invariant feature transform method (Lowe, 2004); *ii.* automatic computation of the relative orientation of each image (by comparing each image to a master, the order of which is prioritised by the number and distribution of tie-points, followed by the iterative and simultaneous adjustment of all initial orientations for optimal orientation); *iii.* addition of GPS points to the ground control point cubes visible in each image to order to convert from relative to absolute orientation; and *iv.* computation of a Digital Terrain Model where $z=f(x,y)$, over which mosaicked image sets are draped to form the orthoimage, and from which a coloured dense 3D point cloud is constructed (Figure 4.4).

The specific workflow used to generate DEMs was optimised for aerial photo acquisition (Bretar et al., 2013). Tie-points were first computed from a low-resolution image, 1/3 the original resolution for faster tie-point selection, then recalculated at step resolution to full resolution. Image pairs that had > 2 tie-points were used to generate the sparse point cloud (Tool: Tapioca MulScale). Tie-points were then calibrated against the optical properties of the sensor lens to correct for distortion (Tool: Tapioca RadialBasic). A sparse point cloud with camera positions was generated and checked for erroneous positions (Tool: AperiCloud). Bad images were removed where necessary and reanalysed. The absolute point cloud was then georeferenced by first converting the BNG projection to a readable format for MicMac (Tool:

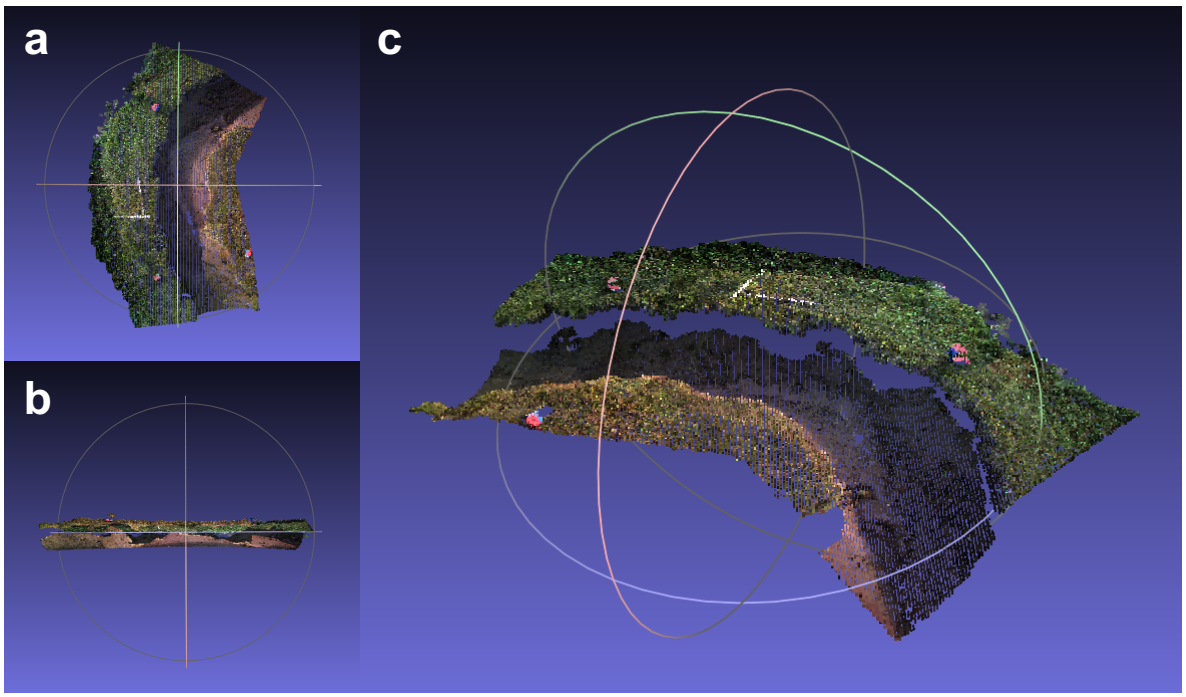

Figure 4.4 Example of a dense point-cloud reconstruction of a saltmarsh creek from **a** bird's eye, **b** side and **c** oblique view. Number of vertices are 4,334,946. White meter sticks in each point cloud are 1 m.

GCPBasclue), then assigning the coordinates of each GCP to the centre of each block visible in each image. At least 3 control points were added where the block appeared in at least two images (Tools: SaisieAppuisInit and SaisieAppuisPredic). The point clouds were optimised to fit between relative camera positions and the added point cloud (Tools: GCPBascule and Campari), then the final orthoimage, dense point cloud, and the DEM models were exported (Tools: MaltOrtho, Tawny and Nuage2Ply). DEMs had a pixel size of 0.0028 x 0.0028 m and elevation accuracy of ± 10 mm. See Appendix X for script used to process the images.

4.2.8 Erosion Rate and Slump Block Extraction

Surface information from all DEMs were extracted using a series of ArcMap 10.4 tools, and batch processed in Python. Prior to exacting predictor and response variables from the DEMs, each creek survey was cropped to a standard size in order to remove erroneous results at the border of each DEM. The target slump blocks were bounded by a polygon visible in the first dataset (14/10/14) with the aid of the orthoimage and hillshading of the DEM, and a series of 25, 50 and 100 cm buffers around each slump block were drawn. The 'marsh platform' and 'creek basin' were also distinguished. An example of geomorphic change in three creeks over the year period are shown in Figure 4.5.

Bathymetric Point Index (BPI) was used to separate the 'creek basin' from the 'marsh platform' using the Benthic Terrain Modeller. BPI calculates the relative elevation difference between DEM raster cells, and assigns positive values for areas that are shallower than their surroundings, and negative values represent locations that are deeper than their surroundings. Larger values represent steeper gradients, whereas values near zero indicate either flat or constant slope surfaces (Gafeira et al., 2015). By this way, topographic features can be identified, and the approach was found an efficient way to differentiate the 'concave' creek from 'convex' marsh platform. BPI is scale-dependent, therefore the number of pixels used in its derivation should broadly represent the feature being reconstructed. As such, all neighbouring cells in an annulus with inner and outer radii of 250 and 500 cells respectively were included (representing typical width of the creeks, and the length of the DEM raster). BPI values are represented as integers, which required that creek DEMs be converted to mm before BPI processing in order to remove decimal places. Once the BPI model was constructed, values above 0 were classified as 'marsh platform' (concave), and BPI values below 0 were classified as 'creek basin' and converted to a polyline shapefile. Holes in each shapefile were filled, then

used to crop the original DEM to extract 'creek basin' and 'marsh platform'. DEMs were then converted back to meters.

Rate of bank edge migration immediately behind each slump block was taken from the distance moved by the creek bank edge between 14/10/14 and 13/10/15. Positional movement was calculated from a transect perpendicular to the creek channel centre, drawn from the centre of a slump block to the marsh platform for time-series for each creek. Change in creek basin area was calculated to measure bank edge erosion for the entire creek basin and for the basin area contained within the buffers around each slump block. Change in volume was used to measure erosion rate of the entire creek basin, individual slump blocks, and the buffers around each slump block. For each time-series, volume of each creek basin was taken above a reference plane set at 0 m OD. Volume of each slump block, and surrounding buffers, were taken above a reference plane defined by the minimum elevation of each slump block in 14/10/14. Volume of slump blocks in 14/10/14 were taken as initial slump block size, and the average elevation within the boundary of each slump block polygon was also taken to calculate initial mean slump block elevation.

Rugosity was calculated as a proxy for slump block presence within the creek basin. Arc-Chord Ratio (ACR) was used as a measure of rugosity, as ACR decouples surface roughness from the underlying slope of a surface (Du Preez, 2015). ACR is estimated between neighbouring raster pixels, therefore raster pixel size is important in determining a meaningful ACR value. A pixel size of 0.05 × 0.05 m was chosen to separate slump blocks from smaller-scale deformities on

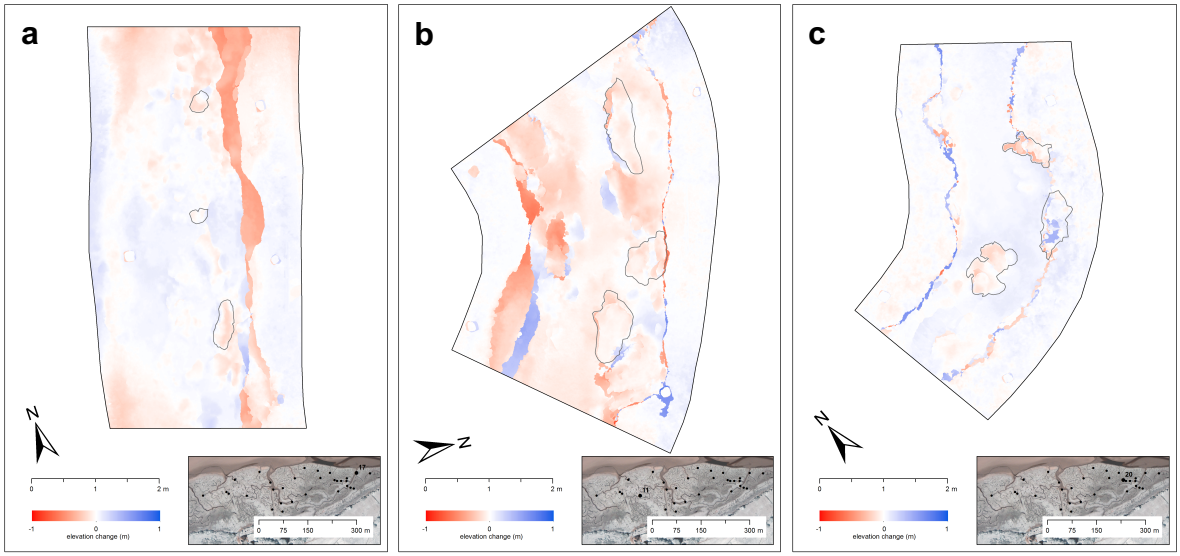

Figure 4.5 Elevation gain (blue) and loss (red) for three creek transects at **a** 1st **b** 2nd and **c** 3rd order creeks between 14/10/14 and 13/10/15. Grey polygons represent the outline of slump blocks.

the creek basin including ripples and debris. Prior to generating a rugosity layer for each 'creek basin', identified from the BPI analysis, the outer 0.05 cm of the creek basin perimeter was cropped to remove the influence of high rugosity values caused by sharp relief at the creek edge. Median rugosity index was then extracted from the rugosity layer as a predictor variable.

4.2.9 Statistical analysis

Relationship between slump block metrics and creek bank change was examined using linear regression. Variables were cube-root transformed where necessary to meet the assumptions of homogeneity of variance, and were checked for outliers. For comparing the means of biotic and abiotic characteristics between vegetated and bare slump blocks, distributions were first verified for normality and homoscedasticity then compared using either parametric Student's t-test or non-parametric Wilcoxon-Mann-Whitney test. Prior to examining the role of biotic and abiotic predictors on slump block and creek bank / basin erosion, multicollinearity between predictors was assessed using Variance Inflation Factor tables to successively remove predictors with VIF scores greater than three (Zuur et al., 2010). Comparison between a maximal mixed-effects model and linear model using 'REML' was done to investigate whether inclusion of slump blocks as random factor significantly improved the model (Zuur et al., 2009). A linear model structure was chosen, and the best-fit model identified using the 'forwards-and-backwards' step-wise regression method with AIC selection in the 'MASS' package (Ripley et al., 2013). The individual contribution of each predictor in the best-fit model to the overall variation explained by model was calculated using the 'relaimpo' package (Grömping, 2006). All statistical analyses were done using R.

4.3 Results

4.3.1 Relationship between hydrology and creek erosion

Between October 2014 and 2015, creek basin volume and bank edge change were determined across five spatial scales: immediately behind a slump block (1 cm), 25, 50 and 100 cm within the perimeter of a slump block, and for the entire creek section (500 cm: approx. 15 m^2). Creek bank and basin erosion increased with increased spatial scale: The mean rate of bank erosion immediately behind a slump block was -3.09 ± 8.20 cm yr^{-1}. Mean expansion in creek basin area (i.e. creek area widening) was 1.45 ± 9.95, 1.40 ± 9.43 and 1.95 ± 8.61 cm^2 yr^{-1} for 25, 50 and 100 cm around each block respectively. Mean creek basin volume expansion were 28.41 ± 128.37, 60.39 ± 276.87 and 152.07 ± 615.38 cm^3 yr^{-1} for 25, 50 and 100 cm around each

block respectively. For the entire creek section, mean creek basin area and volume were 1.97 ± 17.08 cm^2 yr^{-1} and 1303.32 ± 2,9392.22 cm^3 yr^{-1} respectively. Mean peak current speed and inundation period between peak flows (the main perceived drives of creek erosion) were 0.36 ± 0.18 m s^{-1}, and 175 ± 25 minutes respectively. There were no significant relationships between either bank edge change or creek basin volume change with peak current speed inundation period between peak flows (Figure 4.6).

4.3.2 Direct influence of slump blocks on creek bank erosion

Slump maximum erosion and expansion rates were -159 and 101 cm^3 yr^{-1} respectively. Slump block volumes initially ranged between 0.002 and 0.250 m^3 (0.02 to 0.68 m^2), and the difference in height between the highest and lowest block was 80 cm. Bank erosion-expansion rate was positively related to block rate change ($P < 0.001$, $R^2 = 0.18$) (Figure 4.7 a), and there was no significant relationship of either initial block volume or height of a block in the creek with the rate of creek bank erosion (Figure 4.7 b and c). When grouped according to whether

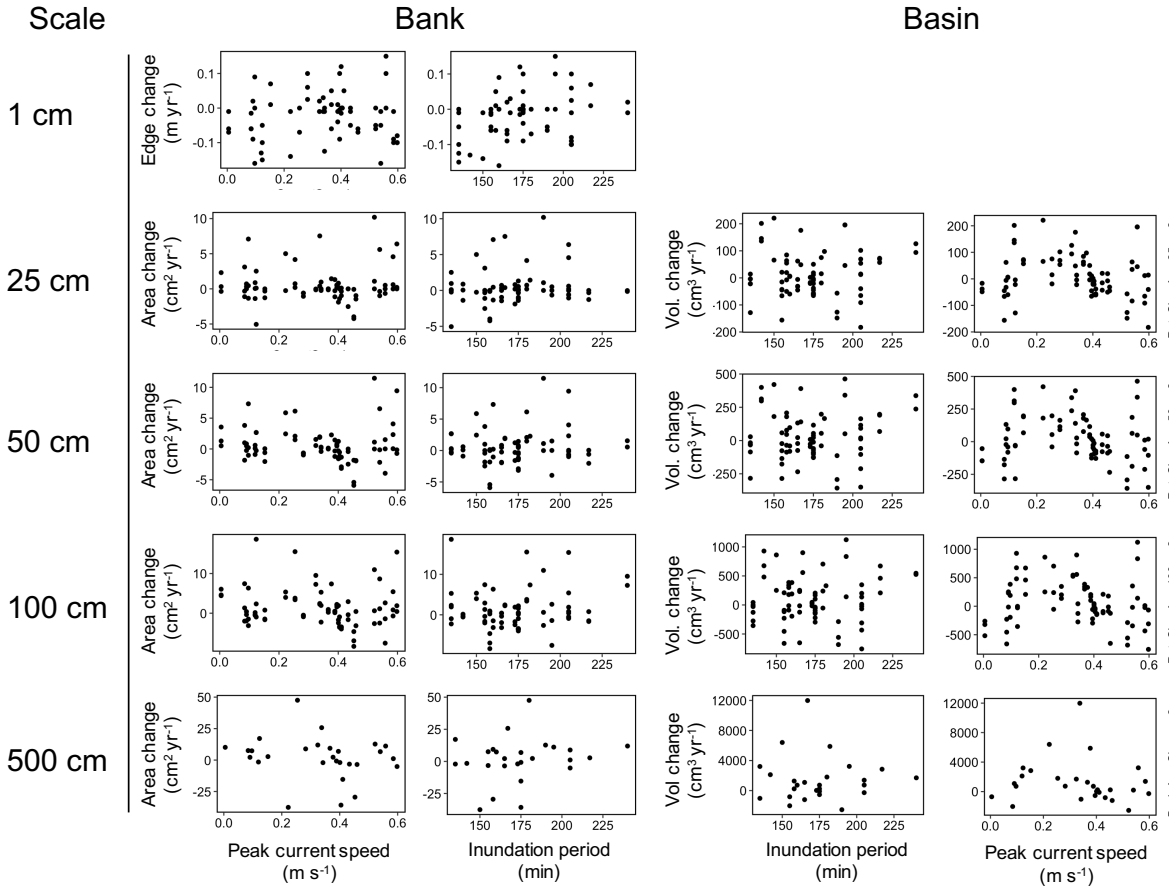

Figure 4.6 Relationships between hydrological forcing (peak current speed and inundation period) and change in creek bank erosion (migration of the creek bank edge, area of the creek bank and volume change of the creek basin) at five spatial scales: creek bank erosion immediately behind a block (1 cm), bank-basin change within 25, 50 and 100 cm of a slump block, and bank-basin change at the entire creek transect scale (500 cm).

blocks were ‘vegetated’ or ‘bare’, erosion-expansion rates of the creek bank had a stronger relationship with vegetated blocks ($P < 0.001$, $R^2 = 0.42$; blue line in Figure 4.7 a) than bare blocks ($P = 0.007$, $R^2 = 0.15$; red line in Figure 4.7 a). Bank erosion was significantly, but weakly, related to increases in initial volume of ‘vegetated’ blocks ($P = 0.031$, $R^2 = 0.14$; blue line in Figure 4.7 b), and to increases in the height of ‘bare’ block within the creek ($P = 0.012$, $R^2 = 0.13$; red line in Figure 4.7 c).

The rate of creek volume change within 25 cm of a slump block was positively related to slump block rate of volume change for all blocks ($P < 0.001$, $R^2 = 0.50$; Figure 4.8 a), and when ‘vegetated’ and ‘bare’ blocks were considered separately ($P < 0.001$, $R^2 = 0.39$; blue line, and $P < 0.001$, $R^2 = 0.48$; red line in Figure 4.8 a respectively). This relationship persisted across the 50 and 100 cm buffer around each block, but became progressively weaker (Figures 4.8 b and c). There were no relationships between the rate of volume change around a slump block and initial slump block volume at any scale (Figures 4.8 d-f). There was a weak relationship between rates of volume change and block elevation within the 25 cm boundary of slump blocks ($P = 0.030$, $R^2 = 0.05$; Figure 4.8 g), which was stronger when bare slump block alone was considered ($P = 0.012$, $R^2 = 0.12$; red line in Figure 4.8 g), indicating that blocks situated below ~ 1.6 m increase rate gain in volume and increase rate loss in volume above 1.6 m. This relationship strengthened slightly with increasing scales of 50 and 100 cm buffers around each slump block (Figures 4.8 h and i).

Within a 25 cm perimeter around each slump blocks, change in the area of the creek basin had a significant positive relationship with slump block volume change ($P = 0.002$, $R^2 = 0.10$; Figure 4.9 a), that was more pronounced with bare blocks ($P = 0.001$, $R^2 = 0.19$; red line in Figure 4.9 a) relative to the vegetated blocks. Therefore, positive rates of slump block accretion were associated with bank expansion, whereas positive rates of slump block erosion were associated with bank erosion. This trend disappeared over the larger scales of 50 and 100 cm (Figures 4.9 b and c). Rate change in creek area showed a weak significant increase as the size of slump blocks increased within 25 cm of the block ($P = 0.015$, $R^2 = 0.06$; Figure 4.9d), and was significant for vegetated blocks ($P = 0.005$, $R^2 = 0.21$; blue line in Figure 4.9 d), but not significant for bare blocks. This trend became weaker over 50 and 100 cm buffers for vegetated blocks only (Figures 4.9 e and f). No significant relationship was observed between rate change in creek area and height of the block in the creek across 25, 50 and 100 cm scales (Figures 4.9 g-i).

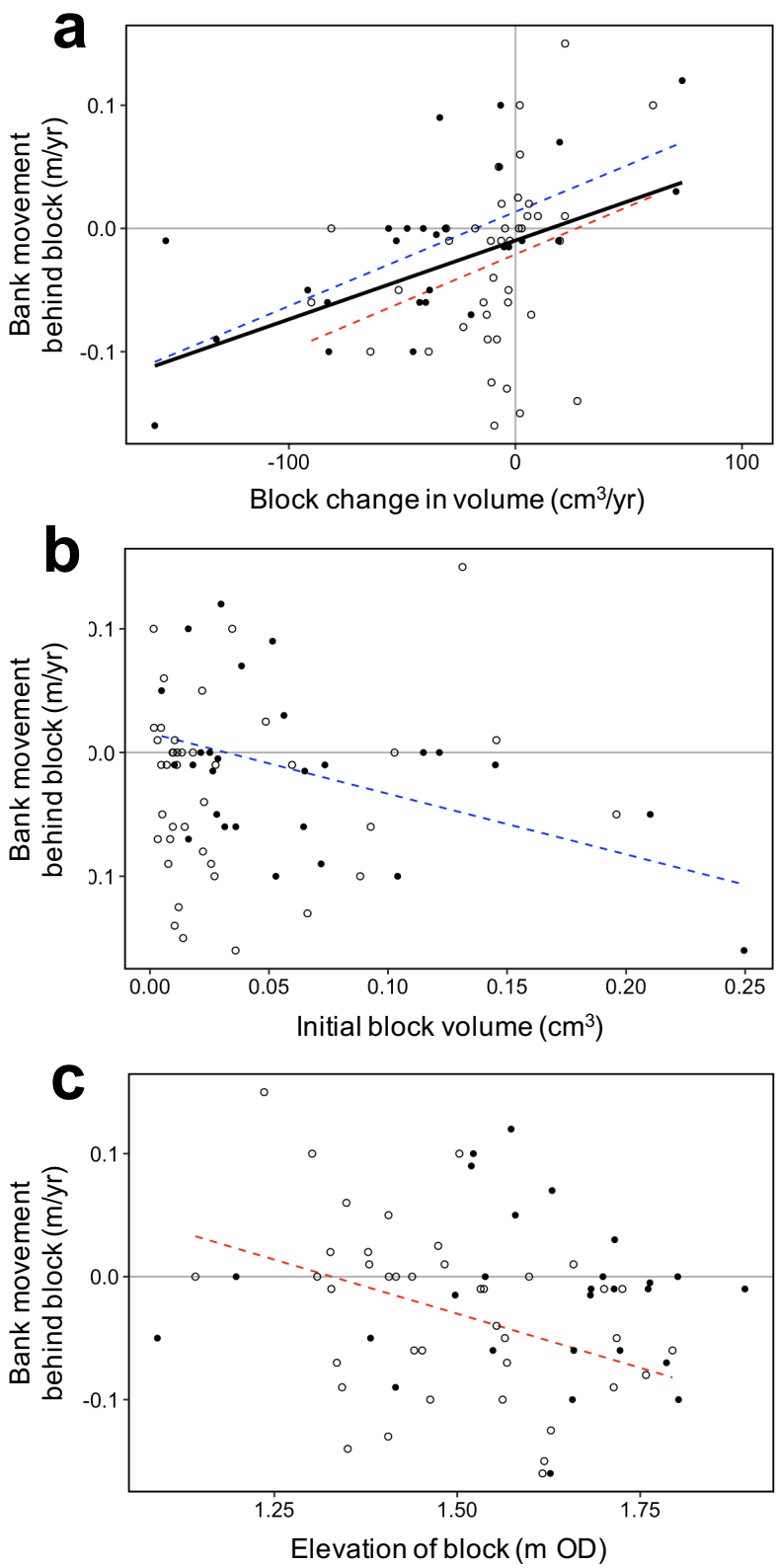

Figure 4.7 Relationship between the rate of creek bank erosion or accretion directly behind a slump block with **a** rate change in slump block volume, **b** initial slump block volume and **c** elevation of the slump block in the creek. Solid black line represents a trend line if significant for the entire dataset. 'Vegetated slump blocks are represented as filled circles with a blue dashed trend line if significant, whereas 'bare' slump blocks are represented as hollow circles with a red dashed trend line if significant.

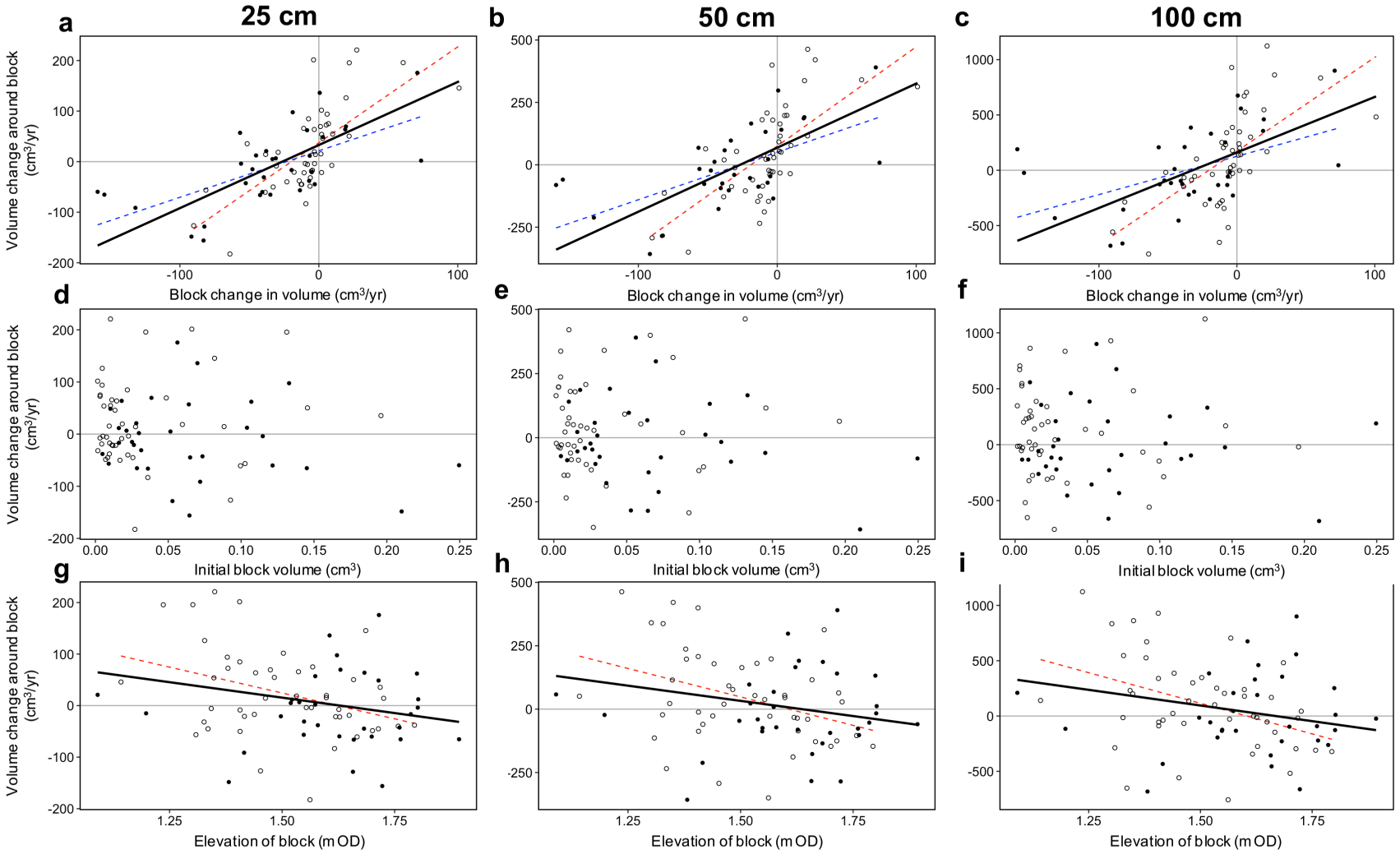

Figure 4.8 Relationship between the rate of volume change within a 25, 50 and 100 cm buffer around each slump block and **a-c** rate change in slump block volume, **d-f** initial slump block volume and **g-i** elevation of the slump block in the creek. Solid black line represents a trend line if significant for the entire dataset. 'Vegetated slump blocks are represented as filled circles with a blue dashed trend line if significant, whereas 'bare' slump blocks are represented as hollow circles with a red dashed trend line if significant.

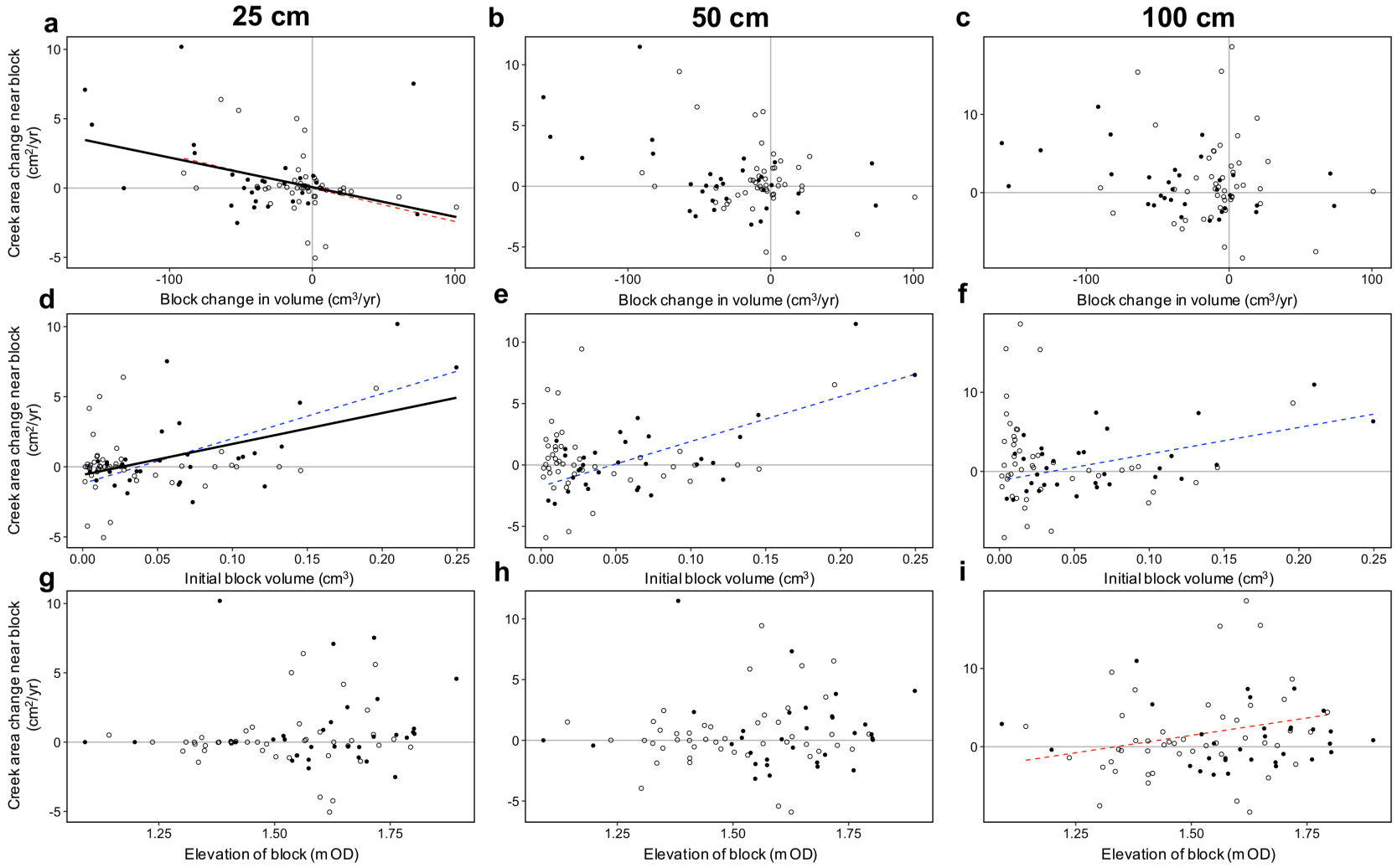

Figure 4.9 Relationship between the rate change in the creek basin of each creek within a 25, 50 and 100 cm buffer around each slump block and **a-c** rate change in slump block volume, **d-f** initial slump block volume and **g-i** elevation of the slump block in the creek. Solid black line represents a trend line if significant for the entire dataset. 'Vegetated slump blocks are represented as filled circles with a blue dashed trend line if significant, whereas 'bare' slump blocks are represented as hollow circles with a red dashed trend line if significant.

Across the entire creek, the largest volume gain was 11,985 cm^3 yr^{-1}, and the largest loss was -2,548 cm^3 yr^{-1}. Largest expansion of the creek basin was 48 cm^2 yr^{-1}, whilst the largest loss was -38 cm^2 yr^{-1}. Rate change in channel area or rate of channel volume change were not significantly related to change in rugosity (a proxy for slump block abundance) (Figures 4.10 a and b).

4.3.3 Relative importance of biotic and abiotic factors on slump block erosion

Average rate of volume loss in slump blocks was five times greater when slump blocks were vegetated (~ -35 cm^3 yr^{-1}) compared to bare (~ -7 cm^3 yr^{-1}) blocks, however when volume loss rate was standardized by initial slump block volume, there was no significant difference. Vegetated blocks were larger (~ 0.07 m^3) than bare blocks (~ 0.03 m^3) and were situated at higher elevations in the creek (~ 1.6 m OD) than bare blocks (1.5 m OD). There were no significant differences in flow and soil characteristics between vegetated / bare slump blocks (Table 4.1).

Step-wise regression produced a best-fit model that found three variables explained 17% of the overall variation in slump block erosion (Table 4.2). Grain size (clay-silt fraction) and root content accounted for ~40% of the model variation each, whilst current speed was marginally significant and explained 20% of model variation. For each significant variable, slump block erosion decreased with higher clay-silt content, higher root content (Figures 4.11 a and b), and erosion rate increased with increasing current speed (Figure 4.11 c). When separate step-wise regression was done for 'vegetated' and 'bare' slump block erosion rates, and best fit models compared (Table 4.2), the most noticeable differences were: i. the overall model variation rose

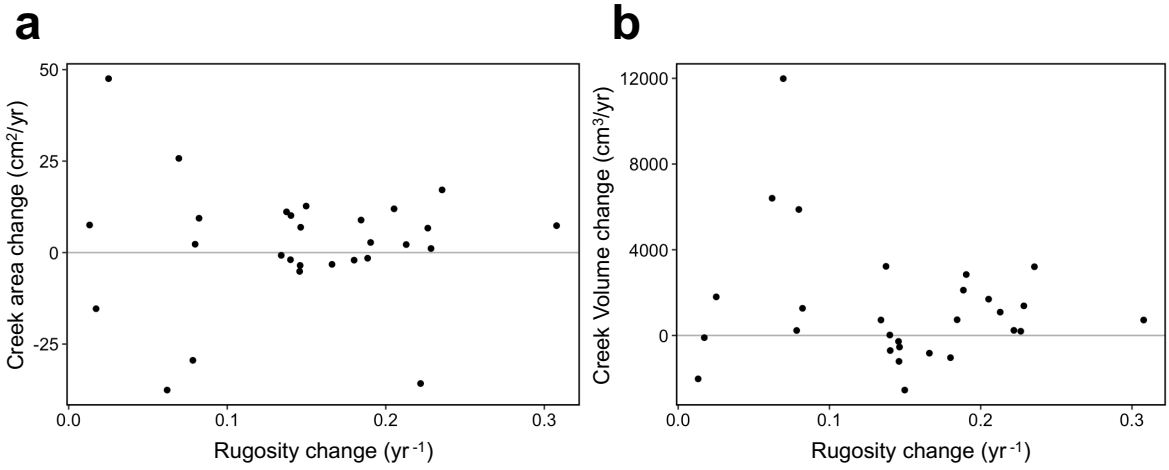

Figure 4.10 Relationship between rugosity change (a proxy for the presence of slump blocks in a creek) and **a** change in creek basin area, and **b** change in creek basin volume.

from the 'full' model to 50% and 28% for 'vegetated' and 'bare' blocks respectively, ii. there was a shift in the type of variable that exerted the greatest influence in the best fit models, where root content accounted for 60% of model variation when only 'vegetated' blocks were considered, and current speed and clay-silt fraction explained 50% and 40 % of the model variation respectively when only 'bare' blocks were considered. Significant relationships are shown in Figures 4.11 d-h.

4.4 Discussion

From a year-long analysis of saltmarsh creek evolution, this study showed that short-term erosion of the marsh edge leads to the emergence of slump blocks that provide a localised and long-term protection against further bank edge erosion, independent of the wider hydrological regime. Specifically, the study shows that *i.* the rate of slump block erosion-accretion is related to the retreat-expansion of the creek edge and volume gain-loss at the creek bank; *ii.* creek edge and slump block erosion have a stronger relationship when blocks are 'vegetated', and erosion of 'bare' blocks located lower in the creek are associated with greater volume loss at the creek bank; *iii.* tidal flood speed and duration were not significant drivers of either creek bank volume loss or edge erosion at any scale; *iv*. longer-lived blocks had higher root content when blocks were 'vegetated', and higher clay-silt fraction with lower flow rates when blocks were 'bare';

Table 4.1 Characteristics of vegetated and bare slump blocks. Values represent means ± SD.

	Vegetated (n=35)	Bare (n=49)	P
Metrics			
Slump block erosion (cm^3/yr)	-34.88 ± 52.45	-7.17 ± 31.02	*
Initial slump block volume (m^3)	0.065 ± 0.058	0.034 ± 0.044	***
Standardized block erosion	-0.0006 ± 0.00095	-0.00012 ± 0.00141	n.s.
Elevation (m OD)	1.61 ± 0.17	1.50 ± 0.15	***
Flow			
Peak current speed (m/s)	0.312 ± 0.181	0.346 ± 0.164	n.s.
Inundation time (min)	170.93 ± 21.74	176.12 ± 26.67	n.s.
Distance from marsh edge (m)	96.55 ± 51.02	101.02 ± 66.99	n.s.
Soil			
Clay-Silt Fraction (%)	45.28 ± 22.40	52.44 ± 20.24	n.s.
Organic matter content (%)	3.48 ± 1.99	3.82 ± 1.39	n.s.
Bulk Density (g/cm^3)	1.10 ± 0.19	1.06 ± 0.14	n.s.
Moisture Content (%)	42.13 ± 13.13	44.43 ± 10.23	n.s.
Root Content (g)	1.10 ± 0.90	1.35 ± 1.01	
Surface			
Vegetation height (cm)	6.50 ± 4.13	-	-
Plant cover (%)	65.75 ± 45.27	-	-
Species Richness	3.19 ± 1.55	-	-

*$P < 0.05$, **$P < 0.01$, ***$P < 0.001$, n.s. = not significant.

and *iv*. the effect of slump blocks on both creek bank erosion and migration diminished at larger scales, suggesting their influence on marsh erosion was localised.

While the study did not experimentally manipulate slump block presence/absence, and therefore cannot identify a causative effect of blocks on bank erosion, rates of both creek bank and creek basin erosion are more closely associated with slump block erosion than current flow or tidal inundation (the perceived dominant mechanism for long-term marsh evolution). This observation indicates that, in parts of the creeks where slump blocks were present, the rate of block dissolution was more important in determining bank erosion than the exposure to diurnal current flow alone. The direct mechanistic role of slump blocks in armouring bank erosion has previously been demonstrated (Gabet, 1998), however our study highlights that the ability of a block to reduce bank erosion is dependent on the rate of slump block erosion. Increasing resistance of slump blocks against erosion were associated with a shift from creek bank erosion to accretion. Slump block-associated infill and creek bank expansion has been reported to occur in a microtidal clay-rich marsh of San Francisco Bay, US, where blocks form low-elevation 'tables' that trap sediment immediately behind and in the vicinity of slump blocks and eventually become colonised by saltmarsh plants (Gabet, 1998; Mariotti et al., 2016). Slump block controls have also been described in macrotidal, sand-rich marsh in north-west UK marsh, where blocks are sufficiently large to impede water flow in the creek and cause sedimentation behind the blockage (Yapp et al., 1917; Goudie, 2013). Along marsh creeks in the hypertidal Severn estuary, UK, intermittent phases of creek bank failure have been followed by prolonged periods of mud-lamina accumulations on top of and behind slump blocks, that appear to have occurred cyclically at least five times over 300 years (Allen, 1985). These indicate slump blocks can provide a resilience mechanism in contrasting marsh systems.

Table 4.2 Predictor variables of slump block erosion (rate of volume change), identified from best-fit models (step-wise regression) when all slump blocks are considered, only vegetated blocks are considered, and only bare blocks are considered.

Model variables	Estimate	SE	*t*-Value	*P* value	R^2
Best model fit: vegetated and bare slump blocks (AIC = 653.83, F = 4.06, *df* = 3, 59, *P* = 0.011 *, R^2 = 0.17, n = 63)					
Clay-silt fraction (%)	0.875	0.303	2.884	0.005 **	0.41
Root content (g)	15.450	5.466	2.827	0.006 **	0.42
Peak current speed (ms^{-1})	-12.745	5.803	-2.196	0.032 *	0.17
Best model fit: vegetated slump block only (AIC = 277.31, F = 5.07, *df* = 4, 21, *P* = 0.006 **, R^2 = 0.49, n = 26)					
Root content (g)	52.049	13.194	3.945	7.410×10^{-4} ***	0.59
Plant cover (%)	-0.695	0.243	-2.861	0.009 **	0.24
Species richness	22.061	8.176	2.698	0.013 *	0.14
Elevation (m OD)	82.119	51.615	1.591	0.127 n.s.	0.04
Best model fit: bare slump blocks only (AIC = 348.79, F = 4.24, *df* = 3, 33, *P* = 0.012 *, R^2 = 0.28, n = 37)					
Peak current speed (ms^{-1})	-80.577	26.214	-3.074	0.004 **	0.51
Clay-silt fraction (%)	0.779	0.277	2.811	0.008 **	0.38
Root content (g)	8.117	4.308	1.844	0.068 n.s.	0.11

*$P < 0.05$, **$P < 0.01$, ***$P < 0.001$, n.s. = not significant.

In addition to the similarities in mechanism to contrasting systems, our study indicated that the relative importance of 'vegetated' and 'bare' blocks on bank erosion processes were subtly different: high-elevation vegetated block erosion had a stronger association with creek edge retreat rate, whereas erosion of low-elevation bare blocks had a stronger effect on volume loss of the creek bank, and promoted accretion where blocks were located lower in the creek. 'Vegetated' and 'bare' blocks collectively may therefore influence bank erosion by affecting

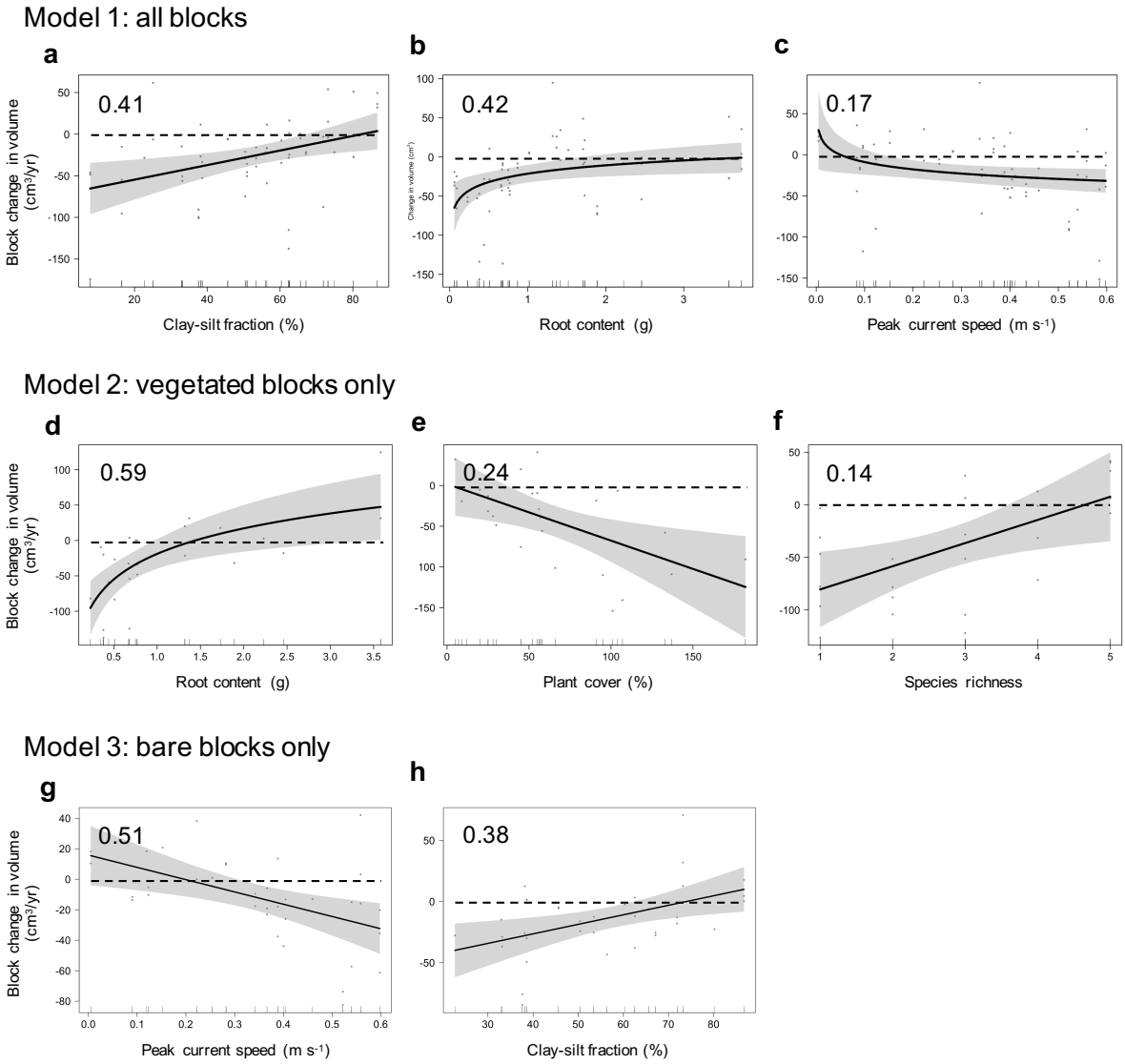

Figure 4.11 Relationships between the rate change in slump block volume and significant predictor variables identified from three separate stepwise regression models. In model 1, where all slump blocks are considered, **a** clay-silt fraction, **b** root content, and **c** peak current speed were significant predictors. In model 2, where only vegetated blocks are considered, **d** root content, **e** plant cover, and **f** species richness were significant predictors. In model 3, where only bare blocks are considered, **g** peak current speed, and **h** clay-silt fraction were significant predictors. The y-axes are scaled by the linear predictor. Value in the top-left corner is the relative importance of a given variable in the model. Data points represent distribution of standardized partial residuals. Dashed lines indicate the threshold between block erosion and accretion. Solid lines represent model-fit though the data. Grey ribbon represents the 95% confidence interval. Tick marks along the bottom of each plot denote deciles of the distribution of each predictor value.

different parts of the erosion process (Figure 4.12). The process of bank erosion requires both the removal of sediment at the base of a cliff (end-point control; Thorne and Tovey (1981)) and the erosion of weaker soil located between the root layer and deeper compacted soils (Chen et al., 2012). The position where blocks are deposited may be a crucial control on the potential resistance and recovery capacity of slump blocks. Contributions of individual slump blocks on creek bank and basin erosion were found to be highly localised, with a rapid decline of influence on the surrounding creek basin / edge over a larger spatial scale, placing constraints on the capacity of slump blocks to act as a 'resilient mechanism' to promote marsh edge recovery.

It is likely that creek bank erosion produces 'vegetated' blocks, which migrate nearer the bank basin over time via soil creep, by which process the soil is slowly moved downslope by gravity (Mariotti et al., 2016). Vegetated slump blocks can facilitate the spread of vegetation down the creek bank and onto any accumulated sediment between blocks (Allen, 1989; 2000), responsible for low-elevation tables described by Gabet (1998). At further depth into the creek, however, few vegetated slump blocks were identified in this study. Plant-bearing slump blocks may migrate sufficiently low in the tidal frame at the point bar, so that the capacity of plants to tolerate inundation stress is exceeded and blocks become bare (Kim et al., 2012), and are smaller in size than vegetated blocks due to prolonged exposure to tidal current action (Friedrichs and Perry, 2001). This study was not of sufficient length to capture soil creep, however it is hypothesised that a 'conveyor belt' mechanism ensures the long-term role slump blocks have in protecting marsh banks form erosion: shifting their importance from protecting the loose layer from erosion, to then protecting the basal zone from erosion (Figure 4.12). The dual-role of slump blocks on regulating bank erosion and in cases promoting recovery has not previously been described, and may represent an important mechanism for controlling local bank erosion rates. Bank erosion therefore appears to initiate a negative feedback cycle whereby the products of bank erosion can promote local-scale recovery similar to other self-organized processes observed within the marsh system including seaward marsh edge collapse and recovery (van de Koppel et al., 2005) and salt-pan expansion and contraction (Wilson et al., 2014; Mariotti, 2016).

The capacity of blocks to resist erosion and promote recovery of the creek was dependent on their rate of erosion. Higher root content was more important in reducing 'vegetated' block erosion, whereas lower flow rates alongside higher clay-silt fraction in the soil were more

important in reducing erosion rates of 'bare' slump blocks. The role of root-rich soils in resisting erosion through cohesion and binding is well established grasslands (Reid and Goss, 1981; Gyssels and Poesen, 2003; De Baets et al., 2006; Reubens et al., 2007), and are recognised as important erosion control in exposed bank of ecohydrological landscapes (van Eerdt, 1985; van Hulzen et al., 2007; Gedan et al., 2011, Francalanci et al., 2013; Gurnell, 2014; Ford et al., 2016). It is plausible that roots were not an important explanatory variable for controlling erosion in 'bare' slump blocks because the binding capacity of roots can become compromised by vegetation loss and root death (Dawson et al., 2000; Silliman et al., 2012). Current flow and clay-silt content therefore become more important in controlling 'bare' block erosion. Increased clay-silt content in the soil is recognised to increase soil cohesion and resist erosion (Feagin et al., 2009), and blocks situated lower in the creek are therefore exposed across the entire surface to tidal inundation for longer than 'high-elevation' vegetated blocks. Whilst high hydrological action is effective at removing failed bank debris along creek banks (Allen, 1989), channel change is limited by intrinsic properties of bank sediments that act to resist erosion alongside tidal currents that are too weak to remove debris from the bank base (Allen, 2000).

The stability of saltmarsh soils has been shown to decrease with grazing pressure (Smith and Odum, 1981), eutrophication (Deegan et al., 2012), vegetation die-back (Lottig and Fox, 2007),

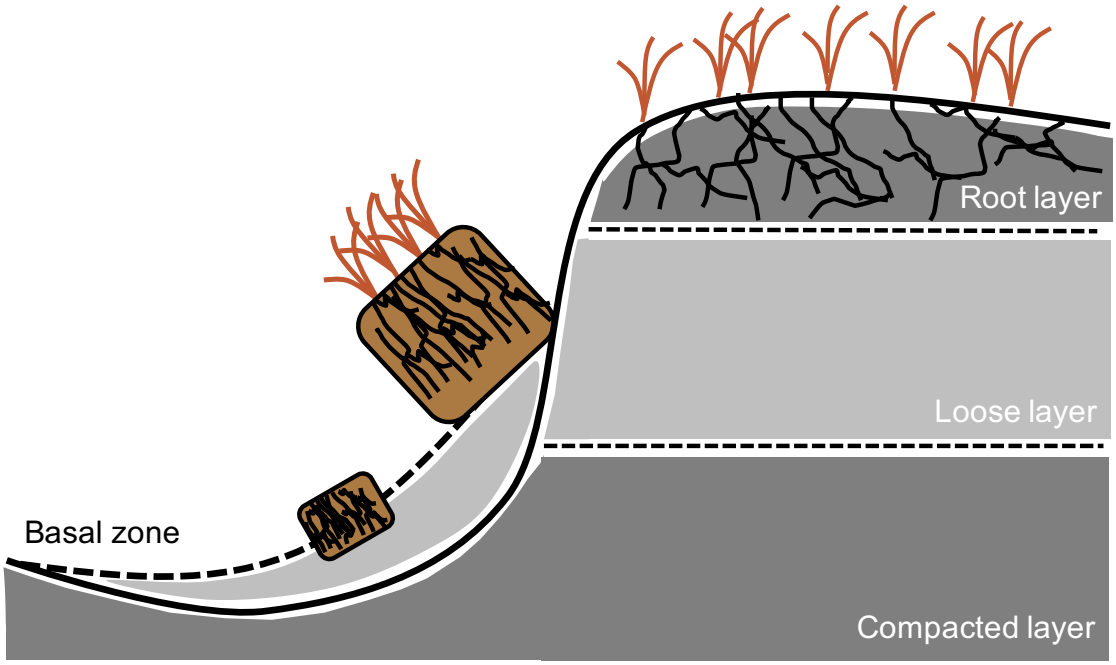

Figure 4.12 Hypothetical condition where slump block placement at the creek bank optimise bank stability and promote marsh accretion. Dark grey regions are less susceptible to erosion, whereas light grey regions are vulnerable to erosion.

bioturbation (Hughes and Paramor, 2004) and soil hypoxia (Ursino et al., 2004) that compromise the binding capacity roots. Compromised root structure would increase 'vegetated' slump blocks erosion rates and inhibit their capacity to resist bank erosion and promote recovery. Moreover, marsh systems with sea level rise and low sediment supply are characterised by increases in marsh creek width and depth as a result of changes in the flowing tidal prism (D'Alpaos et al., 2007; Stefanon et al., 2012), thereby displacing blocks too deeply within the creek to influence both soil erosions beneath the root layer or influence basal end-point removal (Figure 4.12). Slump blocks therefore provide a resilience mechanism that may account for observations of low creek migration despite marsh edge erosion, until the capacity of marsh systems to recover from creek edge erosion is compromised, leading to rapid creek erosion and internal marsh dissection, as observed in coastlines with rising relative sea level and low sediment supply (van der Wal and Pye, 2004; Ganju et al., 2015).

4.5 Conclusions

The results presented here indicate that slump blocks provide a 'dual-role' in protecting against bank erosion, with young vegetated blocks armouring the upper bank and old bare blocks armouring the base. However, this relationship was weak, and was an effect that is localised to within several centimetres of a block. The importance of root content in regulating slump block erosion indicates a strong biotic influence over hydrological forcing on the fate of creek bank erosion. This is, however, less prominent for bare blocks where intensity of current flow and clay-silt becomes important. Lower rates of slump block erosion result in a shift to accretion, which promotes the recovery of the bank edge. Across a longer timescale, it is likely that bank edge erosion and accretion represent a cyclical, self-organizing process similar to other such cycles commonly observed in saltmarshes. However, reductions in the biotic influence on slump block erosion through compromised vegetation health may overcome the protective role of slump blocks, leading to a loss of slump block influence on bank erosion.

5 General discussion

This thesis sought to understand how biological and physical factors interact over different spatio-temporal scales to shape erosion-accretion processes of an important coastal landscape: the salt marsh. To that aim, the thesis constructed a predictive framework for study that involved three spatio-temporal scales (*instantaneous*, *event* and *engineering* scales: Figure 1.8) and then examined the patterns and drivers of marsh change at these scales. The study had the over-arching prediction that the influence of biological drivers on coastal geomorphology would reduce with increase in spatio-temporal scale, whilst the influence of physical factors would increase. The patterns and drivers of lateral marsh change were explored at the scale of creeks (*instantaneous*), estuaries (*event*) and geographical regions in Great Britain (*engineering*). The following discussion will dissect findings of each experimental chapter to inform how marsh dynamics change with scale, how scale and context being considered alter interpretations of ecosystem resilience, and how scale and context could affect management decisions. Section 5.1 summarises the patterns of change observed in this thesis, and addresses the research questions. Section 5.2 considers how lateral marsh dynamics may enhance marsh resilience. Section 5.3 considers how the holistic view of lateral marsh change should inform management options. Limitations of the work and future research avenues are discussed in sections 5.4 and 5.5.

5.1 Holistic lateral marsh change

The first questions posed by this thesis was *at what point can an observation of marsh change made in one dimension (here; 'creek', 'estuary' or 'region') inform changes operating at other dimensions?* When all scales are considered together, it appears that, for Great Britain, observation of marsh change made at one dimension do not necessarily explain lateral marsh change at another, because the key drivers involved in determining lateral marsh dynamics differ at each scale. The study showed that concentrations of suspended sediment and rate of relative sea level rise drove estuarine lateral marsh expansion or erosion trends over 150 years (*Chapter 2*). For three of the estuaries that had shown net marsh expansion, observations of several single marshes revealed rapid and cyclical phases of expansion-erosion over shorter timescales of ~20 years, which was not associated with sea level rise or sediment supply, but with migrating tidal channels (*Chapter 3*). Along the creek network of an eroding marsh, slump blocks that had plants growing on them resisted erosion, trapped sediment, and drove an

erosion-accretion cycle at the creek bank. At the scale of several years, creek lateral dynamics were influenced not by sea level rise, sediment supply, or the meandering of estuary tidal channels, but by the presence of vegetation (*Chapter 4*).

Sediment supply and the rate of relative sea level rise represented a clear 'top-down' control of environmental processes on the overall fate of marshes at the regional-scale. At the creek-scale, the presence of vegetated slump blocks along creek banks likely enhances the stability of an entire saltmarsh creek network (*Chapter 3*). By the localised, indirect role of plants in armouring and recovering creek banks, a 'bottom-up' control of biological processes on marsh stability emerges. At the intermediate 'estuary-scale' domain, both the physical forcing of migrating tidal channels and the capacity of pioneer marsh species to colonize the point-bar of migrated channels were important for understanding lateral marsh dynamics (*Chapter 3*). When all scales are considered together, the role of plants became less important when explaining patterns of lateral marsh change at larger spatial and longer temporal scales. This finding addresses the second question raised by the thesis, questioning *how important biotic processes influence larger-scale lateral marsh dynamics.*

Patterns and drivers of marsh change at different dimensions provide a 'holistic' view of lateral marsh change in estuaries, which appears to show a series of marsh erosion-expansion cycles nested at the three spatial domains investigated here (Figure 5.1). Cycles of marsh expansion and erosion are well documented (Yapp et al., 1917; Jakobsen, 1954; van Straaten, 1954; Greensmith and Tucker, 1965; Allen, 2000; van de Koppel et al., 2005; Pedersen and Bartholdy, 2007; van der Wal et al., 2008; Haslett and Allen, 2014). Studies of regime shift between salt marshes and tidal flats (and vice versa) have a common theme in that they consider lateral marsh dynamics at relatively localised scales of 'single saltmarsh' sites. By having a 'complete' view of the main drivers that control lateral marsh change, it is possible to interpret the likelihood that marsh loss is either the consequence of channel meandering, so will also follow marsh expansion elsewhere in the estuary, or is the consequence of changes are indicative of deficient sediment flux, so are likely to remain as tidal flats over geological scales until sea levels fall again (Cowell and Thom, 1994). There remains considerable debate as to whether vegetation change in ecosystems across the globe is best viewed as a short-term perturbation in landscape evolution, or as a fundamental shift in environmental conditions (Phillips, 1995; D'Alpaos, 2011; Wang and Temmerman, 2013; Mariotti and Carr, 2014; Bouma et al., 2016; Cao et al., 2017; *Chapter 4*). Findings from this thesis demonstrate the

value of interpreting landscape dynamics at a range of spatial- and temporal-scales, that may reveal cycles of ecosystem change driven either by internal, biotic processes or external environmental forcing.

5.2 Intermediate disturbance as a driver of ecosystem persistence

The continuous release and accumulation of sediments that drive lateral marsh dynamics at creek- estuary- and regional-scales appeared to be natural, and could be a fundamental mechanism of marsh resilience, ensuring long-term persistence of the marsh along a given coastline. This thesis observed that Northern marshes of the UK showed a net increase in extent over 100 years (*Chapter 2*), yet had high rates of individual marsh erosion and expansion (*Chapter 3*). The primary driving force of morphodynamic change in UK estuaries is tidal amplitude (Prandle et al., 2005). Northern estuaries have large tides and are therefore subject to greater disturbance, reflected in the sandier nature of the sediment (Goudie, 2013) and high frequency of channel meandering (*Chapter 2*). In contrast, marshes located in the South

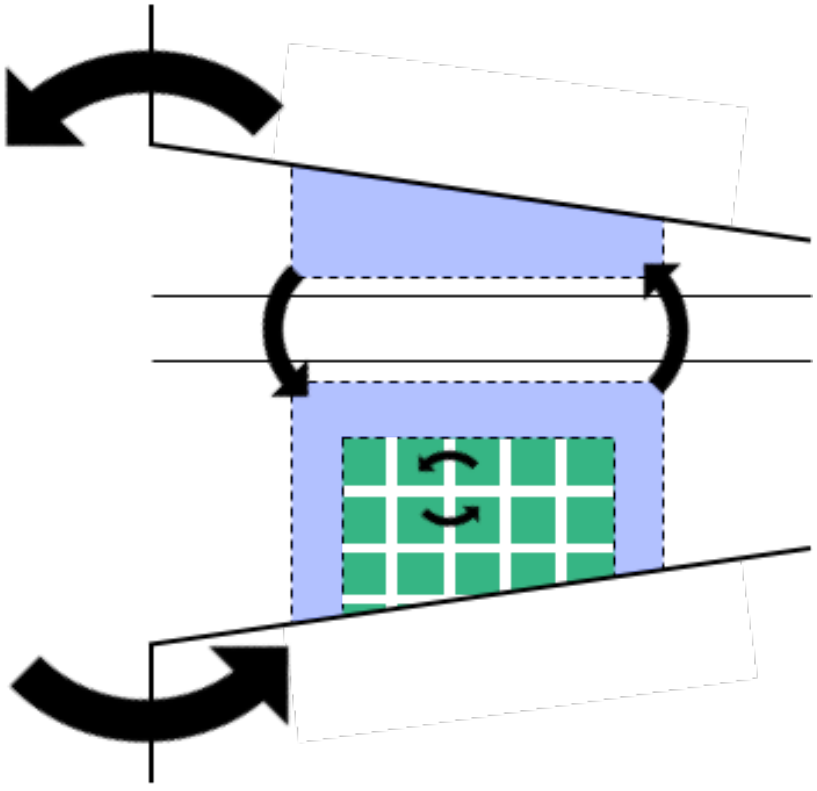

Figure 5.1 Representation of saltmarsh dynamics within an estuary, and how different scales reveal different lateral marsh dynamics: Erosion-expansion cycles occur along saltmarsh creeks (green box and small arrows); marshes expand and erode upon opposite sides of the estuary in response to tidal channel migration (blue box and medium arrows); sediment flux at the regional scale affects the size of the area over which marshes could potentially expand (large arrows). Identifying these patterns provide a holistic view of lateral marsh change within estuaries.

showed net marsh decline, but erosion rates were lower than when marshes in the north eroded. Southern estuaries are meso-tidal and have comparably lower-energy environment, with cohesive muds low channel migration rates (Bray et al., 2017). Within estuaries, tides can enhance sediment deposition through: importing sediment from outside the estuary via tidal asymmetry; transporting sediment from subtidal parts of the estuary to the intertidal; holding suspended sediment in suspension for longer, thus becoming more available for the marsh edge, and; eroding intertidal habitats and releasing sediment for accumulation elsewhere in the estuary (Schuerch et al., 2014). High hydrological forcing by tides may be causing rapid lateral erosion whilst simultaneously creating new areas for marsh growth (as seen in the north). Lower hydrological forcing may cause less extreme/frequent phases of marsh erosion, but may also reduce sediment transport/remobilisation, preventing marshes from expanding/remaining stable under sea level rise (as in the south). However, settlement of sediment can be prevented if levels of hydrological forcing are too extreme, thus inhibit marsh formation (Hu et al., 2015a). Intermediate disturbance levels may therefore be optimal for sustaining marsh erosion-accretion phases and long-term persistence in estuaries. Intermediate levels of disturbance are already recognised as an important ecological driver in enhancing species diversity (Connell, 1978; Grime, 1998), and are critical in the emergence of unique landscapes such as island braided fluvial ecosystems (Francis et al., 2009; Corenblit et al., 2011). This thesis indicates estuarine marsh systems function in a similar way, with insufficient, or too high hydrological dynamics causing the lateral decline of marshes (Figure 5.2).

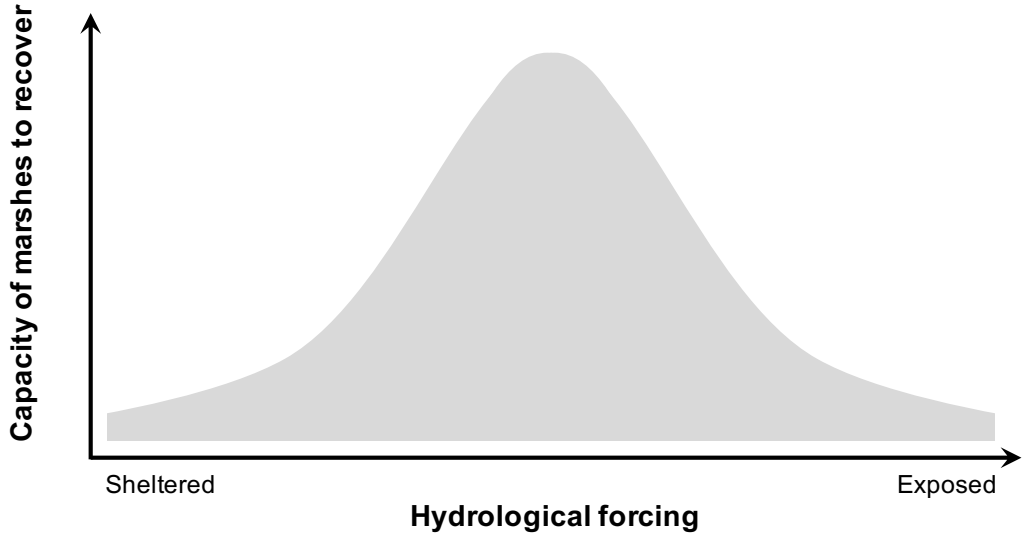

Figure 5.2 Capacity of marshes to recover from disturbance along a gradient of hydrological forcing. Recovery potential is at its highest in intermediate levels of forcing, where enough energy can redistribute sediment within the estuarine system, but is not so large as to prevent the establishment of pioneer marsh growth onto the displaced sediment.

Intermediate disturbance may also be ensuring pioneer species, which underpin recovery from disturbance (Cao et al., 2017), persist in the long-term within estuaries. Estuaries where the channel periodically migrate, western and eastern portions of the pioneer zone are always being eroded and expanded, but the net change in area extent is zero (Figure 5.3; intermediate). Here, there is a persistent pool of pioneer species that could facilitate new marsh growth following disturbance (Erfanzadeh et al., 2010), and thus long-term marsh persistence within the estuary. In low-energy, sheltered environments, the lack of disturbance allows low/mid marsh species to outcompete pioneer species, thus reducing the overall pool of pioneer zones (Figure 5.3; sheltered). In the event of a disturbance event, recovery rates would be hampered by smaller recruitment size. Similar conditions have been found in riparian systems where proportions of bare substrate and young, mature cohorts of pioneer vegetation within the fluvial corridor remained constant despite phases of erosion and accretion (Fisher et al., 2007; Tabacchi et al., 2009).

Marshes studies in *Chapter 2* appear to capture a shift in marsh plant composition from pioneer and low-marsh species dominating the lower portions of estuaries, whilst mid- and upper-marsh species populated upper reaches of the estuary. The shift in plant composition likely follows a gradient of reduced tidal forcing higher up the estuary. Marshes within the mid- and lower-estuary may therefore be erosion-prone, but have a high capacity for recovery, and can persist in more dynamic regions of the estuary. *Chapter 2* did, however, observe net marsh expansion in the outer estuary (likely caused by sediment influx from tidal asymmetry and *Spartina* invasion), so cannot comment on whether the marshes are held in a transient 'pioneer/low-marsh' state by periodic rapid phases of erosion through tidal channel migration (although this has been observed in other marshes situated in lower estuaries (Pringle, 1995)). Conversion of marshes from pioneer- to upper-marsh zones may, however, not represent a loss of resilience. Marshes in the upper estuary are likely to be more resistant to erosion due to the action of plants enriching soil organic matter and thus resistance to erosion (see section 3.4.4). Within a single estuary, there may hypothetically exist two distinct marsh configurations across the length of an estuary in response to a gradient of hydrological forcing: high-estuary 'resistor' marshes, which engineer soils to resist erosion and persist over long periods, and lower- and mid-estuaries 'recoverer' marshes, which are erosion-prone, but have a high capacity for recovery and therefore maintain a dynamic persistence in the lower estuary. Alternative expressions of the same ecosystem type across hydrological forcing gradients may optimise marsh resilience, as has recently been described in barrier sand dunes (Stallins and Corenblit,

2017). Intermediate disturbance events may therefore preserve pioneer cohorts and thus facilitate faster colonisation as the coastal environment changes in the long term. In addition to the deficit of sediment observed in marshes across Southern England, lower periodic hydrological disturbance may be adding an additional stress to the marshes, thus attributing to the net decline here, whilst marshes in the north have been expanding (*Chapter 2*).

5.3 Consequences for ecosystem service provision and management

Conserving existing wetland ecosystems and restoring lost / degraded systems is a key management goal of multilateral environmental agreements around the globe (Matthews, 1993; CBD, 2010; Griggs et al., 2013). Principally, modern management objectives seek to maximise and diversity the number of ecosystem services that wetlands provide (Laurila-Pant et al., 2015). This thesis has highlighted how dynamic marshes can be, which have important implications for managers. The likely success of restoration schemes, as well as the types of services being managed for, depend on understanding marsh dynamics.

5.3.1 Understanding scale in marsh management

Understanding the patterns and drivers of marsh change that operate at centennial, regional scales is necessary for: *i.* identifying where marsh systems are vulnerable to erosion, and *ii.* the identification of which components of the system may require management intervention (*Chapter 2*).

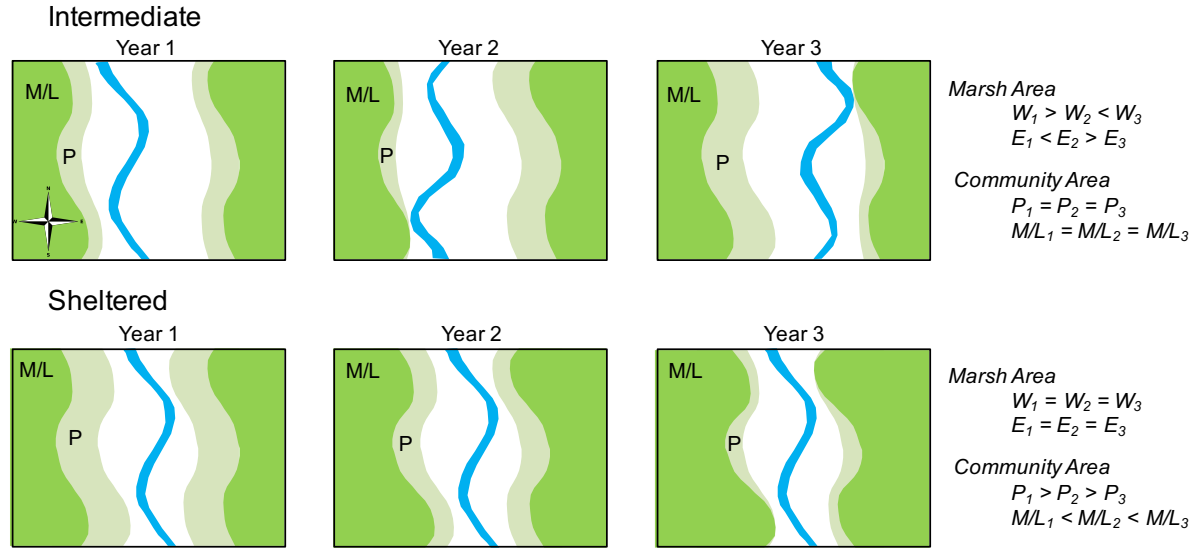

Figure 5.3 Model of how hydrological forcing (blue tidal channel) can sustain the proportion of pioneer marsh habitat (light green) over time, and thus the species needed for recovery following disturbance in an intermediate disturbance environment, compared to a sheltered system. In each case, there is no net change in marsh area over time. P represents pioneer marsh zone, M/L represents Mid- and low-marsh zone.

When local or short-term scales alone are considered by management, incorrect interpretation of the drivers and patterns of change can be made. There are numerous examples of studies that demonstrate trends of marsh erosion or expansion at short- and small-scales, and upscale their findings to explain larger-scale trends of marsh change over time (Castillo et al., 2000; Cox et al., 2003; Feagin et al., 2009). Local trends of erosion have been traditionally viewed as indicator of large-scale marsh decline (Hatvany et al., 2015). However there is a growing body of work highlighting that erosion-accretion phases can by cyclical at the marsh scale (van der Wal et al., 2008; Chauhan, 2009; Haslett and Allen, 2014) and that erosion at one location need not necessarily indicate marsh loss over larger spatial scales (as demonstrated by tidal channel erosion and marsh expansion elsewhere in the estuary *Chapter 3*). To demonstrate how an incorrect interpretation of net marsh loss for the entire estuarine system could be made, compare change in marsh extent of GT: GT has been consistently eroding from 1946 to 2011 (Figure 3.4 a). Marshes in the entire estuary, however, have been expanding (Figure 3.3 a-c). Similarly, a long-term historical perspective of change (150 years) can lead to different interpretations of marsh health. In the case of the Solent, the marshes are at present in rapid decline. However, historical perspective reveals marsh area extent is returning to levels that existed before *Spartina* colonisation (*Chapter 2*). A similar pattern of 'artificially' expanded marshes was revealed through historical analysis by Kirwan et al. (2011), who showed marsh expansion was the consequence of deforestation by European settlers, which led to increasing sediment runoff and deposition at the coast. Considering longer-term timescales can help to reveal how changes in sediment, water and plant health account for present-day marsh sizes and configurations.

As well as issues with upscaling patterns of erosion and accretion to characterise trends at larger- and longer-scales, key drivers regulating marsh change at these scales can also be overlooked. Attempts to identify the main drivers of marsh change, and predicted rates of decline, have previously been made for the UK (Pye and French, 1993a, Pye and French, 1993b, Carpenter and Pye, 1996). These studies have tended to only generalise patterns of marsh change in northern regions, and focus on patterns and causes of erosion along vulnerable marshes of the Essex-Kent and Solent regions. After having upscaling trends of marsh change in Essex-Kent and Solent regions to the UK, it was recently shown that marsh areal extent loss had been overestimated across England and Wales: Pye and French (1993a) estimated marshes would erode by -100 ha/yr. However, marsh change between 1989 and 2009 had varied between +1 and -83 ha/yr (Phelan et al., 2011). Large ranges in the rate change of marsh areal

extent are the result of differences in methodologies used when estimating marsh extent. Differences between the predicted rate of marsh change by Pye and French (1993b) and the observed change documented by Phelan et al. (2011) is partially due to understating the trend of net marsh expansion observed along northern UK. Misidentification of the key drivers responsible for driving marsh change may also have influenced the overstatement of marsh loss rates across GB. *Chapter* 2 found sediment supply and sea level rise were the dominant drivers of marsh area change, whereas Pye and French (1993b) identified storminess and sea level rise as key drivers of change across the country. Findings from this thesis highlight the value of linking historical rates of marsh change with empirical values of the perceived key drivers of marsh change. Use of empirical data may identify different drivers of marsh change over long- and short-terms. For managers, it is risky to consider patterns and drivers of marsh change at one site, and upscale the trend in marsh change across a wider area. A robust interpretation at relevant scales can provide insight into which drivers are most important and potentially put in measures to target them.

There is a prevailing tendency for monitoring strategies to consider the mechanisms of landform change informed by the relatively small temporal spatial scales of experimental studies (Macgregor and van Dijk, 2014, French et al., 2016). Calls have been made to recognise in management plans that ecosystem dynamics change at scales of space and time (e.g., Haslett et al., 2010). Incorporating scale has been important for the UK experience when understanding coastal morphodynamics. National initiatives, like the FutureCoast project (Burgess et al., 2004), have been able to characterise shoreline status and identify sediment cells across the coastline (Cooper and Pontee, 2006), which represent the boundaries within which dominant physical drivers can be identified and predicted at a relevant scale to managers (French et al., 2016). Identifying sediment cells can be used to manage local problems in the context of broader-scale sediment pathways. Having demonstrated the importance of identifying scales of marsh change and the role of large-scale long-term controls on marsh extent change, better understanding of coastal morphodynamics needs to be a priority for effective identification of issues and thus conservation of coastal landscapes, such as salt marshes.

5.3.2 Recommendations for management thinking

Site managers must recognise that dynamics of marsh change are moderated by top-down control of sediment supply (*Chapter 2*) and bottom-up control of plant fecundity (*Chapter 4*).

Moreover, for estuarine marshes, channel meandering can trigger erosion and accretion phases, which are more extreme in the mid- and lower-estuary compared to the upper-estuary which tends to remain stable (*Chapter 3*). There also appears to be a trade-off between:

i. estuaries subject to higher hydrological dynamics that help maintain long-term marsh persistence, but cause rapid phases of lateral erosion-accretion over the short term, and;
ii. estuaries with lower hydrological dynamics that exhibit less extreme rates of marsh erosion-expansion, but are ultimately more vulnerable to erosion in the long-term.

Reconciling this level of complexity in managing saltmarsh extent effectively presents a challenging task for the manager. However, being able to recognise the holistic view of marsh dynamics is needed to inform effective (and realistic) management outcomes. This thesis suggests three key practices that should be adopted in management thinking.

Firstly, several simple metrics that can identify the limits of lateral marsh extent - be that at the regional, estuarine, or creek scale - to aid in the long-term management of saltmarshes in a given estuary. At regional scale, identifying SSC and SLR can inform the likelihood that marshes will grow, decline, or remain dynamically stable (*Chapter 2*); Within estuaries, the likelihood of marsh establishment is high within 25% of estuary width, especially in the upper estuary, based on historical positions of tidal channels, and was applicable across three estuaries (*Chapter 3*); existence of vegetated blocks in the creeks indicates risk of internal dissection of marshes is lower (*Chapter 4*). Similar approaches of identifying marsh limits along wave-influenced coastal zones (Bouma et al., 2014, Hu et al., 2015b) can provide managers with the means of identifying the limits of change upon which natural dynamics of erosion-accretion can occur, thereby reducing the level of complexity of marsh erosion-accretion cycles to an 'average' area that marshes will occur at any given scale.

Secondly, sediment flux and relative sea level rise are especially important drivers of marsh change at the large-scale (*Chapter 2*), average position of tidal channels (*Chapter 3*) and plant health that confers the ability to resist erosion after slump block formation (*Chapter 4*). Monitoring efforts here in particular can be used to predict the vulnerability of a site.

Thirdly, careful consideration must be given to the type of ecosystem services that are being managed for, given the context of lateral marsh change described in this thesis. Figure 5.4

represents the often contradictory needs for different ecosystem services. Differences in the rates of lateral erosion over time and along different portions of the coastline highlight the challenge faced by managers in maximising ecosystems services delivered across the tidal landscape scale whilst accepting change in marsh extent over time. Whilst the effects of changes in the biological components of marshes on ecosystem service delivery are being recognised (Koch et al., 2009), less emphasis has been placed on how morphodynamics could affect ecosystem services, and represents a major research gap.

Natural morphodynamics is especially pertinent for marshes that are being heavily managed, such as those across the German portion of the Wadden Sea coastline, whose extents are carefully controlled (Figure 5.4B), and areas across Southern UK, where considerable investment is being made into restoring degraded marsh systems through managed realignment (Wolters et al., 2005).

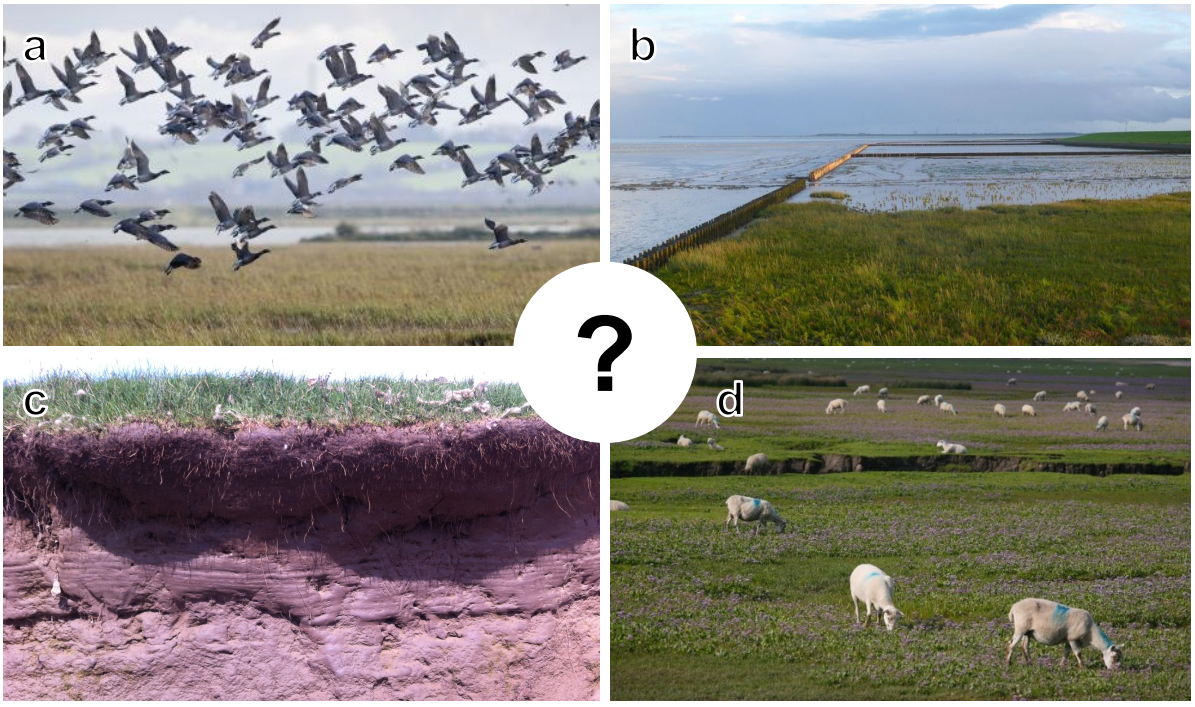

Figure 5.4 Examples of ecosystem services whose functioning may require different morphodynamics to persist over time. **a** For waders, vegetation patches of varying height and density are required for species' selection preference of nest sites to be met (Sharps, 2015). If the area is subject to erosion in the winter, but the marsh expands elsewhere in the immediate locale and maintains structurally diverse vegetation profile, it is unlikely this service will be diminished in the long-term. **b** For the same area, lateral erosion without recovery would necessarily diminish the degree of coastal protection afforded by that marsh (wave dissipation is strongly correlated with marsh width (Shepard et al., 2011)). **c** Stable marshes may, however, ensure any carbon sequestered into the ground remain locked over longer periods of time than along marshes that periodically erode and expand, and **d** increase the profitability of grazing for agriculture. This would alter floral composition and soil conditions (Davidson et al., 2017), and impact on nesting sites at high stocking densities (Sharps et al., 2017). The question mark at the centre represents the choice faced by managers in how the system should be managed for specific ecosystem service outcomes (images: **a** Russell Savory; **b** Oldenberg University; **c** C. Ladd, and; **d** JL Butchers).

5.4 Study Limitations

This study has shed light on some of the patterns and drivers of lateral marsh erosion and expansion that become apparent at different spatio-temporal scales, which are important to recognise when managing potentially vulnerable saltmarsh systems. The scope and applicability of findings in this thesis have their limitations, and are discussed below.

5.4.1 Large-scale predictors of marsh change

Chapter 2 considered the main drivers of lateral marsh change across the UK, and used available data on the perceived key drivers of marsh change. Given that the central focus was on meso- to macro-tidal estuaries, this study likely revealed different dynamics to those operating along open coastlines, or micro-tidal systems. Limitations of using change in storm frequency as a predictor variable are discussed in section 2.4.3. A fully integrated wind-fetch modelling application (e.g., Rohweder et al., 2008) may have provided a better predictor of marsh edge erosion than storm events alone. This study also used an analytically-derived estimate of suspended sediment concentration (SSC) were outlined in the method section and considered acceptable for the main analysis, but still only represents an estimated value. Given the importance of SSC as a predictor of lateral marsh change, sufficient empirical data on SSC near the marsh edge should be used when estimating marsh edge vulnerability in the future (Ganju et al., 2015).

An important consideration in long-term studies of saltmarsh morphodynamics is the response rate of coastline configuration to sudden and substantial phases of modification, such as reclamation. Restoring coastal equilibrium in response to such changes could take centuries and have a longer lasting impact on lateral marsh dynamics than the timescale considered in this thesis (Jongepier et al., 2015). In addition, this thesis did not consider plant species composition change over time over large spatial scales. Although change in marsh areal extent may provide insight into marsh vulnerability, this picture is incomplete without change in vegetation composition, which may inform whether certain community types are being lost (Huckle et al., 2004) and whether this could impact on future marsh resilience.

5.4.2 Influence of bio-physical processes visible at the estuarine scale

Chapter 3 examined the impacts of channel meandering on the size and dynamics of marsh extent in three tidally-dominated estuaries. Although important associations between

meandering channels and maximum attainable marsh size were made, the study was unable to adjudicate whether marsh growth also influenced the position of tidal channels. Flume studies have shown how flow displacement by vegetation can produce narrow, deep, and less mobile channels, and so increase the surface area available for plant growth across riparian systems (Gran and Paola, 2001), and similar processes of plants modifying channel water flow is seen on a much smaller scale in marsh creeks (Temmerman et al., 2005; van der Wal et al., 2008) and at the edges of coastal marshes (Pedersen and Bartholdy, 2007). It may be that, across the entire estuary, marshes have a partial control on influencing flow paths and thus the position of tidal channels.

5.4.3 Role of plants in influencing creek bank evolution

Chapter 4 used an observational study to examine the role of failed bank debris in armouring against creek erosion and facilitating accretion, to present the existence of a short-term dynamic conferring long-term resilience along creek banks. This study, however, could only identify an association between creek erosion and slump block erosion rate (which in turn was strongly influenced by the presence/absence of vegetation) and could not identify a causative effect of blocks on bank erosion. The use of a manipulation experiment, whereby idealised slump blocks are made (presence/absence of vegetation, age of roots since plant death) and exposed to channel flow in a laboratory setting, could demonstrate this.

5.5 Future research

Since the 1970s, there has been considerable research interest into the functioning and value of saltmarshes (Garbutt et al., 2017), and a growing recognition of the importance of understanding lateral marsh dynamics on long-term marsh resilience (Kirwan et al., 2016). This thesis has contributed to the understanding of the patterns and drivers of marsh change across several spatio-temporal scales, and has identified a number of areas for further research.

5.5.1 Satellite data to inform marsh extent, sediment availability, and ecosystem health

This thesis highlights the importance of estimating the areal extent of marshes over multiple time periods in order to determine trends of large-scale expansion, erosion or stability (*Chapter 2*) as has been done in other areas of the globe including Netherlands (Jongepier et al., 2015) and the U.S. (Kirwan et al., 2011) through maps and soil cores. Only a few parts of the globe have historical records dating back over the past 100 years, therefore establishing an inventory

of global marsh extent should be considered crucial in order to measure lateral change into the future. The most up-to-date baseline has been recently complied by Mcowen et al. (2017), however significant portions of the globe remain unmapped, notably boreal regions which remain difficult to access. Cost reductions, high image resolution and revisit times of satellites coupled with modelling are now making it possible to survey inaccessible areas of the globe with minimal ground-truthing (Zarco-Tejada et al., 2018). Future research should capitalise on advances in remote sensing in order to establish a baseline of marsh extent, particularly in regions susceptible to rapid change. In addition to change in aerial marsh extent, efforts should be made to monitor change in floral composition from, for example, hyperspectral satellite images (Belluco et al., 2006), as other environmental processes than sediment supply have been liked to saltmarsh change at subtropical and boreal latitudes including the conversion of saltmarshes to mangrove or unvegetated tidal flat ecosystems due to increased temperature and reduced precipitation (Osland et al., 2016; Gabler et al., 2017).

Chapter 2 showed that trends of marsh expansion and decline across Great Britain can be explained by the balance between sediment supply and relative sea level rise, and similar studies elsewhere have demonstrated the importance of sediment supply to patterns of saltmarsh change (Syvitski et al., 2005; Mariotti and Fagherazzi, 2010; Weston, 2014; Jongepier et al., 2015; Kirwan et al., 2016; Ganju et al., 2017). In addition to establishing a baseline of marsh extent change, efforts should be made in establishing SSC availably of coastlines along the globe. This would provide a simple metric where marshes, and other hydro-sedimenary systems, are most vulnerable. In addition of being able to record colour, near infra-red and LiDAR, satellites can be used to detect SSC in waters. With high revisit times it would be possible to determine average SSC concentrations, and how they vary over time (Dogliotti et al., 2015).

5.5.2 Establishing marsh extent change in boreal regions

Understanding how intertidal habitats in boreal regions are changing is of particular importance as Artic regions have been subject to some of the fastest ecological changes as a consequence of climate change in the world (e.g. Martini et al., 2009). Potential impacts of climate change include:

- Changes in sediment flux to the coast form ice rafting, known to be an important sediment source for marshes in Arctic regions (van Proosdij et al., 2006), due to global warming and increased ice melt;
- Reductions in sea ice through global warming altering wave exposure profiles along coastlines, that could cause substantial modification of soft-sediment coastlines, and;
- Changes in the floral composition of saltmarshes due to warmer air temperatures (Gedan and Bertness, 2010) that may impact on wader populations, and alter grazer dynamics in the region known to be an important driver of habitat composition (Zacheis et al., 2001), and potentially facilitate northward shifts of pioneer species like *Spartina* spp., whose northern limit has been shown to be increasing with warmer temperatures around the globe (Loebl et al., 2006) and therefore could lead to the expansion of marshes.

The paucity of research in Arctic regions represents a major knowledge gap. Understanding how marshes in these regions are likely to change is of global interest to better inform global carbon storage capacity of marshes, their importance for supporting migratory bird populations, and as a model of coastal morphodynamic evolution in response to climate change.

5.5.3 Identifying erosion-expansion cycles as a connected system

Chapter 3 identified how fluctuations in tidal channel position induce compensatory erosion-expansion patterns in marshes. Phases of erosion and expansion appear to be connected within a defined spatial unit, like an estuary, that once identified can help determine the space over which lateral marsh dynamics occur, and the limit to which they can potentially expand to. As discussed above, such connectivity may be crucial for underpinning marsh resilience and long-term persistence within estuaries. Across the UK, great effort has already been placed in identifying compartmentalised hydro-sedimentary coastal cells, whose dynamics are primarily responsible for coastal morphodynamics in that cell at the centennial scale. Coastal morphodynamic models can then be developed to predict future coastline evolution and has

already been used to inform landscape-scale management plans in the UK, which is almost unique in the globe (French et al., 2016). For saltmarshes, identifying sediment cells, and thus the connectivity between marshes (in terms of sediment and seed pool) is crucial for predicting marsh vulnerability. Impairing sediment cycles through dredging activity or land reclamation could lead marsh loss in the long-term. A concerned effort should be placed on identifying the connectivity between marshes from a hydro-sediment environment at a global scale to better predict marsh vulnerability.

5.5.4 Indirect controls on soil erodibility

Chapter 4 showed how vegetated portions of eroded debris resisted against erosion once deposited at the base of creeks. It was hypothesised that live roots conferred more strength against erosion, allowing slump blocks to resist erosion and allow the blocks to accumulate sediment and promote recovery. Several studies have identified the benefits of roots in binding soils, however it remains unclear how management options impact on below-ground root growth. Understanding how different management options might affect below-ground plant growth is especially pertinent of UK marshes, where most marshes are grazed (MEA, 2005; Davidson et al., 2017). Grazing can compact soils and alter plant community (Schrama et al., 2012), the degree to which vary according to grazer type (Elschot et al., 2013). The role of plant roots in binding soils has been shown to depend on plant diversity and soil composition (Ford et al., 2016). Investigations should therefore be made into how alternative grazing regimes would influence soil erosion rates, and thereby the later role of eroded deposits in resisting creek edge erosion.

The presence of slump blocks is not only observed along creeks, but also occur along seaward margins of eroding marshes (Allen, 2000), and were observed during site visits for this thesis as often forming ‘debris fields’ along the marsh profile (Figure 5.5). There is, at present, considerable research interest in understanding the precise mechanisms that trigger shifts in marsh erosion or expansion over the short-term (Bouma et al., 2016; Cao et al., 2017). Allen (1989) has documented cases where debris fields facilitate the seaward growth of marshes, however to the best of my knowledge, no consideration has yet been given to whether debris fields function in a similar capacity to those observed in creeks, of moderating soil erosion rates, that could potentially define the point in which marshes shift from lateral erosion to expansion.

Through improved understanding of lateral marsh dynamics across various scales considered by this thesis, it is hoped a more holistic view of the controls on marsh extent change can better inform management options and ensure natural marsh functioning can be safeguarded into the future.

Figure 5.5 Example of eroded marsh surface debris along the seaward marsh edge in Dwyryd estuary, Wales (Image: C. Ladd).

6 References

Aagaard, T., Nielsen, J., Jensen, S. G. and Friderichsen, J. (2004) 'Longshore sediment transport and coastal erosion at Skallingen, Denmark', *Danish Journal of Geography,* 104(1), pp. 5-14.

Alber, M., Swenson, E. M., Adamowicz, S. C. and Mendelssohn, I. A. (2008) 'Salt marsh dieback: An overview of recent events in the US', *Estuarine, Coastal and Shelf Science,* 80(1), pp. 1-11.

Allen, J. (1985) 'Intertidal drainage and mass-movement processes in the Severn Estuary: Rills and creeks (pills)', *Journal of the Geological Society,* 142(5), pp. 849-861.

Allen, J. (1989) 'Evolution of salt-marsh cliffs in muddy and sandy systems: A qualitative comparison of British west-coast estuaries', *Earth Surface Processes and Landforms,* 14(1), pp. 85-92.

Allen, J. (2000) 'Morphodynamics of Holocene salt marshes: A review sketch from the Atlantic and Southern North Sea coasts of Europe', *Quaternary Science Reviews,* 19(12), pp. 1155-1231.

Altieri, A. H., Bertness, M. D., Coverdale, T. C., Axelman, E. E., Herrmann, N. C. and Szathmary, P. L. (2013) 'Feedbacks underlie the resilience of salt marshes and rapid reversal of consumer-driven die-off', *Ecology,* 94(7), pp. 1647-1657.

An, S., Gu, B., Zhou, C., Wang, Z., Deng, Z., Zhi, Y., Li, H., Chen, L., Yu, D. and Liu, Y. (2007) '*Spartina* invasion in China: Implications for invasive species management and future research', *Weed Research,* 47(3), pp. 183-191.

Angeler, D. G., Allen, C. R., Garmestani, A. S., Gunderson, L. H., Hjerne, O. and Winder, M. (2015) 'Quantifying the adaptive cycle', *PLoS One,* 10(12), pp. 1-17.

Angelini, C., Griffin, J. N., van de Koppel, J., Lamers, L. P., Smolders, A. J., Derksen-Hooijberg, M., van der Heide, T. and Silliman, B. R. (2016) 'A keystone mutualism underpins resilience of a coastal ecosystem to drought', *Nature Communications,* 7:12473, pp. 1-8.

Baart, F., van Gelder, P. H., De Ronde, J., van Koningsveld, M. and Wouters, B. (2011) 'The effect of the 18.6-year lunar nodal cycle on regional sea-level rise estimates', *Journal of Coastal Research,* 28(2), pp. 511-516.

Bai, J., Xiao, R., Cui, B., Zhang, K., Wang, Q., Liu, X., Gao, H. and Huang, L. (2011) 'Assessment of heavy metal pollution in wetland soils from the young and old reclaimed regions in the Pearl River Estuary, South China', *Environmental Pollution,* 159(3), pp. 817-824.

Baily, B. (2011) 'Ordnance Survey data collection and the mapping of tidal features', *Sheetlines,* 90, pp. 4-17.

Baily, B. and Collier, P. (2010) 'The Development of the photogrammetric mapping of tidal lines by the Ordnance Survey', *The Cartographic Journal,* 47(3), pp. 262-269.

Baily, B. and Inkpen, R. (2013) 'Assessing historical saltmarsh change: An investigation into the reliability of historical saltmarsh mapping using contemporaneous aerial photography and cartographic data', *Journal of Coastal Conservation,* 17(3), pp. 503-514.

Baily, B. and Pearson, A. W. (2007) 'Change detection mapping and analysis of salt marsh areas of central southern England from Hurst Castle Spit to Pagham Harbour', *Journal of Coastal Research*, 23(6), pp. 1549-1564.

Balke, T. (2013) 'Establishment of biogeomorphic ecosystems: A study on mangrove and salt marsh pioneer vegetation', Unpublished PhD Thesis, *Radboud University, Netherlands.*

Balke, T., Herman, P. M. and Bouma, T. J. (2014) 'Critical transitions in disturbance-driven ecosystems: Identifying Windows of Opportunity for recovery', *Journal of Ecology,* 102(3), pp. 700-708.

Balke, T., Klaassen, P. C., Garbutt, A., van der Wal, D., Herman, P. M. and Bouma, T. J. (2012) 'Conditional outcome of ecosystem engineering: A case study on tussocks of the salt marsh pioneer *Spartina anglica*', *Geomorphology,* 153-154, pp. 232-238.

Balke, T., Stock, M., Jensen, K., Bouma, T. J. and Kleyer, M. (2016) 'A global analysis of the seaward salt marsh extent: The importance of tidal range', *Water Resources Research*, 52(5), pp. 3775-3786.

Ball, D. (1964) 'Loss-on-ignition as an estimate of organic matter and organic carbon in non-calcareous soils', *European Journal of Soil Science,* 15(1), pp. 84-92.

Barnosky, A. D., Matzke, N., Tomiya, S., Wogan, G. O., Swartz, B., Quental, T. B., Marshall, C., McGuire, J. L., Lindsey, E. L. and Maguire, K. C. (2011) 'Has the Earth's sixth mass extinction already arrived?', *Nature,* 471(7336), pp. 51-57.

Barwis, J. H. (1977) 'Sedimentology of some South Carolina tidal-creek point bars, and a comparison with their fluvial counterparts', *in:* Miall, A.D. (Ed.), Fluvial Sedimentology, *Canadian Society of Petroleum Geologists, Canada* vol. 5, pp. 129-160.

Beets, D. J. and van der Spek, A. J. (2000) 'The Holocene evolution of the barrier and the back-barrier basins of Belgium and the Netherlands as a function of late Weichselian morphology, relative sea-level rise and sediment supply', *Netherlands Journal of Geosciences,* 79(1), pp. 3-16.

Bell, F. W. (1997) 'The economic valuation of saltwater marsh supporting marine recreational fishing in the southeastern United States', *Ecological Economics,* 21(3), pp. 243-254.

Belluco, E., Camuffo, M., Ferrari, S., Modenese, L., Silvestri, S., Marani, A. and Marani, M. (2006) 'Mapping salt-marsh vegetation by multispectral and hyperspectral remote sensing', *Remote Sensing of Environment,* 105(1), pp. 54-67.

Biggs, R., Carpenter, S. R. and Brock, W. A. (2009) 'Turning back from the brink: Detecting an impending regime shift in time to avert it', *Proceedings of the National Academy of Sciences,* 106(3), pp. 826-831.

Blott, S. J. and Pye, K. (2012) 'Particle size scales and classification of sediment types based on particle size distributions: Review and recommended procedures', *Sedimentology,* 59(7), pp. 2071-2096.

Blott, S. J., Pye, K., van der Wal, D. and Neal, A. (2006) 'Long-term morphological change and its causes in the Mersey Estuary, NW England', *Geomorphology,* 81(1), pp. 185-206.

Bookstein, F. L. (1997) 'Morphometric tools for landmark data: Geometry and biology', *Cambridge University Press, Cambridge, UK*, pp. 1-435.

Bouma, T., De Vries, M., Low, E., Peralta, G., Tánczos, I. v., van de Koppel, J. and Herman, P. J. (2005) 'Trade-offs related to ecosystem engineering: A case study on stiffness of emerging macrophytes', *Ecology,* 86(8), pp. 2187-2199.

Bouma, T., van Belzen, J., Balke, T., van Dalen, J., Klaassen, P., Hartog, A., Callaghan, D., Hu, Z., Stive, M. and Temmerman, S. (2016) 'Short-term mudflat dynamics drive long-term cyclic salt marsh dynamics', *Limnology and Oceanography,* 61(6), pp. 2261-2275.

Bouma, T. J., van Belzen, J., Balke, T., Zhu, Z., Airoldi, L., Blight, A. J., Davies, A. J., Galvan, C., Hawkins, S. J. and Hoggart, S. P. (2014) 'Identifying knowledge gaps hampering application of intertidal habitats in coastal protection: Opportunities & steps to tak e', *Coastal Engineering,* 87, pp. 147-157.

Bradley, S., Milne, G., Teferle, F. N., Bingley, R. and Orliac, E. (2009) 'Glacial isostatic adjustment of the British Isles: New constraints from GPS measurements of crustal motion', *Geophysical Journal International,* 178(1), pp. 14-22.
Braudrick, C. A., Dietrich, W. E., Leverich, G. T. and Sklar, L. S. (2009) 'Experimental evidence for the conditions necessary to sustain meandering in coarse-bedded rivers', *Proceedings of the National Academy of Sciences,* 106(40), pp. 16936-16941.
Bray, M., Carter, D. and Hooke, J. (2017) '2012 Update of Bray, M., Carter, D. and Hooke, J. 2004 SCOPAC Sediment Transport Study', *New Forest District Council, UK*. Available at: www.scopac.org.uk/sts (Accessed: 05/06/18).
Bretar, F., Arab-Sedze, M., Champion, J., Pierrot-Deseilligny, M., Heggy, E. and Jacquemoud, S. (2013) 'An advanced photogrammetric method to measure surface roughness: Application to volcanic terrains in the Piton de la Fournaise, Reunion Island', *Remote Sensing of Environment,* 135, pp. 1-11.
Bridson, R. (1980) 'Saltmarsh, its accretion and erosion at Caerlaverock National Nature Reserve Dumfries', *Transactions of the Dumfriesshire and Galloway Natural History and Antiquarian Society,* 55, pp. 60-67.
Brown, J. M. and Davies, A. (2010) 'Flood/ebb tidal asymmetry in a shallow sandy estuary and the impact on net sand transport', *Geomorphology,* 114(3), pp. 431-439.
Brown, J. M. (2007) 'Coastal area modelling: Sand transport and morphological change', Unpublished PhD Thesis, *University of Wales, UK*.
Buck, A. L. (1993) 'An inventory of UK estuaries', *Joint Nature Conservation Committee, Peterborough, UK*, vol. 3, pp. 1-200.
Bunnefeld, N. and Phillimore, A. B. (2012) 'Island, archipelago and taxon effects: mixed models as a means of dealing with the imperfect design of nature's experiments', *Ecography*, 35(1), pp. 15-22.
Burd, F. (1992) 'Historical study of sites of natural sea wall failures in Essex', no. 15, English Nature Research Report, *Universrtity of Hull, Institute of Estuarine and Coastal Studies, Hull, UK*, pp. 1-95, Available at: http://publications.naturalengland.org.uk/publication/33021 (Accessed: 05/06/18).
Burgess, K., Jay, H. and Hosking, A. (2004) 'Futurecoast: Predicting the future coastal evolution of England and Wales', *Journal of Coastal Conservation,* 10(1), pp. 65-71.
Burningham, H. (2008) 'Contrasting geomorphic response to structural control: The Loughros estuaries, northwest Ireland', *Geomorphology,* 97(3), pp. 300-320.
Bush, L. E. and Davies, A. J. (2013) 'Historic aerial imagery to monitor temporal change in intertidal habitats', CCW Scientific Report Series no. 1047, *Countryside Council for Wales, UK,* pp. 1-103.
CH2M HILL (2013a) 'North West Estuaries Processes Reports, Duddon Estuary', Report prepared by CH2M HILL for the North West and North Wales Coastal Group, August 2013, *Sefton Council, UK*, pp. 1-53.
CH2M HILL (2013a) 'North West Estuaries Processes Reports, Kent Estuary', Report prepared by CH2M HILL for the North West and North Wales Coastal Group, August 2013, *Sefton Council, UK*, pp. 1-50.
CH2M HILL (2013a) 'North West Estuaries Processes Reports, Leven Estuary', Report prepared by CH2M HILL for the North West and North Wales Coastal Group, August 2013, *Sefton Council, UK*, pp. 1-48.
Cahoon, D., Hensel, P., Spencer, T., Reed, D., McKee, K. and Saintilan, N. (2006) 'Coastal wetland vulnerability to relative sea-level rise: Wetland elevation trends and process controls' *in:* Verhoeven, J.T.A., Beltman, B., Bobbink, R., and Whigham, D.F. (Eds.), Wetlands and Natural Resource Management, *7th INTECOL International Wetland Conference*, *Netherlands*, pp. 271-292.

Callaghan, D., Bouma, T., Klaassen, P., van der Wal, D., Stive, M. and Herman, P. (2010) 'Hydrodynamic forcing on salt-marsh development: Distinguishing the relative importance of waves and tidal flows', *Estuarine, Coastal and Shelf Science,* 89(1), pp. 73-88.

Cao, H., Zhu, Z., Balke, T., Zhang, L. and Bouma, T. J. (2017) 'Effects of sediment disturbance regimes on *Spartina* seedling establishment: Implications for salt marsh creation and restoration', *Limnology and Oceanography,* 63(2), pp. 647-659.

Carpenter, K. and Pye, K. (1996) 'Saltmarsh change in England and Wales: Its history and causes', Technical Report W12, HR Wallingford, *Environment Agency, Bristol, UK,* pp. 1-126.

Carr, A. (1962) 'Cartographie Record and Historical Accuracy', *Geography,* 47(2), pp. 135-144.

Carrascal, L. M., Galván, I. and Gordo, O. (2009) 'Partial least squares regression as an alternative to current regression methods used in ecology', *Oikos,* 118(5), pp. 681-690.

Castillo, J., Luque, C., Castellanos, E. and Figueroa, M. (2000) 'Causes and consequences of salt-marsh erosion in an Atlantic estuary in SW Spain', *Journal of Coastal Conservation,* 6(1), pp. 89-96.

CBD (2010) 'The strategic plan for biodiversity 2011-2020 and the Aichi biodiversity targets', Document UNEP/CBD/COP/DEC/X/2, *Secretariat of the Convention on Biological Diversity, Nagoya, Japan,* pp. 1-4, Available at: https://www.cbd.int/doc/strategic-plan/2011-2020/Aichi-Targets-EN.pdf (Accessed: 05/06/18).

CCO (2011) 'Annual Local Monitoring Report 2011 - Solway Firth', Channel Coastal Observatory, *Allerdale Borough Council, UK*. Available at: https://www.channelcoast.org/northwest/latest/index.php?link=&dla=download&id=12&cat=1/Solway%20Pages%20from%20Allerdale_Monitoring_Report_2011.pdf (Accessed: 12/03/18).

Chater, E. and Jones, H. (1957) 'Some observations on *Spartina townsendii* H. and J. Groves in the Dovey Estuary', *Journal of Ecology,* 45(1), pp. 157-167.

Chauhan, P. P. S. (2009) 'Autocyclic erosion in tidal marshes', *Geomorphology,* 110(3), pp. 45-57.

Chen, Y., Collins, M. B. and Thompson, C. E. (2011) 'Creek enlargement in a low-energy degrading saltmarsh in southern England', *Earth Surface Processes and Landforms,* 36(6), pp. 767-778.

Chen, Y., Thompson, C. and Collins, M. (2012) 'Saltmarsh creek bank stability: Biostabilisation and consolidation with depth', *Continental Shelf Research,* 35, pp. 64-74.

Christensen, J. H. and Christensen, O. B. (2003) 'Climate modelling: Severe summertime flooding in Europe', *Nature,* 421(6925), pp. 805-806.

Cleveland, R. B., Cleveland, W. S. and Terpenning, I. (1990) 'A seasonal-trend decomposition procedure based on loess', *Journal of Official Statistics*, 6(1), pp. 3-73.

Close, C. (1912) 'Instructions to examiners and field revisers (PRO OS 45/3)', *Ordnance Survey, UK,* pp. 1-45.

Coco, G., Zhou, Z., van Maanen, B., Olabarrieta, M., Tinoco, R. and Townend, I. (2013) 'Morphodynamics of tidal networks: Advances and challenges', *Marine Geology,* 346, pp. 1-16.

Connell, J. H. (1978) 'Diversity in tropical rain forests and coral reefs', *Science,* 199(4335), pp. 1302-1310.

Cooper, N. J., Cooper, T. and Burd, F. (2001) '25 years of salt marsh erosion in Essex: Implications for coastal defence and nature conservation', *Journal of Coastal Conservation,* 7(1), pp. 31-40.

Cooper, N. and Pontee, N. (2006) 'Appraisal and evolution of the littoral 'sediment cell' concept in applied coastal management: Experiences from England and Wales', *Ocean & Coastal Management,* 49(7-8), pp. 498-510.

Corbel, G., Allen, J. T., Woolf, D. K. and Gibb, S. (2007) 'Wind trends in the Highlands and Islands of Scotland 1960–2004 and their relation to the North Atlantic Oscillation', *AMS 87th Annual Meeting, 19th Conference on Climate Variability and Change, USA*, pp. 1-6.

Corenblit, D., Baas, A. C., Bornette, G., Darrozes, J., Delmotte, S., Francis, R. A., Gurnell, A. M., Julien, F., Naiman, R. J. and Steiger, J. (2011) 'Feedbacks between geomorphology and biota controlling Earth surface processes and landforms: A review of foundation concepts and current understandings', *Earth-Science Reviews,* 106(3), pp. 307-331.

Corenblit, D., Tabacchi, E., Steiger, J. and Gurnell, A. M. (2007) 'Reciprocal interactions and adjustments between fluvial landforms and vegetation dynamics in river corridors: A review of complementary approaches', *Earth-Science Reviews,* 84(1), pp. 56-86.

Costanza, R., d'Arge, R., De Groot, R., Farber, S., Grasso, M., Hannon, B., Limburg, K., Naeem, S., O'neill, R. V. and Paruelo, J. (1997) 'The value of the world's ecosystem services and natural capital', N*ature,* 387(6630), pp. 253-260.

Costanza, R., Pérez-Maqueo, O., Martinez, M. L., Sutton, P., Anderson, S. J. and Mulder, K. (2008) 'The value of coastal wetlands for hurricane protection', *AMBIO: A Journal of the Human Environment,* 37(4), pp. 241-248.

Cowell, P. and Thom, B. (1994) 'Morphodynamics of Coastal Evolution', *in:* Carter, R. W. G. and Woodroffe, C. D. (Eds.), Coastal Evolution: Late Quaternary Shoreline Morphodynamics, *Cambridge University Press, Cambridge, United Kingdom,* pp. 33-86.

Cox, R., Wadsworth, R. and Thomson, A. (2003) 'Long-term changes in salt marsh extent affected by channel deepening in a modified estuary', *Continental Shelf Research,* 23(17), pp. 1833-1846.

Crawley, M. J. (2013) 'The R Book', *John Wiley & Sons Ltd., Chichester, UK*, vol. 2, pp. 785-808.

Crosby, S. C., Sax, D. F., Palmer, M. E., Booth, H. S., Deegan, L. A., Bertness, M. D. and Leslie, H. M. (2016) 'Salt marsh persistence is threatened by predicted sea-level rise', *Estuarine, Coastal and Shelf Science,* 181, pp. 93-99.

Cundy, A. B. and Croudace, I. W. (1996) 'Sediment accretion and recent sea-level rise in the Solent, southern England: Inferences from radiometric and geochemical studies', *Estuarine, Coastal and Shelf Science,* 43(4), pp. 449-467.

D'Alpaos, A. (2011) 'The mutual influence of biotic and abiotic components on the long-term ecomorphodynamic evolution of salt-marsh ecosystems', *Geomorphology,* 126(3), pp. 269-278.

D'Alpaos, A., Lanzoni, S., Marani, M. and Rinaldo, A. (2007) 'Landscape evolution in tidal embayments: Modeling the interplay of erosion, sedimentation, and vegetation dynamics', *Journal of Geophysical Research: Earth Surface,* 112(F1), pp. 1-17.

Dacey, J. W. and Howes, B. L. (1984) 'Water uptake by roots controls water table movement and sediment oxidation in short *Spartina marsh*', *Science,* 224(4648), pp. 487-489.

Davidson, K. E., Fowler, M. S., Skov, M. W., Doerr, S. H., Beaumont, N. and Griffin, J. N. (2017) 'Livestock grazing alters multiple ecosystem properties and services in salt marshes: A meta-analysis', *Journal of Applied Ecology,* 54(5), pp. 1395–1405.

Davidson, N., Laffoley, D. d'A., Doody, J., Way, L., Gordon, J., Key, R. E., Drake, C., Pienkowski, M., Mitchell, R. and Duff, K. (1991) 'Nature conservation and estuaries in Great Britain', Estuaries Review, *Nature Conservancy Council, Peterborough, UK,* pp. 1-76.

Davy, A. J., Bishop, G. F. and Costa, C. S. B. (2001) '*Salicornia* L.(*Salicornia pusilla* J. Woods, *S. ramosissima* J. Woods, *S. europaea* L., *S. obscura* P.W. Ball & Tutin, *S. nitens* P.W. Ball & Tutin, *S. fragilis* P.W. Ball & Tutin and *S. dolichostachya* Moss)', *Journal of Ecology,* 89(4), pp. 681-707.

Dawson, L., Grayston, S. and Paterson, E. (2000) 'Effects of grazing on the roots and rhizosphere of grasses', *in*: Lemaire, G., Hodgson, J., Moraes, A., Carvalho, P. C. F. and Nabinger, C. (Eds.), Grassland Ecophysiology and Grazing Ecology, *CABI Publishing, Wallingford, UK,* pp. 61-84.

De Baets, S., Poesen, J., Gyssels, G. and Knapen, A. (2006) 'Effects of grass roots on the erodibility of topsoils during concentrated flow', *Geomorphology,* 76(1), pp. 54-67.

de Groot, A. V., Veeneklaas, R. M., Kuijper, D. P. and Bakker, J. P. (2011a) 'Spatial patterns in accretion on barrier-island salt marshes', *Geomorphology,* 134(3), pp. 280-296.

de Groot, A. V., Veeneklaas, R. M. and Bakker, J. P. (2011b) 'Sand in the salt marsh: Contribution of high-energy conditions to salt-marsh accretion', *Marine Geology,* 282(3), pp. 240-254.

Deegan, L. A., Johnson, D. S., Warren, R. S., Peterson, B. J., Fleeger, J. W., Fagherazzi, S. and Wollheim, W. M. (2012) 'Coastal eutrophication as a driver of salt marsh loss', *Nature,* 490(7420), pp. 388-392.

Deser, C., Hurrell, J. W. and Phillips, A. S. (2017) 'The role of the North Atlantic Oscillation in European climate projections', *Climate Dynamics,* 49(9-10), pp. 3141-3157.

Dixon-Gough, R. W. (2006) 'Changes in land use and their implications upon coastal regions: The case of Grange-over-Sands, Northwest England', *in*: Dixon-Gough, R. W. and Bloch, P. C. (Eds.), The Role of the State and Individual in Sustainable Land Management (International Land Management Series), *Ashgate Publishing Ltd., Aldershot, UK,* pp. 14-31.

Dogliotti, A. I., Ruddick, K., Nechad, B., Doxaran, D. and Knaeps, E. (2015) 'A single algorithm to retrieve turbidity from remotely-sensed data in all coastal and estuarine waters', *Remote Sensing of Environment,* 156, pp. 157-168.

Dorji, P., Fearns, P. and Broomhall, M. (2016) 'A semi-analytic model for estimating total suspended sediment concentration in turbid coastal waters of northern Western Australia using MODIS-Aqua 250 m data', *Remote Sensing,* 8(7), pp. 556-579.

Dronkers, J. J. (1986) 'Tidal asymmetry and estuarine morphology', *Netherlands Journal of Sea Research,* 20(2-3), pp. 117-131.

Dronkers, J. J. (2005) 'Dynamics of coastal systems', *Advanced Series on Ocean Engineering, World Scientific*, vol. 25, pp. 1-519.

Du Preez, C. (2015) 'A new arc–chord ratio (ACR) rugosity index for quantifying three-dimensional landscape structural complexity', *Landscape Ecology,* 30(1), pp. 181-192.

Duarte, C. M., Losada, I. J., Hendriks, I. E., Mazarrasa, I. and Marbà, N. (2013) 'The role of coastal plant communities for climate change mitigation and adaptation', *Nature Climate Change,* 3(11), pp. 961-968.

Dyer, K. R. (1973) 'Estuaries: A physical introduction', *John Wiley & Sons Ltd., London*, *UK,* pp. 1-140.

Egels, Y. and Kasser, M. (2003) 'Digital photogrammetry', *Taylor & Francis, London, UK*, pp. 1-376.

Elliott, T. and Gardiner, A. R. (1981) 'Ripple, megaripple, and sandwave bedforms in the macrotidal Loughor Estuary, South Wales, UK', *in:* Nio, S. D., Shuttenhelm, R. T. E. and Van Weering, Tj. C. E. (Eds.), Holocene Marine Sedimentation in the North Sea Basin, *Blackwell Scientific, Oxford, UK,* pp. 51-64.

Ellison, A. M. (1987) 'Effects of competition, disturbance, and herbivory on *Salicornia europaea*', *Ecology,* 68(3), pp. 576-586.

Erfanzadeh, R., Garbutt, A., Pétillon, J., Maelfait, J.-P. and Hoffmann, M. (2010) 'Factors affecting the success of early salt-marsh colonizers: Seed availability rather than site suitability and dispersal traits', *Plant Ecology,* 206(2), pp. 335-347.

Fagherazzi, S., Gabet, E. J. and Furbish, D. J. (2004) 'The effect of bidirectional flow on tidal channel planforms', *Earth Surface Processes and Landforms,* 29(3), pp. 295-309.

Fagherazzi, S., Kirwan, M. L., Mudd, S. M., Guntenspergen, G. R., Temmerman, S., D'Alpaos, A., Koppel, J., Rybczyk, J. M., Reyes, E. and Craft, C. (2012) 'Numerical models of salt marsh evolution: Ecological, geomorphic, and climatic factors', *Reviews of Geophysics,* 50(1), pp. 1-28.

Fagherazzi, S., Mariotti, G., Wiberg, P. and McGlathery, K. (2013) 'Marsh collapse does not require sea level rise', *Oceanography*, 26(3), pp. 70-77.

Fagherazzi, S. and Overeem, I. (2007) 'Models of deltaic and inner continental shelf landform evolution', *Annual Review of Earth and Planetary Science,* 35, pp. 685-715.

FGDC (1998) 'Geospatial Positioning Accuracy Standards, part 3: National standard for spatial data accuracy', no. FGDC-STD-007.3-1998, *Federal Geogrpahic Data Committee, Washington, DC, USA*, pp. 1-25.

Feagin, R., Lozada-Bernard, S., Ravens, T., Möller, I., Yeager, K. and Baird, A. (2009) 'Does vegetation prevent wave erosion of salt marsh edges?', *Proceedings of the National Academy of Sciences,* 106(25), pp. 10109-10113.

Firth, C. R., Collins, P. E., Smith, D. E. and Scottish Natural Heritage, E. (2000) 'Focus on Firths: Coastal Landforms, Processes and Management Options; V: the Solway Firth', Review No. 128, *Scottish Natural Heritage, Department of Geography and Earth Sciences, Brunel University, Iselworth, UK*, pp. 1-128.

Fisher, J. L. (1991) 'Aberdyfi Harbour study. Prepared for Gwynedd Council', Report No. 1046, Shoreline Management Partnership, *Gwynedd Council, Dolgellau, UK,* pp. 1-50.

Ford, H., Garbutt, A., Jones, L. and Jones, D. L. (2013) 'Grazing management in saltmarsh ecosystems drives invertebrate diversity, abundance and functional group structure', *Insect Conservation and Diversity,* 6(2), pp. 189-200.

Ford, H., Garbutt, A., Ladd, C. J. T., Malarkey, J. and Skov, M. W. (2016) 'Soil stabilization linked to plant diversity and environmental context in coastal wetlands', *Journal of Vegetation Science,* 27(2), pp. 259-268.

Francalanci, S., Bendoni, M., Rinaldi, M. and Solari, L. (2013) 'Ecomorphodynamic evolution of salt marshes: Experimental observations of bank retreat processes', *Geomorphology,* 195, pp. 53-65.

Francis, R. and Bekera, B. (2014) 'A metric and frameworks for resilience analysis of engineered and infrastructure systems', *Reliability Engineering & System Safety,* 121, pp. 90-103.

Francis, R. A., Corenblit, D. and Edwards, P. J. (2009) 'Perspectives on biogeomorphology, ecosystem engineering and self-organisation in island-braided fluvial ecosystems', *Aquatic Sciences,* 71(3), pp. 290.

French, J. (2006) 'Tidal marsh sedimentation and resilience to environmental change: Exploratory modelling of tidal, sea-level and sediment supply forcing in predominantly allochthonous systems', *Marine Geology,* 235(1), pp. 119-136.

French, J., Payo, A., Murray, B., Orford, J., Eliot, M. and Cowell, P. (2016) 'Appropriate complexity for the prediction of coastal and estuarine geomorphic behaviour at decadal to centennial scales', *Geomorphology,* 256, pp. 3-16.
Friedrichs, C. T. and Perry, J. E. (2001) 'Tidal salt marsh morphodynamics: A synthesis', *Journal of Coastal Research*, 27, pp. 7-37.
Friess, D. A., Krauss, K. W., Horstman, E. M., Balke, T., Bouma, T. J., Galli, D. and Webb, E. L. (2012) 'Are all intertidal wetlands naturally created equal? Bottlenecks, thresholds and knowledge gaps to mangrove and saltmarsh ecosystems', *Biological Reviews,* 87(2), pp. 346-366.
Gabet, E. J. (1998) 'Lateral migration and bank erosion in a saltmarsh tidal channel in San Francisco Bay, California', *Estuaries and Coasts,* 21(4), pp. 745-753.
Gabler, C. A., Osland, M. J., Grace, J. B., Stagg, C. L., Day, R. H., Hartley, S. B., Enwright, N. M., From, A. S., McCoy, M. L. and McLeod, J. L. (2017) 'Macroclimatic change expected to transform coastal wetland ecosystems this century', *Nature Climate Change*, 7, pp. 142-147.
Gafeira, G. J., Diaz, D. D. and Long, D. (2015) 'Semi-automated mapping and characterisation of coral reef mounds: Mingulay Reef proof of concept', *British Geological Society,* 1, pp. 1-5.
Ganju, N. K., Defne, Z., Kirwan, M. L., Fagherazzi, S., D'Alpaos, A. and Carniello, L. (2017) 'Spatially integrative metrics reveal hidden vulnerability of microtidal salt marshes', *Nature Communications,* 8, pp. ncomms14156.
Ganju, N. K., Kirwan, M. L., Dickhudt, P. J., Guntenspergen, G. R., Cahoon, D. R. and Kroeger, K. D. (2015) 'Sediment transport-based metrics of wetland stability', *Geophysical Research Letters,* 42(19), pp. 7992-8000.
Gao, S. and Collins, M. (1997) 'Formation of salt-marsh cliffs in an accretional environment, Christchurch Harbour, southern England', *in:* Wang, P. and Berggren, W. A. (Eds.) Proceedings of the 30th International Geological Congress, *VSP Press, Amsterdam*, pp. 95-110.
Garbutt, A., de Groot, A., Smit, C. and Pétillon, J. (2017) 'European salt marshes: Ecology and conservation in a changing world', *Journal of Coastal Conservation,* 21(3), pp. 405-408.
Gedan, K. B. and Bertness, M. D. (2010) 'How will warming affect the salt marsh foundation species Spartina patens and its ecological role?', *Oecologia,* 164(2), pp. 479-487.
Gedan, K. B., Kirwan, M. L., Wolanski, E., Barbier, E. B. and Silliman, B. R. (2011) 'The present and future role of coastal wetland vegetation in protecting shorelines: Answering recent challenges to the paradigm', *Climatic Change,* 106(1), pp. 7-29.
Gedan, K. B., Silliman, B. and Bertness, M. (2009) 'Centuries of human-driven change in salt marsh ecosystems', *Marine Science,* 1, pp 117-141.
Gerdol, V. and Hughes, R. G. (1993) 'Effect of the amphipod *Corophium volutator* on the colonisation of mud by the halophyte *Salicornia europaea*', *Marine Ecology Progress Series*, 97(1), pp. 61-69.
Goodman, P. J., Braybrooks, E. M., Marchant, C. J. and Lambert, J. M. (1969) '*Spartina*× *townsendii* H. & J. Groves *sensu lato*', *Journal of Ecology*, 57(1), pp. 298-313.
Goudie, A. (2013) 'Characterising the distribution and morphology of creeks and pans on salt marshes in England and Wales using Google Earth', *Estuarine, Coastal and Shelf Science,* 129, pp. 112-123.
Graf, W. L. (2000) 'Locational probability for a dammed, urbanizing stream: Salt River, Arizona, USA', *Environmental Management,* 25(3), pp. 321-335.
Gran, K. and Paola, C. (2001) 'Riparian vegetation controls on braided stream dynamics', *Water Resources Research,* 37(12), pp. 3275-3283.

Grime, J. (1998) 'Benefits of plant diversity to ecosystems: Immediate, filter and founder effects', *Journal of Ecology,* 86(6), pp. 902-910.
Gray, A. (1972) 'The ecology of Morecambe Bay. v. The salt marshes of Morecambe Bay', *Journal of Applied Ecology*, 9(1), pp. 207-220.
Gray, A. J., Marshall, D. and Raybould, A. (1991) 'A century of evolution in *Spartina anglica*', *Advances in Ecological Research,* 21, pp. 1-62.
Green, M. O. and Coco, G. (2014) 'Review of wave-driven sediment resuspension and transport in estuaries', *Reviews of Geophysics,* 52(1), pp. 77-117.
Greensmith, J. and Tucker, E. (1965) 'Salt marsh erosion in Essex', *Nature,* 206(4984), pp. 606-607.
Griggs, D., Stafford-Smith, M., Gaffney, O., Rockström, J., Öhman, M. C., Shyamsundar, P., Steffen, W., Glaser, G., Kanie, N. and Noble, I. (2013) 'Policy: Sustainable development goals for people and planet', *Nature,* 495(7441), pp. 305-307.
Grömping, U. (2006) 'Relative importance for linear regression in R: The package relaimpo', *Journal of Statistical Software,* 17(1), pp. 1-27.
Gunnell, J. R., Rodriguez, A. B. and McKee, B. A. (2013) 'How a marsh is built from the bottom up', *Geology,* 41(8), pp. 859-862.
Gurnell, A., Tockner, K., Edwards, P. and Petts, G. (2005) 'Effects of deposited wood on biocomplexity of river corridors', *Frontiers in Ecology and the Environment,* 3(7), pp. 377-382.
Hacker, S. D. and Bertness, M. D. (1999) 'Experimental evidence for factors maintaining plant species diversity in a New England salt marsh', *Ecology,* 80(6), pp. 2064-2073.
Haigh, I., Nicholls, R. and Wells, N. 'Rising sea levels in the English Channel 1900 to 2100', *Proceedings of the Institution of Civil Engineers - Maritime Engineering*, 164(2), pp. 81-92.
Halcrow (2010) 'Appendix A – Regional tidal and sediment modelling studies September 2010', Cell Eleven Tidal and Sediment Study (CETaSS) Phase 2 (ii), *Halcrow, Swindon, UK*, pp 1-220.
Harmsworth, G. and Long, S. (1986) 'An assessment of saltmarsh erosion in Essex, England, with reference to the Dengie Peninsula', *Biological Conservation*, 35(4), pp. 377-387.
Harwood, T. R. and Scott, R. (1999) 'A report on *Spartina anglica* control Grange-over-Sands 1998-1999 for South Lakeland District Council', Institute of Terrestrical Ecology, *South Lakeland District Council*, *UK,* pp 1-46.
Haslett, S. K. and Allen, J. R. (2014) 'Salt-marsh evolution at Northwick and Aust warths, Severn Estuary, UK: A case of constrained autocyclicity', *Atlantic Geology,* 50, pp. 1-17.
Hatvany, M., Cayer, D. and Parent, A. (2015) 'Interpreting salt marsh dynamics: Challenging scientific paradigms', *Annals of the Association of American Geographers,* 105(5), pp. 1041-1060.
Haynes, J. and Dobson, M. (1969) 'Physiography, foraminifera and sedimentation in the Dovey Estuary (Wales)', *Geological Journal,* 6(2), pp. 217-256.
He, Q., Altieri, A. H. and Cui, B. (2015) 'Herbivory drives zonation of stress-tolerant marsh plants', *Ecology,* 96(5), pp. 1318-1328.
HMLR (2016) 'HM Land Registry plans: the basis of HM Land Registry applications (PG40s1)', Her Majesty's Land Registry, UK Government, *London, UK*. Available at: https://www.gov.uk/government/publications/land-registry-plans-the-basis-of-land-registry-applications (Accessed: 05/06/18).
Hoitink, A., Hoekstra, P. and van Maren, D. (2003) 'Flow asymmetry associated with astronomical tides: Implications for the residual transport of sediment', *Journal of Geophysical Research: Oceans,* 108(C10), pp. 1-8.

Holling, C. S. (1973) 'Resilience and stability of ecological systems', *Annual Review of Ecology and Systematics,* 4(1), pp. 1-23.
Hothorn, T., Bretz, F., Westfall. (2016) 'Simultaneous Inference in General Parametric Models', *Biometrical Journal*, 50(3), pp. 346-363.
Houser, C. (2010) 'Relative importance of vessel-generated and wind waves to salt marsh erosion in a restricted fetch environment', *Journal of Coastal Research*, 26(2), pp. 230-240.
Howe, G. M. and Thomas, P. (1963) 'Welsh landforms and scenery', *Macmillan & Co. Ltd., Basingstoke, UK*, pp. 1-155.
HR Wallingford (2002) 'Southern North Sea Sediment Transport Study, Phase 2' Sediment Transport Report. Report EX4526, *Great Yarmouth Borough Council by HR Wallingford, CEFAS/UEA, Postford Haskoning and D'Olier, B, Wallingford, UK*, pp. 1-146.
Hu, Z., Belzen, J., Wal, D., Balke, T., Wang, Z. B., Stive, M. and Bouma, T. J. (2015a) 'Windows of opportunity for salt marsh vegetation establishment on bare tidal flats: The importance of temporal and spatial variability in hydrodynamic forcing', *Journal of Geophysical Research: Biogeosciences,* 120(7), pp. 1450-1469.
Hu, Z., Lenting, W., van der Wal, D. and Bouma, T. J. (2015b) 'Continuous monitoring bed-level dynamics on an intertidal flat: Introducing novel, stand-alone high-resolution SED-sensors', *Geomorphology,* 245, pp. 223-230.
Hu, Z., Wang, Z. B., Zitman, T. J., Stive, M. J. and Bouma, T. J. (2015c) 'Predicting long-term and short-term tidal flat morphodynamics using a dynamic equilibrium theory', *Journal of Geophysical Research: Earth Surface,* 120(9), pp. 1803-1823.
Hubbard, J. C. E. (1965) *'Spartina* marshes in southern England: VI. Pattern of invasion in Poole harbour', *The Journal of Ecology*, 53(3), pp. 799-813.
Hubbard, J. C. E. and Stebbings, R. E. (1967) 'Distribution, dates of origin and acreage of *Spartina townsendii* (*s.l.*) marshes in Great Britain', *Proceedings of the Botanical Society of the British Isles,* 7(1), pp. 1-17.
Huckle, J., Marrs, R. and Potter, J. (2004) 'Spatial and temporal changes in salt marsh distribution in the Dee estuary, NW England, determined from aerial photographs', *Wetlands Ecology and Management,* 12(5), pp. 483-498.
Hughes, R. and Paramor, O. (2004) 'On the loss of saltmarshes in south-east England and methods for their restoration', *Journal of Applied Ecology,* 41(3), pp. 440-448.
Hughes, Z. J. (2012) 'Tidal channels on tidal flats and marshes', *in:* Davis, R.A. and Dalrymple, R.W. (Eds.), Principles of Tidal Sedimentology, *Springer, New York, USA*, pp. 269-300.
Hughes, A. L., Wilson, A. M. and Morris, J. T. (2012) 'Hydrologic variability in a salt marsh: Assessing the links between drought and acute marsh dieback', *Estuarine, Coastal and Shelf Science,* 111, pp. 95-106.
Huiskes, A., Koutstaal, B., Herman, P., Beeftink, W., Markusse, M. and De Munck, W. (1995) 'Seed dispersal of halophytes in tidal salt marshes', *Journal of Ecology*, 83(4), pp. 559-567.
Hume, T. M., Snelder, T., Weatherhead, M. and Liefting, R. (2007) 'A controlling factor approach to estuary classification', *Ocean & Coastal Management,* 50(11), pp. 905-929.
Jago, C. (1980) 'Contemporary accumulation of marine sand in a macrotidal estuary, southwest Wales', *Sedimentary Geology,* 26(1-3), pp. 21-49.
Jenny, B. and Hurni, L. (2011) 'Studying cartographic heritage: Analysis and visualization of geometric distortions', *Computers & Graphics,* 35(2), pp. 402-411.

Johnson, D. (2000) 'Ecological restoration options for the Lymington/Keyhaven saltmarshes', *Water and Environment Journal,* 14(2), pp. 111-116.
Jakobsen, B. (1954) 'The tidal area in South-Western Jutland and the process of the salt marsh formation', *Geografisk Tidsskrift,* 53, pp. 49-61.
Jensen, A. and Jefferies, R. (1984) 'Fecundity and mortality in populations of *Salicornia europaea agg.* at Skallingen, Denmark', *Ecography,* 7(4), pp. 399-412.
JNCC (2004) 'Common standards monitoring guidance for saltmarsh habitats', Version August 2004, Updated from February 2004, *Joint Nature Conservation Committee, Peterborough, UK*, pp. 1-24. Available at: http://jncc.defra.gov.uk/pdf/CSM_coastal_saltmarsh.pdf (Accessed: 05/06/18).
Jones, H. P. and Schmitz, O. J. (2009) 'Rapid recovery of damaged ecosystems', *PLoS One,* 4(5), pp. e5653.
Jongepier, I., Soens, T., Temmerman, S. and Missiaen, T. (2016) 'Assessing the planimetric accuracy of historical maps (sixteenth to nineteenth centuries): New methods and potential for coastal landscape reconstruction', *The Cartographic Journal,* 53(2), pp. 114-132.
Jongepier, I., Wang, C., Missiaen, T., Soens, T. and Temmerman, S. (2015) 'Intertidal landscape response time to dike breaching and stepwise re-embankment: A combined historical and geomorphological study', *Geomorphology,* 236, pp. 64-78.
Kestner, F. J. T. (1962) 'The old coastline of the Wash', *The Geographical Journal*, 128(4), pp. 457-471.
Kestner, F. J. T. (1975) 'The loose-boundary regime of the Wash', *The Geographical Journal*, 141(3), pp. 388-414.
Kiehl, K., Eischeid, I., Gettner, S. and Walter, J. (1996) 'Impact of different sheep grazing intensities on salt marsh vegetation in northern Germany', *Journal of Vegetation Science,* 7(1), pp. 99-106.
Kingham (2013) 'The Broad-Scale Impacts of Livestock Grazing on Saltmarsh Carbon Stocks', Unpublished PhD Thesis, *Bangor University, UK*.
Kim, D., Cairns, D. M. and Bartholdy, J. (2013) 'Tidal creek morphology and sediment type influence spatial trends in salt marsh vegetation', *The Professional Geographer,* 65(4), pp. 544-560.
Kim, D., Cairns, D. M., Bartholdy, J. and Morgan, C. L. (2012) 'Scale-dependent correspondence of floristic and edaphic gradients across salt marsh creeks', *Annals of the Association of American Geographers,* 102(2), pp. 276-294.
King, S. E. and Lester, J. N. (1995) 'The value of salt marsh as a sea defence', *Marine Pollution Bulletin,* 30(3), pp. 180-189.
Kirby, R. (2013) 'The long-term sedimentary regime of the Outer Medway Estuary', *Ocean & Coastal Management*, 79, pp. 20-33.
Kirwan, M. L., Guntenspergen, G. R., D'Alpaos, A., Morris, J. T., Mudd, S. M. and Temmerman, S. (2010) 'Limits on the adaptability of coastal marshes to rising sea level', *Geophysical Research Letters,* 37(23), pp. 1-5.
Kirwan, M. L. and Megonigal, J. P. (2013) 'Tidal wetland stability in the face of human impacts and sea-level rise', *Nature,* 504(7478), pp. 53-60.
Kirwan, M. L., Murray, A. B., Donnelly, J. P. and Corbett, D. R. (2011) 'Rapid wetland expansion during European settlement and its implication for marsh survival under modern sediment delivery rates', *Geology,* 39(5), pp. 507-510.
Kirwan, M. L., Temmerman, S., Skeehan, E. E., Guntenspergen, G. R. and Fagherazzi, S. (2016) 'Overestimation of marsh vulnerability to sea level rise', *Nature Climate Change,* 6(3), pp. 253-260.

Koch, E. W., Barbier, E. B., Silliman, B. R., Reed, D. J., Perillo, G. M., Hacker, S. D., Granek, E. F., Primavera, J. H., Muthiga, N. and Polasky, S. (2009) 'Non-linearity in ecosystem services: Temporal and spatial variability in coastal protection', *Frontiers in Ecology and the Environment,* 7(1), pp. 29-37.

Lal, R. (2005) 'Forest soils and carbon sequestration', *Forest Ecology and Management,* 220(1-3), pp. 242-258.

Lanzoni, S. and Seminara, G. (2002) 'Long-term evolution and morphodynamic equilibrium of tidal channels', *Journal of Geophysical Research: Oceans,* 107(C1), pp. 1-13.

Larcombe, P. and Jago, C. F. (1994) 'The late devensian and holocene evolution of Barmouth Bay, Wales', *Sedimentary Geology,* 89(3), pp. 163-180.

Larcombe, P. and Jago, C. F. (1996) 'The morphological dynamics of intertidal megaripples in the Mawddach Estuary, North Wales, and the implications for palaeoflow reconstructions', *Sedimentology,* 43(3), pp. 541-559.

Laurila-Pant, M., Lehikoinen, A., Uusitalo, L. and Venesjärvi, R. (2015) 'How to value biodiversity in environmental management?', *Ecological Indicators,* 55, pp. 1-11.

Lavelle, J., Mofjeld, H. and Baker, E. (1984) 'An *in situ* erosion rate for a fine-grained marine sediment', *Journal of Geophysical Research: Oceans,* 89(C4), pp. 6543-6552.

Leonardi, N., Defne, Z., Ganju, N. K. and Fagherazzi, S. (2016a) 'Salt marsh erosion rates and boundary features in a shallow Bay', *Journal of Geophysical Research: Earth Surface,* 121(10), pp. 1861-1875.

Leonardi, N. and Fagherazzi, S. (2015) 'Effect of local variability in erosional resistance on large-scale morphodynamic response of salt marshes to wind waves and extreme events', *Geophysical Research Letters,* 42(14), pp. 5872-5879.

Leonardi, N., Ganju, N. K. and Fagherazzi, S. (2016b) 'A linear relationship between wave power and erosion determines salt-marsh resilience to violent storms and hurricanes', *Proceedings of the National Academy of Sciences,* 113(1), pp. 64-68.

Li, C., Chen, C., Guadagnoli, D. and Georgiou, I. Y. (2008) 'Geometry-induced residual eddies in estuaries with curved channels: Observations and modeling studies', *Journal of Geophysical Research: Oceans,* 113(C1), pp. 1-14.

Li, H. L., Wang, Y. Y., An, S. Q., Zhi, Y.-B., Lei, G.-C. and Zhang, M.-X. (2014) 'Sediment type affects competition between a native and an exotic species in coastal China', *Scientific Reports,* 4, pp. 1-5.

Li, H. and Yang, S. (2009) 'Trapping effect of tidal marsh vegetation on suspended sediment, Yangtze Delta', *Journal of Coastal Research*, 25(4), pp. 915-924.

Loebl, M., van Beusekom, J. E. and Reise, K. (2006) 'Is spread of the neophyte *Spartina anglica* recently enhanced by increasing temperatures?', *Aquatic Ecology,* 40(3), pp. 315-324.

Lottig, N. R. and Fox, J. M. (2007) 'A potential mechanism for disturbance-mediated channel migration in a southeastern United States salt marsh', *Geomorphology,* 86(3), pp. 525-528.

Lotze, H. K., Lenihan, H. S., Bourque, B. J., Bradbury, R. H., Cooke, R. G., Kay, M. C., Kidwell, S. M., Kirby, M. X., Peterson, C. H. and Jackson, J. B. (2006) 'Depletion, degradation, and recovery potential of estuaries and coastal seas', *Science,* 312(5781), pp. 1806-1809.

Lowe, D. G. (2004) 'Distinctive image features from scale-invariant keypoints', *International Journal of Computer Vision,* 60(2), pp. 91-110.

Lowe, J., Howard, T., Pardaens, A., Tinker, J., Holt, J., Wakelin, S., Milne, G., Leake, J., Wolf, J. and Horsburgh, K. (2009) 'UK Climate Projections science report: Marine and coastal projections', *Met Office Hadley Centre, Exeter, UK*, pp. 1-99.

Macgregor, N. A. and van Dijk, N. (2014) 'Adaptation in practice: How managers of nature conservation areas in eastern England are responding to climate change', *Environmental Management,* 54(4), pp. 700-719.
Malarkey, J., Baas, J. H., Hope, J. A., Aspden, R. J., Parsons, D. R., Peakall, J., Paterson, D. M., Schindler, R. J., Ye, L. and Lichtman, I. D. (2015) 'The pervasive role of biological cohesion in bedform development', *Nature Communications,* 6, pp. 6257.
Manning, A. and Whitehouse, R. J. S. (2012) 'Enhanced UK Estuaries database: Explanatory notes and metadata (SiTE P1). Development of estuary morphological models'. Technical Report. *HR Wallingford, UK*, pp. 1-27.
Marani, M., D'Alpaos, A., Lanzoni, S., Carniello, L. and Rinaldo, A. (2010) 'The importance of being coupled: Stable states and catastrophic shifts in tidal biomorphodynamics', *Journal of Geophysical Research: Earth Surface,* 115(F4), pp. 1-15.
Marani, M., D'Alpaos, A., Lanzoni, S. and Santalucia, M. (2011) 'Understanding and predicting wave erosion of marsh edges', *Geophysical Research Letters,* 38(21), pp. 1-5.
Marani, M., Da Lio, C. and D'Alpaos, A. (2013) 'Vegetation engineers marsh morphology through multiple competing stable states', *Proceedings of the National Academy of Sciences,* 110(9), pp. 3259-3263.
Marani, M., Lanzoni, S., Silvestri, S. and Rinaldo, A. (2004) 'Tidal landforms, patterns of halophytic vegetation and the fate of the lagoon of Venice', *Journal of Marine Systems,* 51(1), pp. 191-210.
Marani, M., Silvestri, S., Belluco, E., Ursino, N., Comerlati, A., Tosatto, O. and Putti, M. (2006) 'Spatial organization and ecohydrological interactions in oxygen-limited vegetation ecosystems', *Water Resources Research,* 42(6), pp. 1-12.
Mariotti, G. (2016) 'Revisiting salt marsh resilience to sea level rise: Are ponds responsible for permanent land loss?', *Journal of Geophysical Research: Earth Surface,* 121(7), pp. 1391-1407.
Mariotti, G. and Carr, J. (2014) 'Dual role of salt marsh retreat: Long-term loss and short-term resilience', *Water Resources Research,* 50(4), pp. 2963-2974.
Mariotti, G. and Fagherazzi, S. (2010) 'A numerical model for the coupled long-term evolution of salt marshes and tidal flats', *Journal of Geophysical Research: Earth Surface,* 115(F1), pp. 1-12.
Mariotti, G. and Fagherazzi, S. (2013) 'Critical width of tidal flats triggers marsh collapse in the absence of sea-level rise', *Proceedings of the National Academy of Sciences,* 110(14), pp. 5353-5356.
Mariotti, G., Kearney, W. and Fagherazzi, S. (2016) 'Soil creep in salt marshes', *Geology,* 44(6), pp. 459-462.
Marker, M. E. (1967) 'The Dee estuary: Its progressive silting and salt marsh development', *Transactions of the Institute of British Geographers*, 41, pp. 65-71.
Marshall, J. R. (1962) 'The morphology of the upper Solway salt marshes', *The Scottish Geographical Magazine,* 78(2), pp. 81-99.
Martini, I. P., Jefferies, R. L., Morrison, R. G. and Abraham, K. F. (2009) 'Polar coastal wetlands: Development, structure and land use', *in:* Perillo, G. M. E., Wolanski, E., Cahoon, D. R. and Brinson, M. M. (Eds.), Coastal wetlands: An integrated ecosystem approach, *Elsevier, Amsterdam*, pp. 119-155.
Matthews, G. V. T. (1996) 'The Ramsar Convention on Wetlands: Its history and development', *Ramsar Convention Bureau, Gland, Switzerland*, pp. 1-90.
Mcowen, C., Weatherdon, L., Bochove, J.-W., Sullivan, E., Blyth, S., Zockler, C., Stanwell-Smith, D., Kingston, N., Martin, C. and Spalding, M. (2017) 'A global map of saltmarshes', *Biodiversity Data Journal,* 5, pp. e11764.

MEA (2005) 'Millennium Ecosystem Assessment. Ecosystems and human well-being: Wetlands and water', *World Resources Institute, Washington DC, USA,* pp. 1-80.
Met Office (2013) 'Met Office Integrated Data Archive System (MIDAS) Land and Marine Surface Stations Data (1853-current)', *NCAS British Atmospheric Data Centre, Liverpool UK*. Available at: http://catalogue.ceda.ac.uk/uuid/220a65615218d5c9cc9e4785a3234bd0 (Accessed: 05/06/18).
Mevik, B.-H., Wehrens, R., Liland, K. H. (2016), 'Partial Least Squares and Principal Component Regression (Version 2.6-0)', *The Comprehensive R Archive Network (CRAN)*. Available at: http://cran.r-project.org/web/packages/pls/ (Accessed: 05/06/18).
Minchinton, T. E. (2006) 'Rafting on wrack as a mode of dispersal for plants in coastal marshes', *Aquatic Botany,* 84(4), pp. 372-376.
Mitchener, H. and Torfs, H. (1996) 'Erosion of mud/sand mixtures', *Coastal Engineering*, 29(1-2), pp. 1-25.
Möller, I., Kudella, M., Rupprecht, F., Spencer, T., Paul, M., van Wesenbeeck, B. K., Wolters, G., Jensen, K., Bouma, T. J. and Miranda-Lange, M. (2014) 'Wave attenuation over coastal salt marshes under storm surge conditions', *Nature Geoscience,* 7(10), pp. 727-731.
Möller, I., Spencer, T., French, J. R., Leggett, D. and Dixon, M. (1999) 'Wave transformation over salt marshes: A field and numerical modelling study from North Norfolk, England', *Estuarine, Coastal and Shelf Science*, 49(3), pp. 411-426.
Moore, R. D., Wolf, J., Souza, A. J. and Flint, S. S. (2009) 'Morphological evolution of the Dee Estuary, Eastern Irish Sea, UK: A tidal asymmetry approach', *Geomorphology,* 103(4), pp. 588-596.
Motta, D., Langendoen, E., Abad, J. and García, M. (2014) 'Modification of meander migration by bank failures', *Journal of Geophysical Research: Earth Surface,* 119(5), pp. 1026-1042.
Murray, A., Knaapen, M., Tal, M. and Kirwan, M. (2008) 'Biomorphodynamics: Physical-biological feedbacks that shape landscapes', *Water Resources Research,* 44(11), pp. 1-18.
Murray, N. J., Clemens, R. S., Phinn, S. R., Possingham, H. P. and Fuller, R. A. (2014) 'Tracking the rapid loss of tidal wetlands in the Yellow Sea', *Frontiers in Ecology and the Environment,* 12(5), pp. 267-272.
Myers, S. S., Gaffikin, L., Golden, C. D., Ostfeld, R. S., Redford, K. H., Ricketts, T. H., Turner, W. R. and Osofsky, S. A. (2013) 'Human health impacts of ecosystem alteration', *Proceedings of the National Academy of Sciences,* 110(47), pp. 18753-18760.
Nicholls, R. J., Wong, P. P., Burkett, V. R., Codignotto, J. O., Hay, J. E., McLean, R. F., Ragoonaden, S. and Woodroffe, C. D. (2007) 'Coastal systems and low-lying areas', *in:* Parry, M. L., Canziani, O.F., Palutikof, J.P., van der Linden, P. J. and Hanson, C. E. (Eds.), Climate change 2007: Impacts, adaptation and vulnerability. Contribution of working group II to the fourth assessment report of the intergovernmental panel on climate change, *Cambridge University Press, Cambridge, UK*, pp, 315-356.
Odd, N. V. M. and Murphy, D. G. (1992) 'Particulate Pollutants in the North Sea', Report SR292, *HR Wallingford, UK*, pp. 1-38.
Odum, W. E. (1988) 'Comparative ecology of tidal freshwater and salt marshes', *Annual Review of Ecology and Systematics,* 19(1), pp. 147-176.

Oliver, R. R. (2013) 'Ordnance Survey maps: A concise guide for historians'. Charles Close Society for the Study of Ordnance Survey Maps, *CPI Bath Press, Bath, UK,* vol 3, pp. 1-256.
Ollerhead, J., Davidson-Arnott, R. G. and Scott, A. (2005) 'Cycles of salt marsh extension and contraction, Cumberland Basin, Bay of Fundy, Canada', *in:* Sanjaume, E. (Ed.), Geomorphologia Littoral I Quaternari: Homenatge al Professor VM Rossello i Verger*, Universitat de Valencia, Spain*, pp. 293-305.
Osland, M. J., Enwright, N. M., Day, R. H., Gabler, C. A., Stagg, C. L. and Grace, J. B. (2016) 'Beyond just sea-level rise: Considering macroclimatic drivers within coastal wetland vulnerability assessments to climate change', *Global Change Biology,* 22(1), pp. 1-11.
Pedersen, J. B. and Bartholdy, J. (2007) 'Exposed salt marsh morphodynamics: An example from the Danish Wadden Sea', *Geomorphology,* 90(1), pp. 115-125.
Pelling, H. E. and Green, J. M. (2014) 'Impact of flood defences and sea-level rise on the European Shelf tidal regime', *Continental Shelf Research,* 85, pp. 96-105.
Perucca, E., Camporeale, C. and Ridolfi, L. (2007) 'Significance of the riparian vegetation dynamics on meandering river morphodynamics', *Water Resources Research,* 43(3), pp. 1-10.
Peterson, G., Allen, C. R. and Holling, C. S. (1998) 'Ecological resilience, biodiversity, and scale', *Ecosystems,* 1(1), pp. 6-18.
Pethick, J. (1994) 'Estuaries and wetlands: Function and form'. *in:* Falconer, R. A. and Goodwin, P. (Eds.), Wetland management, *Thomas Telford Publishing, London, UK*, pp. 75-87.
Pethick, J. (1996) 'Shoreline intervention proposals: Afon Dysynni to Aberdyfi', The Dyfi Estuary and Aberdyfi Coast. Report to the Countryside Council for Wales, *Gwynedd Council, UK*, pp. 1-11.
Petraitis, P. (2013) 'Multiple stable states in natural ecosystems', *Oxford University Press, Oxford, UK*, pp. 1-200.
Pezeshki, S. (2001) 'Wetland plant responses to soil flooding', *Environmental and Experimental Botany,* 46(3), pp. 299-312.
Phelan, N., Shaw, A. and Baylis, A. (2011) 'The extent of saltmarsh in England and Wales: 2006-2009', *Environment Agency, Bristol, UK*, pp. 1-57.
Phillips, J. D. (1995) 'Biogeomorphology and landscape evolution: The problem of scale', *Geomorphology*, 13, pp. 337-347.
Prandle, D. (2003) 'Relationships between tidal dynamics and bathymetry in strongly convergent estuaries', *Journal of Physical Oceanography,* 33(12), pp. 2738-2750.
Prandle, D. (2004) 'How tides and river flows determine estuarine bathymetries', *Progress in Oceanography,* 61(1), pp. 1-26.
Prandle, D., Lane, A. and Manning, A. J. (2005) 'Estuaries are not so unique', *Geophysical Research Letters,* 32(23), pp. 1-5.
Prandle, D., Lane, A. and Wolf, J. (2001) 'Holderness coastal erosion – offshore movement by tides and waves', *in:* Huntley, D., Leeks, G. and Walling, D. (Eds.), Land-Ocean Interaction. Measuring and modelling fluxes from river basins to coastal seas, *IWA Publishing, London, UK,* pp. 209-240.
Pringle, A. (1995) 'Erosion of a cyclic saltmarsh in Morecambe Bay, north-west England', *Earth Surface Processes and Landforms,* 20(5), pp. 387-405.
Prosser, M. V. and Wallace, H. L. (2004) 'Pen Llyn a'r Sarnau cSAC and adjacent areas salt marshes review and National Vegetation Classification survey 2003: Main report', CCW Science Report no. 642, *Countryside Council for Wales, Bangor, UK,* pp. 1-68.

Pyatt, F. B. and Collin, R. L. (1999) 'Geochemical variations in the intertidal deposits within the Dyfi Estuary, West Wales, United Kingdom - A case study', *Environmental Toxicology*, 14(2), pp. 249-261.
Pye, K. and Blott, S. J. (2014) 'The geomorphology of UK estuaries: The role of geological controls, antecedent conditions and human activities', *Estuarine, Coastal and Shelf Science,* 150, pp. 196-214.
Pye, K. and French, P. W. (1993a) 'Erosion and accretion processes on British saltmarshes. Volume 1. Introduction: saltmarsh processes and morphology', *Cambridge Environmental Research Consultants, Cambridge, UK*, pp. 1-89.
Pye, K. and French, P. (1993b) 'Targets for coastal habitat re-creation', English Nature Science Report No. 13, *English Nature, Peterborough, UK*, pp. 1-43.
Ranwell, D. (1967) 'World resources of *Spartina townsendii* (*sensu lato*) and economic use of *Spartina* marshland', *Journal of Applied Ecology,* 4(1), pp. 239-256.
Raybould, A. (2005) 'History and ecology of *Spartina anglica* in Poole Harbour', *in:* Humphreys, J. and May, V. (Eds.), The ecology of Poole Harbour, *Elsevier, Amsterdam*, pp. 71-90.
Rhind, P. and Jones, A. (1995) 'Brackish saltmarsh communities in the Glaslyn Marsh Trust Reserve', *Oceanographic Literature Review,* 12(42), pp. 1118.
Rietkerk, M., Dekker, S. C., de Ruiter, P. C. and van de Koppel, J. (2004) 'Self-organized patchiness and catastrophic shifts in ecosystems', *Science,* 305(5692), pp. 1926-1929.
Rinaldo, A., Fagherazzi, S., Lanzoni, S., Marani, M. and Dietrich, W. E. 'Tidal networks: 3. Landscape-forming discharges and studies in empirical geomorphic relationships', *Water Resource Research*, 35(12), pp. 3919-3929.
Ripley, B. and Venables, B. (2013) 'Modern applied statistics with S-PLUS', vol. 3, *Springer, New York, USA*, pp. 1-500.
Robins, P. E. and Davies, A. G. (2011) 'Application of TELEMAC-2D and SISYPHE to complex estuarine regions to inform future management decisions', *XVIIIth TELEMAC & Mascaret User Club Chatou, France*, pp. 19-21.
Roberts, W., Dearnaley, M. P., Baugh, J. V., Spearman, J. R. and Allen, R. S. (1998) 'The sediment regime of the Stour and Orwell estuaries', *in:* Dronkers, J. J. and Scheffers, M. (Eds.), Physics of Estuaries and Coastal Seas. *Balkema*, *Rotterdam, Netherlands*, pp. 93-102.
Robins, P. E., Skov, M. W., Lewis, M. J., Giménez, L., Davies, A. G., Malham, S. K., Neill, S. P., McDonald, J. E., Whitton, T. A. and Jackson, S. E. (2016) 'Impact of climate change on UK estuaries: A review of past trends and potential projections', *Estuarine, Coastal and Shelf Science,* 169, pp. 119-135.
Robson, A. and Reed, D. (1999) 'Flood estimation handbook. Volume 3. Statistical procedures for flood frequency estimation', *HR Wallingford, UK*, pp. 1-338.
Rohweder, J. J., Rogala, J. T., Johnson, B. L., Anderson, D., Clark, S., Chamberlin, F. and Runyon, K. (2008) 'Application of wind fetch and wave models for habitat rehabilitation and enhancement projects', *USGS, USA,* pp. 1-54.
Scheffer, M., Carpenter, S., Foley, J. A., Folke, C. and Walker, B. (2001) 'Catastrophic shifts in ecosystems', *Nature,* 413(6856), pp. 591.
Scheffer, M., Carpenter, S. R., Lenton, T. M., Bascompte, J., Brock, W., Dakos, V., van de Koppel, J., van de Leemput, I. A., Levin, S. A. and van Nes, E. H. (2012) 'Anticipating critical transitions', *Science,* 338(6105), pp. 344-348.
Schrama, M., Berg, M. P. and Olff, H. (2012) 'Ecosystem assembly rules: The interplay of green and brown webs during salt marsh succession', *Ecology,* 93(11), pp. 2353-2364.

Schuerch, M., Dolch, T., Reise, K. and Vafeidis, A. T. (2014) 'Unravelling interactions between salt marsh evolution and sedimentary processes in the Wadden Sea (southeastern North Sea)', *Progress in Physical Geography,* 38(6), pp. 691-715.
Seminara, G. (2006) 'Meanders', *Journal of Fluid Mechanics,* 554, pp. 271-297.
Sharps, E., Smart, J., Skov, M. W., Garbutt, A. and Hiddink, J. G. (2015) 'Light grazing of saltmarshes is a direct and indirect cause of nest failure in Common Redshank *Tringa totanus*', *Ibis,* 157(2), pp. 239-249.
Shenker, J. M. and Dean, J. M. (1979) 'The utilization of an intertidal salt marsh creek by larval and juvenile fishes: Abundance, diversity and temporal variation', *Estuaries and Coasts,* 2(3), pp. 154-163.
Shepard, C. C., Crain, C. M. and Beck, M. W. (2011) 'The protective role of coastal marshes: A systematic review and meta-analysis', *PLoS One,* 6(11), pp. e27374.
Shi, Z. (1993) 'Recent saltmarsh accretion and sea level fluctuations in the Dyfi Estuary, central Cardigan Bay, Wales, UK', *Geo-Marine Letters,* 13(3), pp. 182-188.
Shi, Z. and Lamb, H. (1991) 'Post-glacial sedimentary evolution of a microtidal estuary, Dyfi Estuary, west Wales, UK', *Sedimentary Geology,* 73(3-4), pp. 227-246.
Shi, Z., Lamb, H. and Collin, R. (1995) 'Geomorphic change of saltmarsh tidal creek networks in the Dyfi Estuary, Wales', *Marine Geology*, 128(1-2), pp. 73-83.
Silinski, A., Fransen, E., Bouma, T. J., Meire, P. and Temmerman, S. (2016) 'Unravelling the controls of lateral expansion and elevation change of pioneer tidal marshes', *Geomorphology,* 274, pp. 106-115.
Silliman, B. R., van de Koppel, J., Bertness, M. D., Stanton, L. E. and Mendelssohn, I. A. (2005) 'Drought, snails, and large-scale die-off of southern US salt marshes', *Science,* 310(5755), pp. 1803-1806.
Silliman, B. R., van de Koppel, J., McCoy, M. W., Diller, J., Kasozi, G. N., Earl, K., Adams, P. N. and Zimmerman, A. R. (2012) 'Degradation and resilience in Louisiana salt marshes after the BP–Deepwater Horizon oil spill', *Proceedings of the National Academy of Sciences,* 109(28), pp. 11234-11239.
Smith, T. J. and Odum, W. E. (1981) 'The effects of grazing by snow geese on coastal salt marshes', *Ecology,* 62(1), pp. 98-106.
Sousa, A. I., Santos, D. B., Da Silva, E. F., Sousa, L. P., Cleary, D. F., Soares, A. M. and Lillebø, A. I. (2017) '‘Blue Carbon’and Nutrient Stocks of Salt Marshes at a Temperate Coastal Lagoon (Ria de Aveiro, Portugal)', *Scientific Reports,* 7, pp. 1-11.
Spearman, J., Baugh, J., Feates, N., Dearnaley, M. & Eccles, D. (2014) 'Small estuary, big port–progress in the management of the Stour-Orwell Estuary system', *Estuarine, Coastal and Shelf Science*, 150, pp. 299-311.
Spencer, T., Brooks, S. M., Evans, B. R., Tempest, J. A. and Möller, I. (2015) 'Southern North Sea storm surge event of 5 December 2013: Water levels, waves and coastal impacts', *Earth-Science Reviews,* 146, pp. 120-145.
Spencer, T., Schuerch, M., Nicholls, R. J., Hinkel, J., Lincke, D., Vafeidis, A., Reef, R., McFadden, L. and Brown, S. (2016) 'Global coastal wetland change under sea-level rise and related stresses: The DIVA Wetland Change Model', *Global and Planetary Change,* 139, pp. 15-30.
Stallins, J. A. (2006) 'Geomorphology and ecology: Unifying themes for complex systems in biogeomorphology', *Geomorphology,* 77(3), pp. 207-216.
Stallins, J. A. and Corenblit, D. (2017) 'Interdependence of geomorphic and ecologic resilience properties in a geographic context', *Geomorphology*, 305, pp. 76-93.
Stefanon, L., Carniello, L., D'Alpaos, A. and Rinaldo, A. (2012) 'Signatures of sea level changes on tidal geomorphology: Experiments on network incision and retreat', *Geophysical Research Letters,* 39(12), pp. 1-6.

Stralberg, D., Brennan, M., Callaway, J. C., Wood, J. K., Schile, L. M., Jongsomjit, D., Kelly, M., Parker, V. T. and Crooks, S. (2011) 'Evaluating tidal marsh sustainability in the face of sea-level rise: A hybrid modeling approach applied to San Francisco Bay', *PLoS One,* 6(11), pp. e27388.

Suykerbuyk, W., Bouma, T. J., Govers, L. L., Giesen, K., de Jong, D. J., Herman, P., Hendriks, J. and van Katwijk, M. M. (2016) 'Surviving in changing seascapes: Sediment dynamics as bottleneck for long-term seagrass presence', *Ecosystems,* 19(2), pp. 296-310.

Syvitski, J. P., Vörösmarty, C. J., Kettner, A. J. and Green, P. (2005) 'Impact of humans on the flux of terrestrial sediment to the global coastal ocean', *Science,* 308(5720), pp. 376-380.

Tabacchi, E., Steiger, J., Corenblit, D., Monaghan, M. T. and Planty-Tabacchi, A.-M. (2009) 'Implications of biological and physical diversity for resilience and resistance patterns within Highly Dynamic River Systems', *Aquatic Sciences,* 71(3), pp. 279-289.

Tal, M. and Paola, C. (2007) 'Dynamic single-thread channels maintained by the interaction of flow and vegetation', *Geology,* 35(4), pp. 347-350.

Temmerman, S., Bouma, T., Govers, G., Wang, Z., De Vries, M. and Herman, P. (2005) 'Impact of vegetation on flow routing and sedimentation patterns: Three-dimensional modeling for a tidal marsh', *Journal of Geophysical Research: Earth Surface,* 110(F4), pp. 1-18.

Temmerman, S., Bouma, T., van de Koppel, J., van der Wal, D., De Vries, M. and Herman, P. (2007) 'Vegetation causes channel erosion in a tidal landscape', *Geology,* 35(7), pp. 631-634.

Temmerman, S., Meire, P., Bouma, T. J., Herman, P. M., Ysebaert, T. and De Vriend, H. J. (2013) 'Ecosystem-based coastal defence in the face of global change', *Nature,* 504(7478), pp. 79-83.

Thorne, C. R. and Tovey, N. K. (1981) 'Stability of composite river banks', *Earth Surface Processes and Landforms,* 6(5), pp. 469-484.

Thrush, S. F., Hewitt, J. E., Dayton, P. K., Coco, G., Lohrer, A. M., Norkko, A., Norkko, J. and Chiantore, M. (2009) 'Forecasting the limits of resilience: Integrating empirical research with theory', *Proceedings of the Royal Society B*, 276(1671), pp. 3209-3217.

Townend, I. H., Wang, Z. B. and Rees, J. (2007) 'Millennial to annual volume changes in the Humber Estuary', *Proceedings of the Royal Society A*, 463(2079), pp. 837-854.

Traini, C., Proust, J.-N., Menier, D. and Mathew, M. (2015) 'Distinguishing natural evolution and human impact on estuarine morpho-sedimentary development: A case study from the Vilaine Estuary, France', *Estuarine, Coastal and Shelf Science,* 163, pp. 143-155.

Traut, B. H. (2005) 'The role of coastal ecotones: A case study of the salt marsh/upland transition zone in California', *Journal of Ecology,* 93(2), pp. 279-290.

Ursino, N., Silvestri, S. and Marani, M. (2004) 'Subsurface flow and vegetation patterns in tidal environments', *Water Resources Research,* 40(5), pp. 1-11.

Valiela, I., Kinney, E., Culbertson, J., Peacock, E., Smith, S. and Duarte, C. M. (2009) 'Global losses of mangrove and salt marshes', *in:* Duarte, C. M. (Ed.), Global Loss of Coastal Habitats Rates, Causes and Consequences, *Fundación BBVA, Spain*, pp. 107-138.

van Belzen, J., van de Koppel, J., Kirwan, M. L., van der Wal, D., Herman, P. M., Dakos, V., Kéfi, S., Scheffer, M., Guntenspergen, G. R. and Bouma, T. J. (2017) 'Vegetation recovery in tidal marshes reveals critical slowing down under increased inundation', *Nature Communications,* 8, pp. 1-7.

van de Koppel, J., van der Wal, D., Bakker, J. P. and Herman, P. M. (2005) 'Self-organization and vegetation collapse in salt marsh ecosystems', *The American Naturalist,* 165(1), pp. 1-12.
van der Wal, D. and Pye, K. (2004) 'Patterns, rates and possible causes of saltmarsh erosion in the Greater Thames area (UK)', *Geomorphology,* 61(3), pp. 373-391.
van der Wal, D., Wielemaker-van den Dool, A. and Herman, P. M. (2008) 'Spatial patterns, rates and mechanisms of saltmarsh cycles (Westerschelde, The Netherlands)', *Estuarine, Coastal and Shelf Science,* 76(2), pp. 357-368.
van der Wegen, M., Wang, Z. B., Savenije, H. and Roelvink, J. (2008) 'Long-term morphodynamic evolution and energy dissipation in a coastal plain, tidal embayment', *Journal of Geophysical Research: Earth Surface,* 113(F3), pp. 1-22.
van Eerdt, M. M. (1985) 'The influence of vegetation on erosion and accretion in salt marshes of the Oosterschelde, The Netherlands', *Vegetatio,* 62(1-3), pp. 367-373.
van Hulzen, J., van Soelen, J. and Bouma, T. (2007) 'Morphological variation and habitat modification are strongly correlated for the autogenic ecosystem engineer *Spartina anglica* (common cordgrass)', *Estuaries and Coasts,* 30(1), pp. 3-11.
van Proosdij, D., Ollerhead, J. and Davidson-Arnott, R. G. (2006) 'Seasonal and annual variations in the volumetric sediment balance of a macro-tidal salt marsh', *Marine Geology,* 225(1), pp. 103-127.
van Straaten, L. M. J. U. (1954) 'Composition and structure of recent marine sediments in the Netherlands', *Leidse Geologische Mededelingen,* 19(1), pp. 1-108.
van Wesenbeeck, B., van de Koppel, J., Herman, P., Bakker, J. and Bouma, T. (2007) 'Biomechanical warfare in ecology; negative interactions between species by habitat modification', *Oikos,* 116(5), pp. 742-750.
van Wesenbeeck, B., van de Koppel, J., MJ Herman, P. and J Bouma, T. (2008) 'Does scale-dependent feedback explain spatial complexity in salt-marsh ecosystems?', *Oikos,* 117(1), pp. 152-159.
Vandenbruwaene, W., Maris, T., Cox, T., Cahoon, D., Meire, P. and Temmerman, S. (2011) 'Sedimentation and response to sea-level rise of a restored marsh with reduced tidal exchange: Comparison with a natural tidal marsh', *Geomorphology,* 130(3), pp. 115-126.
Vitousek, P. M. (1994) 'Beyond global warming: Ecology and global change', *Ecology,* 75(7), pp. 1861-1876.
Walker, B. (1995) 'Conserving biological diversity through ecosystem resilience', *Conservation Biology,* 9(4), pp. 747-752.
Wang, C. and Temmerman, S. (2013) 'Does biogeomorphic feedback lead to abrupt shifts between alternative landscape states?: An empirical study on intertidal flats and marshes', *Journal of Geophysical Research: Earth Surface,* 118(1), pp. 229-240.
Ward, L. G., Kearney, M. S. and Stevenson, J. C. (1998) 'Variations in sedimentary environments and accretionary patterns in estuarine marshes undergoing rapid submergence, Chesapeake Bay', *Marine Geology,* 151(1), pp. 111-134.
Watson, S. J., Kritharas, P. and Hodgson, G. (2015) 'Wind speed variability across the UK between 1957 and 2011', *Wind Energy,* 18(1), pp. 21-42.
Wernette, P., Shortridge, A., Lusch, D. P. and Arbogast, A. F. (2017) 'Accounting for positional uncertainty in historical shoreline change analysis without ground reference information', *International Journal of Remote Sensing,* 38(13), pp. 3906-3922.
Weston, N. B. (2014) 'Declining sediments and rising seas: An unfortunate convergence for tidal wetlands', *Estuaries and Coasts,* 37(1), pp. 1-23.
Wiehe, P. (1935) 'A quantitative study of the influence of tide upon populations of *Salicornia europea*', *The Journal of Ecology*, 23(2), pp. 323-333.

Wilks, P.J. (1979) 'Mid-Holocene sea-level and sedimentation interactions in the Dovey estuary area, Wales', *Palaeogeography, Palaeoclimatology, Palaeoecology*, 26, pp. 17-36.
Wilson, C. A., Hughes, Z. J., FitzGerald, D. M., Hopkinson, C. S., Valentine, V. and Kolker, A. S. (2014) 'Saltmarsh pool and tidal creek morphodynamics: Dynamic equilibrium of northern latitude saltmarshes?', *Geomorphology,* 213, pp. 99-115.
Wolters, M., Garbutt, A. and Bakker, J. P. (2005) 'Salt-marsh restoration: Evaluating the success of de-embankments in north-west Europe', *Biological Conservation,* 123(2), pp. 249-268.
Wolters, M., Garbutt, A., Bekker, R. M., Bakker, J. P. and Carey, P. D. (2008) 'Restoration of salt-marsh vegetation in relation to site suitability, species pool and dispersal traits', *Journal of Applied Ecology,* 45(3), pp. 904-912.
Woodend, A. (2010) 'Definitions of terms used in farm business management. third edition', *Department for Environment, Food and Rural Affairs*, *London*, pp. 1-48.
Woodworth, P. and Player, R. (2003) 'The Permanent Service for Mean Sea Level: An Update to the 21st Century', *Journal of Coastal Research*, 19(2), pp. 287-295.
Woodworth, P., Teferle, F. N., Bingley, R., Shennan, I. and Williams, S. (2009) 'Trends in UK mean sea level revisited', *Geophysical Journal International,* 176(1), pp. 19-30.
Worrall, F., Burt, T. P. and Howden, N. J. (2013) 'The flux of suspended sediment from the UK 1974 to 2010', *Journal of Hydrology,* 504, pp. 29-39.
Yang, S. L., Ding, P. X. and Chen, S. L. (2001) 'Changes in progradation rate of the tidal flats at the mouth of the Changjiang (Yangtze) River, China', *Geomorphology,* 38(1), pp. 167-180.
Yapp, R., Johns, D. and Jones, O. (1917) 'The salt marshes of the Dovey Estuary', *The Journal of Ecology*, 5(2), pp. 65-103.
Zacheis, A., Hupp, J. W. and Ruess, R. W. (2001) 'Effects of migratory geese on plant communities of an Alaskan salt marsh', *Journal of Ecology,* 89(1), pp. 57-71.
Zarco-Tejada, P., Hornero, A., Hernández-Clemente, R. and Beck, P. (2018) 'Understanding the temporal dimension of the red-edge spectral region for forest decline detection using high-resolution hyperspectral and Sentinel-2a imagery', *Isprs Journal of Photogrammetry and Remote Sensing,* 137, pp. 134-148.
Zuur, A., Ieno, E. N., Walker, N., Saveliev, A. A. and Smith, G. M. (2009) 'Mixed Effects Models and Extensions in Ecology with R', *Springer New York, USA*, pp 1-574.
Zuur, A. F., Ieno, E. N. and Elphick, C. S. (2010) 'A protocol for data exploration to avoid common statistical problems', *Methods in Ecology and Evolution,* 1(1), pp. 3-14.

7 Appendices

Appendix I: Estimating error in saltmarsh area cover

Areal extent of salt marshes across Great Britain using maps and aerial photographs were calculated in this study to measure change over time (*Chapters 2 and 3*). In order to quantify an error term associated with these measurements, the Root Mean Squared Error (RMSE), which describes the average deviation of observed points from their true positions (Wernette et al., 2017), was calculated. Four independent RMSE sources are associated with geographical data: displacement of the basemap, to which historical maps and aerial photographs are referenced, from its 'true' location on the Earth's surface ($RMSE_B$); distortions in historical maps and aerial photographs that introduce error when georeferencing to a basemap ($RMSE_G$); interpreter error when digitizing the salt marsh at a given scale ($RMSE_I$), and; errors introduced by the cartographer when presenting spatial data on a map (not relevant for aerial photographs) ($RMSE_M$). Because each error source is independent, RMSE terms can be added for a total error estimate. To determine distances, in meters, below which 95% of the positional errors in delineated salt marsh edges are expected to fall, FGDC (1998) recommend the added RMSE values are multiplied by 1.7308 in order to calculate $RMSE_{95}$, given as:

$$RMSE_{95} = 1.7308\left(\sqrt{\left(RMSE_B{}^2 + RMSE_G{}^2 + RMSE_I{}^2 + RMSE_M{}^2\right)}\right)$$

Maps produced between 1842 and 1952 (Six-inch County Series Edition) by the Ordnance Survey (OS), were produced using ground surveys. Demarcating the seaward limit of the salt marsh accurately is dependent on the cartographer's capacity to survey difficult-to-reach or dangerous areas, and distinguish the edge of the marsh which is often 'fuzzy' (due to patchy growth of plants) (Baily and Collier, 2010; Baily, 2011; Baily and Inkpen, 2013). OS standards on the quality and accuracy of saltmarsh surveying were not stringent (Close, 1912; Baily and Inkpen, 2013) so as a consequence, the marsh edge is sometimes represented as a stamped symbol without a clearly defined margin (Baily and Inkpen, 2013). OS maps produced after 1952 (National Series Edition maps) were compiled using a combination of ground surveys and aerial photographs. Delineating the marsh edge from aerial photographs accurately depends on surveyor capacity to correctly distinguish plants from other features (such as macroalgae patches), and the quality of the image.

There is no specific guidance on set by the OS on demarcating the marsh edge from aerial photographs (OS, pers. Comm., 2018). Baily and Inkpen (2013) assessed how successful OS ground-surveys were at determining the marsh edge by comparing maps with aerial photographs captured near the map publication date. Where maps were surveyed at similar times to when images were taken, both media are in close agreement.

A value for the positional error of digitized marsh edge (map or photo) from the true position ($RMSE_I$) was not given by Baily and Inkpen (2013). To calculate $RMSE_I$, we selected an example marsh boundary; a 5 km section saltmarsh edge in the Wash was digitised to very high resolution (vertice placed every meter) at high magnification to capture the 'true' marsh edge from an OS map. Resolution of the map was then scaled to 1:7,500, and the marsh edge was digitized once more on three different occasions to capture the 'interpreted' marsh edge. Distance from the 'interpreted' line to the 'true' line was calculated every 20 meters along perpendicular lines from the 'true' line. This is the same procedure used when delineating the marsh edge from maps and aerial photographs. $RMSE_I$ is given as:

$$RMSE_I = \sqrt{\left(\frac{\sum d^2}{n}\right)}$$

Where:

d is the distance between the 'true' and 'interpreted' marsh edge

n is the number of distance measurements.

An additional error term, associated with maps produced from ground surveys only, is the interpretation of the surveyor of where the marsh edge lies which is then reproduced on a map as a line or stamp ($RMSE_M$).

Given that marsh edges from maps and photos have been shown to be in close agreement (Baily and Inkpen, 2013), $RMSE_M$, is assumed to be of the same magnitude as $RMSE_I$:

$$RMSE_M = RMSE_I$$

Both $RMSE_M$ and $RMSE_I$ should be included for estimates of marsh extent taken from maps that have drawn from ground surveys.

Distortions can occur in maps and aerial photographs during the survey. For maps, inaccuracies arise when noting positons from traditional trigonometry surveys or modern Geographical Positioning Systems. After publication, historical maps can distort over time through shrinkage and stretching before being digitised. For aerial photographs, tilt, pitch and yaw of the aeroplane will affect the angle at which images were taken, and unevenness of the topography being captured both cause distortions of the image. Both the film and reprints can distort over time once produced. These issues reduce the accuracy of features that maps and aerial photographs were intended to represent once images are georeferenced. This georeferencing distortion, $RMSE_G$, can be calculated by the distance from which the source deviates from a reference position (Jongepier et al., 2016), calculated by:

$$RMSE_G = \sqrt{\frac{\left(\sum {V_{xy}}^2\right)}{n-2}}$$

Where n is the number of points and V_{xy}, is a displacement vector made up of vector distances v_x and v_y (in meters) between the distorted points and the reference positions, calculated as:

$$V_{xy} = \sqrt{\left({v_x}^2 + {v_y}^2\right)}$$

$RMSE_G$ was calculated separately for all maps and photographs to OS 1:2500 basemaps as reference using MapAnalyst (Jenny and Hurni, 2011). 12 well-distributed control points were identified in both the source and 1:2500 maps and the $RMSE_G$ between them was calculated using

a Helmert transformation (Jongepier et al., 2016). Measurements of marsh extent for the Essex-Kent and Solent regions were taken from Cooper et al. (2001) and Baily and Pearson (2007). Cooper et al. (2001) do not report $RMSE_G$ for their survey, however Baily and Pearson (2007) do report a precision value of between ± 3 and 5 m. An average $RMSE_G$ of 4 meters was taken for their survey and applied to Essex-Kent (*Chapter 2*) and Cardigan Bay (*Chapter 2 and 3*) regions where aerial photography was used to delineate marsh extent. All $RMSE_G$ are reported in Table A1.

Table A1 Error terms for maps and photo distortions. $RMSE_G$ for a representative map tile or aerial photograph in each region, expressed in metres.

Region	County First Edition	County First Revision	County Second Revision	County Third Revision	National First Edition	National First Revision	National Second Revision	National Third Revision	Aerial photography
Solway	12.20	7.07	NA	6.03	6.97	NA	NA	6.03	NA
Morecambe	13.78	11.44	6.92	NA	6.03	6.03	6.03	6.03	NA
Cardigan	9.05	9.99	NA	NA	NA	NA	NA	NA	4.00
Wash	7.72	10.00	NA	NA	6.03	9.72	NA	6.03	NA
Essex-Kent	13.34	12.15	12.15	NA	NA	NA	NA	NA	4.00
Solent	9.32	8.85	10.28	10.28	NA	9.74	NA	6.03	4.00

The 1:2500 maps used as a reference for measuring distortions in older maps and aerial photographs in this study are themselves subject to some positional error between the 'real life' position and that recorded on the map known as $RMSE_B$. For the OS 1:2500, $RMSE_B$ of 1.1 meters has been calculated (HMLR, 2016). Values of $RMSE_{95}$ for each map type are shown in Table A2.

Table A2 Total error for marsh extent measures. $RMSE_{95}$ for map and aerial photograph in each region, expressed in meters.

Region	County First Edition	County First Revision	County Second Revision	County Third Revision	National First Edition	National First Revision	National Second Revision	National Third Revision	Aerial photography
Solway	22.94	15.18	NA	NA	13.77	15.04	NA	13.77	NA
Morecambe	25.48	21.74	8.98	NA	13.77	13.77	13.77	8.98	NA
Cardigan	18.05	19.48	NA	NA	NA	NA	NA	NA	9.49
Wash	16.10	19.50	NA	NA	13.77	19.07	NA	13.77	NA
Essex-Kent	24.77	22.87	22.87	NA	NA	NA	NA	NA	9.49
Solent	18.46	17.75	8.98	19.93	NA	19.10	NA	13.77	9.49

$RMSE_{95}$ is a linear measure (units in metres). In order to express $RMSE_{95}$ for areal measures, a buffer area around the inner and outer circumference of each marsh was constructed, where the width was $RMSE_{95}$ calculated for each source (Wernette et al., 2017). The buffer area can be used

to calculate the predicted minimum and maximum size of the marsh. This error term represents a 95% confidence interval for a given measure of marsh extent.

Calculating a buffer area was not possible for values taken from Cooper et al. (2001) and Baily and Pearson (2007), and no error term is reported by these authors. A marsh buffer area was therefore estimated for each study. The buffer area was estimated by resampling marsh extent from aerial photographs of Cardigan Bay, but at the image scales used by Cooper et al. (2001) and Baily and Pearson (2007) (1:5,000 and 1:10,000 respectively). $RMSE_{95}$ was recalculated, then the percentage difference in area extent between delineated marsh extent and maximum/minimum area buffers were calculated for each scale. Marsh extent was found to vary by ±18.4 and ±20.0% at scales of 1:5,000 and 1:10,000 respectively. These error margins were applied to the values of marsh extent taken from Cooper et al. (2001) and Baily and Pearson (2007) as the $RMSE_{95}$ error term.

The final error term for marsh area extent can be considered conservative, because accuracy in delineating the marsh edge in many cases will be much higher. For example, where the back of the marsh is bounded by a clearly-defined embankment that can be mapped to a high degree of accuracy.

After the OS produced first edition maps (County and National Series), revisions were soon needed to keep maps up-to-date in a rapidly developing landscape. However, revisions did not always include complete re-surveys of an area. Revisions tended to be made only for areas heavily used by people, whilst less important features were simply copied over from the previous edition known as ‘partial-revisions’ (Baily and Inkpen, 2013). Salt marshes were not always resurveyed during map revisions, and when revisions occurred, the specific area that had been revised was not always recorded Baily (2011). In this study, revision error was accounted for by comparing map revisions against first editions of each marsh in each estuary. On the assumption that the marsh boundary is likely to change during a ~30 year period, marshes that had near-identical boundaries in both first and revised editions were considered copied, so areal extent was not calculated.

Appendix II: Validating estimated suspended sediment concentration

An analytically-derived measure of fine cohesive suspended sediment concentration (SSC_E) was used in *Chapter 2*, which represents a maximum static time- and depth-averaged value for the entire estuary, to use as a predictor of lateral marsh change in a Partial Least Squares Regression model. While SSC_E derivations have caveats (e.g. they assume a simplified estuarine geometry based on average depth and area in order to estimate SSC_E (Prandle, 2004)), this appendix demonstrates that SSC_E is a good integrative metric of overall long-term sediment supply.

Numerical models have demonstrated that elevated SSC in tidal waters can increase marsh resilience by promoting both vertical accretion (Kirwan et al., 2010) and lateral expansion (Mariotti and Fagherazzi, 2010). However, static measures of SSC alone are not necessarily good metrics of marsh vulnerability because marsh erosion may result in localised increases in SSC and so would not represent an external sediment source (Ganju et al., 2015). Ganju et al. (2017) show that external sediment supply was strongly correlated to the unvegetated/vegetated ratio (UVVR) of marsh extent in microtidal estuaries across the USA. This appendix examines whether SSC_E and UVVR correlate for estuaries across Great Britain as a validation procedure for using SSC_E to predict external sediment supply. The study used a UK-wide saltmarsh extent shapefile (collated by the UK Environment Agency [EA], https://data.gov.uk/dataset/saltmarsh-extents1) to calculate UVVR. The EA shapefile represents the vegetated portions of marshes across the UK, and distinguishes vegetated marshes form bare tidal channels and salt pans. The EA captured colour aerial images with 10 cm resolution for the UK coastline between 2006 and 2009. Images were georeferenced with root mean square error ranging from 10 cm to 1 m. Marsh delineation was done manually, and digitally using various feature-identification techniques. Creeks less than 1.5 m wide and marshes less than 5 m^2 were overlooked. In cases where there was low confidence in mapping results, site visits were made to ground-truth the digitized marsh surface (Phelan et al., 2011). In a GIS, the saltmarsh extent shapefile was used to calculate the area of vegetated portions for each marsh complex within an estuary. A workflow of ArcGIS tools were then applied to outline the overall marsh complex, thereby effectively separating tidal channel and salt pan features from the vegetated marsh surface. The original shapefile was then subtracted from this

'boundary' layer to calculate the area of unvegetated portions within the marsh complex (Figure A1). UVVR was then calculated (A_{UV}/A_V) for all 25 estuaries.

The study found a highly significant relationship between SSC_E and UVVR for the target estuaries (Figure A2), indicating that levels of SSC_E sufficiently reflect the sediment budget of estuary complexes across Great Britain. Moreover, marshes characterised by net erosion (UVVR >0.30) did not display elevated levels of SSC_E caused by the release of sediment during marsh erosion (Ganju et al., 2017), indicating SSC_E can be applied as a metric of sediment availability regardless of whether marshes are expanding or eroding.

To further validate the use of SSC_E as a predictor of lateral marsh change, we substituted SSC_E for UVVR in a Partial Least Squares Regression model, then compared the model results to the original analysis where SSC_E was used. Prior to running the model, inspection of Cleveland dotplots for each variable identified a single major outlier (Portsmouth, Solent) which had a very

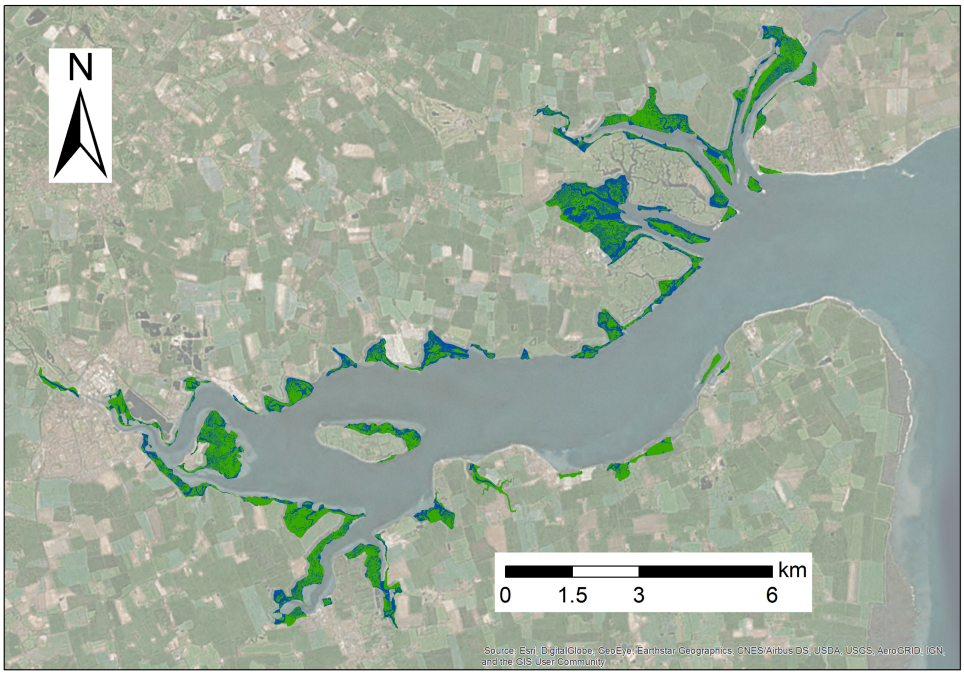

Figure A1 Example of vegetated and unvegetated portions of a marsh. The Blackwater estuary, Essex-Kent region of Great Britain. Unvegetated areas are shown in blue, vegetated surfaces are shown in green. Saltmarsh extent was taken from the UK Environment Agency, and the marsh boundary was determined using a series of polygon processing tools in ArcGIS. Imagery from the ArcGIS World Imagery Basemap.

high UVVR value (UVVR = 2.138). Portsmouth is an industrialised estuary with major shipping lanes running close to the marsh edge, which can increase marsh erosion rates due to the wake caused by passing vessels (Houser, 2010). It is likely that marshes in Portsmouth estuary are especially vulnerable to erosion, resulting in highly fragmented marshes and a high UVVR value. To avoid outlier bias on the robustness of the statistical analysis, this value was subsequently dropped. All variables were then cube-transformed to meet assumptions of normality and equal variance. High correlation existed between UVVR and RSLR (r = 0.75), therefore a Partial Least Squares model was used to examine which variables best explained lateral marsh change. The results showed that RSLR and UVVR in combination best explained the rate of marsh lateral changes in estuaries across Great Britain (Table A3). Marsh expansion had a negative linear relationship with UVVR, and a negative linear relationship with RSLR (Table A3). In summary, greater degradation of the marsh surface (larger UVVR) and higher rates of sea level rise resulted in a greater rate of lateral marsh erosion. By comparing Table A3 with the model results shown in the main text, the use of either SSC_E or UVVR in explaining rate of lateral marsh change resulted in the same conclusion, thereby validating the use of SSC_E as a measure of external sediment supply.

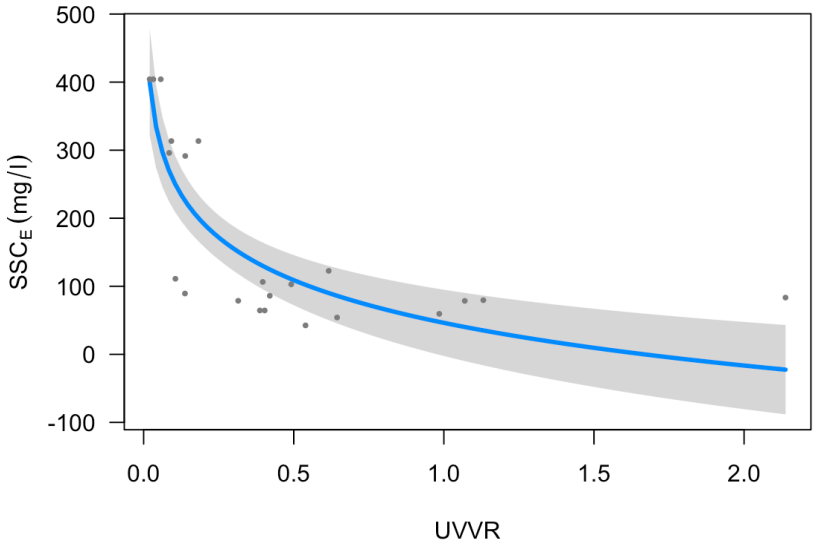

Figure A2 Relationship between two measures of sediment supply. Analytically-derived time- and depth-averaged suspended sediment concentration for each estuary (SSC_E) and unvegetated/vegetated ratio (UVVR), a proxy for net sediment supply. Blue line indicates a best fit and the grey ribbon represents the standard error around the fit. $p < 0.001$, Adjusted $R^2 = 0.69$.

.

Table A3 Model results for key drivers of estuarine-scale marsh change. Partial Least Squares Regression (PLSR) results showing Regression coefficients (RC), Variable Importance in the Projection (VIP) and loading weights (first component) for each predictor variable that best explained rate of saltmarsh change between 1970 and 2016. Bold numerical values show VIP > 1 combined with loading weights > 0.3 to indicate relative importance and main loading in the PLSR model.

Predictor variables	RC	VIP	Loading weights (comp 1)
Percentage variance explained in rate of marsh change = 24.52%			
Relative sea level rise rate	-1.47	**1. 524**	**-0.681**
Unvegetated/vegetated marsh ratio	-1.32	**1.368**	**-0.612**
Bedload sediment flux	0.78	0.812	**0.363**
Wind storm frequency rate	0.32	0.332	0.149
River flood frequency rate	0.19	0.193	-

Appendix III: Literature to support observations of rapid marsh change

Table A4 Literature searched to determine whether marsh change from maps can be considered 'real'.

Region	Area of rapid change	Description and reference
Solway	Rapid expansion and erosion phases of all major marshes in each estuary	OS maps record the expansion and erosion of these larger marshes throughout the Solway region, with a net increase in marsh extent. A study by Marshall (1962) reaches a similar conclusion from interpreting maps (1856-1864) and aerial photographs (1946). Marshall (1962) also investigated aspects of saltmarsh morphology (accretion rates, areas of erosion and expansion and channel configuration) to corroborate their findings, and conclude that there is close agreement between phases of expansion and erosion observed in the field and change recorded from maps. Rapid expansion of Caerlaverock is also described by Bridson (1980) from maps dating back to 1654, in agreement with Marshall (1962). Firth et al. (2000) and CCO (2011) describe the rapid expansion and erosion of different parts of Rockcliffe marsh (Inner Solway) and the marshes in Moricambe Bay since 1776 and 1864 from literature searches and site visits, which were observed in OS maps used in this study.
Morecambe	Rapid erosion and expansion phases in all estuaries	OS maps record the overall expansion of marshes throughout the Morecambe Bay region, with individual marshes undergoing extensive erosion and accretion phases. Of the most drastic change, phases of erosion in Silverdale marsh have been documented by Pringle (1995) from repeat transect measurements between 1983 and 1992, which is out of phase with marsh expansion at Grange-over-Sands on the opposite side of the estuary, described in field surveys by Gray (1972). All estuaries in Morecambe Bay region are considered dynamic, and have experienced rapid changes in saltmarsh extent determined from site visits, historical records and modelling data (Dixon-Gough, 2006, CH2M HILL, 2013a, CH2M HILL, 2013b, CH2M HILL, 2013c). These observations support marsh change observed in OS maps.
Cardigan	Rapid expansion of marshes in the outer estuary	OS maps reveal that marshes throughout the Cardigan Bay region have expanded gradually, with more rapid rates of expansion around the 1950s. Field sketches made during Yapp's (1917) detailed vegetation surveys of the Dyfi estuary in the mid 1910s show a similar extent of saltmarshes to the OS maps. Rapid expansion of the marshes in the outer estuary in the late 1940s is documented by Chater and Jones (1957) from site surveys. Both studies are in agreement with observations of marsh change from OS maps.
Wash	Rapid expansion following reclamation	OS maps document the step-wise loss of marshlands to reclamation, followed by phases of new marsh growth in front of embankments throughout the Wash embayment. Kestner (1962) reconstructed past area cover of salt marsh extent for the Wash by knowing the dates when embankments were constructed. Kestner (1975) later described the mechanism by which sediment deposits in front of the sea wall, allowing marshes to rapidly colonise and expand. These phases of reclamation and new marsh growth are in agreement with marsh change determined from OS maps.
Essex-Kent	Gradual erosion across all estuaries, with some areas of rapid marsh expansion	OS maps record the gradual erosion of marshes across Essex-Kent, with small areas of rapid expansion or erosion subject to embankment / deembankment. Burd (1992) reports in detail the numerous areas of embankment and deembankment from history books, parish and estate records, property deeds, maps and historical surveys from the 17th century onwards. Areas of reclaimed and deembanked marshland is reported by Wolters et al. (2005). Burd (1992) also reports that the government at the time were aware of marsh erosion and more frequent flooding due to land subsidence and rising sea levels. Kirby (2013) and Spearman et al. (2014) also document marsh decline from historical maps and illustrations in the northern and southern parts of the region respectively.
Solent	Rapid expansion across all estuaries	OS maps record the expansion of marshes across the Solent region. Baily and Inkpen (2013) account for the rapid expansion because of the colonisation and spread of the pioneer-marsh hybrid *Spartina townsendii*, and later, fertile allotetraploid species *Spartina anglica*, onto tidal flats across the region. Baily and Inkpen (2013) support this argument by referring to a number of articles published during this period that document the nature and spread of *Spartina spp.* across the region. Baily and Inkpen (2013) did find issues with the accuracy of maps compared to aerial photographs, however much of the error was due to not knowing the date a map was surveyed (only when it was published) when comparing to an aerial photograph, and revision errors where marshes were copied over to successive map editions thus not representing the true marsh extent of that year. Both error terms were accounted for in this study and described in Appendix I.

Appendix IV: Data analysis and model selection

The task for Chapter 2 was to determine which environmental drivers best describe rate of saltmarsh change across Great Britain. Prior to selecting a statistical model, the data was explored to fully to make an informed decision based on the necessary assumptions of different statistical models. Begin by loading the dataset, graphics package `ggplot2`, and some additional functions held in the `additional_functions.R`.

```
library(ggplot2)
source("/Users/Home/Documents/PhD/CHII_uk_marsh_trends/Script/additional_functions.R")
marshes<-read.csv("/Users/Home/Documents/PhD/CHII_uk_marsh_trends/Data/gb_lat_marsh.csv",header=T)
marshes<-marshes[complete.cases(marshes),]
```

Visualising the data. We began our data exploration by investigating how each predictor variable relates to rate of saltmarsh change. To make this easier, we create a new object containing the response and predictor variables only.

```
library(dplyr)
library(tidyr)

marshcheck<-marshes[-c(1:3,5:6,12)]

marshcheck %>%
  gather(-lateral_rate,key="var",value="value") %>%
  ggplot(aes(x=value,y=lateral_rate))+
  geom_point(shape=1)+
  facet_wrap(~var,scales="free_x")+
  theme_bw()
```

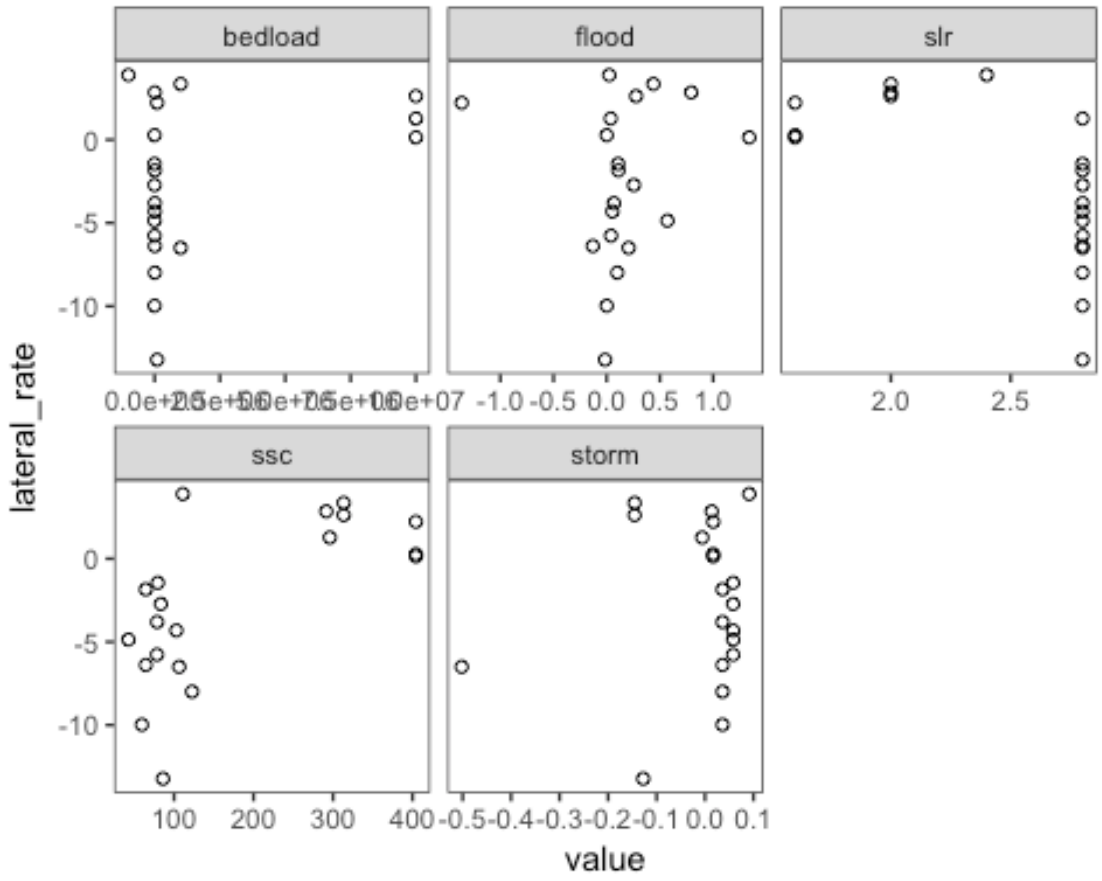

It appears that there may be a negative relationship between relative sea level rise (RSLR) and rate of saltmarsh change, and possibly a positive relationship between estimated suspended sediment concentration (SSC) and rate of marsh change.

Checking for outliers. Use Cleveland dotplots to identify any extreme outliers in the dataset. Outliers might have a significant impact on the results. The data is organised along the y-axis only by row name (i.e. the order in which it was entered into the dataframe).

```
par(mfrow=c(2,3))
lapply(X=c("slr", "storm", "flood","ssc","bedload"), FUN=function(s)
  dotchart(sample(marshcheck[, s]), xlab=s,ylab="Row number"))
```

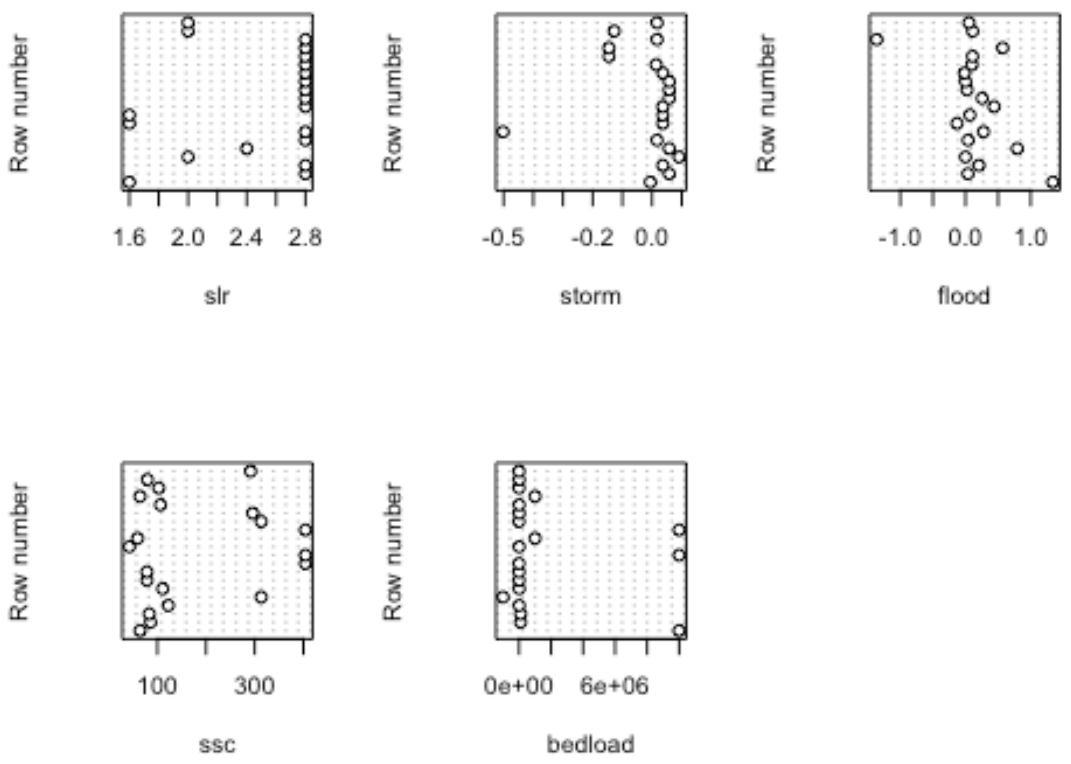

Large variation from the centre of data clusters **suggests** the presence of outliers. Here, storms, floods and bedload predictor variables seem to have issues with extreme values. These are not unprecedented amounts, but may affect our model results. Bare this in mind as the statistical analysis proceeds.

Checking the distribution of variables. To check whether the response variable has a normal distribution, build a boxplot, and scale the y axis to make their ranges comparable.

```
boxplot(scale(marshes$lateral_rate),
              xlab="lateral_rate")
```

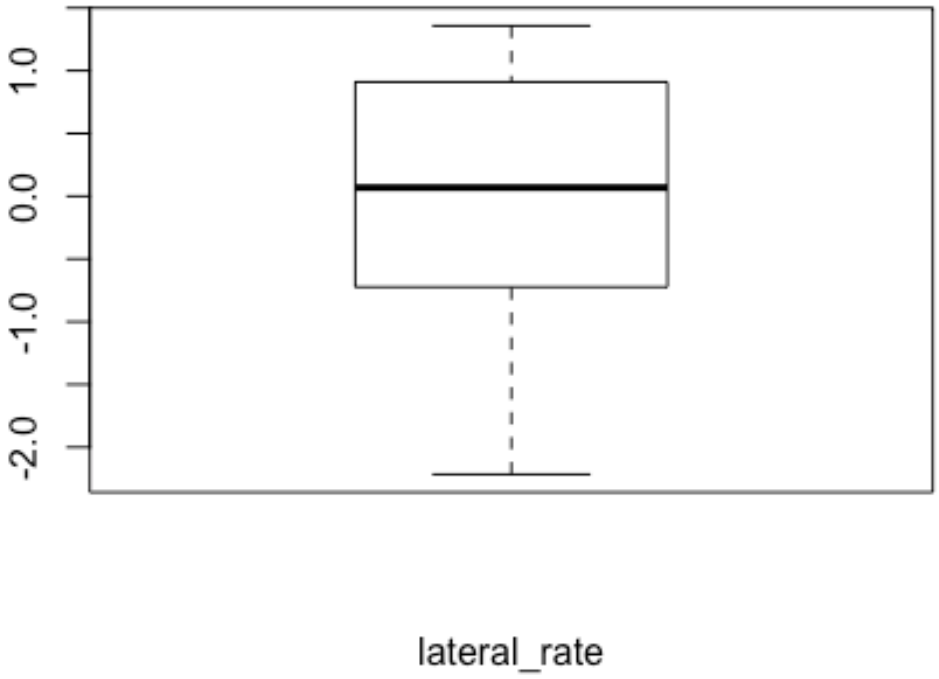


```
shapiro.test(marshes$lateral_rate)

##
##  Shapiro-Wilk normality test
##
## data:  marshes$lateral_rate
## W = 0.95514, p-value = 0.4519
```

There's no evidence of skew. How are the predictor variables distributed?

```
boxplot(scale(marshes[,7:11]))
```

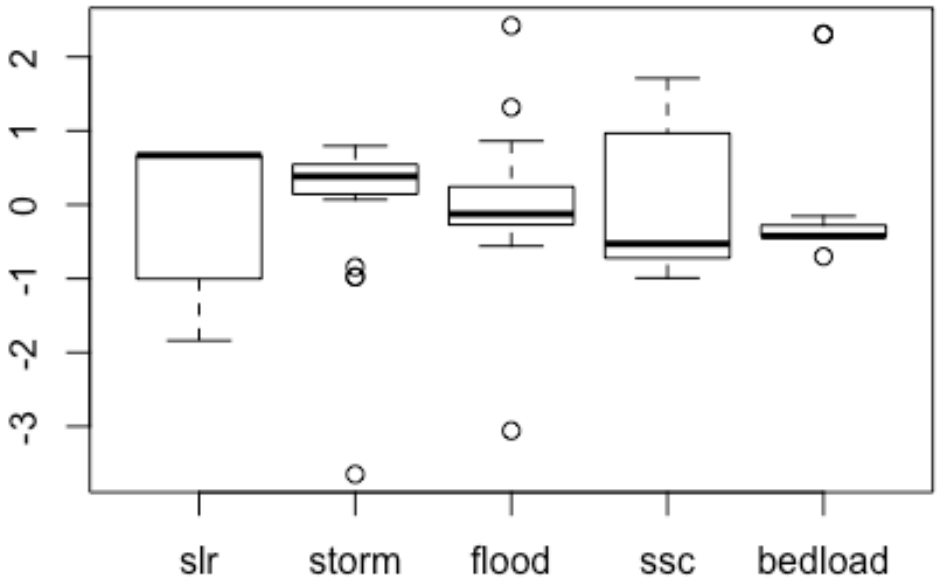

None of the predictor variables have a normal distribution. Transforming the variables may improve this, and also help to deal with outliers. Use a cube root transformation capable of transforming both negative and positive values (see `Math.cbrt` function in the `additional_functions.R` file), and add these to the dataframe.

```
marshes$slr_cbrt<-Math.cbrt(marshes$slr)
marshes$storm_cbrt<-Math.cbrt(marshes$storm)
marshes$flood_cbrt<-Math.cbrt(marshes$flood)
marshes$ssc_cbrt<-Math.cbrt(marshes$ssc)
marshes$bedload_cbrt<-Math.cbrt(marshes$bedload)
boxplot(scale(marshes[,13:17]))
```

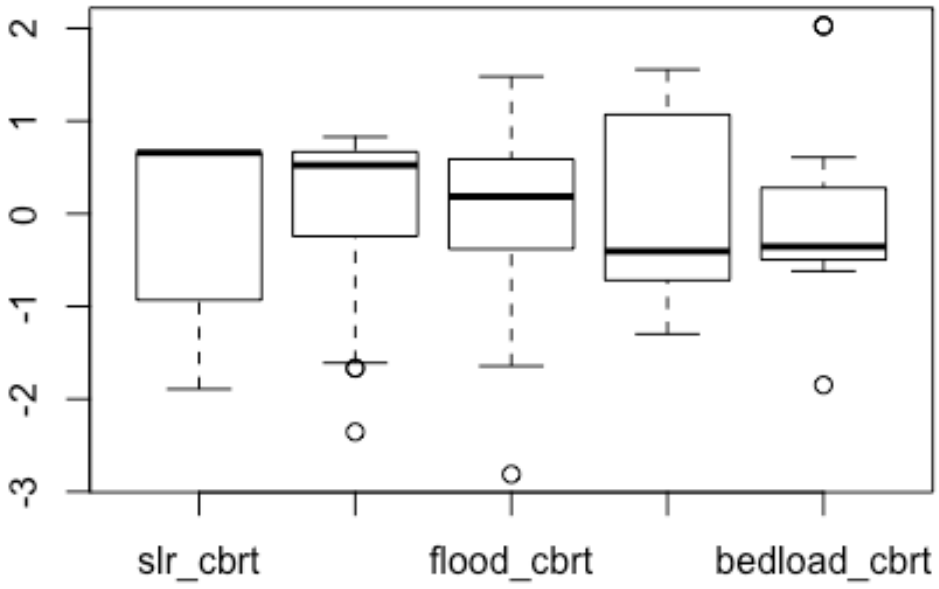

Better. All variables now have a more symmetric distribution and the outliers are no longer extreme. The distribution of our data is suitable for parametric modelling.

Checking for collinearity between predictor variables. Prior to using a parametric model to determine which suite of variables best explains rate of saltmarsh change, check for high collinearity, and reduce it if necessary. Examine the Variance Inflation Factor associated with each predictor variable (see `corvif` function in `additional_functions.R` file) to assess how much variance of an estimated regression coefficient increases if variables are correlated.

```
corvif(marshes[,c("slr_cbrt","storm_cbrt","flood_cbrt","ssc_cbrt","bedload
_cbrt")])

## Correlations of the variables
##
##                slr_cbrt  storm_cbrt   flood_cbrt     ssc_cbrt
## slr_cbrt      1.00000000  0.08735585  0.057292397 -0.883822219
## storm_cbrt    0.08735585  1.00000000 -0.090135044 -0.291960742
## flood_cbrt    0.05729240 -0.09013504  1.000000000  0.005992857
## ssc_cbrt     -0.88382222 -0.29196074  0.005992857  1.000000000
## bedload_cbrt -0.30041408 -0.58719585  0.265328544  0.561011584
##              bedload_cbrt
## slr_cbrt       -0.3004141
## storm_cbrt     -0.5871959
## flood_cbrt      0.2653285
## ssc_cbrt        0.5610116
## bedload_cbrt    1.0000000
```

```
##
##
## Variance inflation factors

## Warning in summary.lm(object): essentially perfect fit: summary may be
## unreliable

##                  GVIF
## slr_cbrt     6.278911
## storm_cbrt   1.581156
## flood_cbrt   1.121972
## ssc_cbrt     8.322387
## bedload_cbrt 2.638079
```

SSC and RSLR are strongly correlated (VIF > 3; Pearson = -0.88). There is no immediate reason why these variables should correlate, but removal of either to deal with collinearity is undesirable as there would be no fair distinction between the relative importance of key variables on rate of marsh change. Given that low collinearity between predictor variables is one of the assumptions of linear models, an alternative approach would be to use the multivariate technique Partial Least Squares Regression (PLSR).

Model 1: Partial Least Squares Regression for all predictors. As opposed to classical stepwise linear regression, where collinearity among the predictors is an issue, PLSR is a statistical tool directly oriented to maximizing the explained variability of the response variable using a set of predictor variables that can be themselves highly correlated (Carrascal et al., 2009). Start by loading the `pls` package and constructing the statistical model for all variables using the transformed variables (including covariates). To select the optimal number of components in the model, employ a "leave-one-out" cross-validation procedure.

```
library(pls)
pls1<-plsr(lateral_rate
           ~ 1 + slr + storm + flood + ssc + bedload,
           data=marshes,
           validation="LOO",
           method = "oscorespls",
           scale=T)
```

Select the optimal number of components to include in the final PLSR model. This can be done by examining a plot of Root Mean Squared Error of Prediction (RMSEP) for each component, and selecting the number of components where RMSEP drastically reduces.

```
plot(RMSEP(pls1))
```

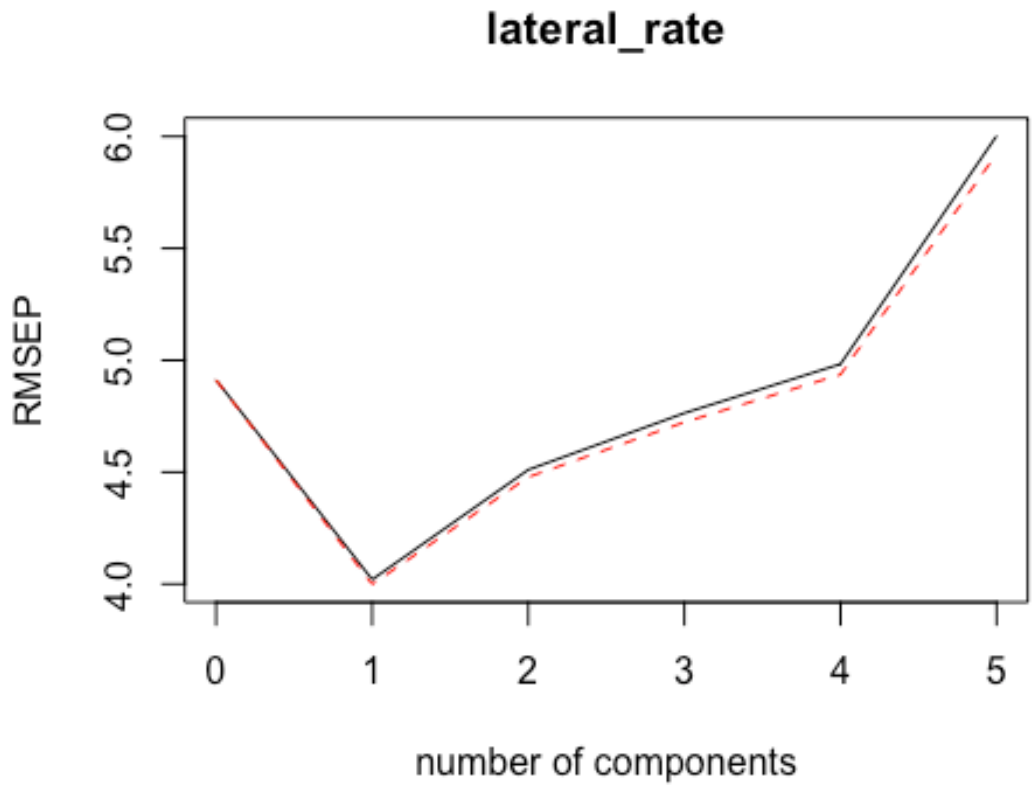

The plot looks unusual. An expected pattern would be for an exponential decline as the number of components increase. This has likely occurred because the number of response variables are quite low. This plot suggests that one component is optimal, however re-run the model without a cross-validation procedure to see if the same answer is returned.

```
plot(RMSEP(plsr(lateral_rate
           ~ 1 + slr + storm + flood + ssc + bedload,
           data=marshes,
           method = "oscorespls",
           scale=T)))
```

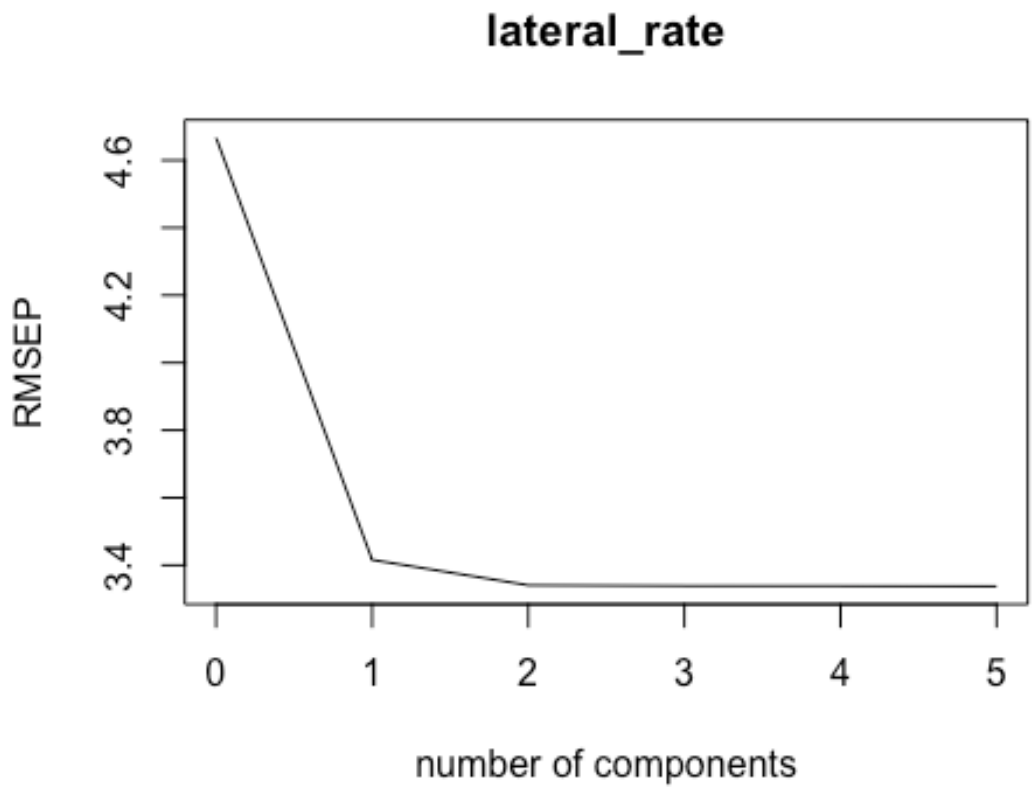

That's better. There's a sharp decline in RMSEP by the first component (from around 4.6 to 3.5), with little change as the number of components increase. This is in agreement with the model when cross-validation is included. See the percentage of variance explained by each model containing a different number of components by examining the R^2 values.

```
R2(pls1)

## (Intercept)      1 comps      2 comps      3 comps      4 comps
##    -0.10803      0.25796      0.06575     -0.04208     -0.14013
##     5 comps
##    -0.65477
```

The model with one components for consideration explains 26% variation in the rate of change in marsh extent. To see which predictor variables were most important in maximizing the explained variability of the response variable, examine the loading weights, regression coefficients and the Variable Importance of the Projection (VIP) values of each predictor for the second component.

```
loading.weights(pls1)

##
## Loadings:
##         Comp 1 Comp 2 Comp 3 Comp 4 Comp 5
## slr     -0.653 -0.134                0.744
## storm    0.126  0.827  0.165 -0.456  0.254
## flood          -0.234  0.965
## ssc      0.660                0.488  0.571
## bedload  0.341 -0.493 -0.195 -0.741  0.233
```

```
##
##                Comp 1 Comp 2 Comp 3 Comp 4 Comp 5
## SS loadings       1.0    1.0    1.0    1.0    1.0
## Proportion Var    0.2    0.2    0.2    0.2    0.2
## Cumulative Var    0.2    0.4    0.6    0.8    1.0
```

```
coef(pls1,ncomp = 1)
```

```
## , , 1 comps
##
##          lateral_rate
## slr       -1.4468554
## storm      0.2798157
## flood      0.1829613
## ssc        1.4632136
## bedload    0.7552285
```

```
VIP(pls1)
```

```
##             slr     storm     flood      ssc   bedload
## Comp 1 1.459086 0.2821811 0.1845079 1.475583 0.7616127
## Comp 2 1.425264 0.4894761 0.2132524 1.439863 0.7812517
## Comp 3 1.424402 0.4893478 0.2260446 1.438986 0.7809235
## Comp 4 1.424241 0.4895316 0.2260318 1.438917 0.7812314
## Comp 5 1.424386 0.4895786 0.2259768 1.438832 0.7811108
```

Variables are considered important when loading weights >0.3 and VIP values are >1.0. The regression coefficients indicate the direction of the relationship between the changes in climate variables and marsh rate.

Conclusion. SSC, RSLR and tidal range were the most important variables that drive rates of marsh change, however be aware that the model only has 26% explanatory power. Proof the findings by applying a different test to the data - build a parametric linear model to explain marsh change after excluding each covariate in turn.

Proofing the PLSR model. In the earlier examination of multiple collinearity, SSC and RSLR collectively had a VIF value of >8. Try and remove all but one from successive VIF tables, and see if they reduce collinearity to a suitable level.

```
corvif(marshes[,c("ssc_cbrt","storm_cbrt","flood_cbrt","bedload_cbrt")]) # SSC only
```

```
## Correlations of the variables
##
##                 ssc_cbrt  storm_cbrt   flood_cbrt bedload_cbrt
## ssc_cbrt      1.000000000 -0.29196074  0.005992857    0.5610116
## storm_cbrt   -0.291960742  1.00000000 -0.090135044   -0.5871959
## flood_cbrt    0.005992857 -0.09013504  1.000000000    0.2653285
## bedload_cbrt  0.561011584 -0.58719585  0.265328544    1.0000000
##
##
## Variance inflation factors

## Warning in summary.lm(object): essentially perfect fit: summary may be
## unreliable
```

```
##                  GVIF
## ssc_cbrt     1.515529
## storm_cbrt   1.545229
## flood_cbrt   1.121638
## bedload_cbrt 2.272715
```

```
corvif(marshes[,c("slr_cbrt","storm_cbrt","flood_cbrt","bedload_cbrt")]) #
RSLR only
```

```
## Correlations of the variables
##
##                 slr_cbrt  storm_cbrt  flood_cbrt bedload_cbrt
## slr_cbrt      1.00000000  0.08735585  0.05729240   -0.3004141
## storm_cbrt    0.08735585  1.00000000 -0.09013504   -0.5871959
## flood_cbrt    0.05729240 -0.09013504  1.00000000    0.2653285
## bedload_cbrt -0.30041408 -0.58719585  0.26532854    1.0000000
##
##
## Variance inflation factors
```

```
## Warning in summary.lm(object): essentially perfect fit: summary may be
## unreliable
```

```
##                  GVIF
## slr_cbrt     1.143407
## storm_cbrt   1.563462
## flood_cbrt   1.111979
## bedload_cbrt 1.852968
```

In each case, the remaining predictor variables have VIF values below 3 and no correlations above 0.75. Outliers and assumptions of normality were previously checked, so construct two separate linear models excluding all-bar-one covariate in turn. Before proceeding with model selection, account for any spatial autocorrelation that might invalidate the model. Use hierarchical clustering to identify groups in the data.

Accounting for spatial autocorrelation can dramatically improve model performance, and help to avoid biased estimates of Type I error (Bunnefeld and Phillimore, 2012). Examine whether there are groupings between our estuaries, based on their pairwise Euclidean distances. If so, this will form a random factor in the model structure.

Start by creating the matrix of Euclidean distances between estuaries.

```
library(gmt)
distance_estuary_matrix=matrix(NA,length(marshes$estuary),length(marshes$e
stuary))
for(est1 in 1:length(marshes$estuary)){
  for(est2 in est1:length(marshes$estuary)){
    distance_estuary_matrix[est1,est2]=geodist(marshes$latitude_wgs[est1],
marshes$longitude_wgs[est1], marshes$latitude_wgs[est2],marshes$longitude_
wgs[est2], units="km")
  }}
distance_estuary_matrix=as.dist(t(distance_estuary_matrix))
full=hclust(distance_estuary_matrix,method="complete")
```

Extract the cophenetic distance between groups to select a value for the inflection point in intra-estuary group variance, and use Elbow plots to validate the selection. First, prepare the data.

```
dist_clust<-data.frame(data.frame(unique(as.numeric(cophenetic(full))))[or
der((unique(as.numeric(cophenetic(full)))),decreasing=T),])
names(dist_clust)<-"distance"
dist_clust$group<-seq.int(nrow(dist_clust))
add_zero<-c(0,26)
dist_clust<-rbind(dist_clust,add_zero)
```

Plot the number of groups against distance to form the clusters.

```
ggplot(dist_clust,aes(distance,group))+
  geom_step()+
  geom_vline(xintercept=90,linetype="longdash")+
  xlab("Distance for cluster formation (km)")+
  ylab("Number of groups")
```

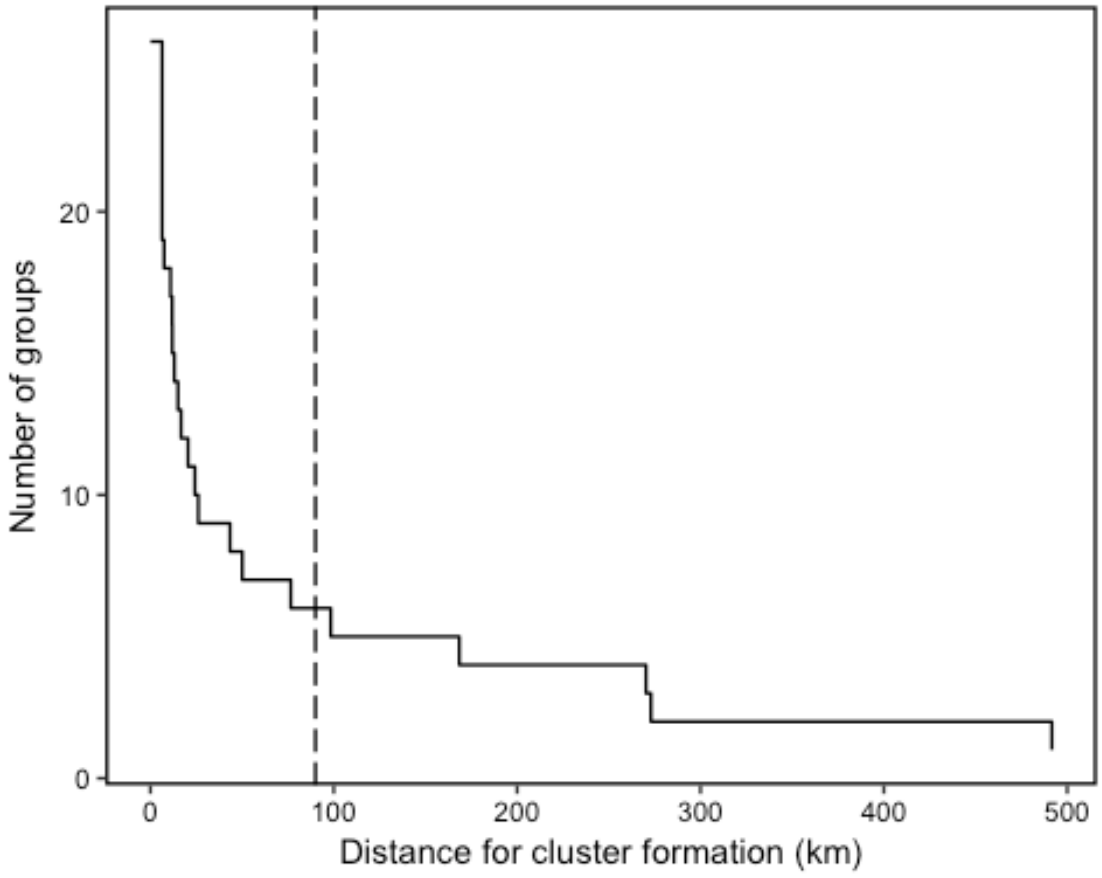

Number of groups reduces exponentially with distance, and there is an 'evening out' at around 90 km, suggesting this is a suitable inflection point to distinguish between groups. This ends up producing 6 distinct hierarchical clusters. Validate the selection of 6 clusters using Elbow plots with k-means clustering method.

```
wss<-(nrow(subset(marshes,select=c(longitude_wgs,latitude_wgs)))-1)*sum(ap
ply(subset(marshes,select=c(longitude_wgs,latitude_wgs)),2,var))
for (i in 2:15) wss[i] <- sum(kmeans(subset(marshes,select=c(longitude_wgs
,latitude_wgs)),
```

```
                                     centers=i)$withinss)
plot(1:15, wss, type="b", xlab="Number of Clusters",
     ylab="Within groups sum of squares")
```

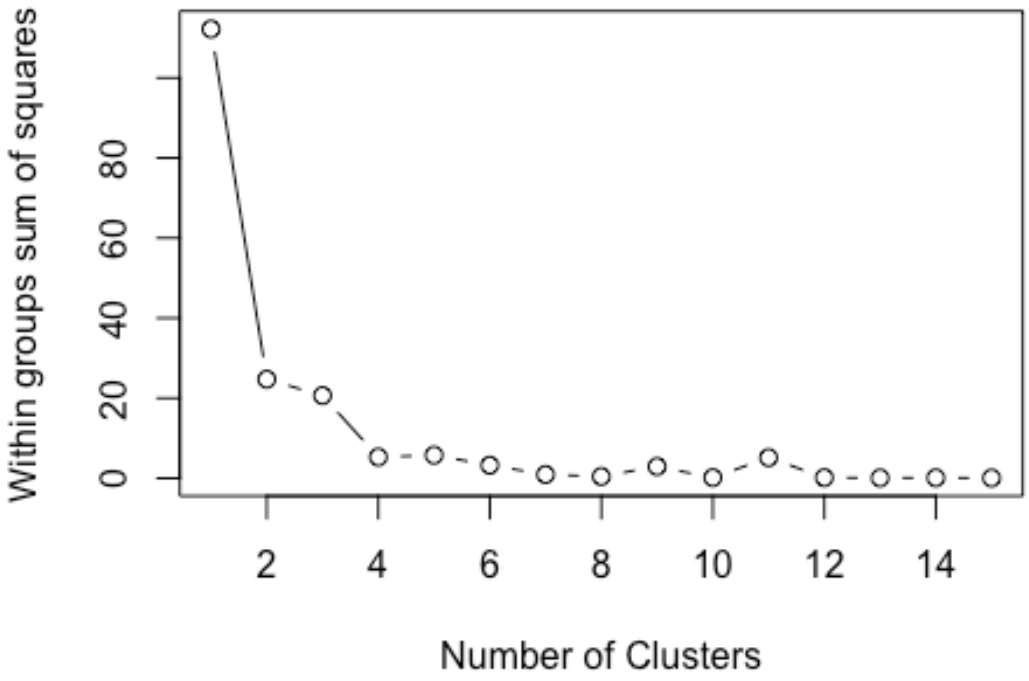

Sum of squares within groups flattens out at 6 groups. This is in agreement with the previous plot, so grouping the estuaries into 6 hierarchical clusters is justified. Cut the hierarchical clustering analysis tree at the 90 inflection point to form our 6 groups, and bind as a new column to the dataframe.

```
group=cutree(full, h=90)
marshes=cbind(marshes,group) # column bind the dataset and the previsouly
determined grouping
marshes$group<-as.factor(marshes$group)
```

Inspect the dataframe `marshes`, Group identity is the same as the region in which each estuary occurs. Build a linear model, and determine whether inclusion of region as a random factor improves the model.

Model selection should be employed to determine whether addition of random effects significantly improves the maximal model. Check to see if adding 'group' as a random factor significantly improves the maximal model using the Restricted Maximum Likelihood (REML) approach.

Build two models: with and without a random effect.

```
library(nlme)
m1<-gls(lateral_rate
        ~ 1 + storm_cbrt+flood_cbrt+ssc_cbrt+bedload_cbrt+slr_cbrt,
```

```
        method = "REML",
        control="optim",
        data=marshes)
m2<-lme(lateral_rate
        ~ 1 + storm_cbrt+flood_cbrt+ssc_cbrt+bedload_cbrt+slr_cbrt,
        random = ~1|group,
        method = "REML",
        control="optim",
        data=marshes)
```

Use anova tables to see if there is a significant difference between the models. Because REML is being used, Significance level needs to be adapted using the L Ratio (Zuur et al., 2009).

```
anova(m1,m2)
```

```
##    Model df      AIC      BIC    logLik   Test  L.Ratio p-value
## m1     1  7 105.6551 110.1285 -45.82754
## m2     2  8 106.3567 111.4692 -45.17837 1 vs 2 1.298353  0.2545
```

```
0.5*(1-pchisq(1.298353,1))
```

```
## [1] 0.1272571
```

There was no significant difference between the models, so the simplest model is favoured (m1). Furthermore, m1 had a lower AIC and is therefore preferred. Switch from gls to lm, to which the model selection using stepwise regression can be applied, which uses a forwards and backwards selection criterion to drop terms based on AIC.

Model 2: Linear model without covariate RSLR. In the first linear model, exclude covariates relative sea level rise and suspended sediment concentration.

```
m3<-lm(lateral_rate
       ~ storm_cbrt+flood_cbrt+ssc_cbrt+bedload_cbrt,
       data=marshes)
step(m3,direction="both")
```

```
## Start:  AIC=53.61
## lateral_rate ~ storm_cbrt + flood_cbrt + ssc_cbrt + bedload_cbrt
##
##                Df Sum of Sq    RSS    AIC
## - storm_cbrt    1     6.622 183.62 52.343
## - bedload_cbrt  1    12.054 189.06 52.926
## <none>                      177.00 53.609
## - flood_cbrt    1    34.097 211.10 55.132
## - ssc_cbrt      1   211.898 388.90 67.352
##
## Step:  AIC=52.34
## lateral_rate ~ flood_cbrt + ssc_cbrt + bedload_cbrt
##
##                Df Sum of Sq    RSS    AIC
## <none>                      183.62 52.343
## + storm_cbrt    1     6.622 177.00 53.609
## - bedload_cbrt  1    32.953 216.58 53.644
```

```
## - flood_cbrt    1    37.382 221.01 54.049
## - ssc_cbrt      1   218.501 402.13 66.021

##
## Call:
## lm(formula = lateral_rate ~ flood_cbrt + ssc_cbrt + bedload_cbrt,
##     data = marshes)
##
## Coefficients:
##  (Intercept)    flood_cbrt      ssc_cbrt  bedload_cbrt
##     -18.5847        2.8705        3.0450       -0.0206
```

The predictor variables that should be retained in the minimal adequate model are assigned to a new model.

```
m4<-lm(lateral_rate
       ~ flood_cbrt+ssc_cbrt+bedload_cbrt,
       data=marshes)
```

Check for heteroscedacity and bias in the model residuals (which violate the assumption of Heterogeneity of Variance)

```
par(mfrow=c(2,2))
plot(m4)
```

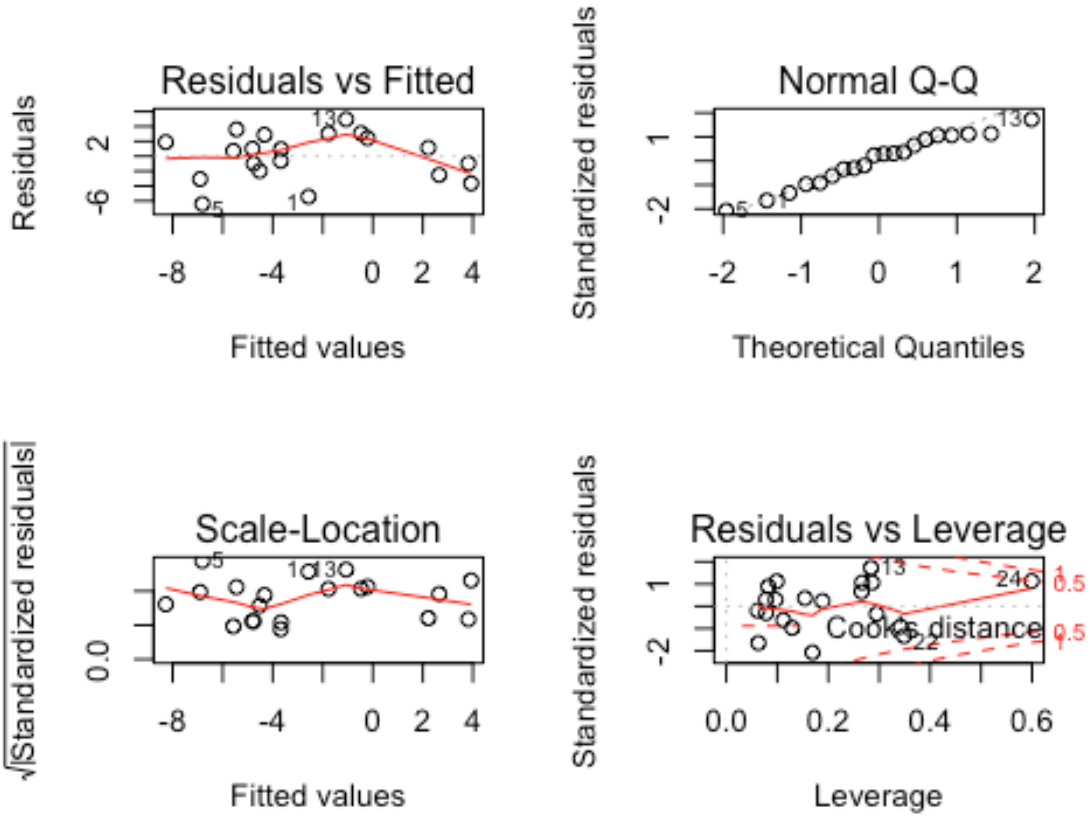

There are no major issues with the model assumptions. Report the various statistics about the data. Use anova tables to identify significant factors in the model using 'type I' sums of squares.

```r
library(relaimpo)
anova(m4)
```

```
## Analysis of Variance Table
##
## Response: lateral_rate
##              Df  Sum Sq Mean Sq F value   Pr(>F)
## flood_cbrt    1  21.294  21.294  1.8555 0.192019
## ssc_cbrt      1 197.676 197.676 17.2244 0.000753 ***
## bedload_cbrt  1  32.953  32.953  2.8713 0.109544
## Residuals    16 183.625  11.477
## ---
## Signif. codes:  0 '***' 0.001 '**' 0.01 '*' 0.05 '.' 0.1 ' ' 1
```

```r
summary(m4)
```

```
##
## Call:
## lm(formula = lateral_rate ~ flood_cbrt + ssc_cbrt + bedload_cbrt,
##     data = marshes)
##
## Residuals:
##     Min      1Q  Median      3Q     Max
## -6.4087 -2.1133  0.8269  2.5405  4.9530
##
## Coefficients:
##               Estimate Std. Error t value Pr(>|t|)
## (Intercept)  -18.58471    3.55460  -5.228 8.28e-05 ***
## flood_cbrt     2.87055    1.59053   1.805 0.089964 .
## ssc_cbrt       3.04495    0.69785   4.363 0.000483 ***
## bedload_cbrt  -0.02060    0.01216  -1.694 0.109544
## ---
## Signif. codes:  0 '***' 0.001 '**' 0.01 '*' 0.05 '.' 0.1 ' ' 1
##
## Residual standard error: 3.388 on 16 degrees of freedom
## Multiple R-squared:  0.5784, Adjusted R-squared:  0.4994
## F-statistic: 7.317 on 3 and 16 DF,  p-value: 0.002633
```

```r
AIC(m4)
```

```
## [1] 111.1008
```

```r
calc.relimp(m4,type=c("lmg"),rela=T)
```

```
## Response variable: lateral_rate
## Total response variance: 22.92356
## Analysis based on 20 observations
##
## 3 Regressors:
## flood_cbrt ssc_cbrt bedload_cbrt
## Proportion of variance explained by model: 57.84%
## Metrics are normalized to sum to 100% (rela=TRUE).
##
## Relative importance metrics:
##
```

```
##                      lmg
## flood_cbrt   0.09943627
## ssc_cbrt     0.81051081
## bedload_cbrt 0.09005292
##
## Average coefficients for different model sizes:
##
##                       1X          2Xs         3Xs
## flood_cbrt   2.05516199  1.822989152  2.87054988
## ssc_cbrt     2.36339279  2.589180582  3.04495472
## bedload_cbrt 0.01291395 -0.001739262 -0.02060277
```

Suspended sediment concentration is highly significant, whereas river flood and bedload sediment flux are not. Visualise the relationship between SSC and rate of saltmarsh change. This is in agreement with the PLSR analysis (so far). Now to see if relative sea level rise is also a significant driver.

Model 3: Linear model without covariate SSC. It was established that no random factor is required in further analyses, so the workflow can proceed straight away in the next model selection excluding covariate SSC in this model.

Build a linear model without suspended sediment concentration.

```
m5<-lm(lateral_rate
       ~ storm_cbrt+flood_cbrt+slr_cbrt+bedload_cbrt,
       data=marshes)
step(m5,direction="both")
```

```
## Start:  AIC=58.34
## lateral_rate ~ storm_cbrt + flood_cbrt + slr_cbrt + bedload_cbrt
##
##                Df Sum of Sq    RSS    AIC
## - bedload_cbrt  1     0.097 224.34 56.349
## - storm_cbrt    1     3.766 228.01 56.673
## <none>                      224.25 58.340
## - flood_cbrt    1    27.273 251.52 58.636
## - slr_cbrt      1   164.653 388.90 67.352
##
## Step:  AIC=56.35
## lateral_rate ~ storm_cbrt + flood_cbrt + slr_cbrt
##
##                Df Sum of Sq    RSS    AIC
## - storm_cbrt    1     4.743 229.09 54.767
## <none>                      224.34 56.349
## - flood_cbrt    1    31.028 255.37 56.940
## + bedload_cbrt  1     0.097 224.25 58.340
## - slr_cbrt      1   189.095 413.44 66.576
##
## Step:  AIC=54.77
## lateral_rate ~ flood_cbrt + slr_cbrt
##
##                Df Sum of Sq    RSS    AIC
## <none>                      229.09 54.767
## - flood_cbrt    1    29.016 258.10 55.153
```

```
## + storm_cbrt    1     4.743 224.34 56.349
## + bedload_cbrt  1     1.074 228.01 56.673
## - slr_cbrt      1   185.166 414.25 64.615

##
## Call:
## lm(formula = lateral_rate ~ flood_cbrt + slr_cbrt, data = marshes)
##
## Coefficients:
## (Intercept)   flood_cbrt     slr_cbrt
##      41.391        2.403      -33.261
```

Fit the new model and check for heteroscedacity and biasy.

```
m6<-lm(lateral_rate
       ~ flood_cbrt+slr_cbrt,
       data=marshes)
par(mfrow=c(2,2))
plot(m6)
```

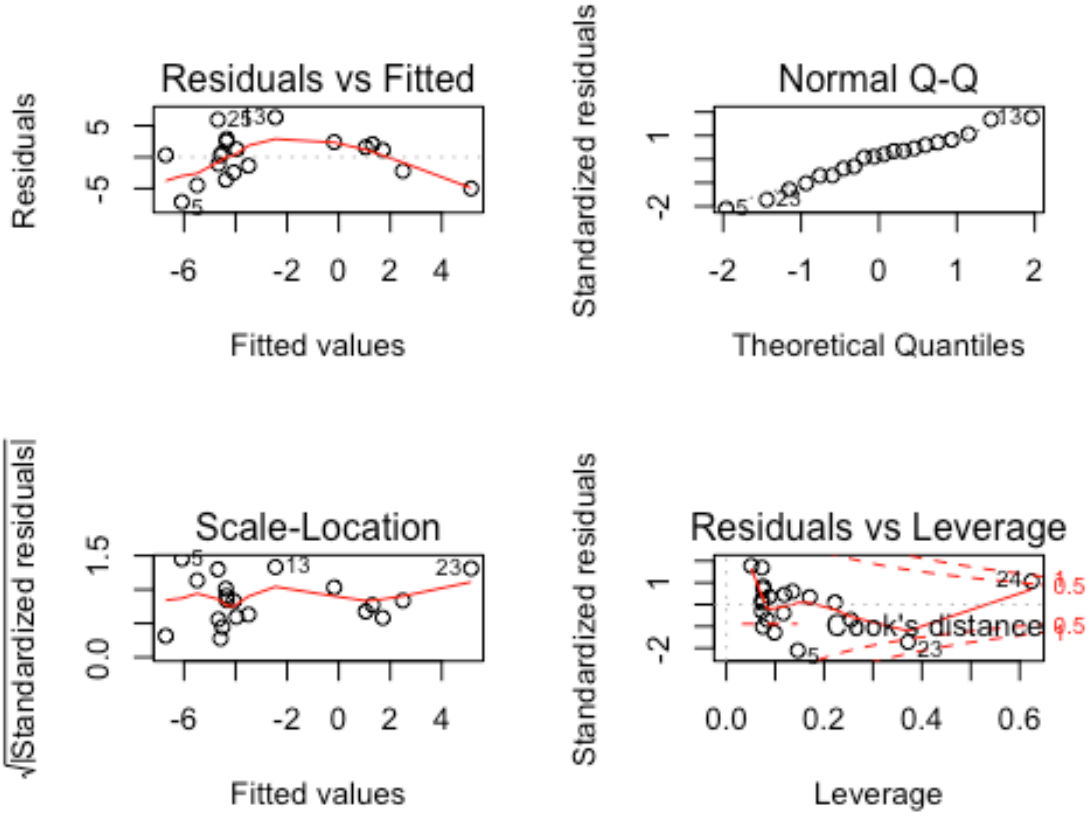

Not too bad. Now examine the anova table.

```
anova(m6)

## Analysis of Variance Table
##
## Response: lateral_rate
##            Df  Sum Sq Mean Sq F value   Pr(>F)
```

```
## flood_cbrt  1  21.294  21.294  1.5802 0.225729
## slr_cbrt    1 185.166 185.166 13.7407 0.001752 **
## Residuals  17 229.088  13.476
## ---
## Signif. codes:  0 '***' 0.001 '**' 0.01 '*' 0.05 '.' 0.1 ' ' 1
```

```
summary(m6)
```

```
##
## Call:
## lm(formula = lateral_rate ~ flood_cbrt + slr_cbrt, data = marshes)
##
## Residuals:
##     Min      1Q  Median      3Q     Max
## -7.1341 -2.2696  0.5115  2.1272  6.3384
##
## Coefficients:
##             Estimate Std. Error t value Pr(>|t|)
## (Intercept)   41.391     12.100   3.421  0.00326 **
## flood_cbrt     2.403      1.638   1.467  0.16053
## slr_cbrt     -33.261      8.973  -3.707  0.00175 **
## ---
## Signif. codes:  0 '***' 0.001 '**' 0.01 '*' 0.05 '.' 0.1 ' ' 1
##
## Residual standard error: 3.671 on 17 degrees of freedom
## Multiple R-squared:  0.474,  Adjusted R-squared:  0.4121
## F-statistic:  7.66 on 2 and 17 DF,  p-value: 0.004248
```

```
AIC(m6)
```

```
## [1] 113.525
```

```
calc.relimp(m6,type=c("lmg"),rela=T)
```

```
## Response variable: lateral_rate
## Total response variance: 22.92356
## Analysis based on 20 observations
##
## 2 Regressors:
## flood_cbrt slr_cbrt
## Proportion of variance explained by model: 47.4%
## Metrics are normalized to sum to 100% (rela=TRUE).
##
## Relative importance metrics:
##
##                  lmg
## flood_cbrt 0.1218395
## slr_cbrt   0.8781605
##
## Average coefficients for different model sizes:
##
##                   1X        2Xs
## flood_cbrt   2.055162   2.402942
## slr_cbrt   -32.506303 -33.260636
```

Relative sea level rise is significant, whereas river flood is not.

Conclusion. From PLSR model, we identified sea level rise and suspended sediment concentration are important predictors of marsh change across Great Britain. This has been validated through separate multiple linear regressions and we consider the analysis robust.

Appendix V: Transect placements across estuaries

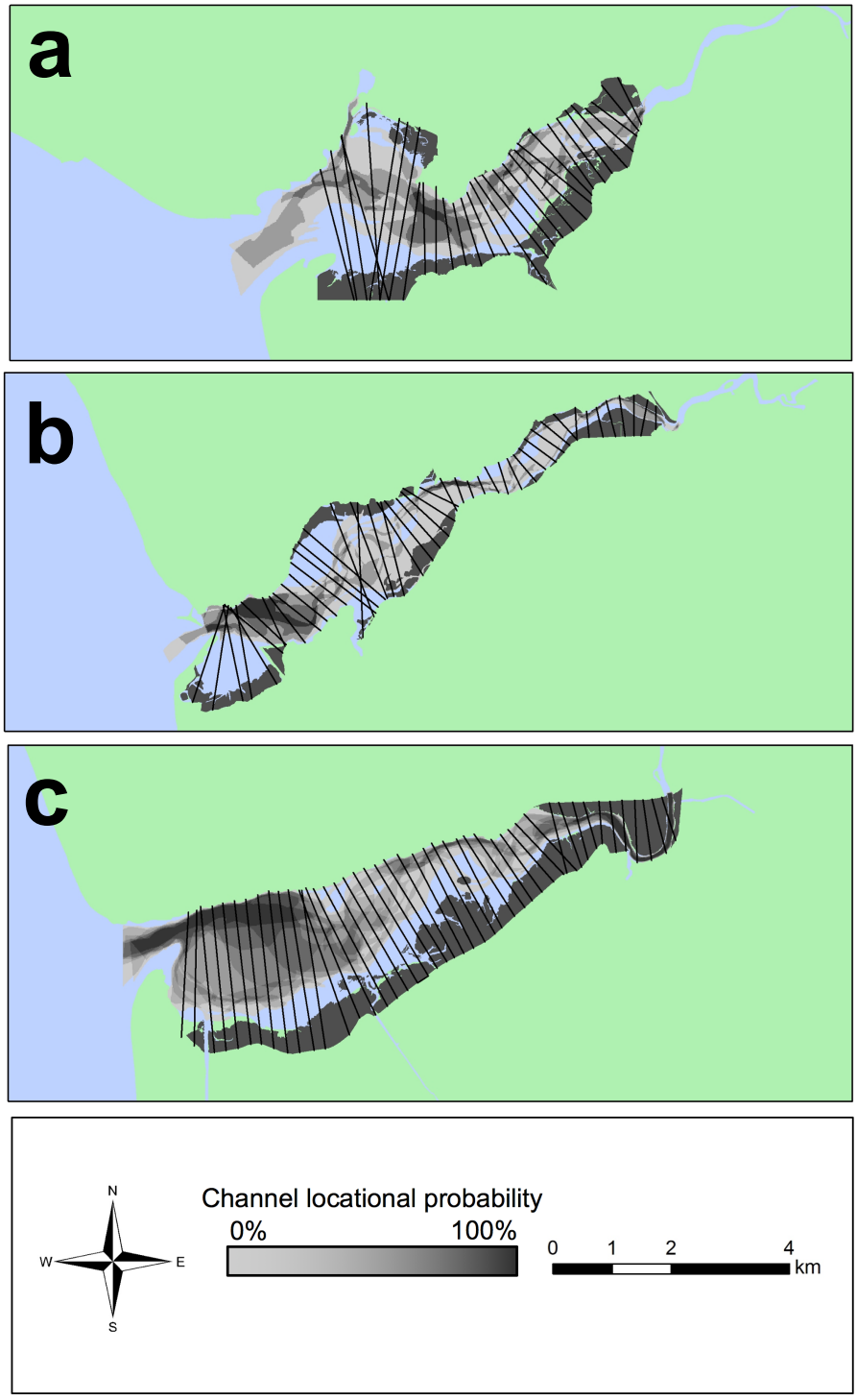

Figure A3 Maps showing the location of transects, channels and marsh for **a** Glaslyn-Dwyryd, **b** Mawddach and **c** Dyfi estuaries. Transects are drawn across each estuary, normal to the centreline. Likelihood of channel occurring in at a specific location in the estuary based on past channel locations are shown in greyscale and saltmarsh extent in grey between 2009-2013.

Appendix VI: Sequential change in marsh extent

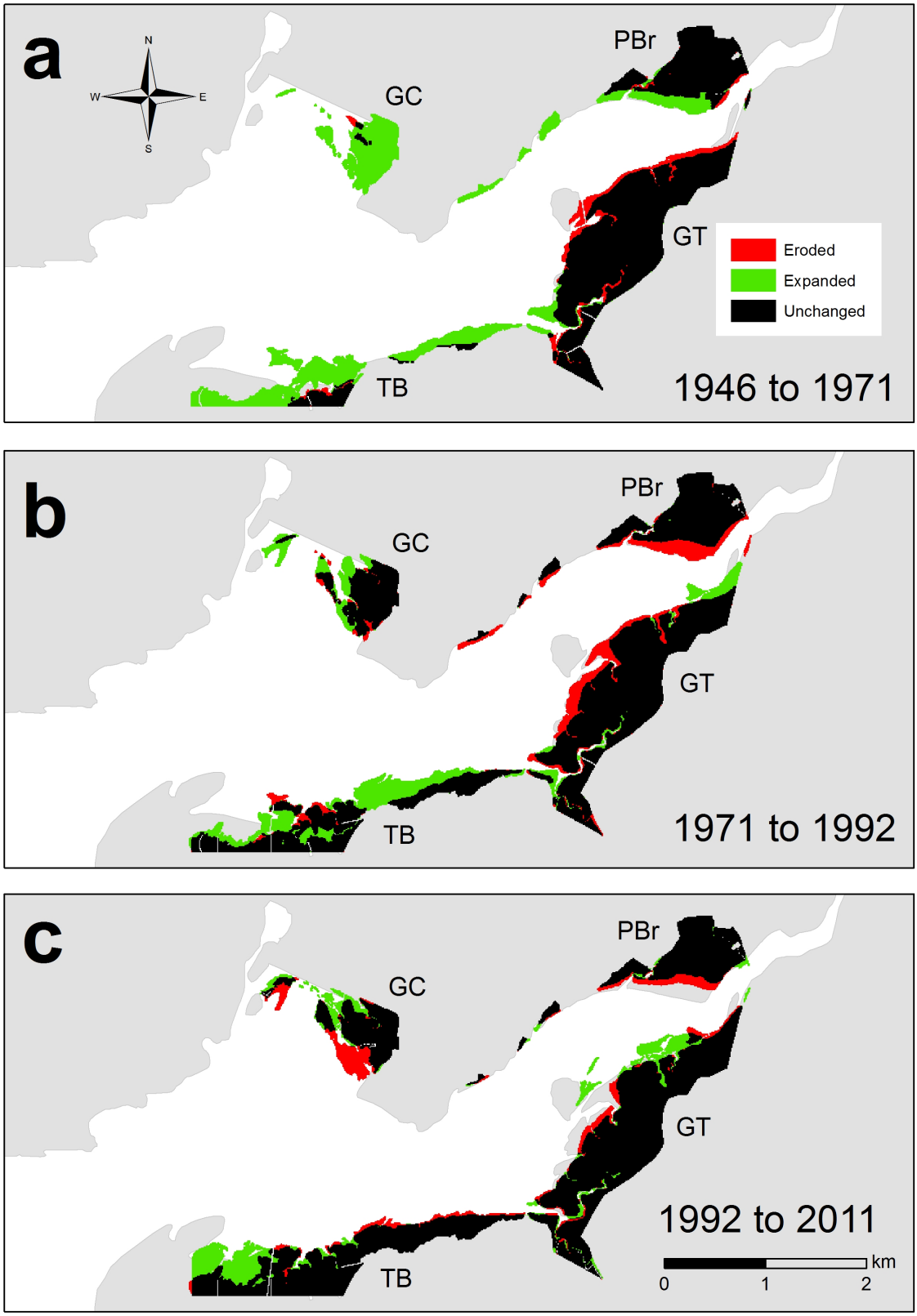

Figure A4 Maps summarising saltmarsh change for Glaslyn-Dwyryd estuary between **a** 1946 and 1971, **b** 1971 and 1992, and **c** 1992 and 2011. Black areas represent stable marsh that has remained unchanged throughout the study period. Red and green areas show areas where marshes have eroded or expanded respectively. Labels refer to the names of saltmarsh complexes (GC: Glaslyn Cob; TB: Traeth Bach; GT: Glastraeth, and; PBr: Pont Briwet).

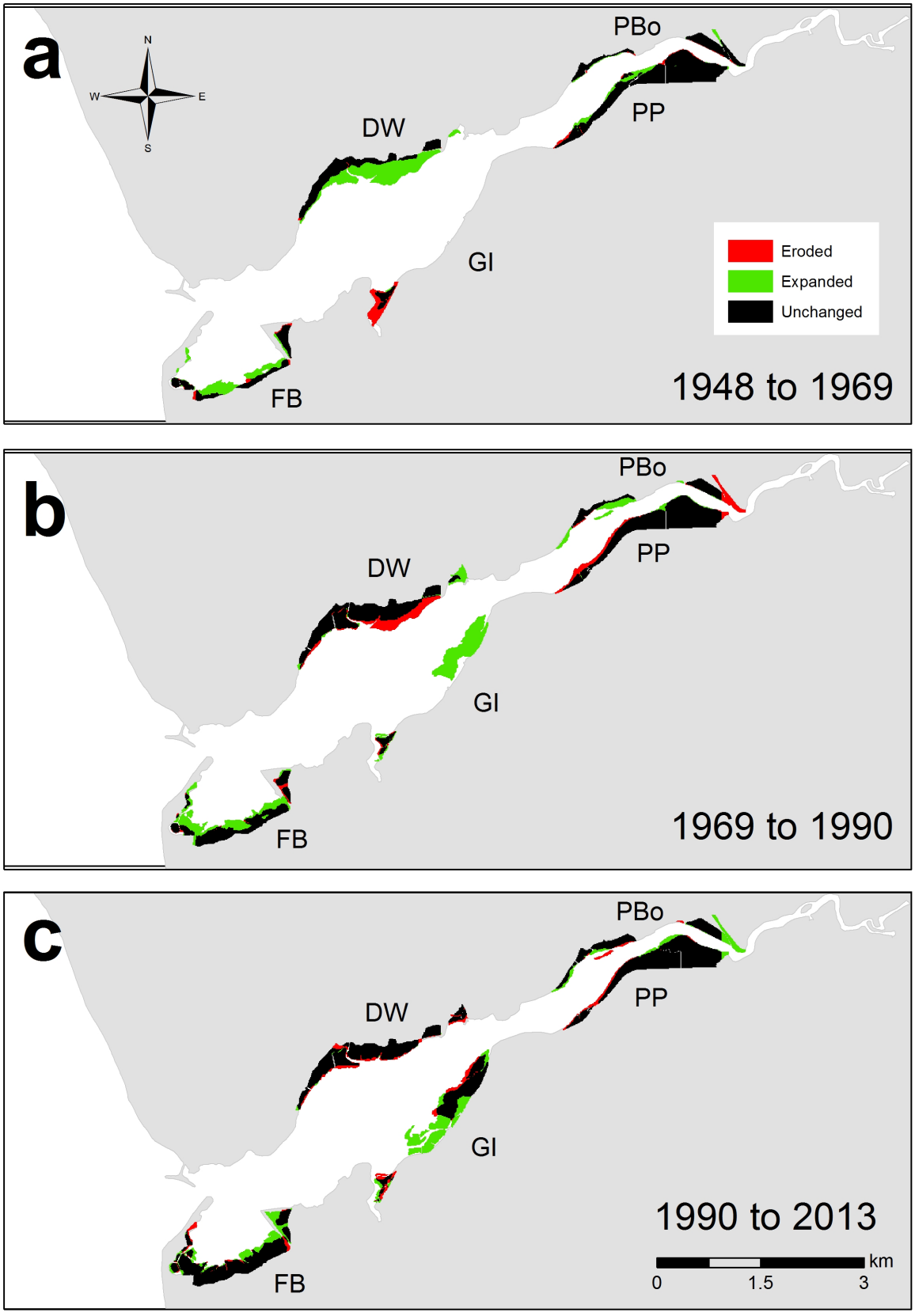

Figure A5 Maps summarising saltmarsh change for Mawddach estuary between **a** 1948 and 1969, **b** 1969 and 1990, and **c** 1990 and 2013. Black areas represent stable marsh that has remained unchanged throughout the study period. Red and green areas show areas where marshes have eroded or expanded respectively. Labels refer to the names of saltmarsh complexes (FB: Fairbourne; DW: Dwynant; GI: Garth Isaf; PP: Penmaenpool, and; PBo: Pont Borthwnog).

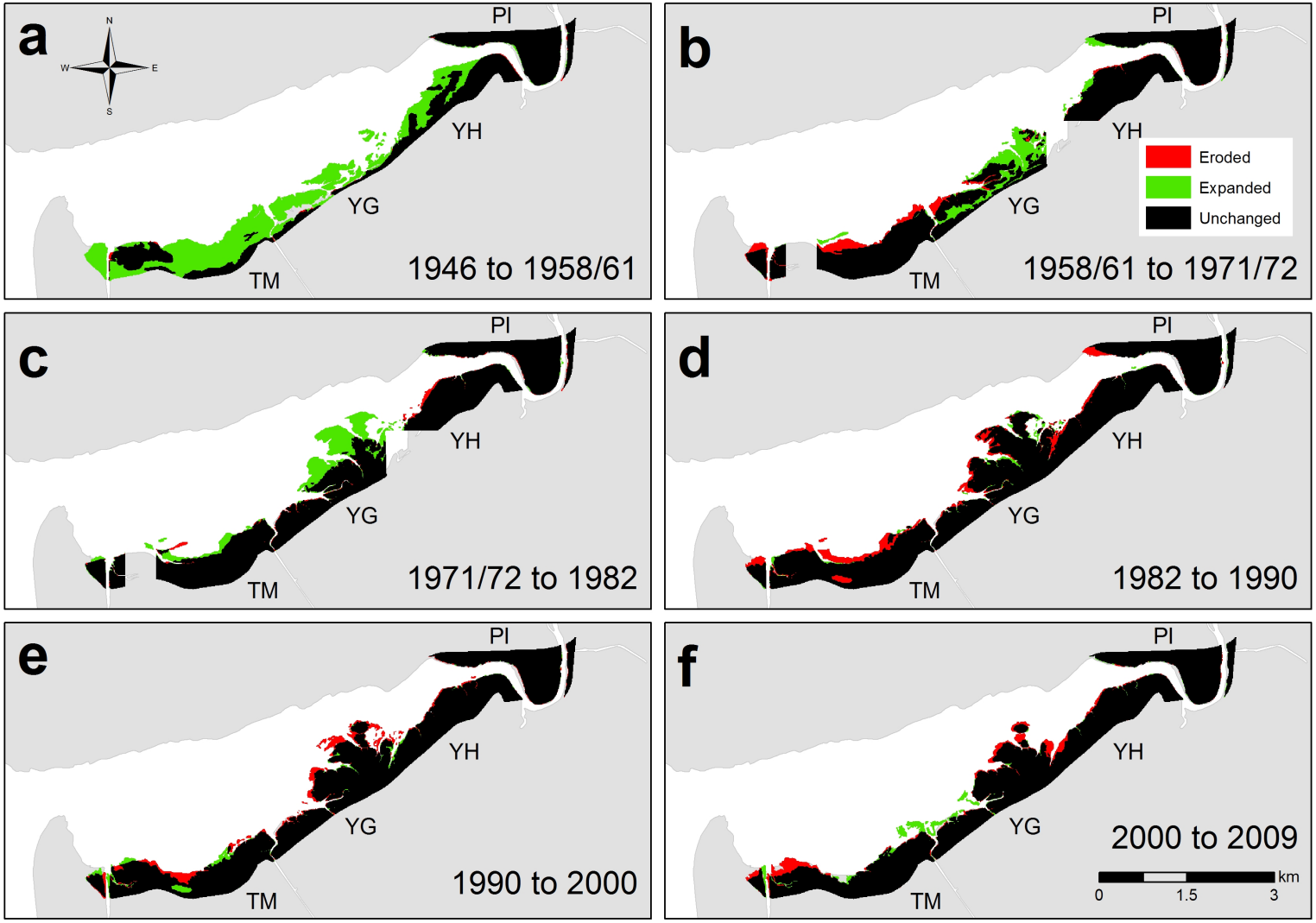

Figure A6 Maps summarising saltmarsh change for Dyfi estuary between **a** 1946 and 1958/61, **b** 1958/61 and 1971/72, **c** 1971/72 and 1982, **d**.1982 and 1990, **e** 1990 and 2000, and **f** 2000 and 2009. Black areas represent stable marsh that has remained unchanged throughout the study period. Red and green areas show areas where marshes have eroded or expanded respectively. Labels refer to the names of saltmarsh complexes (TM: Traeth Maelgwyn; YG: Ynys Greigiog; YH: Ynys Hir and PI: Penmaen Isa).

Appendix VII: Age of saltmarsh deposits

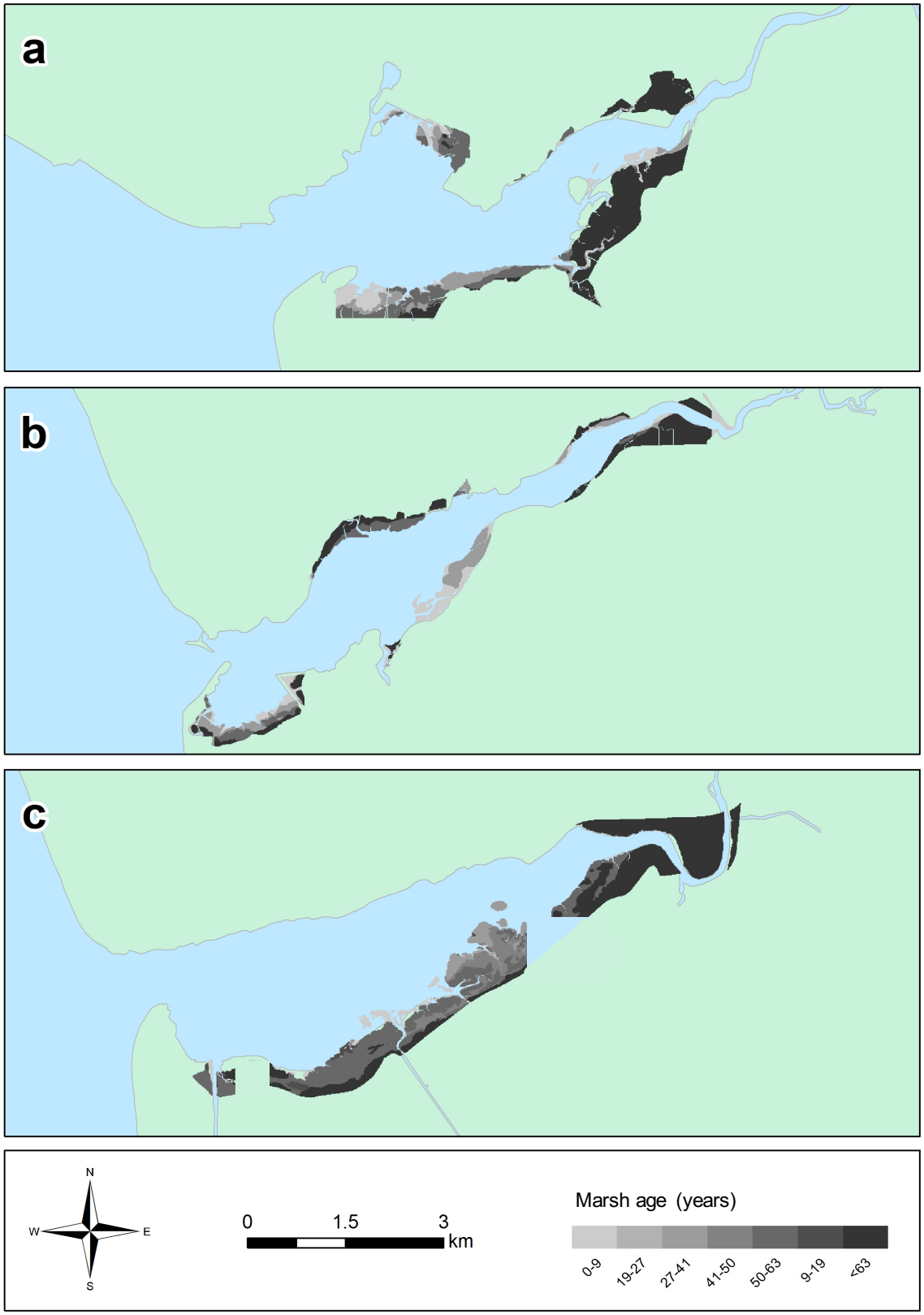

Figure A7 Maps showing the age of marsh deposits (in years) for **a** Glaslyn-Dwyryd, **b** Mawddach and **c** Dyfi estuaries. Darker coloration represents older marsh deposits, and range between 0 and over 63 years.

Appendix VIII: Locational probability of tidal channels

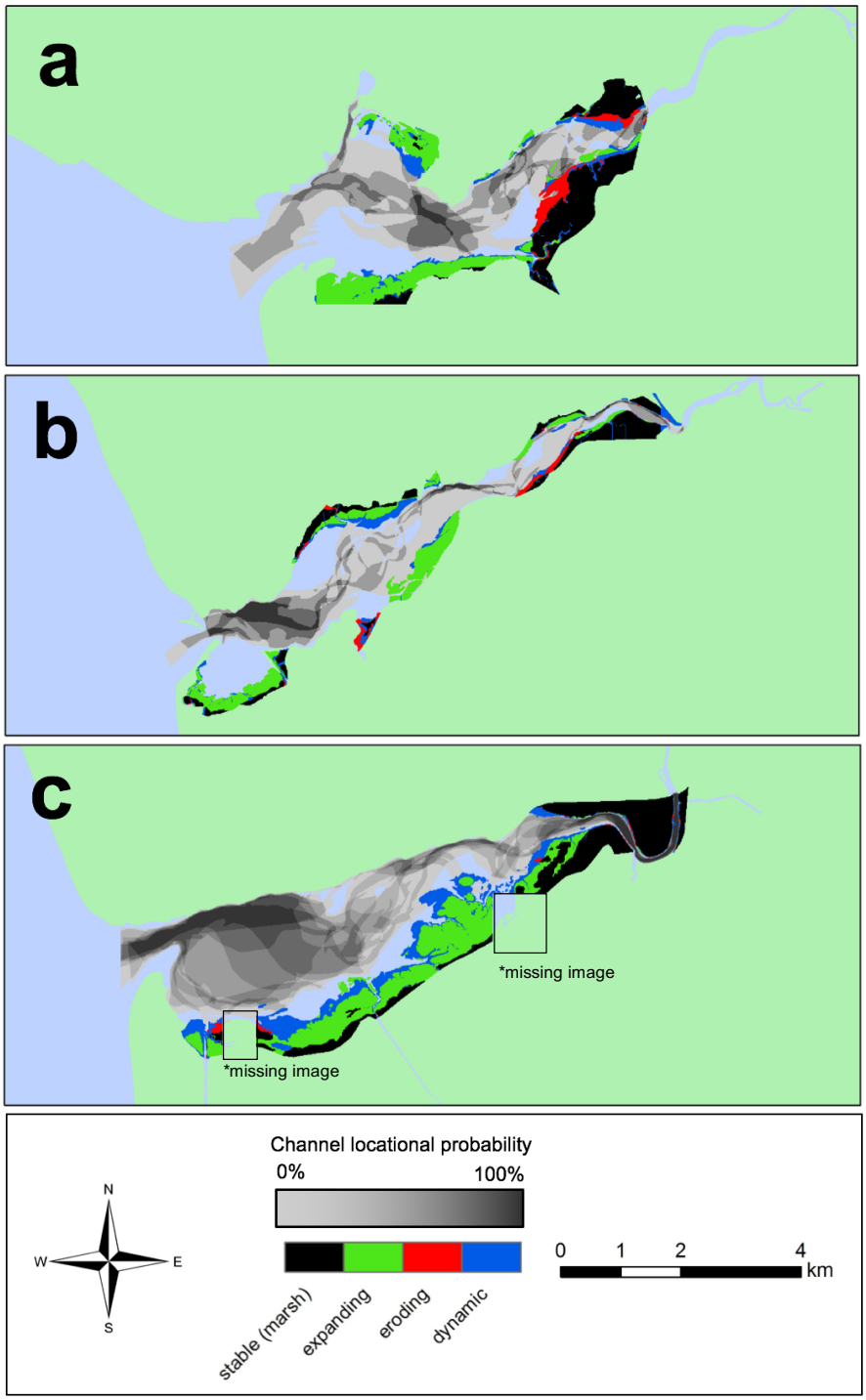

Figure A8 Maps summarising saltmarsh change (colour) and likelihood of channel occurring in at a specific location in the estuary (greyscale) for **a** Glaslyn-Dwyryd, **b** Mawddach and **c** Dyfi estuaries between 1946 and 2013. Black areas represent stable marsh that has remained unchanged throughout the study period. Red and green areas show marsh erosion and expansion respectively. Blue areas represent areas that have fluctuated between marsh and tidal flat at least once during the survey period.

Appendix IX: Detrended wind and river flow data

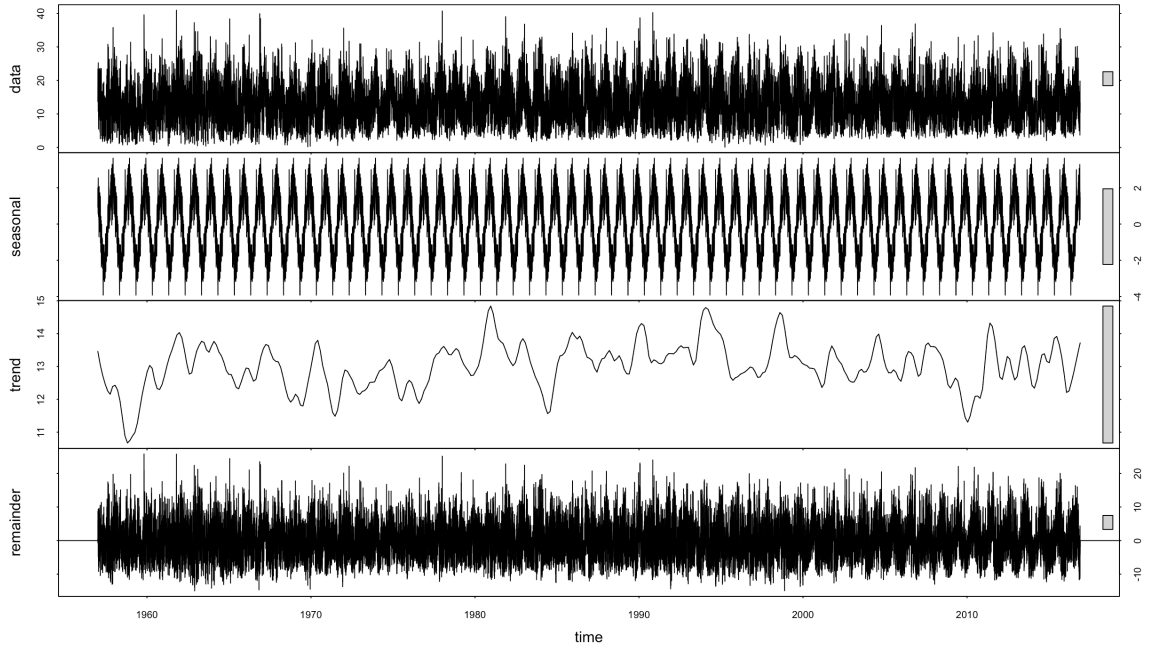

Figure A9 Change in wind speed (m s^{-1}) between 1957 and 2017. Data is presented in four ways: i. Raw data (first panel); ii. seasonal signal (second panel); iii. trend signal (third panel), and; iv. residual data (fourth panel).

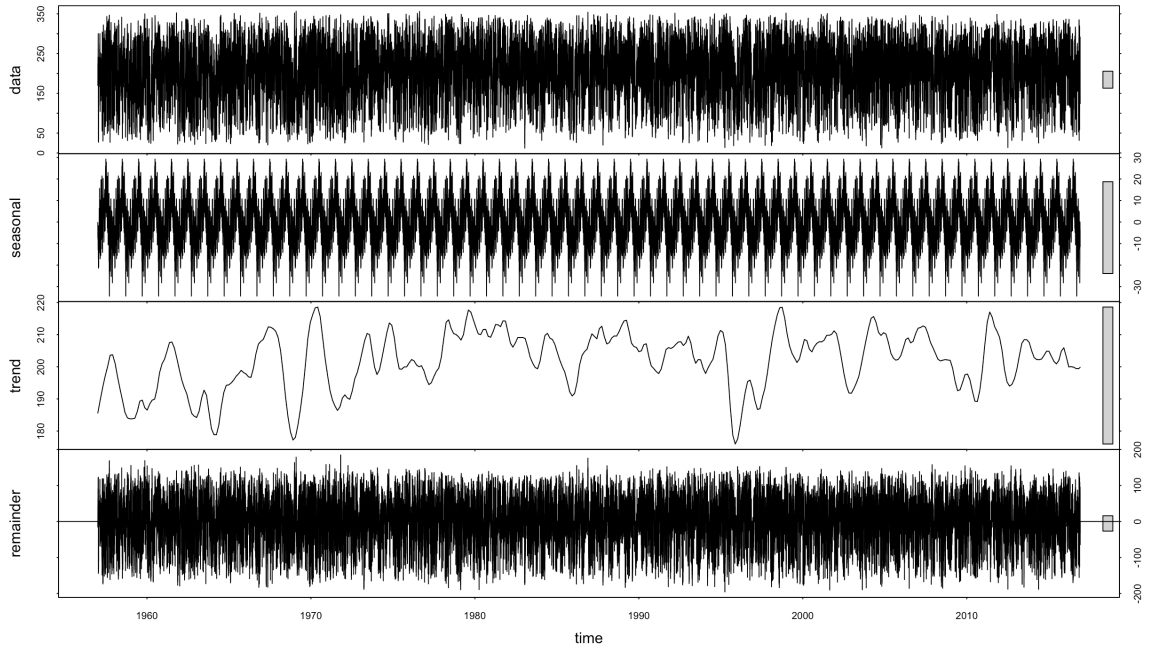

Figure A10 Change in wind direction between 1957 and 2017. Data is presented in four ways: i. Raw data (first panel); ii. seasonal signal (second panel); iii. trend signal (third panel), and; iv. residual data (fourth panel).

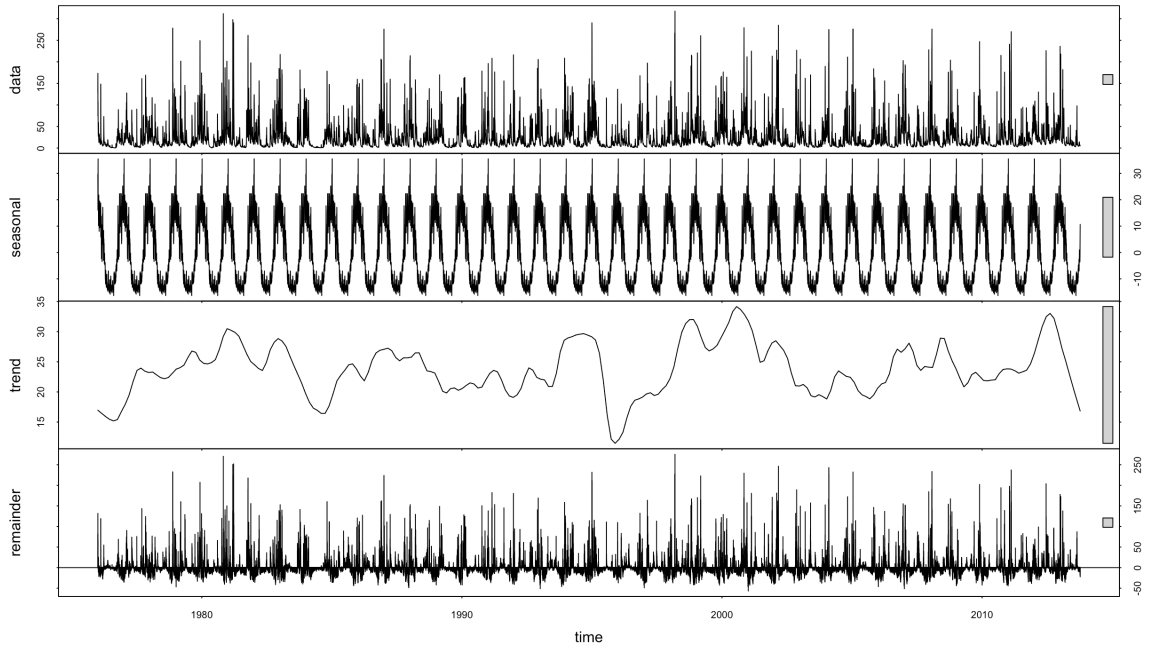

Figure A11 Change in daily river flow (m^3 s^{-1}) between 1962 and 2013. Data is presented in four ways: i. Raw data (first panel); ii. seasonal signal (second panel); iii. trend signal (third panel), and; iv. residual data (fourth panel).

Appendix X: Script for MicMac Structure from Motion

```
DIRMM="${HOME}/micmac/data/creek_data/15_10_13/11"
ALL="${DIRMM}/IMG_[0-9]{4}.JPG"
MIDDLE="${DIRMM}/IMG_(9176|9180|9181|9183).JPG"
EDGES="${DIRMM}/IMG_(9176|9178|9182|9184).JPG"
COORDS="${DIRMM}/gcp01.txt"
NPROC=24

%% find matching picture pairs
Tapioca MulScale ".*JPG" 100 -1 ExpTxt=1 ByP=$NPROC

%% characterize geometric properties of optics
Tapas RadialBasic ".*JPG" Out=Calib ExpTxt=1

%% apply properties to all images
Tapas AutoCal ".*JPG" InCal=Calib Out=All-Rel ExpTxt=1

%% generate sparse point cloud and camera positions
AperiCloud ".*JPG" All-Rel Out=sparse.ply RGB=0 ExpTxt=1

%% convert wgs84 coordinates to british national grid
mm3d GCPConvert AppInFile $COORDS Out=AppOSGB.xml

%% assign coordinates to ground control points (GCP) in a subset of images
SaisieAppuisInit $MIDDLE All-Rel NamePointInit.txt MesureInit.xml

%% calibrate camera orientations with GCPs
GCPBascule $ALL All-Rel OSGB-Init AppOSGB.xml MesureInit-S2D.xml

%% adjust predicted locations of GCPs
SaisieAppuisPredic $ALL OSGB-Init AppOSGB.xml MesureFinale.xml

%% compensate for errors in GCP based on the scene
Campari            ".*JPG"            OSGB-Bascule            OSGB-Compense
GCP=[AppOSGB.xml,0.1,MesureFinale-S2D.$

%% compute dense point clouds
Malt Ortho ".*JPG" OSGB-Compense EZA=1

%% create the orthoimage
mm3d Tawny Ortho-MEC-Malt/ Out=ortho1.tif
```

```
%% convert point cloud to digital elevation model
Nuage2Ply     MEC-Malt/NuageImProf_STD-MALT_Etape_8.xml     Attr=Ortho-MEC-
Malt/ortho1.ti$
```